

Impact of Freight on Highway Infrastructure in New Jersey

FINAL REPORT
September 2015

Submitted by

Hani Nassif, PE, PhD¹
Professor

Kaan Ozbay, PhD³
Professor

Hao Wang, PhD¹
Assistant Professor

Robert Noland, PhD²
Professor

Peng Lou¹
PhD Candidate

Sami Demiroglu, PhD¹
Research Associate

Dan Su, PhD⁴
Visiting Assistant Professor

Chaekuk Na, PhD¹
Research Associate

Jingnan Zhao¹
Research Assistant

Miguel Beltran¹
PhD Candidate

¹ Rutgers Infrastructure Monitoring and Evaluation (RIME) Group

² Bloustein School of Planning
Rutgers, The State University of New Jersey, NJ

³ New York University, NY

⁴ Lamar University, TX



NJDOT Research Project Manager
Kimbrali Davis

In cooperation with

New Jersey
Department of Transportation
Bureau of Research

And

U. S. Department of Transportation
Federal Highway Administration

DISCLAIMER STATEMENT

“The contents of this report reflect the views of the author(s) who is (are) responsible for the facts and the accuracy of the data presented herein. The contents do not necessarily reflect the official views or policies of the New Jersey Department of Transportation or the Federal Highway Administration. This report does not constitute a standard, specification, or regulation.”

1. Report No. FHWA-NJ-2016-004		2. Government Accession No.		3. Recipient's Catalog No.	
4. Title and Subtitle Impact of Freight on Highway Infrastructure in New Jersey				5. Report Date September 2015	
				6. Performing Organization Code Rutgers University	
7. Author(s) Hani Nassif, Kaan Ozbay, Hao Wang, Robert Noland, Peng Lou, Sami Demiroglu, Dan Su, Chaekuk Na, Jingnan Zhao and Miguel Beltran				8. Performing Organization Report No.	
9. Performing Organization Name and Address Rutgers Infrastructure Monitoring and Evaluation (RIME) Group Department of Civil and Environmental Engineering Rutgers, The State University of New Jersey Piscataway, NJ 08854-8014				10. Work Unit No.	
				11. Contract or Grant No.	
12. Sponsoring Agency Name and Address New Jersey Department of Transportation PO 600 Trenton, NJ 08625				13. Type of Report and Period Covered Draft Final Report 09/20/2012 – 09/20/2015	
				14. Sponsoring Agency Code	
15. Supplementary Notes					
16. Abstract Infrastructure systems, such as pavement, bridges, tunnels, and traffic systems, constitute a major part of the national investment and are critical for our society's mobility and economic prosperity. However, overweight vehicles deteriorate our infrastructure at a higher rate relative to other exposure and causes financial impacts that are not explicitly quantified. This project assesses the impact of overweight vehicles (both permitted and non-permitted) on New Jersey's infrastructures, specifically highway pavements and bridges. It conducts a detailed literature review about overweight vehicles on infrastructure from various states, then investigates deterioration models for various types of pavements and bridges, and quantifies the effect of overweight vehicles on service life of pavements and bridges. This study also performs Life Cycle Cost Analyses (LCCA) based on the proposed deterioration models to obtain the damage cost incurred by overweight vehicles. In addition, it develops both a decision-support tool based on the ASSISTME-WIM software and a unified database for the decision support tool that can be used by NJDOT personnel to assess and quantify the associated damage costs to NJDOT infrastructure network due to overweight trucks. The end result provides a tool that enabled the Bureau of Freight Planning and Intermodal Coordination at the New Jersey Department of Transportation (NJDOT) to combine NJDOT's freight and overweight vehicles data with maintenance and traffic data, to estimate the actual damage cost on NJ Highways due to overweight trucks. Using this tool, and based on the analysis of permit records, the estimated state-wide average cost of moving one ton of overweight load per one mile is about \$0.33, in which about approximately 60% of the damage cost is attributed to pavement and 40% to bridges. Based on the current permit fee structure from NJDOT, the damage cost for loads exceeding legal limit is not covered by the weight-based fee. Future work is needed to establish a fee structure based on overweight tons as well as trip miles.					
17. Key Words Overweight trucks, Economic Impact, Highway Bridge, Pavement, Life Cycle Cost Analysis				18. Distribution Statement	
19. Security Classif. (of this report) Unclassified		20. Security Classif. (of this page) Unclassified		21. No of Pages 222	22. Price

ACKNOWLEDGMENTS

The authors would like to thank the New Jersey Department of Transportation (NJDOT) for their support on this project. The former project manager in Bureau of Research, Paul Thomas, is thankfully acknowledged. Their financial support and the technical assistance of NJDOT Engineers in Bureau of Research, Kimbrali Davis and Giri Venkateela, in Bureau of Freight Planning and Services, Paul Truban and Andrew Ludasi, in Bureau of Structural Evaluation, Harshad B. Ringwala and Greg Reinman, and in Pavement Office Susan Gresavage, as well as other Bureaus are gratefully acknowledged. Former post-doc research associate, Ye Xia, is also acknowledged.

TABLE OF CONTENTS

EXECUTIVE SUMMARY	1
INTRODUCTION.....	3
OBJECTIVES	5
LITERATURE REVIEW	6
The Effect of Overweight or Superload Trucks on Bridges and Pavements.....	6
Canada	8
Arizona	8
New York State	8
Connecticut State.....	8
Indiana State.....	9
Louisiana State.....	9
Ohio State	9
Wisconsin State	10
South Carolina State.....	11
Deterioration Model for Highway Bridges	14
Weight Regulations.....	14
<i>Deck Deterioration from Mechanical Loading.....</i>	<i>18</i>
<i>Deck Deterioration from Environmental Factors</i>	<i>20</i>
<i>Fatigue Evaluation.....</i>	<i>23</i>
<i>Current AASHTO LRFD Fatigue Design</i>	<i>25</i>
<i>Current Fatigue Evaluation.....</i>	<i>28</i>
Relevant Studies on Effect of Overweight Traffic on Pavement Damage	40
Life Cycle Cost Analysis of Bridges and Pavements	44
Summary	49
NJDOT WIM Map.....	50
RESEARCH APPROACH.....	53
Data Collection and Development of a Unified Database	53
Data Format	54
Database Software and Structure.....	54
Database Tables.....	55
<i>WIM</i>	<i>55</i>
<i>Weight Class</i>	<i>56</i>
<i>Weight</i>	<i>56</i>
<i>Links</i>	<i>56</i>
<i>AADT</i>	<i>56</i>
<i>Bridges</i>	<i>57</i>
<i>Bridge Condition</i>	<i>57</i>
Processing WIM Data.....	58
Processing NBI Data.....	61
<i>Bridge Classification.....</i>	<i>63</i>

Deterioration and Service Life Prediction Models for Highway Bridges	69
<u>Selection of prototype bridges for analysis.....</u>	<u>69</u>
<u>Deterioration models for Bridge Girders.....</u>	<u>70</u>
<i>Steel Girders</i>	<i>70</i>
<i>Prestressed Concrete Structures.....</i>	<i>75</i>
<i>Effect of Truck Classifications on Girder Deterioration</i>	<i>78</i>
<u>Deterioration models for Bridge Deck.....</u>	<u>78</u>
<i>Service Life of Highway Bridge Deck in New Jersey.....</i>	<i>78</i>
<i>Loading on Bridge Deck</i>	<i>79</i>
<i>Correlation between Truck Loading and Deck Service Life.....</i>	<i>83</i>
<i>Economic impact of overweight trucks on bridge decks.....</i>	<i>89</i>
Deterioration and Prediction Models for Pavement.....	92
<u>Impact of Overweight Truck on Pavement Life</u>	<u>92</u>
<i>WIM Data and Axle Load Spectra.....</i>	<i>92</i>
<i>M-E Analysis Using Different Loading Scenarios.....</i>	<i>97</i>
<u>Allocation of Pavement Damage Cost Using Mechanistic-Empirical Pavement</u>	
<u>Analysis (Pavement-ME).....</u>	<u>99</u>
<i>Development of Load Equivalency Factor for Individual Pavement Distress</i>	
.....	99
<i>Development of Tire Pressure Equivalency Factor</i>	<i>103</i>
<u>Life Cycle Cost Analysis.....</u>	<u>107</u>
<u>Marginal Pavement Damage Cost.....</u>	<u>108</u>
<u>Allocation of Pavement Damage Cost Using Pavement Performance Data .</u>	<u>112</u>
<i>Pavement Structure and Maintenance Activities.....</i>	<i>113</i>
<i>Pavement Life Estimated from Field Data</i>	<i>115</i>
<u>Load Equivalency Factor and Equivalent ESALs</u>	<u>117</u>
<u>Pavement Damage Cost per Truck</u>	<u>120</u>
Greenhouse Gas Emissions and Fuel Consumption Attributable to Overweight	
Freight Vehicles	124
<u>Methods and Assumptions</u>	<u>124</u>
<i>Fuel Consumption</i>	<i>125</i>
<i>Average Speed.....</i>	<i>129</i>
<i>Greenhouse Gases.....</i>	<i>129</i>
<u>Results</u>	<u>129</u>
<u>Conclusions.....</u>	<u>134</u>
Development of a Decision-support Tool and Data-driven Life Cycle Cost	
Analysis.....	135
<u>Decision Support Tool.....</u>	<u>135</u>
<i>Software Architecture</i>	<i>137</i>
<i>Functional Requirements.....</i>	<i>137</i>
<u>Data driven Life Cycle Cost Analysis</u>	<u>137</u>
<i>Methodology and Approach</i>	<i>138</i>

<i>General Methodology of LCCA</i>	138
<i>LCCA Procedure</i>	140
<i>Uncertainties and Reliabilities</i>	143
<u>ASSISTME-WIM Weigh-In-Motion Data Analysis Tool</u>	148
<u>Features of the Web-based Tool:</u>	150
<i>Roadway Damage Cost Calculation</i>	150
<u>Cost Calculations in the Decision Tool</u>	153
<i>Unit Damage Costs</i>	153
<u>Details of the Cost Calculation Steps</u>	155
<i>Details of Roadway Damage Cost Calculation</i>	155
<i>Details of Single Trip Cost Calculation</i>	157
CONCLUSIONS	178
Conclusions for Bridge Part	178
<u>Future Work for Bridge Deterioration Models</u>	179
Conclusions for Pavement Part	179
Conclusions for Decision Tool	180
REFERENCES	181
APPENDIX A OBTAINED DECK DETERIORATION CURVE FROM NBI DATABASE	190
APPENDIX B STRUCTURAL ANALYSIS OF SELECTED BRIDGES	197
Prototype Bridge I: Simple Span Steel Multi-Beam Bridge.....	197
<u>Finite Element Bridge Analysis</u>	197
<i>Material Properties</i>	197
<i>Element Selection and Analysis Report</i>	197
Prototype Bridge II: Simple Span Steel Girder-Floorbeam Bridge.....	200
<u>Three Dimensional Finite Element Modeling and Verification</u>	205
<u>Fatigue Truck Model Analysis</u>	206
Prototype Bridge III: Simple Span Prestressed Concrete Multi-Beam Bridges	208
<u>Geometric Modeling</u>	208
<i>Elements</i>	208
<i>Sections</i>	210
<i>Constraint Elements</i>	211

LIST OF FIGURES

Figure 1. Decision support tool structure.....	2
Figure 2. Comparison of different axle-group-weight formulas.....	15
Figure 3. ADTT of interstate highway and deck deterioration.....	19
Figure 4. Flow chart of fatigue evaluation process for bridges	22
Figure 5. Typical S-N curve ⁽⁴⁷⁾	23
Figure 6. AASHTO LRFD fatigue design truck.....	32
Figure 7. General framework of Mechanistic-Empirical analysis approach	37
Figure 8. Map of WIM sites in New Jersey (2012).....	50
Figure 9. Structure of the unified database	55
Figure 10. Locations of NJ-WIM stations.....	57
Figure 11. Growth in volume and loadings on the rural interstate system (1970-2010)	58
Figure 12. Annual average ADTT for various sites from 1993 to 2012 ⁽⁹⁴⁾	59
Figure 13. Distribution of Route Signing Prefix in bridge inventory	64
Figure 14. Distribution of bridge material in bridge inventory	64
Figure 15. Distribution of structural types in simply supported concrete bridges.....	66
Figure 16. Distribution of structural types in continuous concrete bridges.....	66
Figure 17. Distribution of structural types in simply supported steel bridges	67
Figure 18. Distribution of structural types in continuous steel bridges.....	67
Figure 19. Distribution of structural types in simply supported prestressed concrete bridges	68
Figure 20. Distribution of structural types in continuous prestressed concrete bridges	68
Figure 21. Selection of prototype bridges for analysis.....	69
Figure 22. Flowchart for processing deterioration data	80
Figure 23. Flowchart for WIM data processing.....	80
Figure 24. Statistics of “all trucks” dataset from WIM data	81
Figure 25. Comparison of deterioration models for bridges on various highways	82
Figure 26. Effect of axles per day on service life of bridge decks.....	85
Figure 27. Correlation between lifetime axle counts vs equivalent wheel load.....	85
Figure 28. Predicted service life of deck; (a) interstate highway, (b) US numbered highway, and (c) NJ state highway.....	86
Figure 29. Effect of overweight trucks	89
Figure 30. Vehicle class distributions for (a) non-overweight and (b) overweight traffic	94
Figure 31. Axle load spectra of non-overweight traffic on (a) minor road and (b) major road (Class 9 vehicle)	95
Figure 32. Axle load spectra of overweight traffic on (a) minor road and (b) major road.....	96
Figure 33. Reduction ratio of pavement life at different percentages of overweight truck	98
Figure 34. Load equivalency factors for (a) fatigue cracking and (b) AC rutting developed using Pavement-ME	100
Figure 35. Comparisons between load equivalency factors for (a) fatigue cracking and (b) rutting from Pavement-ME analysis and AASHTO road test.....	102
Figure 36. Tire pressure distributions from a TXDOT survey (After Wang and Machemehl 2003)	104
Figure 37. Tire pressure equivalency factors for fatigue cracking and rutting	104

Figure 38. Pavement life comparisons between flexible pavement and composite pavement of (a) major road (b) minor road	106
Figure 39. MPDC of (a) thick flexible pavement (b) composite pavement on major road for 30 and 60-year analysis period	110
Figure 40. MPDC of (a) thin flexible pavement (b) composite pavement on minor road for 30 and 60-year analysis period	111
Figure 41. Flowchart of analyzing impact of truck loading on pavement damage cost	112
Figure 42. Example of deterioration trend of pavement performance (I-80B).....	116
Figure 43. Example of LEFs from AASHO road test-flexible pavement (Structure Number = 5, Terminal $PSI_t = 2.5$).....	119
Figure 44. Example of LEFs from AASHO road test-rigid pavement (Slab thickness = 9 in, Terminal $PSI_t = 2.5$).....	119
Figure 45. IRI progression on US 1 (m/km).....	130
Figure 46. Decision support (DS) tool structure	136
Figure 47. Conceptual cash flow diagram of a project ⁽¹⁰⁹⁾	142
Figure 48. Calculating NPV using Monte Carlo simulation	145
Figure 49. Conceptual probability distribution of LCCA output (NPV)	146
Figure 50. Cumulative probability distribution for two alternatives in LCCA	146
Figure 51. ASSISTME-WIM web user interface	150
Figure 52. Flowchart for calculation of roadway LCC	151
Figure 53. Flowchart for calculating permit cost for a truck	152
Figure 54. Flowchart of damage cost calculation	156
Figure 55. Flowchart for calculating permit cost for a truck	158
Figure 56. Average and Median Miles for Each Weight Categories	160
Figure 57. Average and Median Weight for Each Mileage Categories	160
Figure 58. Distribution of trip length in each weight category	161
Figure 59. Distribution of weight in each of trip length category	167
Figure 60. Damage and permit costs for weight categories (per ton per mile)	171
Figure 61. Damage and permit costs for trip length categories (per ton per mile).....	171
Figure 62. Surface plot of permit costs (per ton per mile) by weight and by trip length	172
Figure 63. Surface plots of (a) low, (b) average, (c) high damage costs (per ton per mile) by weight and by trip length	172
Figure 64. Damage and permit costs for weight categories (per ton per mile) using marginal unit pavement costs	174
Figure 65. Damage and permit costs for trip length categories (per ton per mile) using marginal unit pavement costs	174
Figure 66. Comparison of average trip costs based on trip length using marginal unit pavement costs	175
Figure 67. Percentage of damage cost paid through the current permit fee structure.	175
Figure 68. Surface plots of (a) low, (b) high damage costs (per ton per mile) by weight and by trip length using marginal unit pavement costs.....	177
Figure 69. Finite element models for (a) Structure No. 1307-155, and (b) Structure No. 0428-164	198
Figure 70. HS-20 design truck for fatigue	199
Figure 71. Exterior girder bottom flange stress at splice cutoff, located 24 ft. from midspan, due to HS-20 including impact (Str. No. 1307-155)	199

Figure 72. Newark Bay Bridge	201
Figure 73. Field instrumentation equipment	201
Figure 74. Weight-In-Motion sensor locations	202
Figure 75. Instrumentation on Span W14 (Type A span) (ft.)	203
Figure 76. Cross section of instrumented Span W14 (Type A span) (ft.)	203
Figure 77. Configuration and axle weights of calibration truck	204
Figure 78. FE Model for Span W14	205
Figure 79. Comparison of strain profiles under truck loading on south lane (17 ft. from curb): (a) main girder Sensor B3238, (b) S4 Sensor B3684, and (c) floorbeam FLB 4 Sensor B3685	206
Figure 80. (a) AASHTO fatigue truck model (b) modified AASHTO fatigue truck model	207
Figure 81. (a) Distribution of gross weight; (b) Distribution of trucks in each.....	207
Figure 82. Integration points of two-node linear beam B31	209
Figure 83. Integration points of a four-node shell element (ABAQUS)	210
Figure 84. Integration points on I section	210
Figure 85. 3-D FE model for prestressed concrete bridge.....	212
Figure 86. 3-D FE model for prestressed concrete girder	212

LIST OF TABLES

Table 1 - Summary of overweight load study from various states	7
Table 2 - Unit cost summary from Ohio DOT ⁽²¹⁾	10
Table 3 - Overweight damage for South Carolina ⁽²⁶⁾	12
Table 4 - Transformed unit cost for South Carolina ⁽²⁶⁾	13
Table 5 - Table of Maximum Gross Weights (lbs.) in New Jersey (N.J.S.A. 39:3-84) ...	16
Table 6 - Fatigue detail constant, A, by category x10 ⁷ (AASHTO LRFD 2010 Table 6.6.1.2.5-1).....	27
Table 7 - Constant amplitude fatigue threshold by category (AASHTO LRFD 2010 Table 6.6.1.2.5-3).....	27
Table 8 - Cycles per truck passage, n (AASHTO LRFD 2010 Table 6.6.1.2.5-2).....	27
Table 9 - Partial load factors: R_{sa} , R_{st} , and R_s ⁽⁴⁷⁾	29
Table 10 - Resistance factor for evaluation, minimum, or mean fatigue life, R_R ⁽⁴⁷⁾	31
Table 11 - Summary of pavement damage cost studies	43
Table 12 - Description and location for NJ-WIM sites (NJDOT)	51
Table 13 - Number of WIM Sites by road type	59
Table 14 - Statistics for interstate highway, US highway, and state highway routes	60
Table 15 - List of items selected in this study.....	62
Table 16 - NBI bridge condition ratings explanation.....	63
Table 17 - Bridge material code definition in NBI database.....	65
Table 18 - Summary of bridge girder life cycle cost analysis for Prototype Bridge I.....	71
Table 19 - Summary of bridge girder life cycle cost analysis for Prototype Bridge II....	73
Table 20 - Summary of bridge girder life cycle cost analysis for Prototype Bridge III....	76
Table 21 - Summary of bridge deck life cycle cost analysis	90
Table 22 - WIM data at the selected sites	93
Table 23 - Summary of pavement structures	97
Table 24 - M-E pavement design criteria.....	97
Table 25 - Representative pavement structures used for major road.....	105
Table 26 - Representative pavement structures used for minor road.....	105
Table 27 - Traffic Volume Assumption Matrixes	105
Table 28 - WIM stations and mileposts at selected sites.....	113
Table 29 - Pavement structures at selected sites.....	114
Table 30 - Treatment and cost data at selected sites.....	114
Table 31 - Average SDI at selected sites after maintenance treatments.....	115
Table 32 - Predicted pavement service life using SDI data	117
Table 33 - ESAL calculation in 30-year and 60-year analysis period	120
Table 34 - Unit pavement damage costs (FY2015 \$ per ESAL lane-mi).....	121
Table 35 - Example of pavement damage cost per truck on Interstate highways	122
Table 36 - Example of pavement damage cost per truck on state roads.....	123
Table 37 - MOVES Vehicle Types.....	126
Table 38 - Conversions of MOVES Vehicle Types to HDM4 Vehicle Types	128
Table 39 - HCM 2010 Inputs	129
Table 40 - Predicted Fuel Consumption and Costs Attributable to Highway Use by Overweight Trucks over 20 years - Asphalt	131

Table 41 - Predicted GHG Emissions Attributable to Highway Use by Overweight Trucks over 20 years - Asphalt	131
Table 42 - Predicted Fuel Consumption and Costs Attributable to Highway Use by Overweight Trucks over 20 years - Concrete	132
Table 43 - Predicted GHG Emissions Attributable to Highway Use by Overweight Trucks over 20 years - Concrete.....	132
Table 44 - Estimated total excess fuel consumption, costs, and GHG emissions attributable to overweight trucks over 20 years.....	133
Table 45 - Equations of economic indicators.....	139
Table 46 - Types of data needed for calculating the other cost items ⁽¹¹²⁾	147
Table 47 - Unit pavement damage costs of interstate highway (\$ per ESAL lane-mi).	153
Table 48 - Cost ratio for each Class (Class unit cost/basic unit cost).....	154
Table 49 - Mileage statistics of permit vehicles by weight categories.....	159
Table 50 - weight statistics of permit vehicles by mileage categories	159
Table 51 - Average damage costs for different overweight and trip length categories	176
Table 52 - Summary of selected bridges.....	197
Table 53 - Str. No. 1307-155.....	200
Table 54 - Str. No. 0428-164.....	200
Table 55 - Str. No. 1023-153.....	200
Table 56 - Location of each sensor	204
Table 57 - Stress range caused by site specific fatigue trucks and estimated remaining fatigue life.....	208

EXECUTIVE SUMMARY

Infrastructure systems constitute a major part of the national investment and are critical for our society's mobility as well as its economic prosperity. The U.S. has an estimated \$25 trillion dollars invested in civil infrastructure systems, including installations that transport, transmit, and distribute people, goods, energy, resources, services, and information. The infrastructure system components such as road pavements, bridges, highways, traffic systems, tunnels, and other systems are assets that should be protected and properly managed. Yet, the degree of deterioration due to the exposure to environmental attack as well as overweight trucks is high. Federal, state, and local governments are tasked with making major decisions to allocate limited funds available for the repair, maintenance, and rehabilitation of New Jersey's infrastructure network. These decisions should be based on integrating various databases from critical infrastructure systems (e.g., bridges, roadway pavement, etc.) and their deterioration and condition models with traffic modeling at the network level, to help perform economic forecasting and life cycle cost analyses.

New Jersey Department of Transportation's (NJDOT) Freight Services has undertaken a major study to collect and process data that is essential for monitoring large trucks (i.e., truck length greater than 102") and their movement on side routes in various cities. To achieve this objective, data from various existing permanent Weigh-In-Motion (WIM) stations were collected and processed to monitor the volume and pattern of large truck movements in NJ. In addition, NJDOT started collecting electronic data on special permits for overweight trucks. Collecting unbiased data and monitoring truck movement, weight data, and axle configuration, provides the basis for understanding the impact of these factors on the State's highway infrastructure. New Jersey is expending significant efforts and resources on maintaining and repairing roadway infrastructures that will be adversely affected due to a growth in the frequency and an increase in the number of heavy and overweight trucks over the last decade. State agencies know a great deal about the factors that cause damage in roads, pavements, and bridges, however, it needs utilize this information and provide a decision-support tool to help maintain and manage NJ's infrastructure systems.

The scope of this project is illustrated in Figure 1 that incorporates four components:

- Develops a ***unified database*** of all available data relating to the condition rating of PMS, bridge management system (BMS) and inventory, Weigh-In-Motion (WIM) truck weight spectra, etc.;
- Utilizes pavement and bridge ***deterioration models*** to evaluate the impact of overweight trucks on the service life of pavement and bridges;
- Conducts ***Life-Cycle Cost Analysis*** (LCCA) to analyze the associated cost that the movement of freight has on the highway system;

- Develops a **decision-making tool** incorporating future growth, prediction models, environmental impact, and impact of changes in truck regulations and policy.

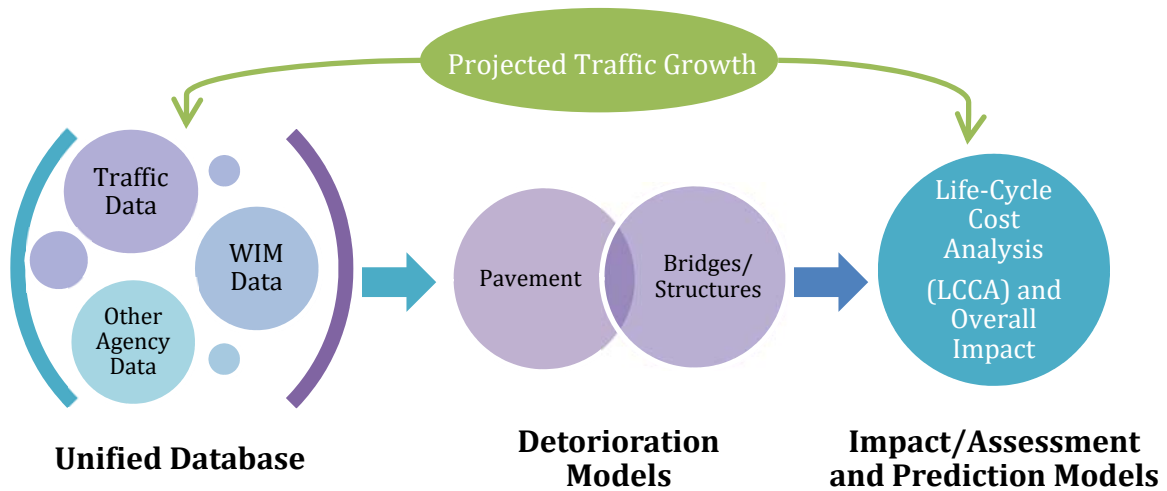


Figure 1. Decision support tool structure

This project assessed the impact of overweight vehicles (both permitted and non-permitted) on New Jersey’s infrastructure systems, specifically highway pavements and bridges. It conducted a detailed literature review about overweight vehicles on infrastructure from various states, then investigated the deterioration models for various types of pavements and bridges, and quantified the effect of overweight vehicles on service life of pavements and bridges. For bridges, both bridge decks and bridge girders were considered. Two loading scenarios were assumed to quantify the effect of overweight trucks. In Case 1, “all trucks” represents current truck traffic with all overweight trucks, and in Case 2, “legal truck traffic” excludes overweight trucks. For pavements, the service life reduction was estimated using two different approaches, mechanistic-empirical (M-E) pavement analysis and analysis using pavement performance data from pavement management systems (PMS), for a wide ranges of pavement structures and traffic condition. This study also performed a Life Cycle Cost Analysis (LCCA) based on the proposed deterioration models to obtain the damage cost incurred by overweight vehicles. In addition, it developed both a decision-support tool based on the ASSISTME-WIM software and a unified database. Both software and unified database were applied by the Bureau of Freight Planning and Intermodal Coordination to combine NJDOT’s freight and overweight vehicles data with maintenance and traffic data, and to estimate the actual damage cost on NJ highways due to overweight trucks. As a case study, this tool was applied on selected permit records from 2011. Based on the analysis of permit records, the estimated state-wide average cost of moving one ton of overweight load for one mile is about \$0.33, in which about 60% of the damage cost is attributed to pavement and 40% to bridge. Based on current permit fee structure from NJDOT, the damage cost for loads exceeding legal limit is not covered by the weight-based fee. Future work is needed to establish a fee structure based on overweight tons as well as trip miles.

INTRODUCTION

Highway agencies are responsible for protecting the billions of taxpayer dollars invested in highway infrastructure. As such, for the purposes of safety and system preservation, trucking operational characteristics (i.e., size and weight) is regulated by the federal and state legislation and policies. The federal commercial vehicle maximum standards on the interstate highway system are: 1) single axle: 20,000 lbs., 2) tandem axle: 34,000 lbs., and 3) gross vehicle weights: 80,000 lbs. However, almost every state highway agency has its own legal load limits that are also based on single- or tandem-axle loads and the gross weight of the vehicle. Some agencies also have limits on the load per unit of tire width. These load limits are imposed with the intention to keep the loading conditions as consistent as possible with the methodology used to design the highway facility. The effect of truck loads on infrastructure is important in the effort of upgrading and maintaining the transportation infrastructure. Permits help regulate the operation of overweight as well as oversized trucks by ensuring the safety of bridges and minimizing damage to pavements while promoting commerce and the movement of goods and services. The impact of heavy truck loads on road pavement was studied by the AASHTO Road tests performed in the 1950s. The data from the tests has shown that the damage to the pavement can be as large as to the fourth power as the load increases.

The State of New Jersey Transportation's Freight Services has established a major study to collect and process data that is essential for monitoring large trucks (truck length greater than 102ft.) and their movements on side routes in various cities. To achieve this objective, data from various existing permanent fixed Weigh-In-Motion (WIM) stations is being collected and processed to monitor the volume and pattern of large truck movements in New Jersey. In addition, NJDOT started collecting electronic data on special permits for overweight trucks. The collection of unbiased data and monitoring of truck movement, weight data, and axle configuration provide the basis for understanding their impact on the State's highway infrastructures. The movements of large trucks on side routes can adversely affect the performance of road infrastructure and would disrupt the traffic pattern in various cities. The implications on the cost of maintaining safe roads and their integrity are obvious. Major decisions must be made to allocate the limited funds available for repair, rehabilitation, and/or replacement. Accordingly, the State will expend significant effort and resources on maintaining and repairing roadway infrastructure that will be adversely affected. A great deal is known about the factors that cause damage in roads, pavements and bridges; however, the State needs to utilize this information and provide a decision-support tool to help maintain and manage infrastructure systems. Such a tool should incorporate four components:

1. Develop a ***unified database*** of all available data relating to the condition rating of pavement management systems (PMS), bridge management system (BMS) and inventory, Weigh-In-Motion (WIM) truck weight spectra, etc.
2. Utilize pavement and bridge ***deterioration models*** to evaluate the impact of overweight truck on the service life of pavement and bridges;
3. Conduct a ***Life-Cycle cost analysis*** (LCCA) to analyze the associated cost that the movement of freight has on the highway system;

4. Develop a **decision-making tool** incorporating future growth, prediction models, environmental impact, and impact of changes in truck weight and size regulations and policy.

In recent years, several studies have estimated the truck damage using mechanistic-empirical (M-E) approaches. Unlike early design approaches converting mixed traffic into equivalent single-axle loads (ESALs), recent M-E models use axle-load spectra data from WIM stations. The advanced modeling capabilities drive federal and state transportation agencies to shift from the old empirical AASHTO Pavement Design Guide (1986, 1993) to the new Mechanistic Empirical Design Guide (NCHRP 1-37, 2004) ^(1, 2, 3). Parker and Hussain (2006), utilizing traffic data from the States of Florida, New Jersey, and New York, used KENLAYER software and pavement performance models to quantify the pavement damage caused by vehicles with different gross weights, number of axles, tire pressures, speeds, and load distributions on individual axles ⁽⁴⁾. Similarly, Hong et al. (2007) proposed a site-specific methodology for load-related pavement construction cost estimation using Mechanistic-Empirical Pavement Design Guide (MEPDG) ⁽⁵⁾. However, the pavement damage cost associated with trucks was not quantified.

Previous research and practice show that any increase in legal truck weight would shorten the time to repair or replace the bridges. The importance of identifying the impact of overweight trucks has been recognized by many state departments of transportation. Yoder et al. (1979) investigated the impact of a GVW limit increase for Indiana DOT, which represents an early effort in this area ⁽⁶⁾. Byrd, Tallamy, MacDonald, and Lewis (BTML) conducted a study in 1987 for New York State DOT on the effects of permit truck weights with special interest on steel fatigue-induced costs ⁽⁷⁾. Moses completed a study on the effects of proposed new truck weights on bridges for TRB ⁽⁵⁾. The results were summarized in TRB Special Reports 225 (1990) and 227 (1990) ^(8, 9). This study assessed the costs of fatigue life reduction and substandard load ratings caused by a variety of proposed new truck-weight limits, which was the first effort of including new bridges as a cost impact category. Moses (1989) also reported incremental costs for the new load limit scenarios considered, which are useful when more specific data are not available ⁽¹⁰⁾. A subsequent study by Mohammadi et al. (1998) incorporated more probabilistic treatment of fatigue damage to better understand the cost impact on bridges ⁽¹¹⁾. A beta distribution is assumed for the stress range, a Weibull distribution for the fatigue resistance (Ang and Tang, 1975) ⁽¹²⁾. The bridge is said to have failed in fatigue when the sum of the Miner's Rule has reached unity. Heywood and Pearson (1997) from Australia, Saber et al. (2008) in Louisiana Department of Transportation and Development, Chang and Garvin (2007), Altay et al. (2003) in University of Minnesota, and so on, conducted research on the effects of increasing truck weight on bridges ^(see references 13, 14, 15, and 16).

In summary, the objective and methodology employed in this project is consistent with highway agency practice, as guided by current AASHTO specifications. It also represents the-state-of-the-art in analysis techniques and uses the available data to the fullest extent. The improvements discussed above have been implemented in the methodology.

OBJECTIVES

The main objective of this project is to assess the impacts of overweight vehicles (both permitted and non-permitted) on New Jersey's infrastructure systems, specifically highway pavements and bridges. In addition, this project has aimed at developing a decision-support tool based on the ASSISTME-WIM software. A unified database will be utilized for the decision support tool that can be used by NJDOT personnel to assess and quantify the associated damage costs to NJDOT infrastructure network due to overweight trucks. It is our expectation that this decision-support tool will be utilized to manage the collected data for future use in making maintenance and operation decisions. The research methodology can be broadly classified into the following key scopes:

- **Review state-of-the-art practice and collect all available data.** The research team has reviewed the current practices on pavement and bridge deterioration models of other state agencies, and collected all available weigh-in-motion (WIM) data from NJDOT.
- **Develop deterioration models of pavement and bridges.** The research team has categorized the bridges into 4 groups (prestressed concrete bridge, steel girder bridge, reinforced concrete bridge, and concrete deck) and the pavements into 4 groups (major and minor road with thick and thin pavement). The National Bridge Inventory (NBI) data are also utilized for the development of deterioration models.
- **Design a unified database and decision-support tool to utilize all available data.** The research team has utilized the findings from the literature reviews and current practices, and updated the ASSISTME-WIM software that houses and organizes the WIM data. The updated ASSISTME-WIM software will integrate with models developed to assess the impact of loads on pavement and bridge on highways as identified from the literature. The software had an easy-to-use user interface to enable DOT personnel to use the tool in decision-support and planning capacities.
- **Evaluate life cycle costs and environmental impacts.** The developed deterioration models of pavement and bridge based on truck weights and loads enable the further development of life-cycle analysis that resulted in better policies for long-term maintenance and investment in New Jersey's road network. These techniques enabled the evaluation of both costs and environmental impacts.

LITERATURE REVIEW

The research team assembled and reviewed the most relevant literature regarding current practice, technical literature, research findings of recently completed and ongoing projects, and procedures from domestic and foreign sources. Moreover, they completed literature searches of all related research work done by FHWA, NCHRP, SHRP, and other DOT's regarding impact of heavy trucks on highway infrastructure. The research team found that heavy trucks have significant effect on highway bridges and pavements in terms of load carrying capacity, serviceability, and structure maintenance. In addition to the effect of overweight and superload trucks on highway infrastructure, the effect of raising truck load limits on highway bridges and pavements was also reviewed. A detailed literature search was completed regarding the following topics related to this study:

1. Effect of overweight or superload trucks on bridges and pavements;
2. Deterioration models for highway bridges;
3. Deterioration models for highway pavements; and
4. Life cycle cost analysis of highway bridges and pavements.

The Effect of Overweight or Superload Trucks on Bridges and Pavements

Due to the increasing number of permits issued for overweight trucks, the impact of overweight trucks on highway infrastructure mainly on bridges and pavements has caused lots of concern in North America. Simple analysis methods are not well established for local agencies to estimate the impact on bridges subjected to overloads. Some state DOTs already initiated studies to help quantify the structural or economic impacts of overweight trucks. These states include Connecticut, Indiana, Louisiana, Ohio, Wisconsin, and South Carolina. The search is summarized in Table 1.

Table 1 - Summary of overweight load study from various states

State Details	CT	IN	LA	OH	WI			SC	This Study
Authors and Year	Culmo et al. 2004	Bowman et al. 2005	Roberts et al. 2005	Swearingen et al. 2009	Bae, Oliva 2009 and 2012	Lin et al. 2012*	Adams et al. 2013**	Chowdhury et al. 2013	Nassif et al. 2015
Infrastructure considered	Bridge	Bridge	Pavement, Bridge	Pavement, Bridge	Bridge	Bridge	Pavement	Pavement, Bridge	Pavement, Bridge
Bridge Members	Girder	Girder	Girder, Deck	Girder	Girder, Deck	Deck	N.A.	Girder	Girder, Deck
WIM Involvement	No	Yes	No	No	No	No	No	Yes	Yes
Economic Analysis	No	No	Yes	Yes	Yes	Yes	Yes	Yes	Yes
LCCA Involvement	N.A.	N.A.	Yes	No	Yes	No	No	No	Yes
Cost Recovery	N.A.	N.A.	Yes	Yes	N.A.	No	Yes	Yes	Yes

* Investigate the deck only

** Report on practice review

Canada

1995- Fatigue Based Methodology for Managing Impact of Heavy-Permit Trucks on Steel Highway Bridges (Canada) ⁽¹⁷⁾

As one of earliest studies on this topic, Dicleli and Bruneau conducted research on the impact of heavy-permit trucks on steel highway bridges in 1995 ⁽¹⁷⁾. They investigated ultimate and cumulative effects of the overloads and found that the selected bridges had adequate ultimate capacity to accommodate the overweight. However, the cumulative fatigue damage was a concern for the large number of passing overweight trucks. In addition, the authors stated that the concept of infinite fatigue life cannot be relied on due to the involvement of overweight trucks and a reasonably large number of special permits could only cause a small reduction in fatigue life.

Arizona

2006- Estimating the Cost of Overweight Vehicle Travel on Arizona Highways ⁽¹¹³⁾

Straus and Semmens performed a study to quantify state highway damage on the basis of the impacts of overweight vehicles. They gave an estimate that overweight vehicles imposed uncompensated damages somewhere between \$12 million and \$53 million per year to Arizona roadway, including bridges and pavements.

New York State

2015- Effects of Overweight Vehicles on NYSDOT Infrastructure ⁽¹¹⁴⁾

Ghosn et al. performed a study to estimate the effect of different categories of overweight trucks on NYSDOT pavements and bridges. The results showed that trucks carrying divisible load permits cost \$50 million in damage to New York bridge infrastructure per year, trucks with special hauling permits cause \$2 million per year in additional costs, while illegally overweight trucks may be responsible for \$43 million per year, totaling \$95 million per year. For pavement network, the cost due to overweight trucks is about \$145 million per year, divided into \$78 million per year for divisible load permits, \$7 million per year for special hauling permits, and \$60 million per year for illegally overweight trucks.

Connecticut State

2004-Behavior of Steel Bridges under Superload Permit Vehicles ⁽¹⁸⁾

M.P. Culmo et al. presented a study on the behavior of selected steel bridges under specific superload permit trucks ⁽¹⁸⁾. The authors discussed six specific superload trailer types and their effect on bridges in terms of bridge span length, lateral load distribution, and dynamic load allowance. They obtained strain data from testing and compared this data to the response from structural analysis. The results showed that a conventional

line girder analysis can be employed with minor adjustments in assumption to analyze the effect of superloads on highway bridges, and impact can be taken as zero for trucks crossing at walking speed.

Indiana State

2005- Fatigue of Older Bridges Due to Overweight and Oversized Loads ⁽¹⁹⁾

In 2005, J.A. Reisert et al. reported a study on the fatigue of older bridges in Northern Indiana due to overweight and oversized loads ⁽¹⁹⁾. The authors collected field measurements of truck axle loads spectrum and bridge response. Both two dimensional and three dimensional models were built to predict the structural response under identified truck loads from WIM data. Based on the WIM database, new 3-axle and 4-axle fatigue trucks were developed, and a statistical database of resistance parameters was incorporated. Then remaining fatigue life was estimated for selected bridges on the heavy weight corridor.

Louisiana State

2005- Effects of Hauling Timber, Lignite Coal, and Coke Fuel on Louisiana Highways and Bridges ⁽²⁰⁾

F.L. Roberts et al. presented a study on the effect of overweight permitted vehicles hauling timber, lignite coal, and coke fuel on highway pavements and bridges ⁽²⁰⁾. They used three loading scenarios in the analysis, 80,000 lbs. (interstate weight limit), 86,600 lbs. (permit practice of the time), and 100,000 lbs. (proposed permit weight limit). They analyzed the identified highway routes and bridges on which commodities hauling take place, including approximately 1,400 control sections and 2,800 bridges. Results indicate that permit fees paid by timber trucks should increase from the current \$10 per year to around \$346/year/truck for a GVW of 86,600 lbs. when axles are equally loaded and \$4,377/year/truck if 48-kip axle load are permitted. The current permit fee for lignite coal should remain at current levels. The legislature should not consider raising the GVW level to 100,000 lbs. because the pavement overlay costs double over those at 86,600 lbs. GVW and the bridge repair costs become significant. In many cases, the bridge costs per passage of a loaded truck amount to \$8.90, meaning that the cost of bridge damage per truck per year can easily exceed \$3,560.

Ohio State

2009- Impacts of Permitted Trucking on Ohio's Transportation System and Economy ⁽²¹⁾

In 2009, Ohio Department of Transportation performed a study of the impacts of permitted trucking on Ohio's transportation system and economy ⁽²¹⁾. In the study, a three-tiered approach was employed for the pavements cost. The basic cost is shared by all users. Structural costs are shared by all trucks in accordance with their impact and overweight costs were attributed entirely to permitted vehicles. The resulting

allocations employing this method result in a \$122 million allocation to overweight vehicles annually. For bridges, the study used the incremental method to quantify the damage directly in dollar terms. The bridge impact costs total \$22 million annually. The annual trip and trip length were estimated as 24.8 annual trips of an average length of 98.8 mi. The calculated unit costs are \$0.05 per ESAL-mi plus \$0.008 per mi as shown in Table 2. Table 2 also lists the breakdown of each cost category considered. Both unit costs, ESAL-mi and mi cost, allocate three categories. For a permit cost calculation example, when looking specifically at the 5-axle trucks with the GVW was 113,006 lbs. which would produce nearly 17 ESALs and the trip length was 152 mi, the permit cost was \$129.20 (17 ESALs x 152 Mi x \$0.05 per ESAL mi) plus \$1.22 (152 mi x \$0.008 per mi), which is equal to \$130.42.

Table 2 - Unit cost summary from Ohio DOT ⁽²¹⁾

Cost Categories Allocated	ESAL-mi	Mi
(1) Load Bearing Damage (in Millions)	\$89.353	/
(2) 1" Overlay for Over Weight (in Millions)	\$29.274	/
(3) Bridge Asset Consumption (in Millions)	\$21.195	/
(4) Bridge (Millions)	/	\$0.860
(5)+(6) Pavement, VMT (Millions)	/	\$3.186
Total Annual (in Millions)	\$139.822	\$4.046
Total ESAL mi or Mi (in Millions)	2,785	523
Unit Cost	\$0.05	\$0.008
Expenses Considered		
(1) Load bearing structural pavement thickness		
(2) Additional 1.0" pavement thickness due to overweight trucks		
(3) Bridge Asset Consumption		
(4) Bridge Preservation Cost		
(5) 3.0" minimum pavement thickness and 6.0" aggregate		
(6) 2.0" overlays		

Wisconsin State

2009 and 2012- Bridge Analysis and Evaluation of Effects under Overload Vehicles-Phase I and II ^(22, 23)

H. Bae and M. Oliva initiated the evaluation of bridges under overload vehicles in 2009; the first phase was mainly focused on the structural analysis of bridges under the overweight trucks ^(22, 23). They developed finite element models of 118 multi-girder bridges and performed 16 load cases of overload vehicles for each multi-girder bridge. Afterward, they proposed the girder distribution factor equations for multi-girder bridges

under overload vehicles and found that intermediate diaphragms under overload vehicles are not a concern. As an extension of first phase, the authors aimed in evaluating the long-term cost impact of vehicles on bridges with life cycle cost analysis. Finally, they investigated the long-term behavior of concrete decks and steel girder bridges, then developed a means to assign cost to the overloads.

2012- Impact of Overweight Vehicles on Bridge Deck Deterioration ⁽²⁴⁾

Many researchers have stated that the deterioration of bridge decks is a complicated results of different failure modes, such as corrosion, fatigue, global or local flexural crack and so on. Z. Lin et al. from University of Wisconsin-Milwaukee performed an investigation of the impact of overweight trucks on bridge deck deterioration using laboratory tests and numerical simulations ⁽²⁴⁾. The laboratory tests simulated the combined effect of mechanical stresses and freeze-thaw cycles on concrete cylinders and the results confirmed that the mechanical loading combined with freeze-thaw cycles significantly increased the permeability of air-entrained concrete and may accelerate the deterioration of concrete elements such as bridge decks. The numerical simulation of bridge decks analyzed the stress level in both transverse and longitudinal direction. In addition, they proposed empirical equations to predict the stress under heavy wheel load.

2013-Aligning Oversize/Overweight Permit Fees with Agency Costs: Critical Issues ⁽²⁵⁾

T. Adams et al. performed a review of current permitting practice from different states, and fee structure ⁽²⁵⁾. The preliminary trends for overweight and oversize demands in the foreseeable future were outlined and the different infrastructure impacts of OSOW loads were documented, such as pavement, bridge, safety, congestion, and environment. At last, they proposed a methodology to quantify the cost but it was without validation.

South Carolina State

2013- Rate of Deterioration of Bridges and Pavements as Affected by Trucks ⁽²⁶⁾

The Clemson University group analyzed the rate of deterioration of bridges and pavements affected by trucks for the South Carolina DOT ⁽²⁶⁾. They evaluated the effect of overweight trucks and super-load trucks. The cost for bridges consisted of annual bridge fatigue damage costs for superstructure (girders only) and annual bridge maintenance costs (data obtained from DOT). The unit cost directly from the report is shown in Table 3. Table 4 shows the transformed unit cost in dollar per mi per ton.

Table 3 - Overweight damage for South Carolina ⁽²⁶⁾

Truck Type	Bridge (Per Mi)			Pavement (Per Mi)			Combine Pavement and Bridge (Per Mi)		
	A	B	C	A	B	C	A	B	C
2-axle, 35-40 kips	\$0.0040	\$0.0058	\$0.0018	\$0.35	\$0.67	\$0.32	\$0.3522	\$0.6748	\$0.3225
3-axle, single unit, 46-50 kips	\$0.0062	\$0.0075	\$0.0013	\$0.24	\$0.39	\$0.14	\$0.2475	\$0.3933	\$0.1459
3-axle, combination, 50-55 kips	\$0.0075	\$0.0094	\$0.0020	\$0.44	\$0.74	\$0.30	\$0.4443	\$0.7444	\$0.3002
4-axle, single unit, 63.5-65 kips	\$0.0061	\$0.0067	\$0.0006	\$0.35	\$0.45	\$0.10	\$0.3585	\$0.4601	\$0.1016
4-axle, combination, 65-70 kips	\$0.0067	\$0.0092	\$0.0025	\$0.48	\$0.82	\$0.33	\$0.4885	\$0.8247	\$0.3363
5-axle, 80-90 kips	\$0.0074	\$0.0111	\$0.0037	\$0.45	\$0.83	\$0.38	\$0.4583	\$0.8421	\$0.3838
6-axle, 80-90 kips	\$0.0101	\$0.0139	\$0.0038	\$0.25	\$0.43	\$0.18	\$0.2585	\$0.4408	\$0.1823
6-axle, 90-100 kips	\$0.0101	\$0.0191	\$0.0090	\$0.25	\$0.66	\$0.42	\$0.2585	\$0.6835	\$0.4250
6-axle, 100-110 kips	\$0.0101	\$0.0262	\$0.0161	\$0.25	\$0.99	\$0.74	\$0.2585	\$1.0124	\$0.7539
7-axle, 80-90 kips	\$0.0115	\$0.0152	\$0.0037	\$0.13	\$0.24	\$0.11	\$0.1428	\$0.2556	\$0.1128
7-axle, 90-100 kips	\$0.0115	\$0.0201	\$0.0087	\$0.13	\$0.38	\$0.24	\$0.1428	\$0.3955	\$0.2528
7-axle, 100-110 kips	\$0.0115	\$0.0267	\$0.0152	\$0.13	\$0.56	\$0.43	\$0.1428	\$0.5880	\$0.4452
7-axle, 110-120 kips	\$0.0115	\$0.0354	\$0.0239	\$0.13	\$0.81	\$0.68	\$0.1428	\$0.8440	\$0.7012
7-axle, 120-130 kips	\$0.0115	\$0.0469	\$0.0355	\$0.13	\$1.13	\$0.99	\$0.1428	\$1.1729	\$1.0302
8-axle, 80-90 kips	\$0.0121	\$0.0157	\$0.0036	\$0.10	\$0.18	\$0.08	\$0.1140	\$0.2005	\$0.0865
8-axle, 90-100 kips	\$0.0121	\$0.0204	\$0.0083	\$0.10	\$0.29	\$0.18	\$0.1140	\$0.3059	\$0.1919
8-axle, 100-110 kips	\$0.0121	\$0.0265	\$0.0144	\$0.10	\$0.44	\$0.34	\$0.1140	\$0.4668	\$0.3529
8-axle, 110-120 kips	\$0.0121	\$0.0344	\$0.0223	\$0.10	\$0.62	\$0.51	\$0.1140	\$0.6497	\$0.5358
8-axle, 120-130 kips	\$0.0121	\$0.0446	\$0.0325	\$0.10	\$0.86	\$0.76	\$0.1140	\$0.9029	\$0.7890

Note:

A: Per mi Damage for a Truck Loaded at the Legal Weight Limit

B: Per mi Damage for an Overweight Truck Loaded up to the Maximum Overweight Limit

C: Additional per mi Damage for an Overweight Truck above the Legal Weight limit up to the Maximum Overweight Limit

Table 4 - Transformed unit cost for South Carolina ⁽²⁶⁾

Truck Type	Bridge (per Mi Per Ton)	Pavement (per Mi Per Ton)	Combine (per Mi Per Ton)
	C	C	C
2-axle, 35-40 kips	\$0.00009000	\$0.01603500	\$0.01612500
3-axle, single unit, 46-50 kips	\$0.00005200	\$0.00578400	\$0.00583600
3-axle, combination, 50-55 kips	\$0.00007273	\$0.01084364	\$0.01091636
4-axle, single unit, 63.5-65 kips	\$0.00001846	\$0.00310769	\$0.00312615
4-axle, combination, 65-70 kips	\$0.00007143	\$0.00953714	\$0.00960857
5-axle, 80-90 kips	\$0.00008222	\$0.00844667	\$0.00852889
6-axle, 80-90 kips	\$0.00008444	\$0.00396667	\$0.00405111
6-axle, 90-100 kips	\$0.00018000	\$0.00832000	\$0.00850000
6-axle, 100-110 kips	\$0.00029273	\$0.01341455	\$0.01370727
7-axle, 80-90 kips	\$0.00008222	\$0.00242444	\$0.00250667
7-axle, 90-100 kips	\$0.00017400	\$0.00488200	\$0.00505600
7-axle, 100-110 kips	\$0.00027636	\$0.00781818	\$0.00809455
7-axle, 110-120 kips	\$0.00039833	\$0.01128833	\$0.01168667
7-axle, 120-130 kips	\$0.00054615	\$0.01530308	\$0.01584923
8-axle, 80-90 kips	\$0.00008000	\$0.00184222	\$0.00192222
8-axle, 90-100 kips	\$0.00016600	\$0.00367200	\$0.00383800
8-axle, 100-110 kips	\$0.00026182	\$0.00615455	\$0.00641636
8-axle, 110-120 kips	\$0.00037167	\$0.00855833	\$0.00893000
8-axle, 120-130 kips	\$0.00050000	\$0.01163846	\$0.01213846

Note:

C: Additional per mi Damage for an Overweight Truck above the Legal Weight limit up to the Maximum Overweight Limit

Deterioration Model for Highway Bridges

In this part, the deterioration models for bridge deck and girders are reviewed in regards to the long-term behavior of highway bridges.

Weight Regulations

Bridges on the Interstate Highway System were designed to carry a wide variety of vehicles and their expected loads. However, in 1950s and later, as the tradeoff between concerns over the deterioration of existing bridge infrastructure and the pressure of increasing truck weight limitations from the trucking industry became prominent, the weight-to-length ratio of a vehicle crossing a bridge was limited by the Bridge Formula shown in (1), which was enacted by Congress in 1975. This was introduced as a program called “Federal-Aid Highway Act”, which restricted the gross vehicle weight and the weights of different axle types. In addition to Bridge Formula weight limits, the Federal law limited single axles to 20,000 lbs., tandem axles (axles closer than 96 in apart) to 34,000 lbs., and gross vehicle weight to 80,000 lbs. This formula was calibrated to keep girder overstressing of HS20 bridges under 5 percent and of HS15 bridges under 30 percent.

$$W = 500 \times [LN/(N-1)+12N+36] \quad (1)$$

where

W = the overall gross weight on any group of two or more consecutive axles to the nearest 500 lbs.;

L = the distance in ft. between the outer axles of any group of two or more consecutive axles; and

N = the number of axles in the group under consideration.

Federal Highway Administration (FHWA) developed another weight formula shown in (2), called TTI formula. The formula has the same criterion as Bridge Formula. The formula is given as:

$$\begin{aligned} W &= 34000+1000L && \text{For } L < 56 \text{ ft.} \\ W &= 62000+500L && \text{For } L > 56 \text{ ft.} \end{aligned} \quad (2)$$

In 1990, TRB proposed a modification on the TTI formula that reduced the limits on axle loads while allowing higher gross weights. This modified TTI formula only limits the stress of HS20 bridges and not HS15 bridges. The formula is given as:

$$\begin{aligned}
 W &= 26000 + 2000L && \text{For } L < 23 \text{ ft.} \\
 W &= 62000 + 500L && \text{For } L > 23 \text{ ft.}
 \end{aligned}
 \tag{3}$$

As demonstrated in Figure 2, the TTI formula allows higher weights for short vehicles, and tandem and tridem axle groups compared to the Bridge Formula. For longer vehicles, however, the TTI formula allows smaller GVWs than Bridge Formula. The modified TTI formula has higher limitations than TTI formula when vehicles or axle group longer than 8 ft.

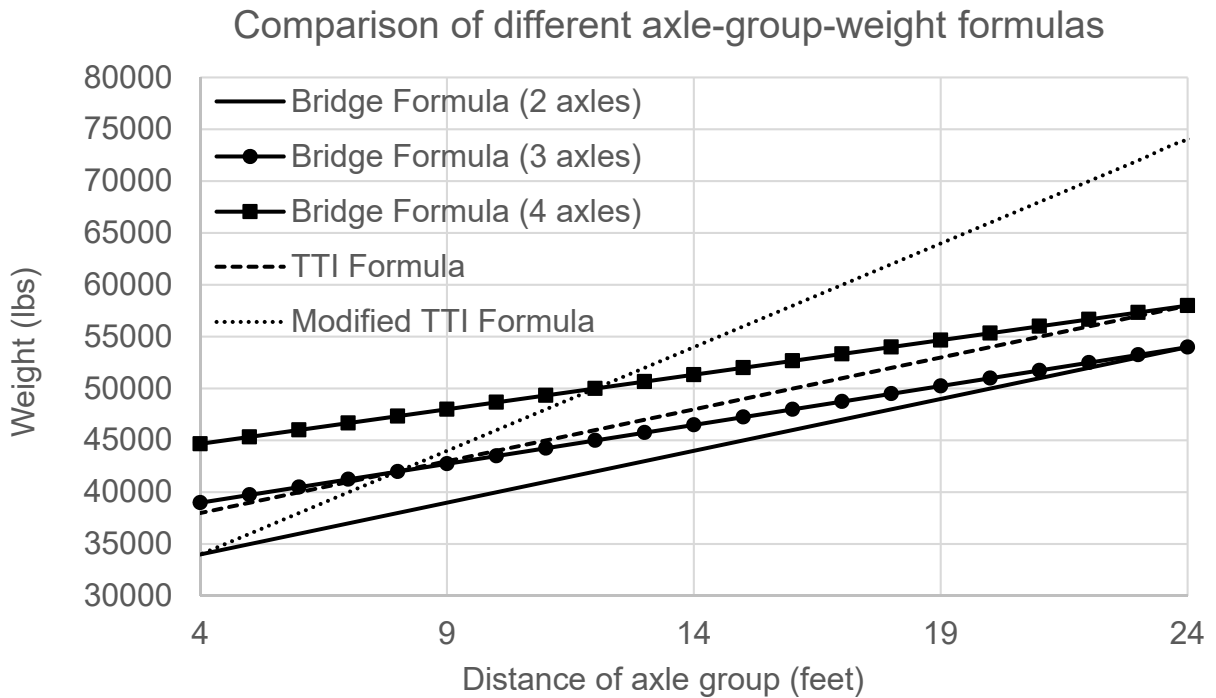


Figure 2. Comparison of different axle-group-weight formulas

In New Jersey, the vehicle dimensional and weight limitations is stated in New Jersey Statutes Annotated (N.J.S.A) 39:3-84. All oversize and overweight permits are governed by Rules and Regulations promulgated by the Chief Administrator, NJ Motor Vehicle Commission at N.J.A.C. 13:18-1.1, et seq. A table of maximum gross weight in New Jersey is provided as listed in Table 5. From the table, the weight limitations in New Jersey follow the Bridge Formula.

Table 5 - Table of Maximum Gross Weights (lbs.) in New Jersey (N.J.S.A. 39:3-84)

Length(ft.)	2 axles	3 axles	4 axles	5 axles	6 axles	7 axles
3	22400	22400	22400	22400	22400	22400
4	34000	34000	34000	34000	34000	34000
5	34000	34000	34000	34000	34000	34000
6	34000	34000	34000	34000	34000	34000
7	34000	34000	34000	34000	34000	34000
8	34000	34000	34000	34000	34000	34000
9	39000	42500	42500	42500	42500	42500
10	40000	43500	43500	43500	43500	43500
11	41000	44000	44000	44000	44000	44000
12	42000	45000	50000	50000	50000	50000
13	43000	45500	50500	50500	50500	50500
14	44000	46500	51500	51500	51500	51500
15	44800	47000	52000	52000	52000	52000
16	44800	48000	52500	58000	58000	58000
17	44800	48500	53500	58500	58500	58500
18	44800	49500	54000	59000	59000	59000
19	44800	50000	54500	60000	60000	60000
20	44800	51000	55500	60500	66000	66000
21	44800	51500	56000	61000	66500	66500
22	44800	52500	56500	61500	67000	67000
23	44800	53000	57500	62500	68000	68000
24	44800	54000	58000	63000	68500	74000
25	44800	54500	58500	63500	69000	74500
26	44800	55500	59500	64000	69500	75000
27	44800	56000	60000	65000	70000	75500
28	44800	57000	60500	65500	71000	76500
29	44800	57500	61500	66000	71500	77000
30	44800	58500	62000	66500	72000	77500
31	44800	59000	62500	67500	72500	78000
32	44800	60000	63500	68000	73000	78500
33	44800	60500	64000	68500	74000	79000
34	44800	61500	64500	69000	74500	80000
35	44800	62000	65500	70000	75000	80000
36	44800	63000	66000	70500	75500	80000
37	44800	63500	66500	71000	76000	80000
38	44800	64500	67500	71500	77000	80000
39	44800	65000	68000	72500	77500	80000
40	44800	66000	68500	73000	78000	80000

Length(ft.)	2 axles	3 axles	4 axles	5 axles	6 axles	7 axles
41	44800	66500	69500	73500	78500	80000
42	44800	67200	70000	74000	79000	80000
43	44800	67200	70500	75000	80000	80000
44	44800	67200	71500	75500	80000	80000
45	44800	67200	72000	76000	80000	80000
46	44800	67200	72500	76500	80000	80000
47	44800	67200	73500	77500	80000	80000
48	44800	67200	74000	78000	80000	80000
49	44800	67200	74500	78500	80000	80000
50	44800	67200	75500	79000	80000	80000
51	44800	67200	76000	80000	80000	80000
52	44800	67200	76500	80000	80000	80000
53	44800	67200	77500	80000	80000	80000
54	44800	67200	78000	80000	80000	80000
55	44800	67200	78500	80000	80000	80000
56	44800	67200	79500	80000	80000	80000
57	44800	67200	80000	80000	80000	80000
58	44800	67200	80000	80000	80000	80000
59	44800	67200	80000	80000	80000	80000
60	44800	67200	80000	80000	80000	80000
61	44800	67200	80000	80000	80000	80000
62	44800	67200	80000	80000	80000	80000
63	44800	67200	80000	80000	80000	80000
64	44800	67200	80000	80000	80000	80000
65	44800	67200	80000	80000	80000	80000
66	44800	67200	80000	80000	80000	80000
67	44800	67200	80000	80000	80000	80000
68	44800	67200	80000	80000	80000	80000
69	44800	67200	80000	80000	80000	80000
70	44800	67200	80000	80000	80000	80000

Deterioration of Bridge Decks

The bridge deck is a bridge component that usually undergoes more deterioration than any other component due to its direct exposure to heavy and more frequent truck traffic, environmental conditions, and de-icing salts. Therefore, measuring the deterioration of bridge decks can be quite complicated. Previous studies have demonstrated that transverse cracks and water penetration during service decreased the ultimate punching shear and fatigue strengths of the concrete decks ^(27, 28, 29). However, the interaction between the deck deterioration and the overweight loading were not quantified explicitly. The current AASHTO Manual for Bridge Evaluation indicates that the de-icing salts and truck traffic volume affect the deck deterioration rate, but the evaluation of bridge decks is limited to visual inspections only ⁽³⁰⁾. In reality, a combination of mechanical loading and environmental factors would lead to the end of service life.

Moreover, due to the increasing truck traffic both in weight and frequency on the highway network, there is a need to correlate the effect of overweight trucks with concrete deck deterioration. Figure 3 shows the changes of ADTT over years on I-195 (Site 195) and I-287 (Site 287) as well as the deterioration curve of a bridge deck near Site 195. It shows that while ADTT is increasing over the 20 years, the bridge deck rating is decreasing over the same period. This study, which is part of an ongoing project sponsored by the NJDOT, was performed to evaluate the relationship between overweight trucks and the accumulated damage they would cause on concrete decks.

Deck Deterioration from Mechanical Loading

Previous studies indicated fatigue and overstressing are the two major problems caused by mechanical loading and found that fatigue and overstressing are two possible deterioration modes that are independent phenomena ^(31, 32, 33). Starting from late 1970s, laboratory tests were performed to investigate the failure modes of reinforced concrete decks as a whole. The test results showed that the fatigue of reinforced concrete deck is governed by the punching shear failure of concrete ^(33, 34, 35). It was also noted that during experimental tests, both the simulation of axle loads and simulation of the boundary conditions are the two most important factors (see references 28, 29, 32 and 33). The stationary pulsating load simulation did not yield the cracking pattern observed in the field and overestimated the fatigue life. It was concluded that the moving wheel load simulation was better in correlating with field conditions. From available test data, all the fatigue models for bridge decks yielded models such as in (4) which was conservative in predicting the fatigue life for orthotropic concrete decks. Since the rear

wheel usually has dual tires with a print of 20 inch by 8 inch while steering wheel is usually a single tire, the value for steering wheel weight was increased by 1/0.67.

$$\log(P/P_u) = a - b \log(N_{pf})$$

$$P = \left(\sum f_i(p_i) \times p_i^{17.95} \right)^{1/17.95}$$
(4)

where

P_u is the ultimate strength of the deck, N_{pf} is the number of cycles to failure,

a and b are the parameters of regression line,

P is the equivalent wheel load from wheel weight distribution,

p_i is the value of wheel weight (kips) in wheel weight distribution, and

$f_i(p_i)$ is the frequency for that weight.

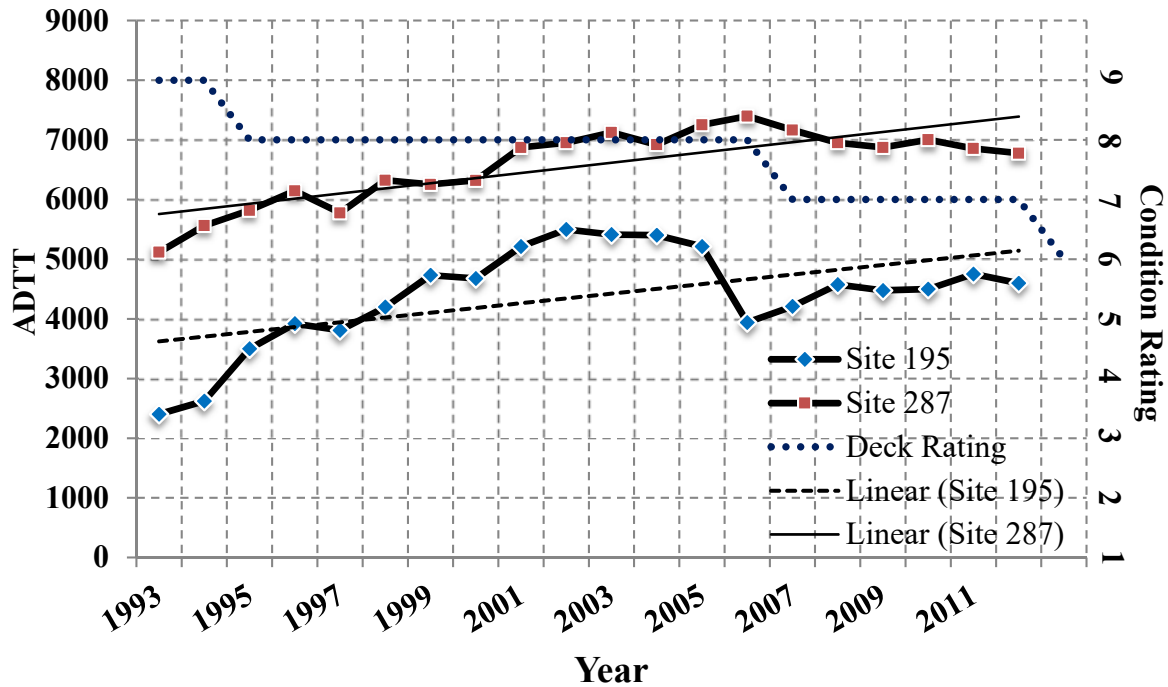


Figure 3. ADTT of interstate highway and deck deterioration

Overstressing of bridge decks is described as the susceptibility of the bridge deck to cracking under the effect of truck loads. A recent study investigated the impact of overweight vehicles on bridge deck deterioration based on the combined effect of overstressing and freeze-thaw⁽³⁶⁾. Laboratory tests were also performed to evaluate the freeze-thaw cycles on the durability of concrete under mechanical loading. Additionally, numerical simulations were conducted to estimate the stress level of RC decks under overweight vehicle with heavy axle loads. Empirical equations were proposed to calculate the stress of deck concrete subjected to overweight trucks as follows:

$$\begin{aligned}\sigma_x &= \frac{3pS}{t^2(S+12)} \\ \sigma_z &= \sigma_{z0} + \frac{6pS}{5t^2(S+12)}\end{aligned}\tag{5}$$

where

σ_x is the transverse stress;

σ_z is the longitudinal stress;

σ_{z0} is the initial longitudinal stress;

p is wheel load;

S is the girder spacing; and

t is the thickness of deck slab.

Deck Deterioration from Environmental Factors

Experience has demonstrated that highway bridges are vulnerable to damage from environmental attack, such as corrosion, freeze-thaw and alkali-silica reaction.

The corrosion of the reinforced concrete deck will lead to a reduction in the cross-sectional area of the reinforcing steel or loss of bond, which may further lead to the loss of strength and unserviceability. Various models of this type of failure are developed based on the mechanism of the diffusion of chlorides through the protective concrete cover, showing that the corrosion will be initiated once the chloride concentration exceeds a threshold (see references 37, 38, 39 and 40).

Deterioration of Bridge Girders

The increase in legal truck weight would shorten the time for repair or replacement of many bridges. Yoder et al. (1979) investigated the impact of a GVW limit increase for Indiana DOT including those on bridges⁽⁶⁾. The following cost impacts were included in this effort for bridges: (a) strength related costs, (b) steel fatigue-related costs, and (c) deck deterioration costs. The strength-related costs refer to inadequate load carrying capacity of bridges under the new permissible load. The steel fatigue-related costs were also estimated to be negligibly small, based on the data available at the time. Impact costs associated with bridge deck deterioration were estimated using an assumption that cost increase is linearly related to the maximum permitted GVW. This study represents an early effort in this area.

NCHRP Report 495 (2003) proposed a recommended methodology for estimating the impact of changes in truck weight limits on bridge network costs⁽⁴¹⁾. Step-by-step instructions for applying the methodology were included in the report along with detailed application of the methodology. Four cost-impact categories are covered in the methodology: 1) Fatigue of existing steel bridges, 2) Fatigue of existing RC decks, 3) Deficiency due to overstress for existing bridges, and 4) Deficiency due to overstress for new bridges. The fatigue life evaluation procedure is the core part of the procedure.

In 1985, NCHRP Project 12-28, "Fatigue Evaluation Procedures for Steel Bridges", was initiated. The goal of the principle investigators, Moses, Schilling, and Raju, was to develop fatigue design procedures that more accurately reflect fatigue-loading conditions. Probabilistic techniques were employed to ensure consistent levels of reliability. There has been extensive work done on field-testing of bridges to determine remaining fatigue life. For the most part, the investigator installs strain gages to key fatigue prone detail locations on a bridge structure and monitors strain/stress levels for a given period of time. The cumulative damage is calculated based on Miner's Rule, and along with the ADTT for the location, the fatigue life is calculated based on the recommendations of Moses et al, 1987⁽⁴²⁾. The remaining fatigue life is simply the total life less the current service life of the structure.

Nowak, Nassif, and Frank (1993) published the findings of a fatigue evaluation of a steel bridge⁽⁴³⁾. The bridge under study was instrumented to determine the remaining fatigue life. Strain gages were installed such that fatigue critical members were monitored. Additionally, all girders in one span were instrumented to determine the load distribution. This was found to be crucial to understanding the actual vs. assumed load distribution. Analytical results showed high stresses in the exterior girders, making those

members most fatigue critical. However, the measured stresses were much less than the calculated stresses. Sensors indicated that the connection of the floor beams to the exterior girder was behaving like a fixed moment connection. Furthermore, the floor beam was responding as a beam fixed against rotation but undergoing a relative displacement between the supports at the exterior and first interior girders.

This fatigue study provided a more complete analysis, given the calibration runs and information on truck superposition, and also provided an important contribution to the state of the art for fatigue study of bridges. The major steps proposed are roughly consistent with those proposed in Task 3.

Remaining fatigue life estimation is the most challenging part of this project for bridges. The fatigue analysis should follow The Manual For Bridge Evaluation (2011) and AASHTO Specifications (2012) to be consistent with current practice ^(44, 45).

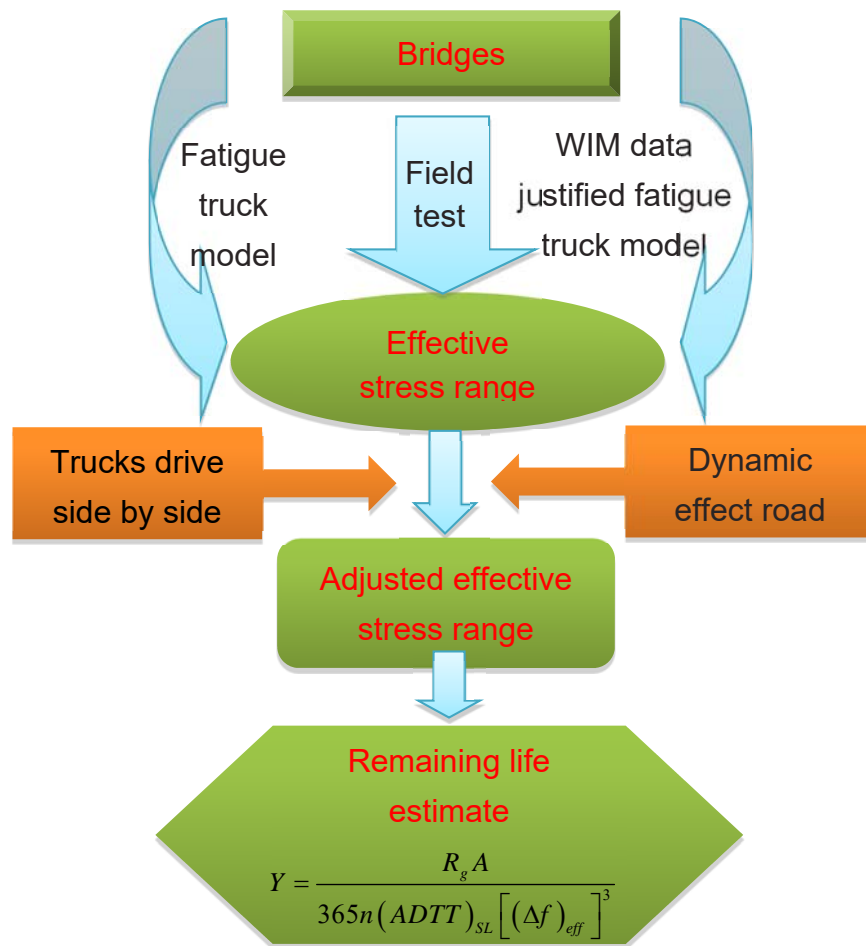


Figure 4. Flow chart of fatigue evaluation process for bridges

Fatigue Evaluation

Fatigue is a mode of failure whereby a crack develops and propagates within metal under loads that are less than the design ultimate strength of the structure. The ASTM definition: “The process of progressive localized permanent structural change occurring in a material subjected to conditions which produce fluctuating stresses and strains at some point or points and which may culminate in cracks or complete fracture after a sufficient number of fluctuations” (ASTM E206-72)⁽⁴⁶⁾.

Fatigue failures were noted by engineers as early as 1829 (Munse 1990)⁽⁴⁷⁾. This phenomenon was studied in conveyor chains used in coal mines by Albert in 1837 (Schutz 1996)⁽⁴⁸⁾. A more notable researcher in fatigue was Wohler. He developed deflection gages for in-service monitoring to study why railcar axles were failing in 1858. He developed one of the earliest “safe-life” approaches to fatigue design, stating that if bearings were designed for 200,000 mi of service, then the fatigue life of the axles should be designed likewise.

The S-N Diagram

The fatigue resistance of a structure depends on the loading level (stress range) and the frequency of loading. The relationship between stress ranges and loading cycles is often shown using a S-N or Wohler plot, Figure 5⁽⁴⁷⁾.

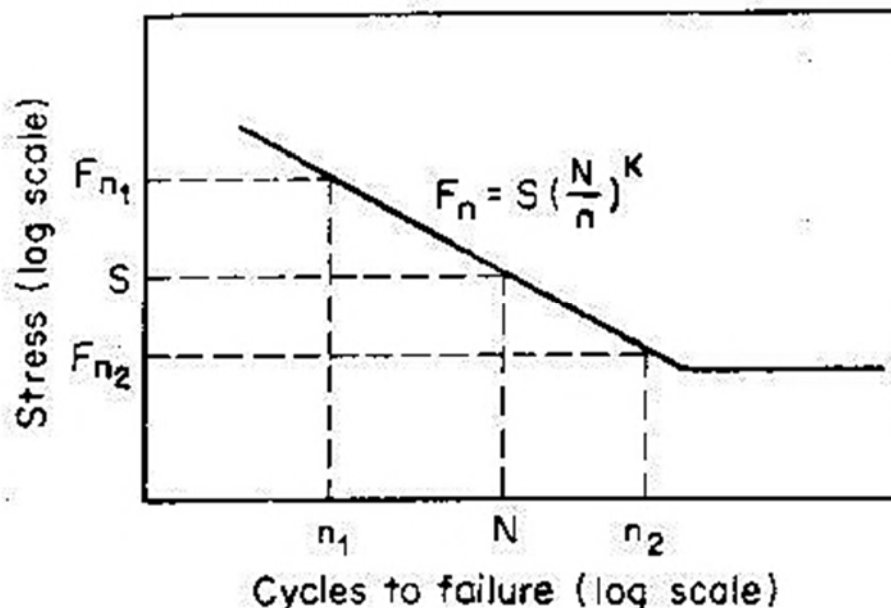


Figure 5. Typical S-N curve⁽⁴⁷⁾

The scale of the S-N plot is log-log to show the ultimate number of cycles to failure, often greater than 2,000,000. Additionally, the horizontal line to the right of the abscissa represents the stress level of infinite life. At this level the metal element can theoretically endure an infinite number of cycles without propagating a fatigue crack. The S-N curves vary by type of metal and also by geometry of the element. For example, notched or corroded elements will fail under much lower loads and a fewer number of cycles.

Effective Stress

The effective stress, also nominal stress, of a load history is defined as a stress that causes the same amount of fatigue damage as the actual load history for the given number of cycles. The equation, Miner's Law (root mean cube stress), is given as:

$$S_r = \left(\sum f_i S_{ri}^3 \right)^{1/3} \quad (6)$$

where

f_i =the fraction of stress ranges at level i ;

S_{ri} =the stress range magnitude of interval i ; and

S_r =effective stress range.

Extensive laboratory testing has proven Miner's Rule is applicable to bridge members (Schilling 1978)⁽⁴⁹⁾. When calculating the effective stress, a minimum sufficient number of cycles should be present to avoid falsely high effective stresses from a few high range cycles.

There is no consensus among fatigue researchers as to how to calculate the effective stress from an observed experimental record. Field data includes many low range stress cycles due to sensor noise and vibration. These minute cycles cause a negligible contribution to the fatigue damage. Rainflow processing modes within data acquisition systems offer a lower threshold below which cycles are omitted. The choice threshold has an influence on the value of the effective stress. Since effective stress is calculated as a root-mean-cube weighted average, a large number of minute stress cycles cause a significant drop in the calculated effective stress. Fisher et al. (1998) recommends taking a lower cutoff such that the number of observed stress cycles approximately equals the average daily truck traffic at the bridge location⁽⁵⁰⁾.

Cumulative Damage Estimation

Multiple laboratory test specimens subject to repeated loading cycles at constant amplitudes are used to generate these S-N curves. However, the loading patterns of actual structures contain random variable amplitude stress cycles. Therefore, a means to find an equivalent damage accumulation is needed. The linear cumulative damage rule, or the Palmgren-Miner Rule, herein referred to as Miner's Rule, is used to relate variable amplitude behavior to constant amplitude behavior (Miner 1945)⁽⁵¹⁾. The failure criterion is defined as when the damage reaches unity. Miner's Rule, in its simplest form, is given as:

$$\sum_i \frac{n_i}{N_i} = \frac{n_1}{N_1} + \frac{n_2}{N_2} + \frac{n_3}{N_3} + \dots = 1 \quad (7)$$

where

n_i = number of stress cycles at level σ_i ; and

N_i = number of stress cycles to produce failure at σ_i .

The damage caused by a load history is not immediately clear from the number of cycles or the maximum stress range. In other words, the most damaging load history is not necessarily the one with the highest number of cycles. The most damaging load history is most likely the history that contains a large number of mid-to-high range cycles (Socie and Pompetzki 2004)⁽⁵²⁾. Therefore, it is critical that the cumulative damage method be applied to normalize each load history for comparison.

Current AASHTO LRFD Fatigue Design

AASHTO LRFD Specifications (2012) categorized fatigue as load- and distortion-induced fatigue⁽⁴⁵⁾. Distortion-induced fatigue often occurs in the web at a welded connection plate near a flange when proper detailing practices are not followed. This will not provide a rigid load path to transmit force in the transverse member and develop significant secondary stresses that induce fatigue crack (Fisher et al. 1990)⁽⁵³⁾.

Distortion induced stresses cause cracking very early into service of bridges with vulnerable details. The resulting stresses can be as high as 30 ksi in the web gap. Distortion prone details are often the result of designers' desire to avoid welding transverse stiffeners to tension flanges. Another example are the gusset plates welded to tension portions of webs to connect lateral bracing members. The cause of distortion is often unanticipated secondary bending or vibration of lateral bracing (Moses 1987)⁽⁴²⁾. Distortion induced fatigue is difficult to model since it depends heavily on the

specific detail and loading conditions. Therefore, this type of fatigue cracking is not easily predicted using the current code provisions. Field testing must be done to measure out-of-plane displacements and stress concentrations at vulnerable details.

For load-induced fatigue considerations, the force effect considered shall be the live load stress range. For each components and details specified in Table 6.6.1.2.3-1 of AASHTO LRFD Specifications, the following equation shall be satisfied ⁽⁴⁵⁾:

$$\gamma(\Delta f) \leq (\Delta F)_n \quad (8)$$

where

γ is the load factor for fatigue load combination;

(Δf) is the force effect, live load stress range due to the passage of the fatigue load in ksi; and

$(\Delta F)_n$ is the nominal fatigue resistance.

The fatigue resistance is defined as:

$$(\Delta F)_n = \left(\frac{A}{N} \right)^{\frac{1}{3}} \geq \frac{1}{2} (\Delta F)_{TH} \quad (9)$$

where

$N = (365)(75)n(\text{ADTT})_{SL}$;

A = detail category constant;

n = number of stress range cycles per fatigue truck passage;

$(\text{ADTT})_{SL}$ = single-lane ADTT; and

$(\Delta F)_{TH}$ = constant-amplitude fatigue threshold (AASHTO 2010 6.6.1.2.5).

The current code, as with the previous AASHTO code, and the American Welding Society (AWS) code, specify detail categories for welded and bolted connections (Table 6). The categories are denoted by letter and include: A, B, B', C, D, D', E, and E'. Category A details include rolled beam sections and are considered the most fatigue resistant details. Category E', however, are the most susceptible to fatigue damage and include longitudinally loaded fillet-welded attachments.

Table 6 - Fatigue detail constant, A, by category $\times 10^7$ (AASHTO LRFD 2010 Table 6.6.1.2.5-1)

Detail Category	Constant, A, $\times 10^8$
A	250.0
B	120.0
B'	61.0
C	44.0
C'	44.0
D	22.0
E	11.0
E'	3.9

Table 7 - Constant amplitude fatigue threshold by category (AASHTO LRFD 2010 Table 6.6.1.2.5-3)

Detail Category	Threshold (ksi)
A	24.0
B	16.0
B'	12.0
C	10.0
C'	12.0
D	7.0
E	4.5
E'	2.6

Table 8 - Cycles per truck passage, n (AASHTO LRFD 2010 Table 6.6.1.2.5-2)

Longitudinal Members	Span Length	
	>40 ft.	<40ft
Simple Span Girders	1.0	2.0
Continuous Girders		
1) near interior support	1.5	2.0
2) elsewhere	1.0	2.0
Cantilever Girder	5.0	
Trusses	1.0	
Transverse Members	Spacing	
	>20ft	<20ft
	1.0	2

The fatigue design is based on a single lane loaded. Therefore, the average daily truck traffic is used for determination of fatigue loading. Multiple truck loading is considered rare (Moses 1987)⁽⁴²⁾. Special provisions are given for cases when multiple truck situations may occur. For example, bunching of trucks may occur on a bridge near traffic signals or uphill on two or more lane bridge. For these cases, a 15 percent increase in fatigue truck weight is prescribed.

Current Fatigue Evaluation

The current evaluation provisions for highway bridges are set forth in the American Association of State Highway Officials (AASHTO) The Manual for Bridge Evaluation (MBE 2011)⁽⁴⁵⁾. The current methodology was the recommendation of Bowman, Fu, Zhou, Connor and Godbole as part of the NCHRP Report 721, “Fatigue Evaluation of Steel Bridges”⁽⁴²⁾. The principle inputs for fatigue design are the average daily truck traffic, percentage of truck traffic, and connection detail category.

The manual identifies two levels of fatigue evaluation: the infinite-life check and the finite-life calculations. The bridge details are subject to the more complex finite-life fatigue evaluation when they fail the infinite-life check.

Step 1: Estimating stress ranges

The calculated effective stress range shall be estimated as

$$(\Delta f)_{eff} = R_s \Delta f \quad (10)$$

where

R_s = The stress range estimate partial load factor, calculated as $R_{sa}R_{st}$, unless otherwise specified; and

Δf = Measured effective stress range, or 75 percent of the calculated stress range due to the passage of the fatigue truck as specified in LRFD Design Article 3.6.1.3, or a fatigue truck determined by a truck survey or weight-in-motion study.

Due to the uncertainty in the calculation of effective stress range at a particular fatigue detail including both uncertainty associated with analysis, represented by the analysis partial load factor, R_{sa} , and uncertainty associated with assumed effective truck weight represented by the truck-weight partial load factor, R_{st} . The values of partial load factors are listed in Table 9.

Table 9 - Partial load factors: R_{sa} , R_{st} , and R_s ⁽⁴⁷⁾

Fatigue-Life Evaluation Methods	Analysis Partial Load Factor, R_{sa}	Truck-Weight Partial Load Factor, R_{st}	Stress-Range Estimate Partial Load Factor, R_s^a
For Evaluation or Minimum Fatigue Life			
Stress range by simplified analysis, and truck weight per LRFD Design Article 3.6.1.4	1.0	1.0	1.0
Stress range by simplified analysis, and truck weight estimated through weigh-in-motion study	1.0	0.95	0.95
Stress range by refined analysis, and truck weight per LRFD Design Article 3.6.1.4	0.95	1.0	0.95
Stress range by refined analysis, and truck weight by weigh-in-motion study	0.95	0.95	0.90
Stress range by field-measured strains	N/A	N/A	0.85
For Mean Fatigue Life			
All methods	N/A	N/A	1.00

The effective stress range may be estimated through field measurements of strains at the fatigue-prone detail under consideration under typical traffic condition. The effective stress range shall be taken as the cube root of the sum of the cubes of the measured stress ranges, as given in:

$$(\Delta f)_{eff} = R_s \left(\sum \gamma_i \Delta f_i^3 \right)^{\frac{1}{3}} \quad (11)$$

where

γ_i = Percentage of cycles at a particular stress range; and

Δf_i = The particular stress range.

When field-measured strains are used to generate an effective stress range, R_s , for the determination of evaluation or minimum fatigue life, the stress-range estimate partial load factor shall be taken as 0.85. When field-measured strains are used to generate an effective stress range, R_s , for the determination of mean fatigue life, the stress-range estimate partial load factor shall be taken as 1.0.

Step 2: Determination of fatigue-prone details

Bridge details are only considered to be prone to load induced fatigue damage if they are experiencing a net tensile stress. Therefore, fatigue evaluation is needed only if:

$$2 R_s (\Delta f)_{tension} > f_{dead-load\ compression} \quad (12)$$

where

$(\Delta f)_{tension}$ = Factored tensile portion of the stress range due to the passage of a fatigue truck; and

$f_{dead-load\ compression}$ = unfactored compressive stress at the detail due to dead load.

Step 3: Infinite-Life Check

The fatigue details satisfy the infinite-life check if the following equation satisfied, otherwise step 4 is needed.

$$(\Delta f)_{max} \leq (\Delta F)_{TH} \quad (13)$$

where

$(\Delta f)_{max}$ = maximum stress range expected at the fatigue-prone detail, which may be taken as $2.0(\Delta f)_{eff}$;

$(\Delta F)_{TH}$ = constant-amplitude fatigue threshold given in Table 7.

Step 4: Estimating Finite Fatigue Life

Three levels of finite fatigue life could be estimated: 1) the minimum expected fatigue life (which equals the conservative design fatigue life), 2) the evaluation fatigue life (which equals a conservative fatigue life for evaluation), and 3) the mean fatigue life (which equals the most likely fatigue life).

The total finite fatigue life of a fatigue-prone detail, in years, shall be determined as:

$$Y = \frac{R_R A}{365 n (ADTT)_{SL} [(\Delta f)_{eff}]^3} \quad (14)$$

where

R_R = Resistance factor specified for evaluation, minimum, or mean fatigue life as given in Table 10;

A = Detail-category constant given in LRFD Design in Table 6;
n = Number of stress-range cycles per truck passage estimated by Table 8, or through the use of influence lines, or by field measurements;
 $(ADTT)_{SL}$ = Average number of trucks per day in a single lane average; and
 $(\Delta f)_{eff}$ = The effective stress range as specified in Step 1.

Table 10 - Resistance factor for evaluation, minimum, or mean fatigue life, R_R ⁽⁴⁷⁾

Detail Category ^a	R_R		
	Evaluation Life	Minimum Life	Mean Life
A	1.7	1.0	2.8
B	1.4	1.0	2.0
B'	1.5	1.0	2.4
C	1.2	1.0	1.3
C'	1.2	1.0	1.3
D	1.3	1.0	1.6
E	1.3	1.0	1.6
E'	1.6	1.0	2.5

A fatigue design truck is specified for calculation of stresses. The gross weight and axle spacing is chosen such that the fatigue damage caused by the design truck is similar to that of the actual truck population. The NCHRP Report 299 also gives provisions for calculating a site-specific fatigue truck. The gross weight of the design truck is calculated from the root-mean-cube effective gross weight of the truck population. The distribution of gross vehicle weights has been shown to be greatly site specific (Laman 1996) ⁽⁵⁴⁾. Therefore, a more accurate assessment of fatigue remaining life can be accomplished with local truck weight distributions as:

$$W_{equ} = \left(\sum f_i W_i^3 \right)^{1/3} \quad (15)$$

where

f_i =fraction of gross weights within interval i ; and

W_i =mid width of interval i .

The current fatigue design truck consists of two 32-kip axles that are 30 ft. apart (Figure 6). In order to calculate the member stresses due to the design truck, lateral distribution factors for fatigue are specified. The distribution factors for static design of the members assume an ultimate load condition which produces the maximum load effect.

Fatigue damage, however, is an accumulated damage caused by single truck passages. Therefore, the most likely distribution is chosen for fatigue design, whereas, the most severe is chosen for the static ultimate strength limit state.

The stresses caused by the fatigue truck passage are used to determine the design stress range for fatigue. Depending on the bridge span, the number of cycles caused by a truck is determined. For shorter spans, the design truck shows two distinct peaks, whereas, for longer spans there is one overall peak (Schilling 1984)⁽⁵⁵⁾.

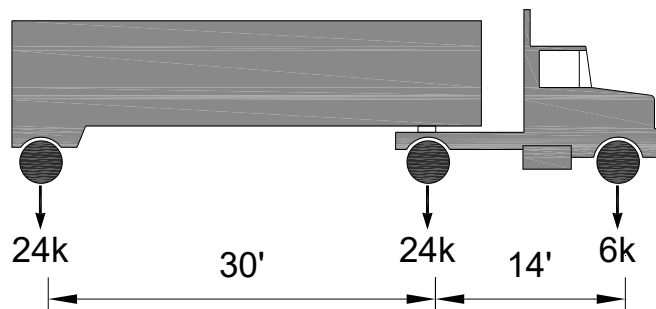


Figure 6. AASHTO LRFD fatigue design truck

Another important consideration in fatigue design is impact or dynamic load amplification. The impact factor used for fatigue is an effective impact factor (Moses 1987)⁽⁴²⁾. The stress range is amplified, not the peak stress. The effective impact factor represents typical bridges with normal road roughness. Factors of 1.10 and 1.10-1.13 for smooth and rough surfaces, respectively, were chosen for the current design provisions.

In 1985, NCHRP Project 12-28, “Fatigue Evaluation Procedures for Steel Bridges”, was initiated. The goal of the principle investigators—Moses, Schilling, and Raju—was to develop fatigue design procedures that more accurately reflect fatigue loading conditions. They employed probabilistic techniques to ensure consistent levels of reliability, included a means for evaluating existing bridges, and developed a quantitative means of assessing remaining life. Additionally, there were guidelines for engineers to develop site specific fatigue design loads and account for future traffic volumes. New factors for load distribution, impact, truck superposition, and cycles per truck were introduced. Factors were developed to represent the typical or average effect of truck loading. Fatigue design was differentiated from static (ultimate) limit state design. Whereas, exceeding the ultimate limit state would result in structural collapse, exceeding the fatigue limit state would simply result in shortened life of a structural component. Corrective actions could be taken to extend the life or replace the structure before serious damage occurred. The

end result of the shift from ultimate to a more tolerant limit state would be a more realistic, cost-efficient design philosophy.

The basis for the material properties needed in fatigue design were developed from laboratory testing of bridge elements. The tests conducted by Keating and Fisher (1985) were done for different samples at constant amplitude stress ranges ⁽⁵⁶⁾. The cycles to failure were plotted on a representative SN curve. There was a significant scatter of the data; therefore, the allowable stress ranges were defined as two standard deviations below the mean stress. The current design SN curves approximate the lower 95 percent confidence limits from test results. The mean SN curves, therefore, provide a higher number of cycles.

There has been extensive research on field testing bridges to determine remaining fatigue life. For the most part, investigators install strain gages to key fatigue-prone detail locations on bridge structures and monitors strain/stress levels for a given period of time. The cumulative damage is calculated based on Miner's Rule, and along with the ADTT for the location, the fatigue life is calculated based on the recommendations (Moses et al, 1987) ⁽⁴²⁾. The remaining fatigue life is simply the total life, less the current service life of the structure.

Hahin, South, Mohammadi, and Polepeddi (1993) applied the new fatigue evaluation procedures proposed by Moses, et al. to numerous bridges in Illinois ⁽⁵⁷⁾. The experimental program consisted of instrumenting fifteen representative steel bridges with strain gages and monitoring stresses at critical details over a 3- to 8-hour periods. Stress cycles were collected using Rainflow techniques. Stress cycles below 0.5 ksi were discarded as noise and were considered a negligible contribution to fatigue damage. Short term data were linearly extrapolated to a 24-hour period. Miner's Rule of linear damage accumulation was used along with fatigue strength coefficients and exponents based on the Munse et al, 50 percent mean data for structural details, given by:

$$N=c(S)^m \quad (16)$$

where

S=stress range (ksi);

c=fatigue strength coefficient;

m=fatigue strength exponent; and

N=number of cycles to major crack formation or failure.

The daily damage caused by truck traffic was computed. Truck volumes were provided by the Illinois Department of Transportation. No indication was made of the truck weight distributions or superposition. Stress cycles were linearly projected by multiplying the daily data out to 25 years. No consideration was made with regard to variability of the stress cycles. The authors, however, do make provisions to account for truck volume and weight increases by compounding the number of cycles annually and increasing the stress magnitudes, respectively. The authors conclude that increasing the truck weights by 10 percent once and the truck volume 5 percent annually, fatigue damage is 4.5 times greater than with no volume or weight change over 25 years. The study is comprehensive with regard to the number of structures instrumented, however, little is known about the truck load spectra. Furthermore, only 3-8 hours of monitoring at 3-4 superstructure locations was conducted for each site. Additional monitoring is needed to verify the assumption that the short test durations represent a typical day of loading. Additional gage locations could also be added to determine load distributions for use in computer modeling similar structures.

A subsequent study by Mohammadi et al. (1998) incorporated a more probabilistic treatment of fatigue damage⁽⁵⁸⁾. A beta distribution is assumed for the stress range and a Weibull distribution is assumed for the fatigue resistance (Ang and Tang 1975)⁽¹²⁾. Different fatigue reliability target levels of 97.7 percent and 99.9 percent are used for redundant and non-redundant members, respectively. The bridge is said to have failed in fatigue when the sum of the Miner's Rule has reached unity. The authors express the expected damage as a statistical term:

$$E(D) = \int_0^{S_{\max}} \frac{\bar{n}}{N(s)} f(s) ds \quad (17)$$

where

S is the stress range expressed as a continuous random variable with f(s) as a probability density function, and

\bar{n} =average number of cycles for all ranges, given by:

$$\bar{n} = \frac{c}{\int_0^{S_{\max}} S^m f(s) ds} \quad (18)$$

where

c and m are empirical constants (Ang and Munse 1975)⁽¹²⁾.

Finally, the fatigue reliability is expressed using Ang and Munse's (1975) equation⁽¹²⁾:

$$L(n) = \exp\left\{-\left[\frac{\bar{n}}{n}\Gamma(1+\alpha)\right]^{1/\alpha}\right\} \quad (19)$$

where

$L(n)$ =fatigue reliability;

Γ =gamma function;

$\alpha=0.108$;

Ω =uncertainty of fatigue life (0.54 for sections with cover plates); and

n =total number of cycles.

A traffic growth factor is implemented similar to the Hahn (1993) paper and fatigue lives are computed⁽⁵⁷⁾. Results are similar to the 1993 paper. Again, no consideration was made with regard to the truck weight distributions.

Deterioration Model for Pavement Structure

An empirical pavement design method was built based on data collected from field experience or experiments. According to known pavement distresses under the specific traffic loadings, the relationship between the observed pavement performance and pavement design is determined.

AASHTO recommends a pavement design procedure that is widely utilized in the U.S. It was established on the basis of the results of AASHTO Road Tests performed in Ottawa, Illinois in the 1950s, which was conducted to determine how traffic loading influenced pavement damage and serviceability. Considering the effect of drainage and environmental factors and including rehabilitation design, the AASHTO 1993 Guide enhanced the pavement design method. The AASHTO 1993 Guide consist of flexible and rigid pavement design.

The pavement performance concept of present serviceability Index (PSI) was developed during AASHTO Road Test in the 1960s. PSI is a combination of values defined by the equation below:

$$PSI = 5.03 - 1.91\log(1 + SV) - 0.01(C + P)^{0.5} - 1.38RD^2 \quad (20)$$

where

SV = longitudinal cracking in the wheel path;

C = cracked area;

P = patched area; and

RD = average rut depth for both wheel paths.

The modified AASHTO Guide design equation for flexible pavements is as follows (Huang 2004).

$$\log\left(\frac{W_{tx}}{W_{t18}}\right) = 4.79 \log(18+1) - 4.79 \log(L_x + L_2) + 4.33 \log L_2 + \frac{G_t}{\beta_x} - \frac{G_t}{\beta_{18}}$$

$$\beta_x = 0.40 + \frac{0.081(L_x + L_2)^{3.23}}{(SN+1)^{5.19} L_2^{3.23}} \quad (21)$$

$$G_t = \log\left(\frac{4.2 - p_t}{4.2 - 1.5}\right)$$

where

W_{tx} = number of applications of given axle;

W_{t18} = number of standard axle passes (single 18 kips axle);

L_x = load in kips of axle group;

L_2 = axle code (1 for single axle, 2 for tandem axles, 3 for tridem axles, and 4 for quad axles);

β_{18} = value of β_x when $L_x = 18$ and $L_2 = 1$;

p_t = terminal serviceability;

SN = structural number, $SN = a_1 D_1 + a_2 D_2 m_2 + a_3 D_3 m_3$,

a_1, a_2, a_3 =layer coefficients for the surface, base, and subbase;

D_1, D_2, D_3 =the thickness of the surface, base and subbase; and

m_2, m_3 =the drainage coefficients for the surface, base and subbase course.

The mechanistic-empirical approach has the capability to accurately estimate pavement damage accumulation over its service life due to truck loading with the input data for traffic, climate, materials and structure. The advantage of this M-E approach is that it combines empirical pavement performance deterioration trends obtained from field data with theoretical predictions of material responses to the applied load conditions. For example, axle loads from the truck loading are applied on a mechanistic pavement structure model and critical pavement responses (stress and strain) are calculated. The responses are then used in an empirical pavement performance model to calculate the number of allowable passes of truck that would induce pavement failure (such as cracking, rutting, roughness degradation, and etc.). Figure 7 shows the general framework for the mechanistic-empirical analysis approach.

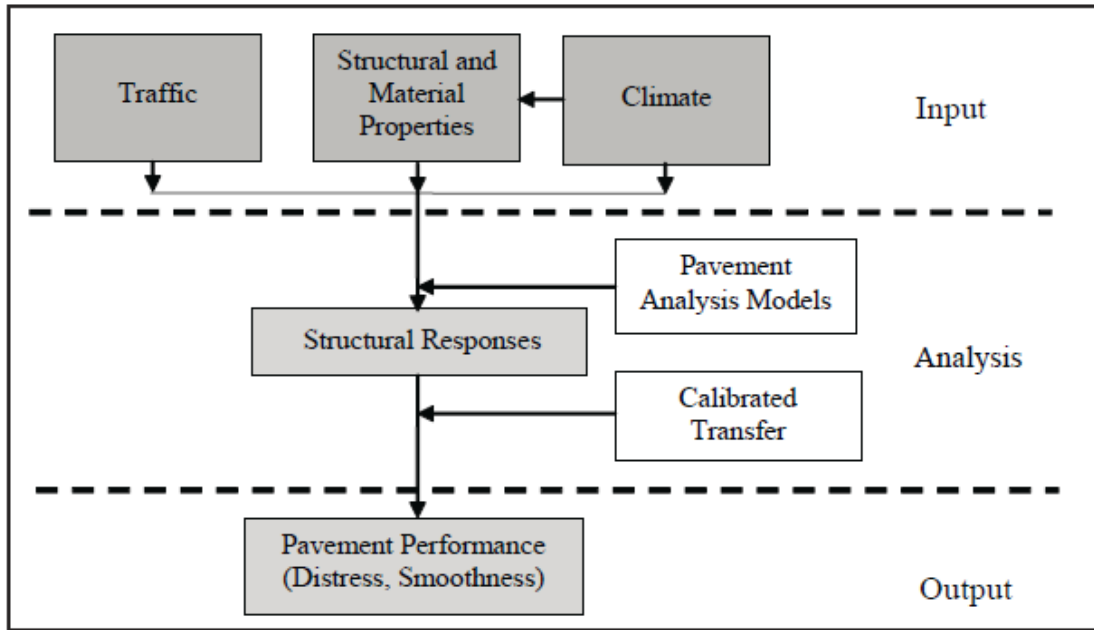


Figure 7. General framework of Mechanistic-Empirical analysis approach

The mechanistic-empirical pavement design guide (MEPDG) was released in draft form at the conclusion of NCHRP 1-37A project in April, 2004. In 2014, Pavement-ME was released as the next generation of AASHTOWare® pavement design software, which builds upon the MEPDG, and expands and improves the features in the accompanying prototype computational software.

In the MEPDG, structural responses (stresses, strains and deflections) are mechanistically calculated based on material properties, environmental conditions, and loading characteristics. These responses are used as inputs in empirical models to predict pavement performance. The accuracy of empirical models is a function of the quality of the input information and the calibration of empirical distress models to observed field performance. The distresses considered for flexible pavements are: rutting, bottom-up fatigue cracking, longitudinal (top-down) cracking, thermal cracking, and roughness (ARA 2004).

The MEPDG has a hierarchical approach for the design inputs, defined by the quality of data available and importance of the project, including:

- Level 1 - Laboratory measured material properties are required (e.g., dynamic modulus for asphalt concrete, nonlinear resilient modulus for unbound materials). Project-specific traffic data is required (e.g., vehicle class and axle load distributions);
- Level 2 - Inputs are obtained through empirical correlations with other parameters (e.g., resilient modulus estimated from CBR values) and state-wide traffic data;
- Level 3 - Inputs are selected from a database of national or regional default values according to the material type or highway class (e.g., soil classification to determine the range of resilient modulus, highway class to determine vehicle class distribution).

The following details the deterioration model used in the MEPDG.

Fatigue Cracking

The equation used for fatigue cracking in MEPDG is:

$$N_f = 0.00432k_1' C(\varepsilon_t)^{-3.291} (E)^{-1.281} \quad (22)$$

where

N_f = number of repetitions to fatigue cracking;

k_1' = correction parameter for different asphalt layer thickness effects;

C = laboratory to field adjustment factor;

ε_t = tensile strain at the critical location; and

E = stiffness of the material.

The Final equation used for top-down fatigue cracking in MEPDG is:

$$FC_{Top} = \left(\frac{1000}{1 + e^{(7.0 - 3.5 \log_{10}(D-10))}} \right) (10.56) \quad (23)$$

where

FC_{top} = top-down fatigue cracking (ft./mi) ; and

D = top-down fatigue damage.

Rutting in Asphalt Mixtures

The equation used for rutting in asphalt mixtures in MEPDG is:

$$\frac{\varepsilon_p}{\varepsilon_r} = k_1 10^{-3.3541} T^{1.5606} N^{0.4791} \quad (24)$$

where

ε_p = accumulated plastic strain at N repetitions of load (in/in);

ε_r = resilient strain of the asphalt material as a function of mix properties, temperature and time rate of loading (in/in);

k_1 = function of total asphalt layers thickness (in) and depth (in) to computational point, to correct for the confining pressure at different depths;

T = temperature (deg F); and

N = number of load repetitions.

$$\begin{aligned} k_1 &= (C_1 + C_2 \cdot \text{depth}) \times 0.328196^{\text{depth}} \\ C_1 &= -0.1039 h_{AC}^2 + 2.4868 h_{AC} - 17.342 \\ C_2 &= 0.0172 h_{AC}^2 - 1.7331 h_{AC} + 27.428 \end{aligned} \quad (25)$$

where

depth = rut depth on asphalt layer; and

h_{AC} = total thickness of the asphalt layers (in).

Rutting in Unbound Materials

The equation used for rutting in unbound materials in MEPDG is:

$$\delta_a(N) = \beta_{s1} \left(\frac{\varepsilon_0}{\varepsilon_r} \right) e^{\left(\frac{\rho}{N} \right)^\beta} \varepsilon_v h \quad (26)$$

where

δ_a = permanent deformation for the layer/sublayer (in);

N = number of traffic repetitions;

β_{CAL} = national calibration factor: 2.23 for granular layers; 1.35 for subgrades,

ε_0 , β , and ρ = material properties;

ε_r = resilient strain imposed in laboratory test to obtain the above listed material properties, ε_0 , β , and ρ (in/in);

ε_v = average vertical resilient strain in the layer/sublayer as obtained from the primary response model (in/in); and

h = thickness of the layer/sublayer (in).

Reflective Cracking

The equation used for reflective cracking in MEPDG is:

$$RC = \frac{100}{1 + e^{(3.5+0.75(Heff))+dt(-0.688584-3.37302(Heff)^{-0.915469})}} \quad (27)$$

where

RC=present of cracks reflected (percent);

t=time (year); and

d=calibration parameter.

Relevant Studies on Effect of Overweight Traffic on Pavement Damage

During the life of pavement, various types of vehicles will pass on the design lane and numerous factors will influence pavement damage. Traffic loading on road pavements is characterized by a number of different types of vehicles with variations in load magnitude, number of axles, and axle configuration. The increasing axle load and/or total vehicle weight shortens the pavement service life and increases the agency cost to maintain pavement condition at an acceptable level. It is expected that the impact of overweight truck on pavement service life is affected by pavement structure, traffic characteristics, and overweight percentage.

To date, a number of research efforts have been devoted to study the reduction of pavement service life and the increase of life cycle cost associated with overweight trucks. Roberts and Djakfar (1999) studied the impact of increasing the legal gross vehicle weight (GVW) limit as compared to the previous legal GVW. They calculated the required overlay thickness for each analysis period and compared the weight scenarios. They found that the greater increasing of GVW led to more significant decreasing of pavement service life and more overlays. However, roads that are designed for heavier traffic had smaller effects from the increasing GVW.

Freeman et al. (2002) conducted a study to determine the effect of higher allowable weight limit provisions on pavement maintenance and rehabilitation cost in Virginia. This study included traffic classification, weight surveys, an investigation of subsurface conditions, and comprehensive structural evaluations. They estimated the cost of damage to roadway pavements with a higher allowable weight limit to be \$28 million over a 12-year period due to the increased overlay thickness. Sadeghi and Fathali (2007) conducted sensitivity analysis to find the significant parameters that influence the deterioration of pavement under truck loading. They obtained the relationships between truckloads and the number of allowable load cycles for each distress. The factors considered in the analysis include asphalt layer thickness, pavement temperature,

subgrade condition, and vehicle speed. Pais et al. (2013) studied the truck factor for the vehicles that travel with axle loads or the total vehicle weight above the maximum legal limits. They also found that the effect of vehicle loads was diminished by increasing the asphalt layer thickness, and subgrade stiffness had little effect on the impact of vehicle loads, if the pavement distress is fatigue cracking.

Previous studies on pavement damage cost caused by heavy trucks have used field performance data (empirical approach) or simulated data (theoretical approach). These studies seek to estimate either the average pavement damage cost (APDC) or the marginal pavement damage cost (MPDC). The average cost is the total MR&R cost divided by the total usage (such as number of ESALs); while the marginal cost is the cost of repairing the damage caused by an additional vehicle on given highway.

Gibby et al. (1990) evaluated the influence of heavy truck on maintenance cost. They used maintenance data, traffic data, weather data, and geometric data of randomly sampled 1100 one-mi section of state highways in California to analyze the relationship between maintenance cost to traffic, weather, and geometry. The conclusion indicated that, in the average traffic, roadway, and climatic conditions, the average annual maintenance cost per heavy truck per day is approximately \$7.67; however, the corresponding cost per passenger car is around \$0.08.

Ghaeli (1997) evaluated the cost of Ontario by separating pavement degradation due to environmental and traffic-associated factors. He conducted life cycle cost to obtain the marginal cost and the marginal costs per ESAL per km per year were found from \$0.001 to \$0.075.

Hajek et al. (1998) used the marginal cost method to analyze pavement cost allocation. They found that the annual life-cycle pavement costs were highly dependent on the highway type. They found marginal pavement cost per ESAL per year for new pavement was from \$0.0025 to \$0.5968; while in-service pavement was from \$0.0013 to \$0.307 (Canadian dollars).

Li and Sinha (2000) concluded that the share of pavement damage attributable to load and non-load factors depends on several factors such as the type of improvement (routine maintenance or rehabilitation), pavement type, and other variables. For routine maintenance, the load and non-load shares were found to be 25-75 for flexible pavements and 30-70 for composite pavements. They found load and non-load fractions of rehabilitation expenditures used to repair pavement damage to be 30-70 for flexible pavements and 40-60 for composite pavements.

Martin (2002) provided an estimate to load-related road wear cost for thin bituminous-surfaced arterial roads in Australia. They developed a statistical relationship between the annual average road maintenance cost and appropriate heavy vehicle road use variables. This study estimated that 65 to 55 percent of road wear cost were attributable to heavy vehicles.

Roberts et al. (2005) found that for lignite coal the tridem axle on the trailer with additional more 8,000 lbs. causes less pavement damage than the tandem axle on the trailer. For timber hauling, there was a gap between the annual damage cost and revenue from overweight permit fee. It indicated that timber trucks were supposed to pay \$346/year for a GVW of 86kips. Fortowsky and Humphreys (2006) concluded two methodologies to estimate freight changes and pavement impacts from freight truck diversion caused by changes of truck weight limits on Interstate highways. They found that the high bound of resurfacing cost was in the range of \$5.97-\$23.89/ daily ESAL-mi; the low bound of resurfacing cost it was between \$9.58 and \$47.84 per daily ESAL-mi, according to highway types.

Saber et al. (2008) investigated the economic impact of heavy sugarcane trucks on Louisiana highways, using 1986 AASHTO Design Guide. They found that the pavement damage caused by a sugarcane truck with a GVW of 100kips to pavement was around \$2,072/year. Ohio Department of Transportation (2009) performed a simplified highway cost allocation study (HCAS) to study the impacts of overweight trucks. It was noted that over 14,500 lane mi of pavement would be designed thinner if no overweight trucks existed and the overweight weight trucks were supposed to responsible for about 122 million dollars per year.

Tirado et al. (2010) estimated the permit fees with different truck-axle loading and configuration based on the incremental damage caused by the heavy truck. The incremental damage was transformed to a permit fee on the basis of the present worth value (PWV) of repairing the pavement. It was found that, aside from the truck gross vehicle weight and axle configuration, pavement structure and damage threshold to rehabilitation heavily affected the permit fee. Ahmed (2012) conducted marginal pavement damage cost estimation and found it in the range of \$0.0033 per ESAL-mi on Interstate highways to \$0.1157 per ESAL-mi on non-national highway systems (NNHS).

Chowdhury et al. (2013) performed a research to estimate pavement deterioration caused by overweight trucks and study the adequacy of standard permitting practices in state agencies. The permit fee was in the range of \$24-\$175 per trip per truck, depending on trip distance, vehicle configuration, and weight. Table 11 lists pavement damage cost summarized from previous literature.

Table 11 - Summary of pavement damage cost studies

Study	Analysis Approach	Traffic Variable & Performance index	MR&R Cost Data	Pavement Damage Cost
Gibby et al. (1990)	Empirical	AADT (cars & small trucks) AADT trucks (>5axles)	Total maint. Cost; California (1984-1987)	Trucks- \$7.60/m/yr Cars - \$0.08/m/yr
Ghaeli (1997)	Empirical	ESAL	Life-cycle cost with maintenance or major resurfacing	\$0.001 to \$0.075 per ESAL per year
Hajek et al. (1998)	Empirical	ESAL	Construction, maint. & rehab. Ontario Data	\$0.0025-0.597 per ESAL-km-year (New pavements) \$0.0013-0.307 per ESAL-mi-year (In- service Pavements)
Li and Sinha (2000)	Empirical	ESAL IRI	Routine maint, rehab & periodic maint. Indiana	\$0.0143-\$0.024 per ESAL-mi
Freeman et al. (2002)	Theoretical	Higher weight limit of vehicle load	Maintenance and rehabilitation cost	\$28 million over a 12-year period
Roberts et al. (2005)	Theoretical	GVW excess 80,000lb	Overlay thickness	\$346/year/truck for a GVW of 86,600 lbs.
Fortowsky et al. (2006)	Empirical	ESAL	Resurfacing cost	\$5.97-\$23.89/daily ESAL-mi; \$9.58-\$47.84/daily ESAL-mi
Saber et al. (2008)	Theoretical	GVW excess 100,000lb	Overlay	\$2,072/year/truck for a GVW of 100,000 lbs.
Ohio DOT (2009)	Empirical	ESAL	Life-cycle cost with maintenance	\$122 million per year
Ahmed (2012)	Empirical	ESAL	Life-cycle cost with maintenance	\$0.0033/ESAL-mi on Interstate highways \$0.1157/ ESAL-mi on non-national highways
Chowdhury et al. (2013)	Theoretical	GVW excess 80,000lb	Construction cost	\$24-\$175 per trip per truck

Life Cycle Cost Analysis of Bridges and Pavements

LCCA is the most renowned evaluation tool for transportation infrastructure management and decision-making support during the project-level analysis. Many professional societies publish literature covering this topic, each with its own objectives. Federal Highway Administration (FHWA) and State Highway Agencies (SHAs) are interested in promoting its application as an evaluation tool capable of achieving higher policy objectives. Highway construction societies are interested in LCCA when its application can provide outcomes that serve a wider spread of their products (e.g., rigid pavements). In contrast, the academics are interested in finding the “right” answers on how to better apply LCCA. The review in this section goes over the major literature provided by the different stakeholders with special emphasis on academic research.

Paterson recorded the acknowledgment of LCCA in the works of Gilipsie in the late nineteenth century (Paterson, 1985) ⁽⁷²⁾. Later, the foremost comprehensive research on LCCA had been credited to Winfrey when he outlined the basis of conducting this analysis in the transportation sector (Winfrey, 1969) ⁽⁷³⁾.

NCHRP Synthesis 122 presented the results of the research exploring the use of LCCA in highway agencies in 1985 (Paterson, 1985) ⁽⁷²⁾. The extent of LCCA application, its complexity, and comprehensiveness during that period was limited, mostly because of the difficulty in performing calculation-intensive analysis in the absence of high performance computing machines available today.

A particular study that developed a synthetic model for the discount rate in LCCA was performed by Philip Cady in 1985 (Cady, 1985) ⁽⁷⁴⁾. According to Cady, the discount rate used in transportation infrastructure LCCA must take into account the effects of increasing costs of highway construction with decreasing construction funds. Arditi and Messiha (1999) surveyed LCCA practices within municipal organizations. The survey in this research focused on the treatment of LCCA input parameters in addition to the overall impacts and consequences of LCCA application ⁽⁷⁵⁾.

A significant manuscript published by the FHWA titled “Life Cycle Cost Analysis in Pavement Design - In Search of Better Investment” constituted a major keystone in LCCA literature (Walls et al, 1998) ⁽⁷⁶⁾. This manuscript is by far the most referenced document in LCCA literature nowadays. Its importance lies in the fact that it provided an easy-to-follow step-by-step process on how to conduct LCCA including numerical examples. The most important contributions were the work-zone user cost calculations and the incorporation of reliability concepts in LCCA application through the Monte Carlo

simulation. More recently, in early 2003, the Office of Asset Management within FHWA released a software package titled “Probabilistic LCCA” that performs the LCCA according to the manuscript described above. The FHWA LCCA guidelines, however, have minimized the significance of user costs during normal operations in the LCCA. It assumes that user costs are comparable across competing alternatives when the pavement serviceability reaches a certain level; consequently, excluding them will not affect the LCCA outcome.

The aim of a major portion of the LCCA literature is to present guidelines for conducting LCCA. A practice-oriented document titled “Life-Cycle Cost Analysis: State-of-the-Practice” was published by the Colorado Department of Transportation (CDOT)⁽⁷⁷⁾. This concise document provides valuable insight for practicing analysts and engineers on the application of LCCA in the bounds of the DOT for distinct and straightforward evaluation.

Lee discusses the fundamentals of LCCA. His research concludes that the LCCA is a restricted form of benefit-cost analysis (BCA) that can be applied in situations where benefits are assumed equal for all alternatives. Lee’s paper provides a noteworthy line of reasoning about the shared scope and consistency between LCCA and BCA (Lee, 2002)⁽⁷⁸⁾.

Another set of “guidelines” in LCCA research is presented by Hall et al (2003)⁽⁷⁹⁾. This paper focuses on the estimation of LCCA components and parameters. The significance of this research is that it presents LCCA transparently; it does not exclude any component, but it provides a general description of each component and the method of estimation.

A publication by the American Concrete Pavement Association (ACPA) titled “Life Cycle Cost Analysis: A Guide for Comparing Alternative Pavement Designs” explains all factors that should be considered in the LCCA and provides guidance on the selection of LCCA-sensitive parameters. It includes useful real-life case studies with detailed numerical calculation that better illustrate the LCCA process. However, a clear focus was made on showing the benefits of lower life cycle cost of rigid pavement (ACPA, 2002)⁽⁸⁰⁾.

In academia, the LCCA literature is mainly focused on LCCA model development. Reigle and Zaniewski (2001) developed a risk-based LCCA model for project-level pavement management⁽⁸¹⁾. Their model was significant regarding two major treatments: (1) it incorporated reliability concepts through the Monte Carlo simulation for the treatment of risk in the pavement design phase, and (2) it integrated a skid-resistance prediction

model for estimating the accident costs in the user costs components for pavement alternatives that differ in their wearing surface skid characteristics.

Another model was developed by Papagiannakis and Delwar (2001) and packaged as a software titled "Pavement Investment Decisions (PID)"⁽⁸²⁾. Their model provides an interface between analysis at the project-level and the network-level. It is unique in its pavement performance index, which combines the measuring criteria of surface distress and structural condition.

A model was introduced by Abaza (2002). This model, called "Optimum Flexible Pavement Life-Cycle Analysis Model", uses the AASHTO pavement life-cycle performance functions to calculate an optimum pavement life cycle disutility⁽⁸³⁾. He introduces a new parameter to be used as a measure that replaces both the pavement life-cycle relative performance and life cycle cost by one effective indicator that assigns monetary value to pavement performance.

Another trend in the LCCA literature focuses on investigating the "what-if" scenarios of LCCA application. This type of research is important and is expected to draw significant interest in the coming years, mainly because conducting LCCA entails making many assumptions about the inherent uncertainty of future parameters. An example of such research is presented by Zayed et al (2002) where they investigated the reasons behind the conflicting results of the LCCA when using deterministic methods versus stochastic methods⁽⁸⁴⁾.

Salem et al. (2003) presented a risk-based approach for estimating life-cycle costs and evaluating infrastructure rehabilitation and construction alternatives⁽⁸⁵⁾. In the study, they utilized highway pavement data to demonstrate the model concept and development. The developed risk-based life-cycle cost model considers the time to failure of each pavement rehabilitation/construction alternative and provides additional knowledge about the uncertainty levels that accompany the estimated life-cycle costs. This paper describes the various components of the developed model, the factors affecting pavement performance and service life, the statistical stratification process of highway pavement networks, and the data input modeling and simulation utilized for the analysis.

NCHRP Report 483, "Life-Cycle Cost Analysis for Bridges," is developed to be used by professionals to undertake life-cycle costing analysis for bridges⁽⁸⁶⁾. First part of the report establishes guidelines and standardizes procedures for conducting life-cycle costing. Second part of the report is useful to all professionals engaged in life-cycle cost analysis either for the repair of existing structures or for the evaluation of new bridge

alternatives. The Guidance Manual outlines the concept of life-cycle costing, identifies sources for data, and explains the methodology by which life-cycle costing can be conducted. The report also provided the bridge life-cycle cost analysis (BLCCA) software in CRP-CD-26. The BLCCA software provides a tool for professionals to apply the life-cycle cost-analysis concepts and methodologies to the analysis of bridges. The software considers agency and user costs and enables the user to consider both vulnerability and uncertainty in the analysis.

Huang et al. (2004) developed a project-level decision support tool for ranking maintenance scenarios for concrete bridge decks deteriorated as a result of chloride-induced corrosion⁽⁸⁷⁾. The approach is based on a mechanistic deterioration model and a probabilistic life-cycle cost analysis. Their analysis includes agency and user costs of alternative maintenance scenarios and considers uncertainties in the agency cost and the corrosion rate in the deterioration model.

Labi and Sinha (2005) investigated the cost effectiveness of various levels of life-cycle preventive maintenance (PM) for three asphaltic concrete pavement functional class families⁽⁸⁸⁾. For each family, they estimated the effectiveness and cost associated with each of several alternative life-cycle PM strategies. For each strategy, they estimated effectiveness as the increase in service life relative to a base-case strategy, and cost as in terms of agency and user costs associated with the treatments comprising that strategy. Using the estimated costs and effectiveness, they developed statistical models to describe the relationship between life-cycle PM effort and its efficacy in extending the pavement life, per unit cost. The study shows that increasing PM is generally associated with increasing cost effectiveness but only up to a certain turning point beyond which cost effectiveness decreases. It determined that the maximum cost effectiveness and the corresponding level of annualized PM are influenced by the pavement functional class and cost components considered.

Daigle and Lounis (2006) developed an approach for life cycle cost analysis of reinforced concrete bridges that takes into account all costs incurred by the owners and users during construction, maintenance rehabilitation and replacement⁽⁸⁹⁾. This approach provides also an estimate of the environmental impacts associated with construction and replacement of bridge decks in terms of greenhouse gas emissions and waste production. The analysis considers all the key stages in the life cycle, which include extraction of raw materials, construction, maintenance, repair and rehabilitation, replacement, and disposal. The total life cycle costs are evaluated by using the present value method.

Chen and Flintsch (2007) proposed a “fuzzy logic” approach for determining the timing of pavement maintenance, rehabilitation, and reconstruction (MR&R) treatments in a probabilistic LCCA model for selecting pavement MR&R strategies⁽⁹⁰⁾. Instead of using predefined service life for initial construction and future rehabilitations, the proposed approach uses performance curves and fuzzy logic triggering models to determine the most effective timing of MR&R activities. They compared their approach with the deterministic and traditional probabilistic approaches in a simple case study. The case study demonstrated that the fuzzy logic–based risk analysis model for LCCA can effectively produce results that are at least comparable to those of the benchmark methods while effectively considering some of the uncertainty inherent to the process.

Kendall et al. (2008) developed an integrated life-cycle assessment and life-cycle cost analysis model to enhance the sustainability of concrete bridge infrastructure⁽⁹¹⁾. The objective of this model is to compare alternative bridge deck designs from a sustainability perspective that accounts for total life-cycle costs including agency, user, and environmental costs. They examined a conventional concrete bridge deck and an alternative engineered cementitious composite link slab design. Despite higher initial costs and greater material related environmental impacts on a per mass basis, the link slab design results in lower life-cycle costs and reduced environmental impacts when evaluated over the entire life cycle. Traffic delay caused by construction comprises 91 percent of total costs for both designs. Costs to the funding agency comprise less than 3 percent of total costs, and environmental costs are less than 0.5 percent. These results show life-cycle modeling is an important decision-making tool since initial costs and agency costs are not illustrative of total life-cycle costs. Additionally, accounting for construction-related traffic delay is vital to assessing the total economic cost and environmental impact of infrastructure design decisions.

Lee et al (2011) developed an LCCA approach for validation of the pavement design on the I-710 Long Beach rehabilitation project with three pavement types: innovative (long-life) asphalt concrete pavement (ACP), standard-life ACP, and long-life Portland cement concrete pavement (PCCP)⁽⁹²⁾. The LCCA followed the Caltrans procedure and incorporated information filed by the project team. The software tools Construction Analysis for Pavement Rehabilitation Strategies (CA4PRS) and Real-Cost were used for quantitative estimates of construction schedule, work zone user cost, and agency cost for initial and future maintenance and rehabilitation activities. Conclusions from the LCCA supported use of the innovative ACP alternative, the one actually implemented in the I-710 Long Beach project (Phase 1), since the innovative ACP alternative had the lowest life-cycle costs over the 60-year analysis period. For example, the life-cycle agency cost for the innovative ACP alternative (\$33.2 million) was about \$7.9 million more cost-

effective than that of the standard-life ACP alternative (\$41.1 million) and about \$17.2 million less expensive than the long-life PCCP alternative (\$50.4 million).

Zhang et al. (2013) developed a new network-level pavement asset management system (PAMS) utilizing life-cycle analysis and optimization methods⁽⁹³⁾. Integrated life-cycle assessment and cost analysis expand the scope of the conventional network-level PAMS from raw material extraction to end-of-life management. To aid the decision-making process, the authors applied a life-cycle optimization model to determine the near-optimal preservation strategy for a pavement network. The authors utilized a geographic information system (GIS) model to enhance the network-level PAMS by collecting, managing, and visualizing pavement information data. The network-level pavement asset management system proposed in this paper allows decision makers to preserve a healthy pavement network and minimize life-cycle energy consumption, greenhouse gas (GHG) emissions, or cost as a single objective, and also meet budget constraints and other agency constraints within an analysis period. A case study of a pavement network in Michigan compares the near-optimal preservation strategy to the Michigan DOT's current preservation practice. Compared with the current preservation plan, the optimal preservation strategy reduces life-cycle energy consumption, GHG emissions, and cost by 20, 24, and 10 percent, respectively.

Summary

Considering the increasing demand for overweight loads from the industry and the accelerated deterioration of these overweight loads on New Jersey highway infrastructure, there is an imperative need to quantify the economic impact of these overweight loads. From the literature search above, several states already put effort on investigating the impact of overweight trucks. However, the methodologies vary from state to state. In order to accurately assess the impact of overweight loads, all available databases were utilized in this study including truck information (WIM), pavement structure information, and bridge information; then a unified database was established.

NJDOT WIM Map

The New Jersey Department of Transportation (NJDOT) has installed over 80 Weigh-In-Motion (WIM) sites throughout the state to monitor long term trends in truck volumes and weights. The locations of these sites are shown in Figure 8 and described in Table 12. Each circle represents one WIM system which includes one or more instrumented lanes, a WIM data logger, and a permanent enclosure. The data from these sites is used for pavement design, long-term freight planning, and enforcement. The functional classification of the sites ranges from two lane country roads, to urban arterials, to major interstate highways. The duration of available data varies by site depending on the installation date. Typically, about thirteen years of data is available for the sites, with some having as much as 20 years of continuous data.

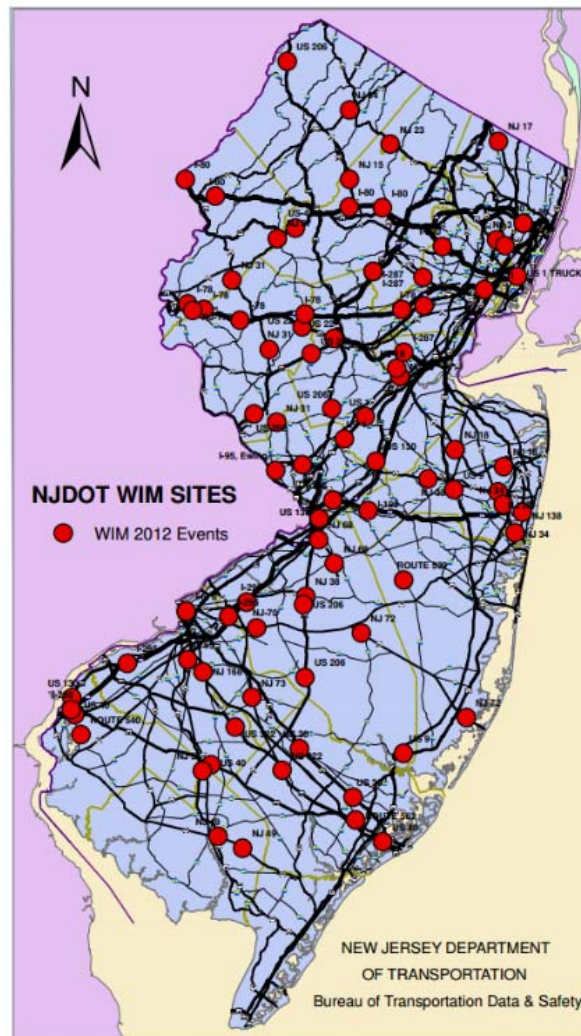


Figure 8. Map of WIM sites in New Jersey (2012)

Table 12 - Description and location for NJ-WIM sites (NJDOT)

ROUTE	LANES	MILE-POST	MUNICIPALITY	COUNTY	SITENAME
Co-539	NB/SB(2)	29.3	Plumstead Twp	Ocean	539
Co-551	NB/SB(2)	6.8	Upper Pittsgrove Twp	Salem	C51
Co-653	NB(2)	2.6	Secaucus Town	Hudson	CLR
Doremus Ave	NB/SB(2)	2.3	Newark City	Essex	DRM
I-195	EB/WB(4)	4	Hamilton Twp.	Mercer	19B
I-195	EB/WB(4)	10.2	Upper Freehold	Monmouth	195
I-280	WB(3)	5.1	Roseland Boro	Essex	280
I-287	NB(3)	31.7	Harding Twp.	Morris	A87
I-287	NB/SB(4)	61.7	Franklin Lakes Boro	Bergen	287
I-295	NB/SB(6)	35.7	Cherry Hill Twp.	Camden	I2C
I-295	NB/SB(6)	39.6	Mt. Laurel Twp.	Burlington	295
I-78	EB/WB(6)	25.7	Readington Twp.	Hunterdon	78D
I-78	WB(4)	34.5	Bernards Twp.	Somerset	78B
I-80	EB(6)/WB(6)	66.2	S. Hackensack	Bergen	SHE/SHW
NJ-124	EB/WB(4)	7.6	Summit City	Union	124
NJ-138	EB/WB(4)	2.6	Wall Twp.	Monmouth	138
NJ-15	NB/SB(4)	7.1	Jefferson Twp.	Morris	15
NJ-168	NB/SB(3)	1.3	Gloucester Twp.	Camden	168
NJ-18	NB/SB(4)	16	Colts Neck Twp.	Monmouth	18B
NJ-18	NB/SB(4)	26.6	Marlboro Twp.	Monmouth	18
NJ-18	NB(3)/SB(2)	44.6	Piscataway Twp.	Middlesex	18D
NJ-23	NB/SB(4)	23.8	West Milford Twp.	Passaic	23
NJ-31	NB/SB(2)	13	East Amwell Twp.	Hunterdon	31B
NJ-31	NB/SB(4)	26.4	Readington Twp.	Hunterdon	31D
NJ-31	NB/SB(2)	40.4	Washington Twp.	Warren	31C
NJ-33	EB/WB(5)	23.5	Manalapan Twp.	Monmouth	33
NJ-34	NB/SB(4)	0.6	Wall Twp.	Monmouth	34
NJ-34	NB/SB(4)	5.7	Wall Twp.	Monmouth	34B
NJ-55	SB(2)	27.4	Vineland City	Cumberland	55C
NJ-55	NB(2)/SB(2)	57.9	Deptford Twp.	Gloucester	552
NJ-68	NB/SB(2)	2.4	Springfield Twp.	Burlington	68
NJ-68	NB/SB(4)	7	Mansfield Twp.	Burlington	68A
NJ-72	EB/WB(2)	2.1	Woodland Twp.	Burlington	72
NJ-73	NB/SB(4)	11.9	Winslow Twp.	Camden	73
NJ-94	NB/SB(2)	33.8	Hardyston Twp.	Sussex	94
NJTPK	NB(2)	0.8	Carneys Point Twp.	Salem	NJT
US-1	NB/SB(6)	12.9	Plainsboro Twp.	Middlesex	1
US-1	NB/SB(4)	18	S. Brunswick Twp.	Middlesex	01A
US-130	NB/SB(4)	57	Bordentown Twp.	Burlington	13B

ROUTE	LANES	MILE-POST	MUNICIPALITY	COUNTY	SITENAME
US-130	NB/SB(4)	70.6	Cranbury Twp.	Middlesex	13A
US-202	NB/SB(4)	3.5	WestAmwell Twp.	Hunterdon	202
US-202	NB/SB(4)	19.2	Branchburg Twp.	Somerset	02B
US-22	EB/WB(4)	26.6	Readington Twp.	Hunterdon	22
US-22	EB/WB(4)	32.3	Bridgewater Twp.	Somerset	22B
US-322	EB/WB(4)	27.5	Monroe Twp.	Gloucester	322
US-40	EB/WB(4)	3	Carneys Point Twp.	Salem	40A
US-40	EB/WB(2)	28.4	Franklin Twp.	Gloucester	40
US-40	EB/WB(4)	61.6	Egg Harbor Twp.	Atlantic	40B
US-46	EB/WB(4)	25.2	Mount Olive Twp.	Morris	46
US-9	NB/SB(4)	111.8	Freehold Twp.	Monmouth	09A
I-295	NB/SB(4)	2.9	Carneys Point	Salem	I2S
US-130	NB/SB(2)	3.4	Penns Grove Boro	Salem	130
NJ-72	EB/WB(4)	25	Stafford Twp.	Ocean	72B
US-1&9	SB(7)	48.1	Newark City	Essex	01C
I-78	EB(3)	5	Greenwich Twp.	Warren	78E
I-78	WB(3)	7.9	Betlehem Twp.	Hunterdon	78W
I-676	NB/SB(4)		Camden City	Camden	676
I-80	EB/WB(6)	32.4	Roxbury	Morris	80B
I-80	EB/WB(8)	38.1	Rockaway	Morris	80C
I-80	EB(4)/WB(3)	8.3	Knowlton	Warren	80A
I-95	NB/SB(6)	1.2	Ewing	Mercer	95
I-95	NB/SB(6)	6.3	Lawrence Twp.	Mercer	95B
NJ-55	NB/SB(4)	37	Vineland City	Cumberland	551
NJ-57	EB/WB(4)	3.5	Greenwich Twp.	Warren	57A
NJ-70	EB/WB(2)	10.3	Evesham Twp.	Burlington	551
NJ-173	EB/WB(4)	2.4	Greenwich Twp.	Warren	173
I-78	EB/WB(6)	14.5	Union	Hunterdon	78A
I-95	NB(2)	2.1	Ewing	Mercer	952
NJ-17	SB(3)	25.5	Mahwah	Bergen	17
NJ-31	NB/SB(4)	30.1	Clinton	Hunterdon	31
NJ-52	NB/SB(4)	1.6	Ocean City	Cape May	52
NJ-440	NB/SB(4)	21.4	Bayonne City	Hudson	169
US-1&9	SB(2)Ex	47.2	Newark City	Essex	01B
US-206	NB/SB(2)	22	Southampton	Burlington	206

Where: NB=Northbound, SB=Southbound

RESEARCH APPROACH

Data Collection and Development of a Unified Database

Public agencies in transportation such as state DOTs and MPOs and their consultants collect large amounts of data from the state highways through the usage of embedded sensors, weigh-in-motion sensors, or video collection technologies. For this project the RIME team identified the main data sources as:

- Volume counts and classification data;
- Weigh-in-motion truck weight data;
- Overweight trucks / permit data;
- Pavement condition and bridge inventory data.

In addition, the data sources outlined above, the project team also considered the use of the data from other agencies from neighboring agencies such as volume counts and WIM data, and pavement condition and bridge inventory data. However, due to limited access to those data sources, only the data provided by NJDOT is used in the development of the database. The vast amount of the data, which is utilized in the development of the database and the software decision tool, is collected by different sources and each source is its own data format. Hence, it is required to handle different data formats in a fast and automated way.

The RIME team has previous experience in the development of software handling large scale data. For example, in a previous research project, the RIME team has developed ASSISTME-WIM that allows for the continuous validation of the WIM data and other characteristics of truck traffic needed for assessing their impact. In the current project, the WIM data also constitute the bulk of the data.

Based on the previous experience, first, a unified database is developed containing all available data relating to the condition rating of pavement management systems (PMS), bridge management system (BMS) and inventory, Weigh-In-Motion (WIM) truck weight spectra, etc. This database consists of many data tables containing different data types. The project team considered to use an open source and fast database platforms that can handle large data effectively and decided on utilizing MySQL platform. Then, the data types, which are needed for analyses, are carefully investigated to define the relationships between the different data types. Defining the relationships are necessary to run queries on the unified database containing multiple data tables. The result set acquired by running the queries will supply the needed input by the deterioration models and Life Cycle Cost analysis.

Data Format

There are three data types that are included in the database:

- WIM Data: This data contains detailed information about the individual trucks passing over the weigh-in-motion station. It includes speed, GVW, class, each axle spacing, and each axle weight of individual trucks with a time stamp.
- Bridge Inventory: This data is obtained from National Bridge Inventory database and it contains the location, structure number, structure length, number of lanes on the structure and other design parameters.
- Volume counts: This data includes roadway information, milepost and hourly volume counts for the most roadways in NJ.
- NJ roadway network: This is a geodatabase of the roadway links which also contains their SRI, start milepost, end milepost, etc.

Database Software and Structure

For managing the database, the project team decided to use MySQL, an open-source and widely used database tool. MySQL provides fast and convenient framework for complex data tables. This is important as our goal is to process complex queries quickly in the background and provide the relevant results to the user in a seamless way.

To combine different data formats in a unified database, the first step is to create data tables containing relevant data from each source and to assign relationships between those tables. Figure 9 shows the structure of the unified database and the relationships between the data tables. In the next section, the database tables and the relationships will be explained.

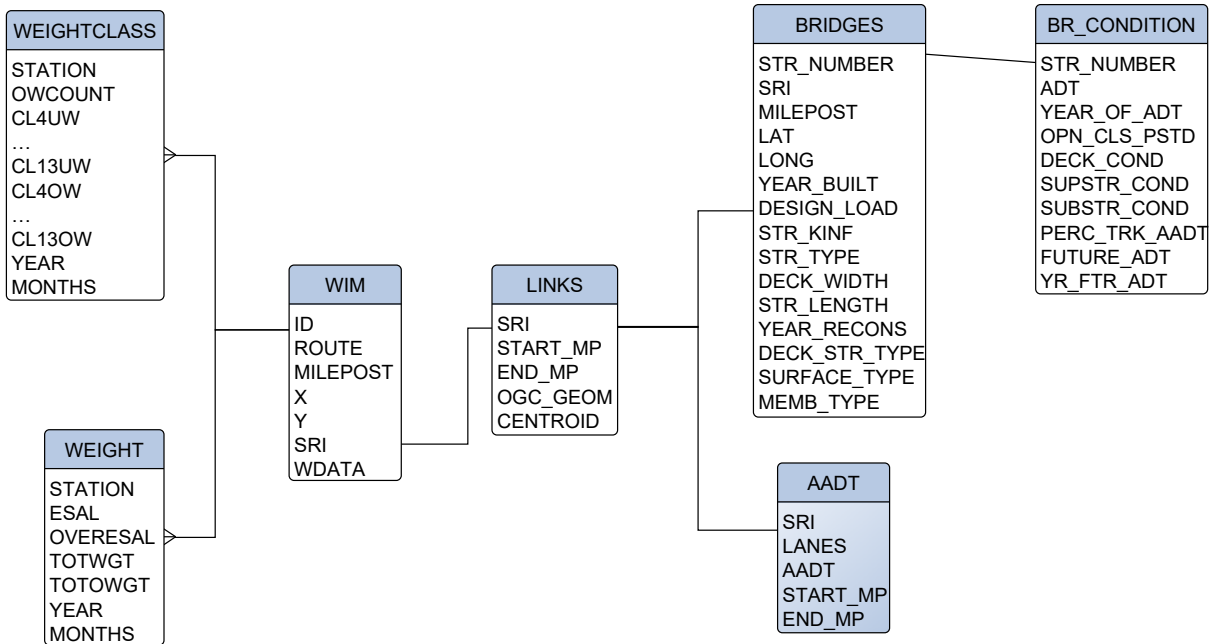


Figure 9. Structure of the unified database

Database Tables

The unified database has 7 main tables. These are:

WIM

There are 88 WIM stations (81 of them reports data) in NJ (see Figure 10) and this table used contains details of the WIM stations (codename, location, coordinates and SRI). The data from the WIM stations forms the bulk of the data used in the analyses. This table is necessary to locate the data from which WIM station will be used in an analysis based on the selected roadway or the link. The table is related to LINKS table through SRI and Milepost fields. Actually, WIM stations in this table also has their own tables where we gather the truck traffic data such as ESALs, weight, etc. However, those tables are not included in the unified database as the data from those tables are processed and, as a result, summary tables are created in the database which are WEIGTCLASS and WEIGHT tables. These two tables are related to WIM table through STATION field (corresponds to ID field in WIM table).

Weight Class

This table generated from the individual weight tables of the WIM stations. It contains the count of overweight count and total overweight and total legal weight of the trucks by class type for the data for the most recent year available. Months field is used to extrapolate the data, if the data for the most recent year is incomplete for the WIM station.

Weight

Similar to WEIGHTCLASS table, WEIGHT table is generated from the weight tables of WIM stations. This table contains the total weight and total over weight of trucks passing over a station for the data of the most recent year. This table also contains total ESALs and total overweight ESALs for each station. To calculate these fields, first, axle weight and axle type (single, tandem, tridem, and quad) are determined for each truck using the load equivalency factors developed and explained in the pavement deterioration models part of this study. Using the overweight criteria for the trucks in NJ, overweight trucks and for legal trucks are separated and total ESALs for each category is calculated for generating the fields in this table. If the station does not have the data for the full year, it is assumed that the traffic trend is same for all year and hence the data extrapolated for the year.

Links

This is a spatial table containing the links in NJ roadway network. This table is needed for geographically referencing the data and displaying it on GoogleMaps. To create this table, first, NJ Roadway network shape file simplified to only include highways and toll roads (surface streets and country roadways are omitted since they are out of scope of this study). Then, a tool named shp2mysql is utilized to create a MySQL dump from the shape file. Later, the dump file is imported a MySQL database spatial table. Since MySQL platform is used in this study, the new spatial feature of it, called ST_AsGeoJSON, is utilized in the decision tool. Using this feature made it possible to query this spatial table and generate dynamic GeoJSON results for selected links which can be displayed easily on GoogleMaps.

AADT

Rutgers team obtained traffic counts from the many different sensors of NJDOT for a previous study. This table contains AADT data for the links on major roadways of NJ. This table is needed if a roadway with no WIM station needs to be analyzed. In this case, using AADT table, truck traffic ratio is generated by comparing the AADT of the closest WIM station to that of the selected roadway (or the link). Then, the truck traffic on the closest WIM station is modified based on this ration and used for the selected roadway.

Bridges

This table contains the locations and the properties of 6918 bridges in NJ since 1992. It is generated using the NBI data. This table used by the decision tool to locate the bridge(s) on the selected roadway or link and their properties (type, length, width, and rehabilitation history) for the cost calculations. The table also provides input for the deterioration models.

Bridge Condition

This table, also generated using NBI data, contains bridge conditions data for the past 23 years. It provides input for the bridge deterioration models.

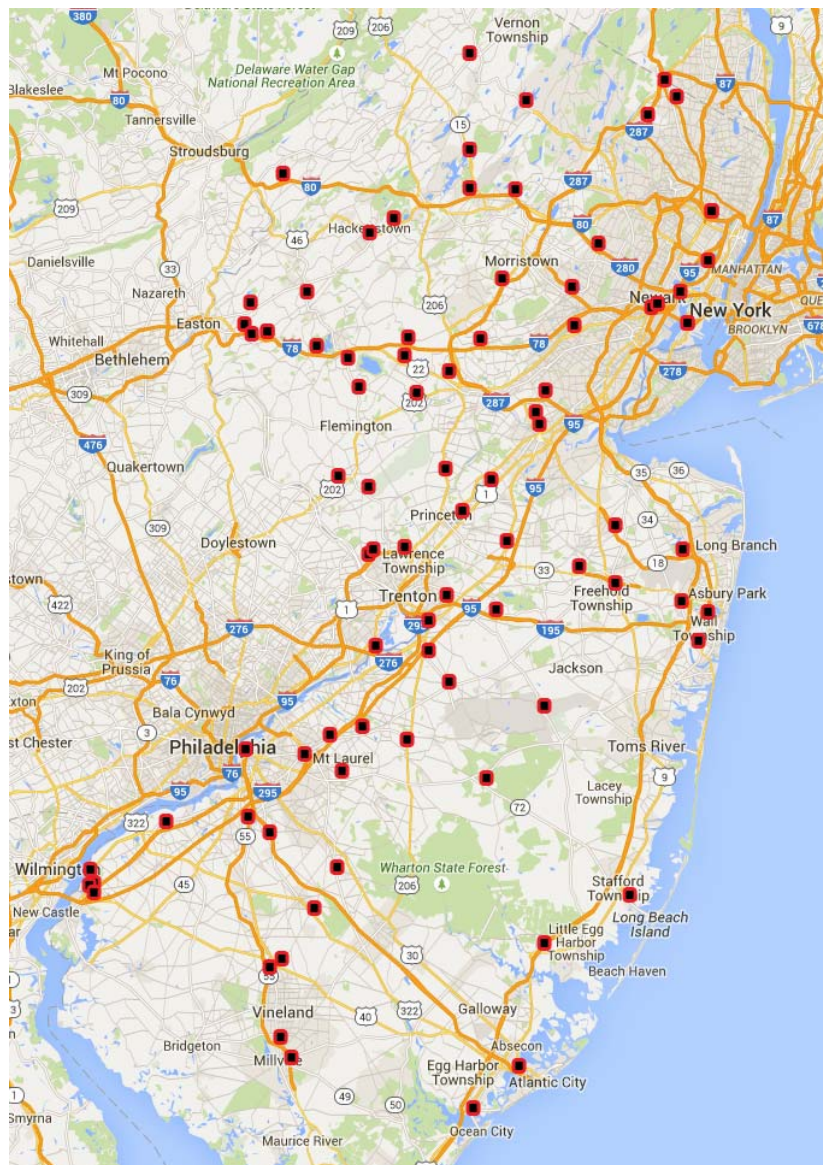


Figure 10. Locations of NJ-WIM stations

Processing WIM Data

Over the past decades, the traffic patterns have changed dramatically because of economic growth as well as the technology innovation in highway transportation industries. FHWA (2011) and FHWA (2015) has concluded that there is sturdy increase in truck traffic over the years. As shown in Figure 11 although the average daily traffic subject to decrease from 2002, the average daily load still shows sturdy increase. This implies that less number of trucks have carried more loads over the years, especially after year of 2002.

The State of New Jersey is located between Philadelphia and New York City, two major metropolitan centers in Northeast America. High volumes of interstate traffic and products are carried by its transportation system. As shown in Figure 10, there are total 90 permanent Weigh-in-Motion (WIM) sites operated by NJDOT. These WIM sites spread across the State of New Jersey and located at different inter-state highway, state highway, and local roads and the WIM data has been collecting from these sites for 10 to 20 years ⁽⁹⁴⁾.

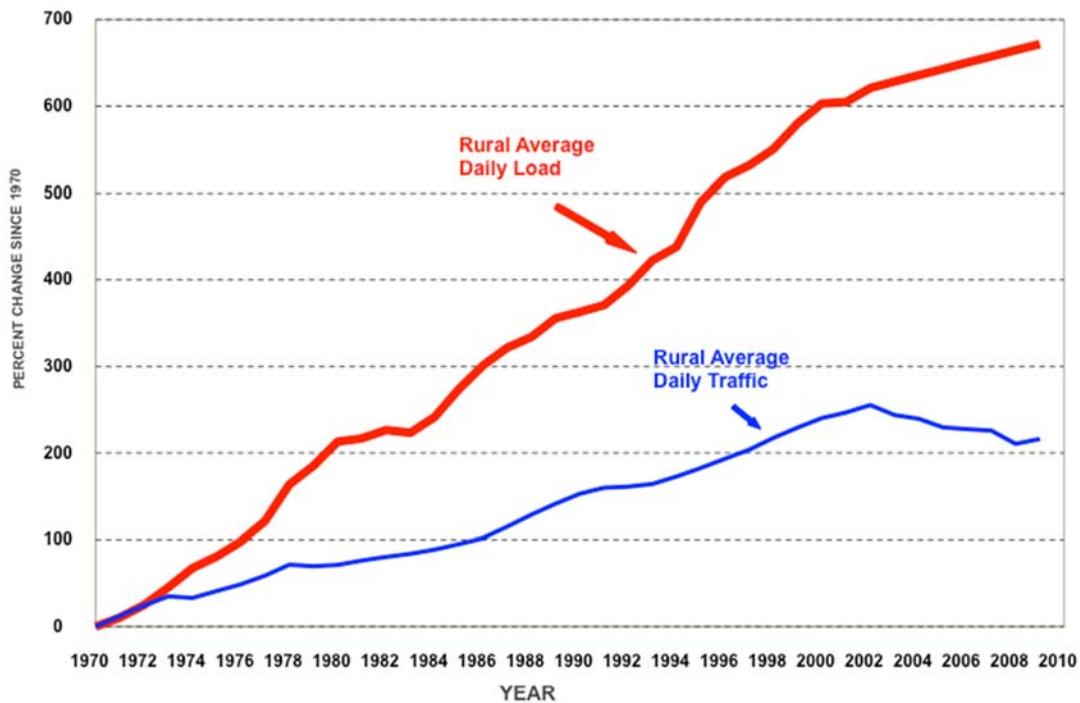


Figure 11. Growth in volume and loadings on the rural interstate system (1970-2010)

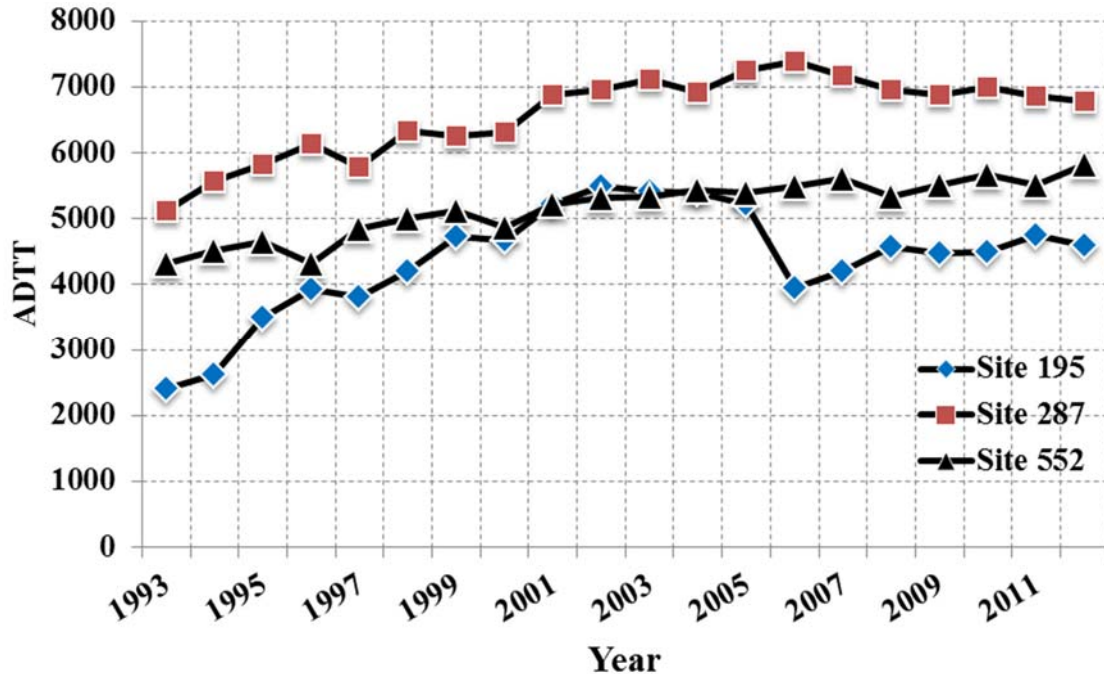


Figure 12. Annual average ADTT for various sites from 1993 to 2012 ⁽⁹⁴⁾

Considering the traffic volume at different sites, as shown in Figure 12, over the years, the characteristics of truck traffic in NJ vary significantly. These variations can be attributed to the rapid development of trucking technology and high demanding on highway transportation. Especially due to popularity of online shopping, more goods are moving around on the road, which changed the traffic patterns on the road.

There are a total of 90 WIM sites that currently operated by NJDOT. As shown in Table 13, among these 90 WIM sites, 23 of them are located at interstate highways, 24 of them are located at US highways, 37 of them are located at State highways, and the other 6 sites are located at local county road. Due to the difference in functionality in different road, the characteristics of the truck traffic on different roads might vary significantly.

Table 13 - Number of WIM Sites by road type

Road Type	Number of Sites
Interstate Highway	23
US Highway	24
State Highway	37
County Road	6
Total	90

Table 14 shows the basic statistics for various interstate highway, US highway, and state highway routes. It is observed even for same type of road the traffic condition varies significantly.

Table 14 - Statistics for interstate highway, US highway, and state highway routes

Route	Ave. Axles per Truck	ADTT	Axles Per Day	Percentage (>80kips)	Percentage (>100kips)	Percentage (>120kips)
I-195	3.41	1993	6792	7.44	3.37	1.47
I-280	3.55	410	1454	3.11	0.39	0.13
I-287	4.54	6169	27997	2.07	0.21	0.03
I-78	4.65	12630	58695	7.94	0.08	0.02
I-80	4.52	1701	7699	3.27	0.49	0.13
I-95	4.05	3050	12346	12.20	2.9	0.46
I-676	3.46	1682	5828	2.6	0.13	0.023
I-295	4.29	6285	26990	2.6	0.17	0.04
US-1	4.10	1589	6509	7.32	0.64	0.12
US-30	2.96	346	1024	3.21	0.41	0.11
US-9	3.07	1400	4297	2.93	0.43	0.06
US-22	3.29	596	1958	6.92	0.35	0.1
US-40	4.00	801	3204	11.31	2.04	0.2
US-46	3.13	441	1380	2.76	0.2	0.03
US-130	4.07	367	1493	1.13	0.3	0.1
US-202	4.10	1065	4367	1.76	0.42	0.05
US-206	3.80	612	2325	3.34	0.49	0.09
US-322	2.89	339	979	4.37	1.44	0.56
NJ-15	3.40	1186	4028	6.13	0.21	0.03
NJ-18	3.65	579	2113	9.75	0.61	0.07
NJ-18	3.14	619	1941	0.55	0.1	0.04
NJ-31	4.10	707	2896	16.33	5.39	1.55
NJ-33	3.24	793	2567	2.58	0.43	0.12
NJ-34	3.09	388	1197	2.08	0.53	0.1
NJ-55	4.15	2674	11089	12.03	0.77	0.17
NJ-68	3.90	204	795	0.54	0.17	0.09
NJ-72	3.70	359	1328	4.23	0.26	0.08
NJ-73	2.86	422	1208	3.39	0.37	0.07
NJ-94	3.23	365	1179	3.31	0.38	0.08
NJ-124	2.71	77	207	0.75	0.21	0.03
NJ-138	3.04	361	1098	1.32	0.05	0.03
NJ-168	2.78	159	441	0.14	0.02	0.01

Processing NBI Data

The National Bridge Inventory (NBI) Database has the most extensive and detailed data on highway bridges in the US. The NBI is a collection of information (database) covering all of the Nation's bridges located on public roads, including Interstate Highways, US highways, State and county roads, as well as publicly-accessible bridges on Federal lands. It presents a State by State summary analysis of the number, location, and general condition of highway bridges within each State. In this project, the NBI data for all New Jersey bridges were collected from Year 1992 to Year 2013. The no-delimiter data were columned by the research group. The Recording and Coding Guide for the Structure Inventory and Appraisal of the Nation's Bridges provides instructions for coding of condition rating for bridge structure (USDOT 1995) ⁽⁹⁵⁾. There are up to 116 data items for bridges which categorized in three main data groups: Bridge Management Items (BRI_MGT_ITEM), Bridge Inventory Items (BRI_INV_ITEM), and Bridge Rating Items (BRI_RAT_ITEM). Each item has specified number which has a specified definition in bridge inspection manual. Based on the needed inputs for bridge deterioration models and bridge cost analysis, a list of items selected in this study was shown in Table 15.

Before processing the NBI data, following preliminary data filtering steps has been done in order to define and select the highway bridge database. After the preliminary filter shown above, 6918 bridges were selected and stored in the unified database.

- items 5a=1 (Route carried "on" the structure);
- items 42a=1 or 4 or 5 or 6 or 7 or 8 (service on the bridge: 1 - Highway, 4 - Highway-railroad, 5 - Highway-pedestrian, 6 - Overpass structure at an interchange or second level of a multilevel interchange, 7 - Third level (Interchange), 8 - Fourth level (Interchange));
- item 49 >=6.1meters (Bridge length >= 6.1 meter);
- item 112=Y (Structure meet or exceed the minimum length specified to be designated as a bridge for National Bridge Inspection Standards purposes);
- Remove not applicable and blank data;
- Remove duplicate data.

Table 15 - List of items selected in this study

#	Data Item	Item # in NBI
1	Structure Number	item 8
2	Route Signing Prefix	item 5B
3	Designated Level of Service	item 5C
4	Route Number	item 5D
5	Directional Suffix	item 5E
6	Functional classification of inventory route	item 26
7	Year Built	item 27
8	Design Load	item 31
9	Structure type	item 43a and 43b
10	Number of spans in Main Unit	item 45
11	Structure length	item 49
12	Deck Width, out-to-out	item 52
13	Year Reconstructed	item 106
14	Deck Structure Type	item 107
15	Wearing Surface/Protective System	item 108
16	Average Daily Traffic	item 29
17	Year of Average Daily Traffic	item 30
18	Structure open, posted, or closed to traffic	item 41
19	Deck condition rating	item 58
20	Superstructure rating	item 59
21	Substructure	item 60
22	Average daily truck traffic	item 109
23	Future Average Daily Traffic	item 114

Deterioration curves were prepared for superstructure and deck. The deterioration level is quantified using condition rating indices, which were also used by NBI. This is a numeric ranking system from “0” to “9”, where “0” represents “Failed Condition” and “9” represents “Excellent Condition” (Table 16). Such condition rating data is available for deck, superstructure and substructure in the NBI database. NJDOT uses the same condition rating system as well. The bridge deterioration curves for the bridges in selected 11 WIM sites are provided in the following figures:

Table 16 - NBI bridge condition ratings explanation

Condition Rating	Interpretations
9	Excellent Condition
8	Very Good Condition – no problems noted.
7	Good Condition – some minor problems.
6	Satisfactory Condition – structural elements show some minor deterioration.
5	Fair Condition – all primary structural elements are sound but may have minor section loss, cracking, spalling or scour.
4	Poor Condition – advanced section loss, deterioration, spalling or scour.
3	Serious Condition – loss of section, deterioration of primary structural elements. Fatigue cracks in steel or shear cracks in concrete may be present.
2	Critical Condition – advanced deterioration of primary structural elements. Fatigue cracks in steel or shear cracks in concrete may be present or scour may have removed substructure support. Unless closely monitored it may be necessary to close the bridge until corrective action is taken.
1	Imminent Failure Condition – major deterioration or section loss present in critical structural components or obvious vertical or horizontal movement affecting structure stability. Bridge is closed to traffic but corrective action may put it back in light service.
0	Failed Condition – out of service; beyond corrective action.

Bridge Classification

Deterioration of bridge elements depend on several important parameters related to bridge design, material, geographical location and environment, and traffic volume and weight. Therefore, it is important to classify bridges based on the values of these parameters so that targeted bridge type can be identified for developing deterioration models in the following bridge analysis part. To achieve this goal, filtered data records are classified based on the following parameters that are discussed in more detail in the following subsections:

- Route Signing Prefix
- Material types
- Structure types
- Bridge ages
- Bridge span length

Route Signing Prefix identified the route signing prefix for the inventory route including interstate highway, U.S. numbered highway, state highway, county highway, city street, federal lands road, state lands road, and other. The distribution is shown in Figure 13.

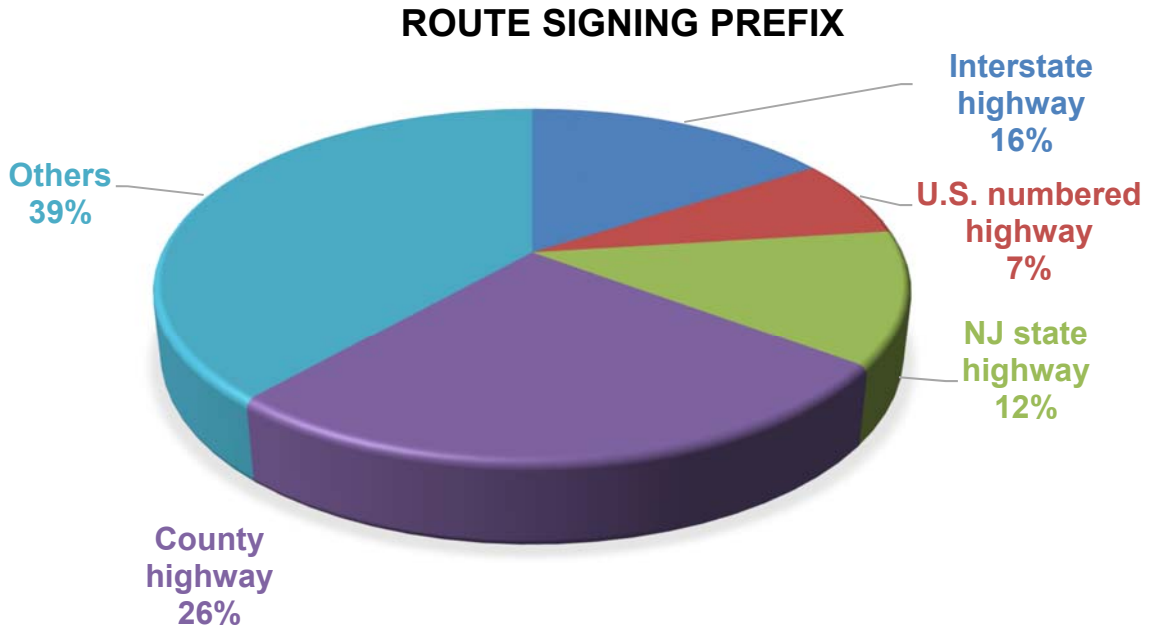


Figure 13. Distribution of Route Signing Prefix in bridge inventory

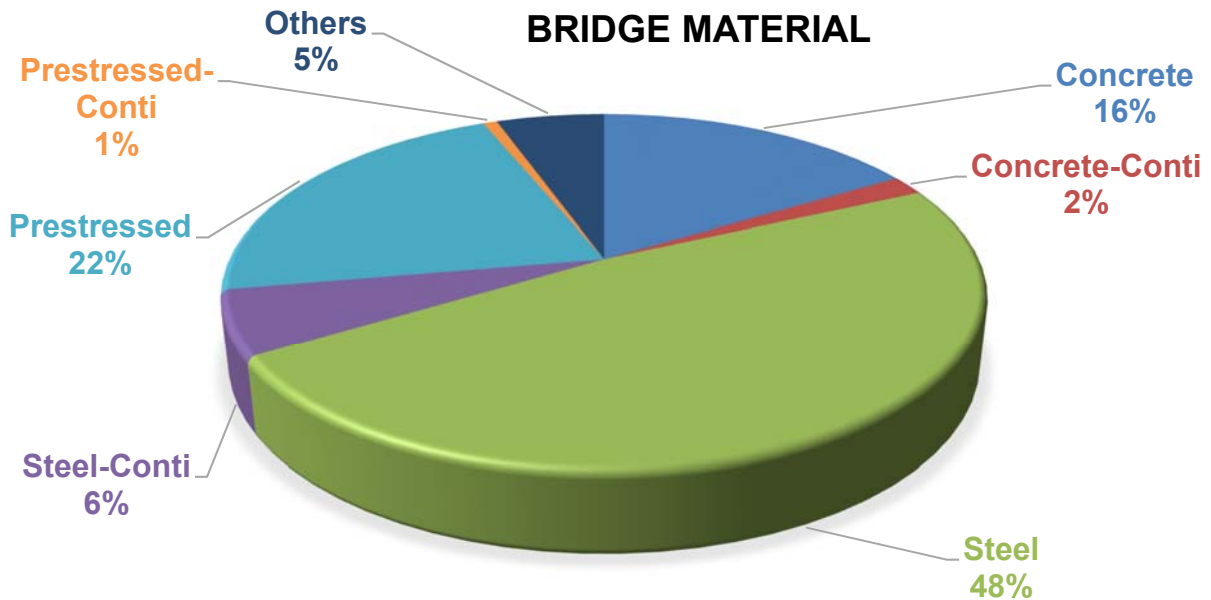


Figure 14. Distribution of bridge material in bridge inventory

There are different types of materials used in bridge superstructure. Material type is presented in item ITEM43A in NBI database using a number from 0 to 9. Figure 14 shows the percentages of using steel, steel continued, reinforced concrete, reinforced concrete continued, prestressed concrete, prestressed concrete continued, and others in bridge superstructure. This figure clearly indicates that most of bridges are simply supported in each types of material. Nearly half of bridges are simply supported steel bridges and the second is simply supported prestressed concrete bridges.

Type of structure represents the structural system of the bridge and is presented in item ITEM43B. Type of structures has numbers from 00 to 22 as described in Table 17. The distribution of structural type for each material type is shown from Figure 15 to Figure 20. For simply supported concrete bridge, most of them are culvert type and while for continuous concrete bridge are slab bridges. For both simply supported and continuous steel bridges, most of them are multi-beam bridge type and girder-floor beam system. For prestressed concrete bridge, the highest proportion is multi-beam structure.

Table 17 - Bridge material code definition in NBI database

Code	Description
1	Slab
2	Stringer/Multi-beam or Girder
3	Girder and Floorbeam System
4	Tee Beam
5	Box Beam or Girders - Multiple
6	Box Beam or Girders - Single or Spread
7	Frame (except frame culverts)
8	Orthotropic
9	Truss - Deck
10	Truss - Thru
11	Arch - Deck
12	Arch - Thru
13	Suspension
14	Stayed Girder
15	Movable - Lift
16	Movable - Bascule
17	Movable - Swing
18	Tunnel
19	Culvert (includes frame culverts)
20	Mixed types
21	Segmental Box Girder
22	Channel Beam
0	Other

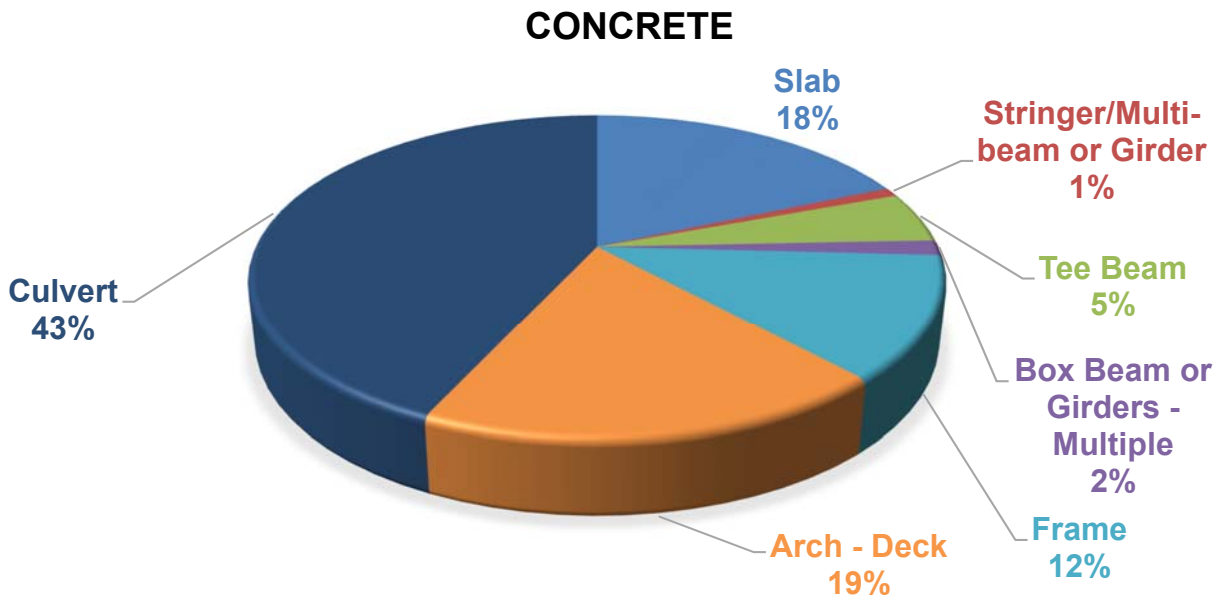


Figure 15. Distribution of structural types in simply supported concrete bridges

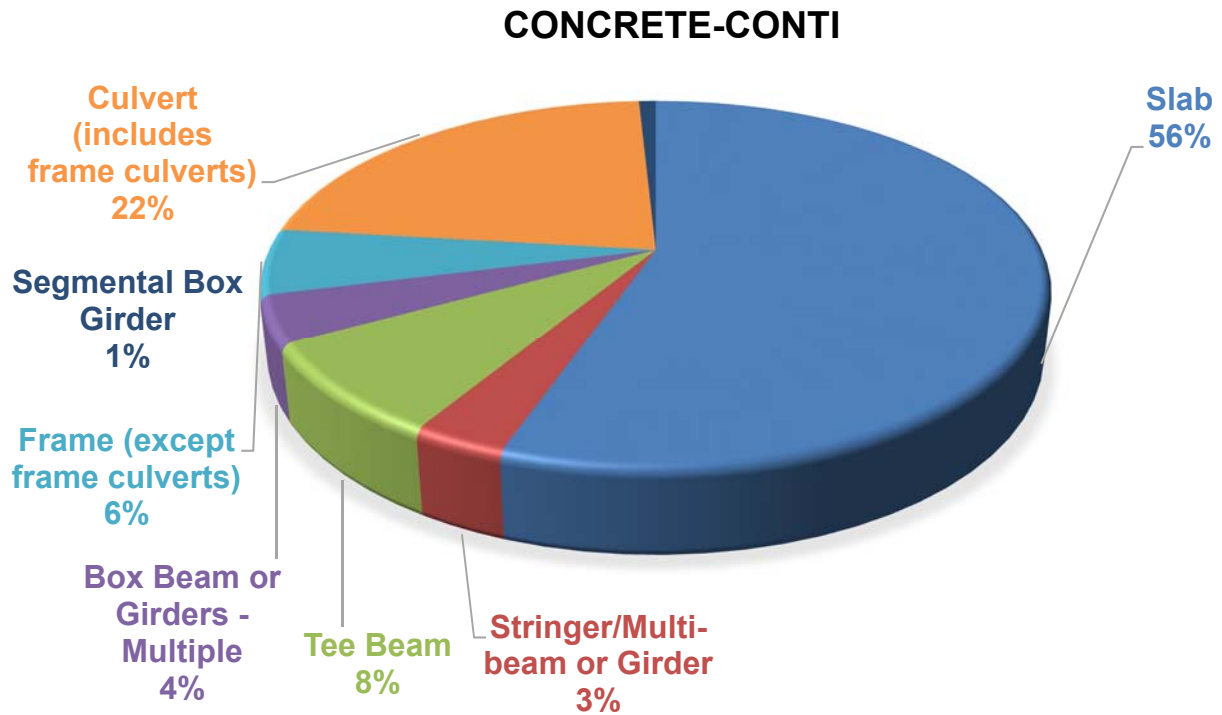


Figure 16. Distribution of structural types in continuous concrete bridges

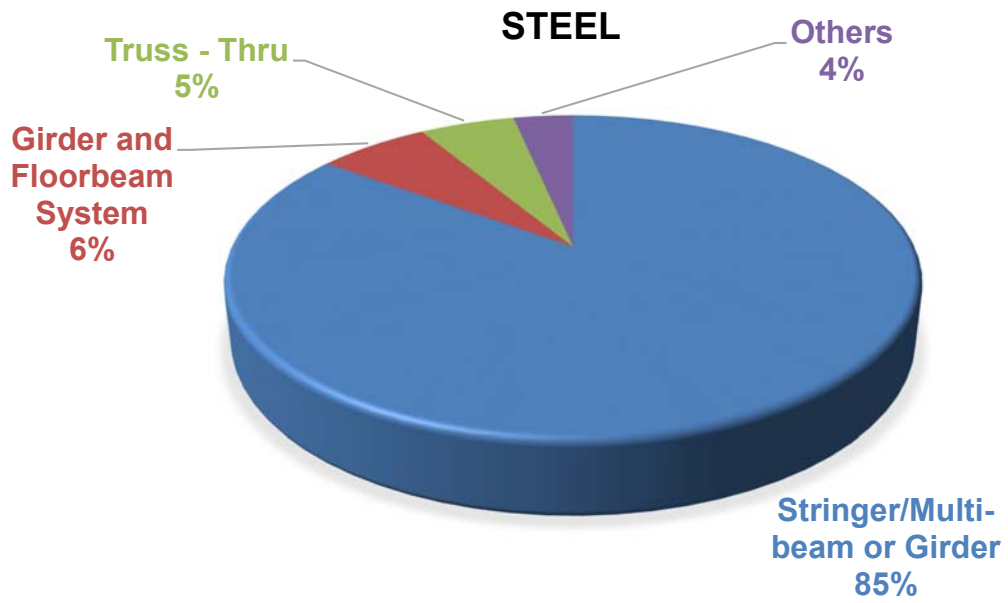


Figure 17. Distribution of structural types in simply supported steel bridges

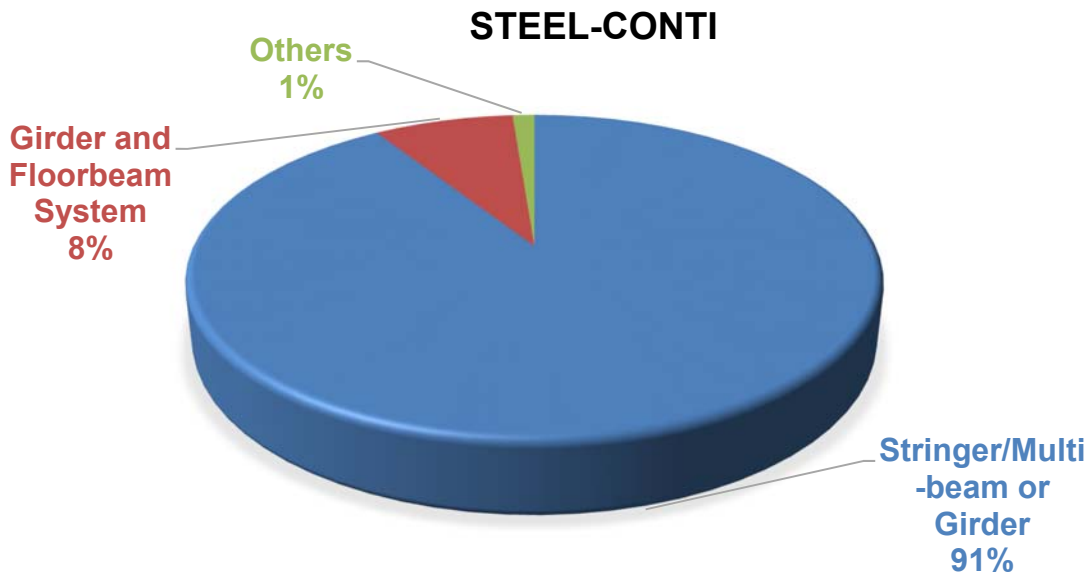


Figure 18. Distribution of structural types in continuous steel bridges

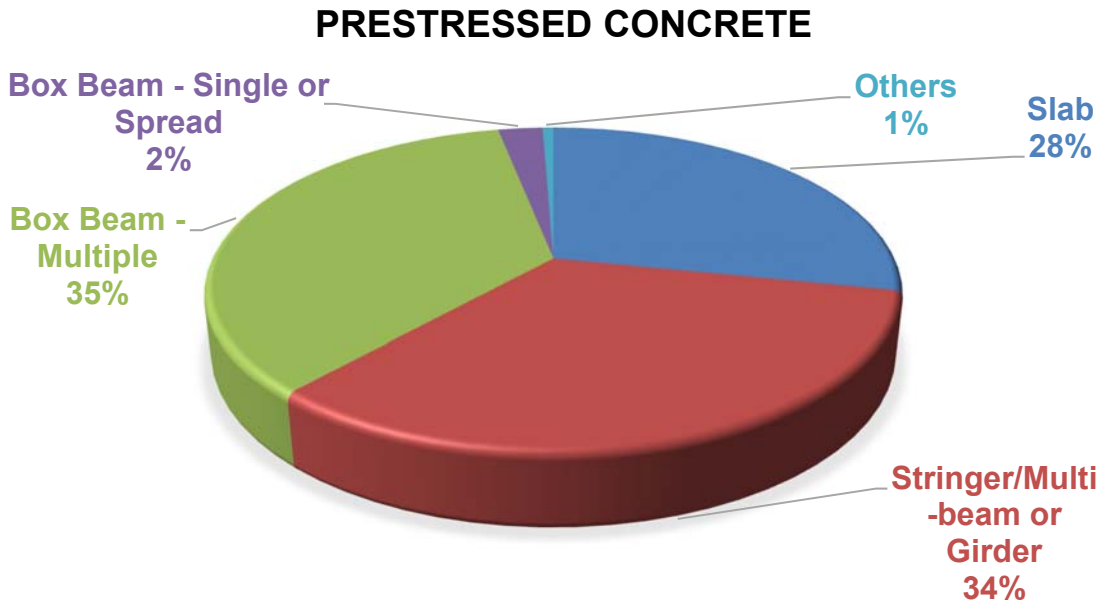


Figure 19. Distribution of structural types in simply supported prestressed concrete bridges

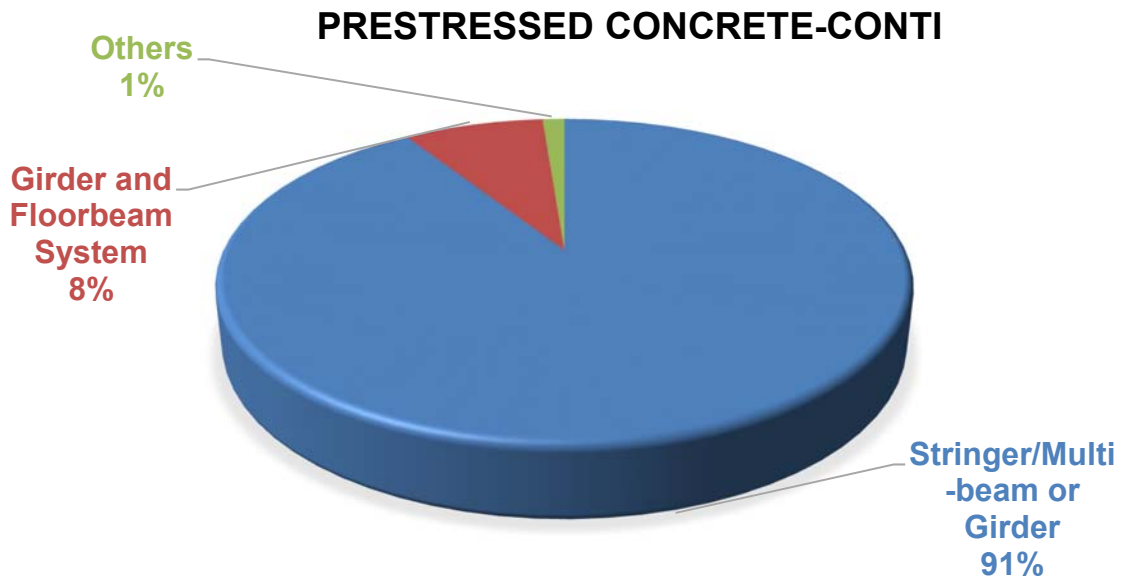


Figure 20. Distribution of structural types in continuous prestressed concrete bridges

Deterioration and Service Life Prediction Models for Highway Bridges

Selection of prototype bridges for analysis

Through a bridge's useful life, it requires both routine and periodic maintenance and occasional rehabilitation work. Especially the deterioration of bridge deck triggers most of the maintenance, rehabilitation, and replacement works since a bridge deck is the most immediate component of a bridge structure exposed to the impact of traffic and climatic changes. In this study, the cost impact of overweight trucks on the highway bridges system is quantified by Bridge Life-Cycle Cost Analysis (BLCCA). However, the estimate of bridge's life cycle costs is dependent on reasoned estimates of the service lives of various bridge components.

From the classification of highway bridge inventory in New Jersey as shown in Figure 21, four types of bridges were selected for analysis including 1) simple span steel multi-beam bridges, 2) simple span steel girder-floorbeam bridge, and 3) simple span prestressed concrete multi-beam bridge.

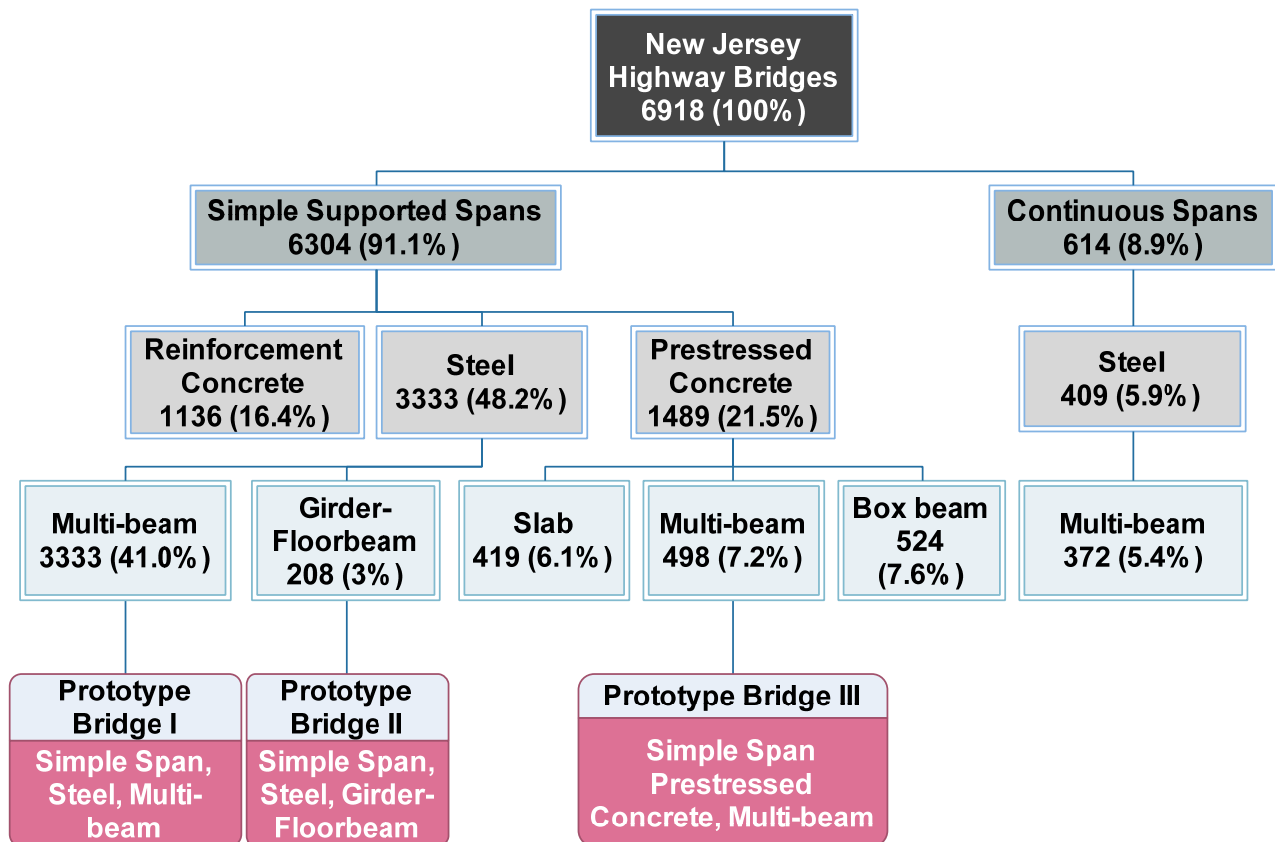


Figure 21. Selection of prototype bridges for analysis

In this study, the economic impact is the fatigue-related cost which are corresponding to bridge deterioration models while routine maintenance cost can be determined from current NJDOT practice and maintenance cost history. In order to quantify the damage cost effect of overweight truck on bridge, three bridge deterioration models are considered in this study and each category will be discussed below:

- Fatigue of existing steel bridge girders,
- Fatigue of prestressed concrete bridges tendons,
- Fatigue of existing RC decks.

Deterioration models for Bridge Girders

Steel Girders

In order to perform bridge life cycle cost for estimation of economic impact of overweight trucks, the service life is needed. The evaluation method employed is based on The Manual for Bridge Evaluation (AASHTO)⁽³⁰⁾. For this method, the remaining life was determined by:

$$Y = \frac{R_g A}{365n (ADTT)_{SL} [(\Delta f)_{eff}]^3} \quad (28)$$

where

R_R = Resistance factor specified for evaluation, minimum, or mean fatigue life as given in Table 7.2.5.2-1, The Manual for Bridge Evaluation (AASHTO)

A = Detail-category constant given in LRFD Design Table 6.6.1.2.5-1, AASHTO LRFD Design Specifications, 2010 [9]

N= Number of stress-range cycles per truck passage estimated, 1 in this case

$(AADT)_{SL}$ = Average number of trucks/day in a single lane averaged over the fatigue life

$(\Delta f)_{eff}$ = The effective stress range

A detailed structural analysis using Finite Element analysis is performed in Appendix B. With regards to prototype bridges, the stress range is obtained under various loading conditions from WIM data. After the structural analysis and fatigue life estimation, this study considers two scenarios to quantify the economic impact of overweight trucks: Case 1 all trucks that represent current truck traffic with all overweight trucks and Case 2 legal truck traffic only without overweight trucks. BLCCA was performed for both scenarios. The annual maintenance costs are assumed to be the same for both scenarios. An analysis period of 75 years was used. The bridge replacement cost is assumed as \$330 per ft². Percentage increases in annual truck traffic are assumed as 2.25, 1.5, and 1.5 for interstate highways, US numbered highways, and NJ state highways, respectively. The discount rate is assumed as 3 percent. The analysis results of BLCCA of Prototype Bridge I and Prototype Bridge II were summarized in Table 18 and Table 19.

Table 18 - Summary of bridge girder life cycle cost analysis for Prototype Bridge I

Route (WIM sites)	Service Year(w)	Service Year(wo)	EUAC(w)	EUAC(wo)	Cost Difference	Overweight part	Permit truck	Life Reduction
	(years)	(years)	(\$/year/ft2)	(\$/year/ft2)	(\$/year/ft2)	(\$/kips/ft2/year)	(\$/kips/ft2/year)	(%)
I-195	131	188	10.59	10.38	0.21	1.03E-07	2.68E-08	30%
I-280(280)	221	238	10.31	10.28	0.03	2.41E-07	4.37E-08	7%
I-287(287)	95	105	10.85	10.76	0.09	1.84E-07	1.80E-08	10%
I-287(A87)	99	103	10.82	10.78	0.04	1.02E-07	9.70E-09	4%
I-78(78A)	56	60	12.43	12.07	0.36	1.90E-07	1.12E-08	7%
I-78(78D)	97	103	10.84	10.78	0.06	1.13E-07	1.03E-08	6%
I-78(78W)	87	102	10.95	10.79	0.16	7.62E-08	1.02E-08	15%
I-80(80B)	143	152	10.54	10.50	0.04	8.28E-08	1.36E-08	6%
I-95(95B)	107	153	10.75	10.49	0.26	1.38E-07	2.01E-08	30%
I-676(676)	162	191	10.46	10.38	0.08	8.13E-07	6.08E-08	15%
I-295(295)	95	104	10.85	10.77	0.08	8.11E-08	9.77E-09	9%
US-1(001)	194	243	10.37	10.27	0.09	1.23E-07	1.70E-08	20%
US-30(30M)	338	364	10.17	10.15	0.02	4.46E-07	5.31E-08	7%
US-9(09A)	240	269	10.28	10.24	0.04	1.46E-07	2.34E-08	11%
US-22(022)	279	336	10.22	10.17	0.05	2.31E-07	3.40E-08	17%
US-40(040)	229	295	10.30	10.21	0.09	1.67E-07	2.58E-08	22%
US-46(046)	324	358	10.18	10.15	0.03	2.79E-07	4.18E-08	9%
US-130(13A)	341	356	10.17	10.16	0.01	3.81E-07	6.17E-08	4%
US-202(02B)	255	273	10.26	10.23	0.02	1.78E-07	2.57E-08	7%
US-206(206)	286	327	10.22	10.18	0.04	1.84E-07	3.19E-08	12%
US-322(322)	323	401	10.18	10.13	0.05	4.48E-07	8.60E-08	19%
NJ-15	214	298	10.32	10.20	0.12	1.21E-07	1.75E-08	28%
NJ-18(18D)	330	343	10.18	10.16	0.01	2.79E-07	3.80E-08	4%
NJ-18(018)	264	324	10.24	10.18	0.06	2.12E-07	3.07E-08	19%

Route (WIM sites)	Service Year(w)	Service Year(wo)	EUAC(w)	EUAC(wo)	Cost Difference	Overweight part	Permit truck	Life Reduction
	(years)	(years)	(\$/year/ft2)	(\$/year/ft2)	(\$/year/ft2)	(\$/kips/ft2/year)	(\$/kips/ft2/year)	(%)
NJ-31	235	330	10.29	10.18	0.11	1.43E-07	3.17E-08	29%
NJ-33	277	317	10.23	10.19	0.04	1.77E-07	2.82E-08	13%
NJ-34	343	378	10.16	10.14	0.02	3.36E-07	5.79E-08	9%
NJ-55(551)	147	210	10.52	10.33	0.19	1.02E-07	1.29E-08	30%
NJ-68	392	406	10.13	10.12	0.01	4.81E-07	7.93E-08	3%
NJ-72	309	369	10.19	10.15	0.05	2.28E-07	3.69E-08	16%
NJ-73	327	388	10.18	10.13	0.04	2.40E-07	4.75E-08	16%
NJ-94	319	379	10.18	10.14	0.05	2.48E-07	3.98E-08	16%
NJ-124	484	507	10.09	10.08	0.01	1.15E-06	1.98E-07	5%
NJ-138	352	393	10.16	10.13	0.03	1.61E-07	4.29E-08	10%
NJ-168	450	466	10.10	10.09	0.01	7.72E-07	1.01E-07	3%

Table 19 - Summary of bridge girder life cycle cost analysis for Prototype Bridge II

Route (WIM site)	Service Life (Case 1)	Service Life (Case 2)	EUAC (Case 1)	EUAC (Case 2)	Cost Difference	Unit Cost (Overweight part)	Unit Cost (whole truck)	Life Reduction
	(years)	(years)	(\$/year/ft ²)	(\$/year/ft ²)	(\$/year/ft ²)	(\$/kips/ft ² /year)	(\$/kips/ft ² /year)	(%)
I-195	93	147	10.88	10.52	0.36	1.77E-07	4.62E-08	37%
I-280(280)	179	197	10.41	10.36	0.04	3.56E-07	6.45E-08	9%
I-287(287)	61	70	12.01	11.40	0.61	1.20E-06	1.18E-07	13%
I-287(A87)	64	68	11.79	11.54	0.25	6.64E-07	6.34E-08	5%
I-78(78A)	31	34	16.74	15.80	0.94	4.89E-07	2.88E-08	9%
I-78(78D)	63	68	11.89	11.52	0.37	7.40E-07	6.77E-08	8%
I-78(78W)	54	67	12.64	11.58	1.06	5.03E-07	6.76E-08	20%
I-80(80B)	104	112	10.78	10.71	0.07	1.46E-07	2.39E-08	7%
I-95(95B)	71	113	11.33	10.70	0.63	3.38E-07	4.94E-08	37%
I-676(676)	122	150	10.64	10.50	0.14	1.33E-06	9.96E-08	19%
I-295(295)	61	69	12.01	11.46	0.55	5.31E-07	6.40E-08	11%
US-1(001)	137	183	10.56	10.40	0.16	2.17E-07	3.00E-08	25%
US-30(30M)	276	302	10.23	10.20	0.03	6.53E-07	7.76E-08	9%
US-9(09A)	181	209	10.40	10.33	0.07	2.43E-07	3.87E-08	13%
US-22(022)	219	274	10.32	10.23	0.08	3.56E-07	5.25E-08	20%
US-40(040)	170	234	10.43	10.29	0.15	2.75E-07	4.24E-08	27%
US-46(046)	263	296	10.25	10.21	0.04	4.13E-07	6.19E-08	11%
US-130(13A)	279	294	10.23	10.21	0.02	5.59E-07	9.04E-08	5%
US-202(02B)	195	213	10.36	10.33	0.04	2.90E-07	4.20E-08	8%
US-206(206)	225	266	10.30	10.24	0.06	2.83E-07	4.91E-08	15%
US-322(322)	262	339	10.25	10.17	0.08	6.50E-07	1.25E-07	23%
NJ-15	156	237	10.48	10.28	0.20	2.01E-07	2.92E-08	34%
NJ-18(18D)	268	281	10.24	10.22	0.02	4.14E-07	5.65E-08	5%

Route (WIM site)	Service Life (Case 1)	Service Life (Case 2)	EUAC (Case 1)	EUAC (Case 2)	Cost Difference	Unit Cost (Overweight part)	Unit Cost (whole truck)	Life Reduction
	(years)	(years)	(\$/year/ft ²)	(\$/year/ft ²)	(\$/year/ft ²)	(\$/kips/ft ² /year)	(\$/kips/ft ² /year)	(%)
NJ-18(018)	204	263	10.35	10.25	0.10	3.33E-07	4.81E-08	23%
NJ-31	176	268	10.42	10.24	0.18	2.30E-07	5.09E-08	34%
NJ-33	216	255	10.32	10.26	0.06	2.76E-07	4.40E-08	15%
NJ-34	282	316	10.22	10.19	0.04	4.86E-07	8.38E-08	11%
NJ-55(551)	95	152	10.86	10.50	0.36	1.95E-07	2.49E-08	38%
NJ-68	330	344	10.18	10.16	0.01	6.72E-07	1.11E-07	4%
NJ-72	248	307	10.27	10.20	0.07	3.39E-07	5.48E-08	19%
NJ-73	266	326	10.24	10.18	0.06	3.50E-07	6.91E-08	18%
NJ-94	257	317	10.25	10.19	0.07	3.64E-07	5.85E-08	19%
NJ-124	421	445	10.12	10.10	0.01	1.50E-06	2.59E-07	5%
NJ-138	290	331	10.21	10.17	0.04	2.31E-07	6.14E-08	12%
NJ-168	388	404	10.13	10.12	0.01	1.03E-06	1.35E-07	4%

Prestressed Concrete Structures

An investigation on the fatigue behavior of pretensioned concrete girders was conducted by Overman et al. (1984)⁽⁹⁷⁾. This study included an extensive literature review and full-scale fatigue tests of flexural prestressed concrete girders. In addition to the behavior of the whole girders, the fatigue behaviors of the girder components such as the concrete, steel rebars and prestressing strands, as well as the interaction between these materials were discussed. According to a study by the American Concrete Institute (ACI) Committee 215 (ACI 1974), progressive cracking may occur in concrete and fatigue failure may occur after a certain number of repetitive loadings even when the maximum stress of the repetitive loadings is less than the concrete's static strength⁽⁹⁸⁾. In the ACI-215 study (ACI 1974), concrete fatigue strength was determined as a fraction of the concrete static strength.

In the Overman's study, it was found that among the different fatigue failure mechanisms of prestressed concrete girders, the most common fatigue failure was the prestressing strands fatigue fracture (Overman et al. 1984)⁽⁹⁷⁾. Especially when cracks occurred in prestressed girders, strands fatigue was more likely to occur at cracked locations because of increased stress range in strands at these cracked locations. To estimate the prestressing strands fatigue life, the following equation by Paulson et al. (1983) can be used⁽⁹⁹⁾:

$$\log N = 11 - 3.5 \times \log \sigma \quad (29)$$

where

N = fatigue life in number of cycles; and

σ = strand stress range.

Using the similar approach for steel bridge girder, the fatigue life of a prestressed concrete can be estimated by the equation below:

$$Y = \frac{\log \left(1 - \frac{(1-u) \times 10^{11-3.5 \log S_r}}{T_o} \right)}{\log u} \quad (30)$$

where

Y is the estimated fatigue life;

u is the annual traffic increase; and

T_o is the single lane ADTT.

Detailed structure analysis using Finite Element method is summarized in Appendix B. With the prototype bridges, the stress range was obtained under various loading condition from WIM data. The summary of BLCCA is shown in Table 20.

Table 20 - Summary of bridge girder life cycle cost analysis for Prototype Bridge III

Route ID	Service Life (Case 1)	Service Life (Case 2)	EUAC (Case 1)	EUAC (Case 2)	Cost Difference	Unit Cost (Overweight part)	Unit Cost (whole truck)	Life Reduction
Unit	(years)	(years)	(\$/year/ft ²)	(\$/year/ft ²)	(\$/year/ft ²)	(\$/kips/ft ² /year)	(\$/kips/ft ² /year)	(%)
I-195	130	196	10.60	10.36	0.23	1.15E-07	3.00E-08	33%
I-280(280)	223	243	10.31	10.27	0.03	2.68E-07	4.84E-08	8%
I-287(287)	95	107	10.85	10.75	0.11	2.08E-07	2.03E-08	11%
I-287(A87)	98	103	10.83	10.78	0.04	1.14E-07	1.09E-08	5%
I-78(78A)	55	59	12.56	12.16	0.40	2.06E-07	1.21E-08	7%
I-78(78D)	98	105	10.83	10.76	0.06	1.25E-07	1.14E-08	7%
I-78(78W)	86	103	10.96	10.78	0.18	8.58E-08	1.15E-08	17%
I-80(80B)	142	152	10.54	10.50	0.04	9.24E-08	1.52E-08	6%
I-95(95B)	105	158	10.77	10.48	0.29	1.56E-07	2.28E-08	33%
I-676(676)	165	199	10.45	10.36	0.09	8.92E-07	6.68E-08	17%
I-295(295)	96	106	10.85	10.75	0.09	8.95E-08	1.08E-08	10%
US-1(001)	191	246	10.38	10.27	0.11	1.41E-07	1.95E-08	22%
US-30(30M)	341	372	10.17	10.14	0.02	5.00E-07	5.95E-08	8%
US-9(09A)	243	276	10.27	10.23	0.05	1.63E-07	2.60E-08	12%
US-22(022)	279	344	10.23	10.16	0.06	2.60E-07	3.83E-08	19%
US-40(040)	224	299	10.31	10.20	0.10	1.93E-07	2.98E-08	25%
US-46(046)	328	366	10.18	10.15	0.03	3.11E-07	4.65E-08	11%
US-130(13A)	345	363	10.16	10.15	0.01	4.27E-07	6.90E-08	5%
US-202(02B)	257	278	10.25	10.23	0.03	1.99E-07	2.88E-08	7%
US-206(206)	287	334	10.22	10.17	0.04	2.06E-07	3.57E-08	14%
US-322(322)	323	413	10.18	10.12	0.06	5.04E-07	9.66E-08	22%
NJ-15	211	306	10.33	10.20	0.13	1.36E-07	1.97E-08	31%
NJ-18(18D)	338	353	10.17	10.16	0.01	3.04E-07	4.16E-08	4%

Route ID	Service Life (Case 1)	Service Life (Case 2)	EUAC (Case 1)	EUAC (Case 2)	Cost Difference	Unit Cost (Overweight part)	Unit Cost (whole truck)	Life Reduction
NJ-18(018)	261	330	10.25	10.18	0.07	2.41E-07	3.49E-08	21%
NJ-31	226	334	10.30	10.17	0.13	1.68E-07	3.71E-08	32%
NJ-33	279	325	10.22	10.18	0.05	1.96E-07	3.13E-08	14%
NJ-34	349	389	10.16	10.13	0.03	3.72E-07	6.41E-08	10%
NJ-55(551)	141	213	10.55	10.33	0.22	1.19E-07	1.51E-08	34%
NJ-68	399	415	10.13	10.12	0.01	5.37E-07	8.85E-08	4%
NJ-72	308	376	10.19	10.14	0.05	2.56E-07	4.14E-08	18%
NJ-73	331	400	10.17	10.13	0.05	2.65E-07	5.23E-08	17%
NJ-94	319	389	10.18	10.13	0.05	2.76E-07	4.43E-08	18%
NJ-124	494	521	10.08	10.07	0.01	1.27E-06	2.19E-07	5%
NJ-138	358	405	10.15	10.12	0.03	1.76E-07	4.69E-08	12%
NJ-168	463	482	10.10	10.09	0.01	8.31E-07	1.09E-07	4%

Effect of Truck Classifications on Girder Deterioration

Deterioration models for Bridge Deck

From the literature review, the deterioration of bridge deck usually comes from various factors. A reliable prediction of service life of deteriorating highway bridge deck under different loading conditions is needed for a rational life-cycle cost analysis.

Service Life of Highway Bridge Deck in New Jersey

The expected trend in the deterioration process is that if there is no improvement made to a bridge member, its condition rating either remains the same or falls to a lower value as the bridge ages. Although there is reconstruction information in the NBI database, there are still lots of unrecorded repair or reconstruction activities on the bridge members due to their sudden increase in condition rating ^(102, 103, 104). Therefore, it is important to check the validity of condition rating by examining the records of each bridge. The flowchart describing validation procedure is shown in Figure 22. The age of a bridge is captured when the rating is downgraded. The deterioration data indicated that outliers consist of the few data points with age less than 10 years and condition ratings below 6 as well as data points with age 40 years or older and condition ratings above 7. In order to partially address this issue, Morcouc developed a criterion for the maximum and minimum age number for each condition rating as follows ⁽¹⁰³⁾:

- Condition rating 9 age less than 0 and more than 30 years;
- Condition rating 8 age less than 0 and more than 40 years;
- Condition rating 7 age less than 0 and more than 50 years;
- Condition rating 6 age less than 10 and more than 60 years;
- Condition rating 5 age less than 20 and more than 70 years;
- Condition rating 4 age less than 30 and more than 80 years.

The deterioration model assumed here was a third order polynomial function of bridge age in years:

$$CR = M_0 + M_1x + M_2x^2 + M_3x^3 \quad (31)$$

where

CR = the Bridge Condition Rating, x is the age of bridge in years; and M_0 , M_1 , M_2 , and M_3 = the parameters from regressions.

Figure 25 shows the deterioration curves of bridges deck on different highways. Previous studies concluded that bridge decks usually experienced replacement when the condition rating downgraded to 4 (see references 102, 103, 104 and 105). Therefore, the service life of bridge decks on each highway is determined at the age of deck when the condition rating downgraded to 4. Note that the service life from Figure 25 represents the mean value of service life on each highway. The average service life of bridge decks on interstate highways, US numbered highways, and NJ state highways are 36.8, 48.4, and 52 years respectively. The bridge decks on interstate highway deteriorated with the highest rate while the decks on NJ State Highway deteriorated much more slowly. The deterioration curve of bridge deck for available highways are provided in Appendix A.

Loading on Bridge Deck

The WIM data was collected from various WIM sites the operated by NJDOT. The raw data contains all traffic including cars and trucks and a significant amount of erroneous data. A refined data processing program was proposed as shown in Figure 23 to extract two datasets: the “all trucks” dataset, and the “legal trucks” dataset. The “all trucks” dataset reflects the actual truck loading on the bridges that can be used to correlate with the service life obtained from previous section and then service life prediction functions based on wheel weight could be obtained. The “legal trucks” dataset was utilized to predict the service life of deck under legal trucks traffic without overweight trucks. By comparing the service lives of deck under these two truck traffic conditions, the reduction in service life of bridge decks can be calculated. Figure 24 shows the comparisons of ADTT, APD, effective truck weight, equivalent wheel load, average APT, and proportion of overweight trucks over all trucks on the three types of highways. We found that interstate highways have significantly higher ADTT and APD comparing to the other two highway types. The median and average ADTT are 3884 and 4293 for interstate highways, 437 and 616 for US numbered highways, and 405 and 635 for NJ state highways. Meanwhile, we found the average axles per trucks on interstate highway are higher than the other two. In addition, most overweight trucks on interstate highways are Class 9 trucks with five axles while those on US numbered highway and NJ state highway are Class 7 trucks that have four axles. It is important to note that on average, NJ State highway has the highest proportion of overweight trucks. As shown in Figure 24 (e) and (f), although the interstate highway has higher effective truck weight than the other two, all three highway types have comparable equivalent wheel loads due to the fact that trucks on interstate highways usually have more axles. The highest equivalent wheel load of 26.1 kips was observed on US-322. Given the similar wheel load level, the reason that decks on interstate highways deteriorated with the highest rate is because of the enormous values of ADTT and APD.

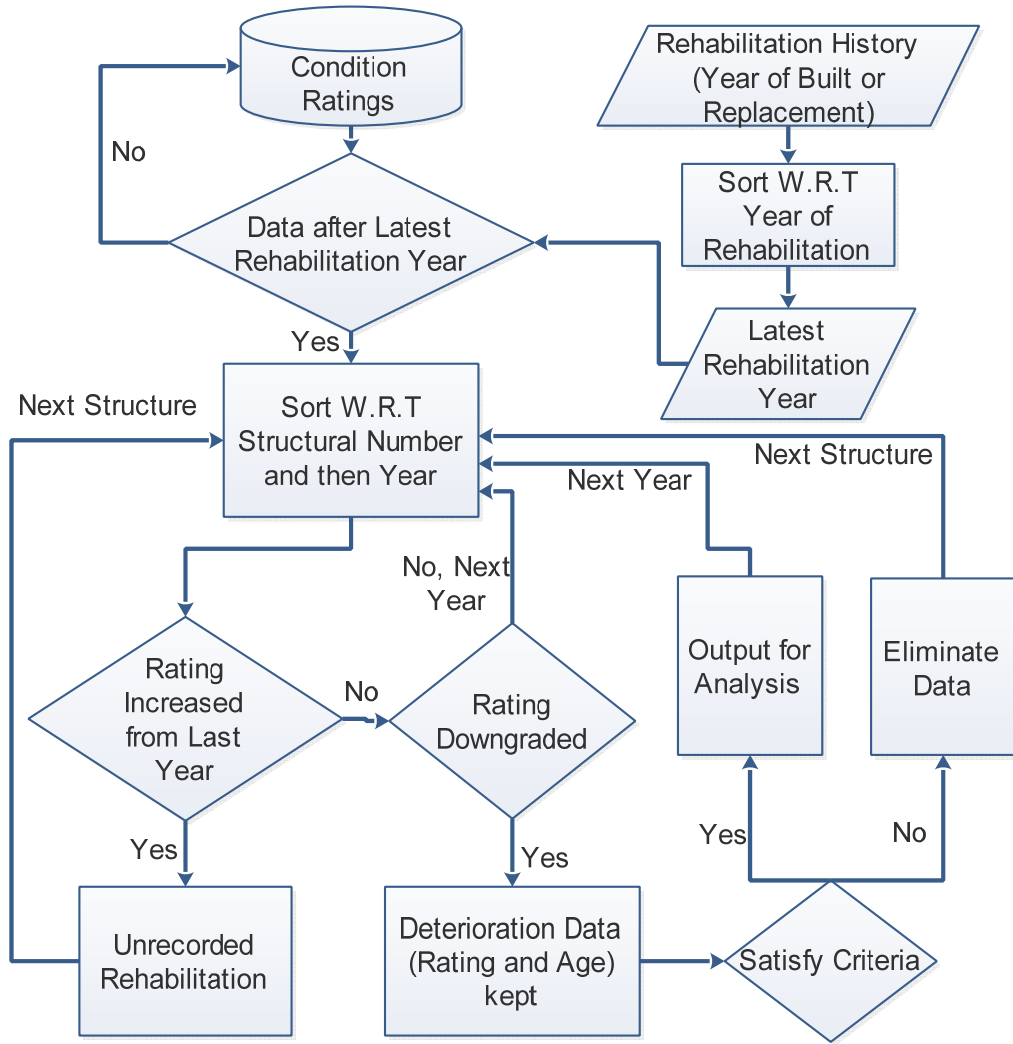


Figure 22. Flowchart for processing deterioration data

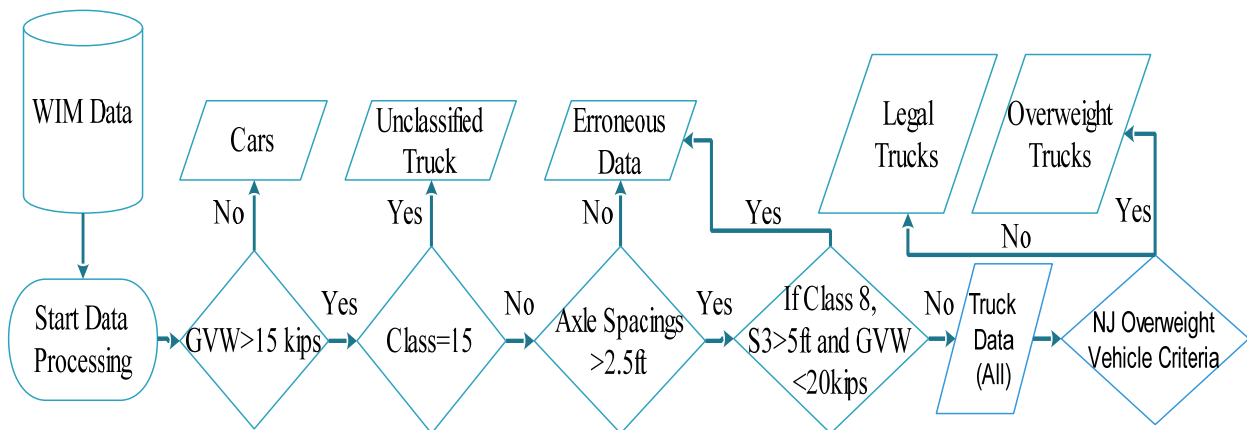
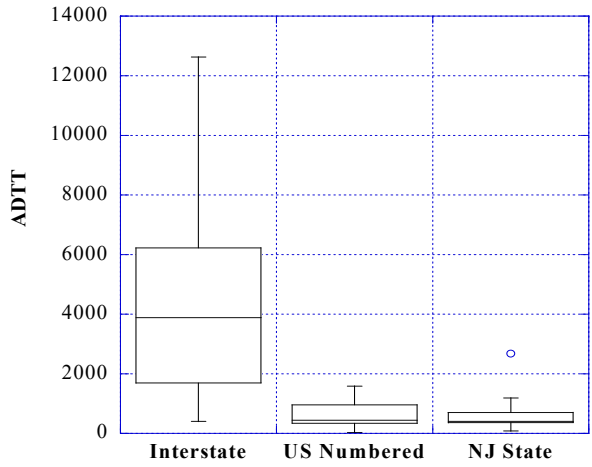
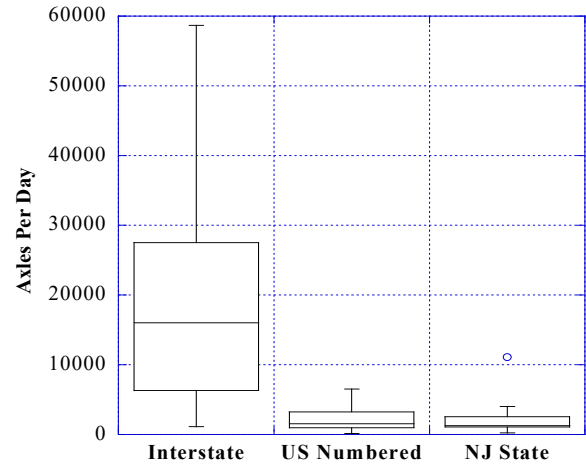


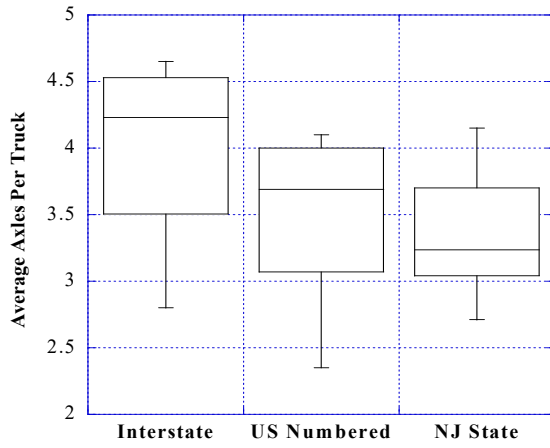
Figure 23. Flowchart for WIM data processing



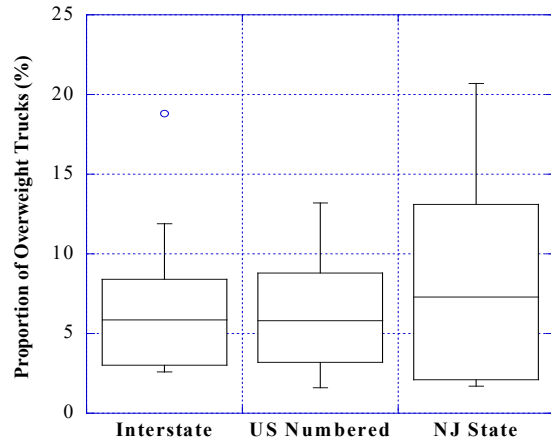
(a)



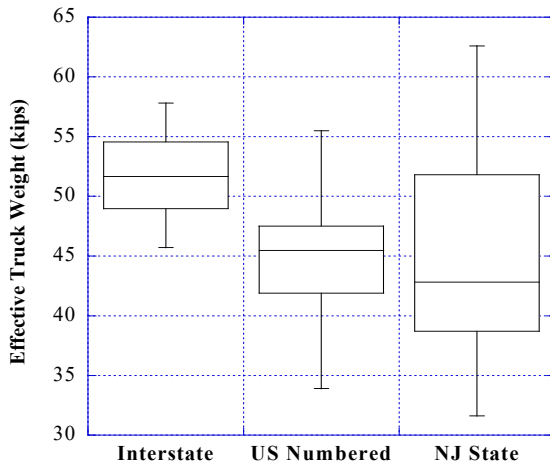
(b)



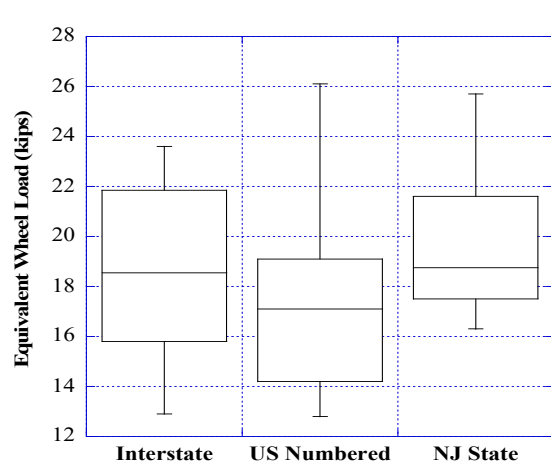
(c)



(d)



(e)



(f)

Figure 24. Statistics of “all trucks” dataset from WIM data

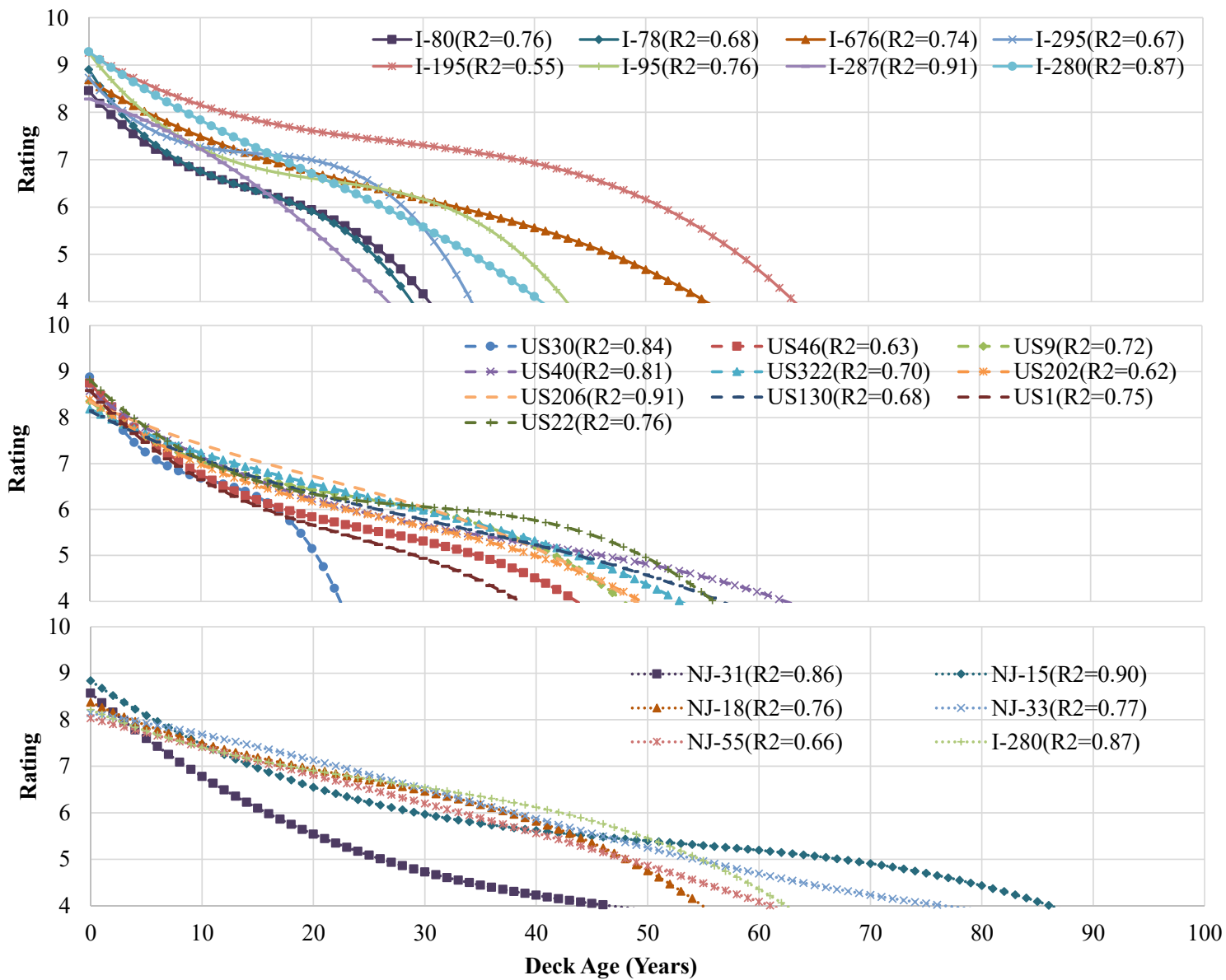


Figure 25. Comparison of deterioration models for bridges on various highways

Correlation between Truck Loading and Deck Service Life

ADTT and APD are considered to be important factors that affect the service life of bridge decks since they indicate the frequency of loading on bridge decks. Datasets that have the comparable wheel weight are extracted and plotted in Figure 26. Different types of highways are treated separately in order to exclude the effect of highway types. Each line in the plot shows that a higher value of APD corresponds to lower service life. Comparing two lines in the same highway, lower wheel load levels correspond to higher service life, when the number of axles per day is held constant. Both parameters play roles in determining the service life of decks. In order to consider both parameters, the capacity of bridge decks herein was defined as the lifetime axle count, N_A , which represents the total number of axles passing the bridge over service life span as below:

$$N_A = \sum_{i=0}^y APD_i * 365 * r \quad (32)$$

where

N_A is the lifetime axle count;

APD_i is average axles per day at year i ;

y is service life in years predicted; and

r is annual truck traffic growth.

The lifetime axle count was plotted versus the equivalent wheel load in Figure 27, and linear regressions were performed for three highway types. Note each data point represents the mean value of lifetime axle counts on one highway that under same equivalent wheel load. The total numbers of bridges considered are 597, 220, and 250 for interstate highway, US numbered highway, and NJ state highway respectively. For interstate highways, US numbered highways, and NJ state highways, the R-squared for linear regression line are 0.83, 0.71, and 0.65 respectively. It is found that service life of decks on interstate highways and NJ state highways are more sensitive than on US numbered highways. Based on the correlations established above, prediction functions are proposed for life axle count based on equivalent wheel load as below, where P is the equivalent wheel load:

$$\begin{aligned}
\text{Interstate } N_A &= 7.2969 \times 10^8 - 2.7825 \times 10^7 \times P \quad R^2=0.83 \\
\text{US Numbered } N_A &= 2.079 \times 10^8 - 6.9013 \times 10^6 \times P \quad R^2=0.71 \\
\text{NJ State } N_A &= 6.9273 \times 10^8 - 2.8852 \times 10^7 \times P \quad R^2=0.65
\end{aligned}
\tag{33}$$

If service life and APD are considered, the functions can be expressed as below. Note, these functions are data-driven models and works for interpretation. In addition, beyond a certain point, the service year of deck is not governed by the wheel loads. Predicted service life of bridge deck is visualized in Figure 28. The annual traffic increase and average APT are taken as 2.25 percent and 4.04, 1.5 percent and 3.53, and 1.5 percent and 3.34 for interstate, US numbered, and NJ state highway respectively where d is the annual truck traffic increase.

$$y = \frac{\log \left[1 + \frac{N_A \times d}{365 \times ADTT \times APT} \right]}{\log(1+d)}
\tag{34}$$

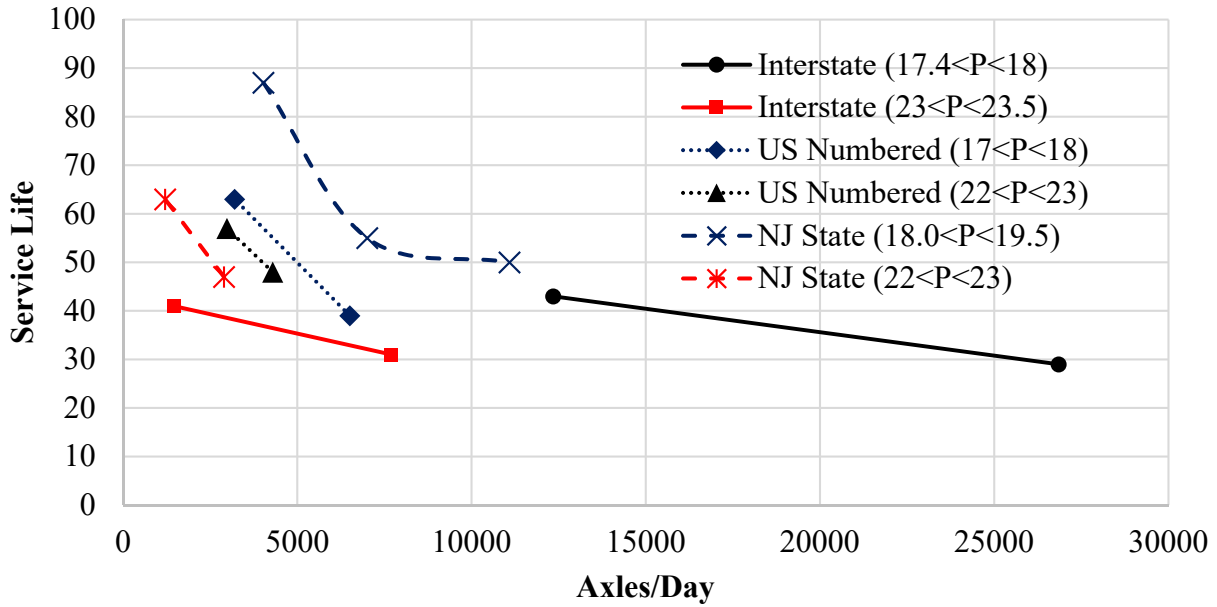


Figure 26. Effect of axles per day on service life of bridge decks

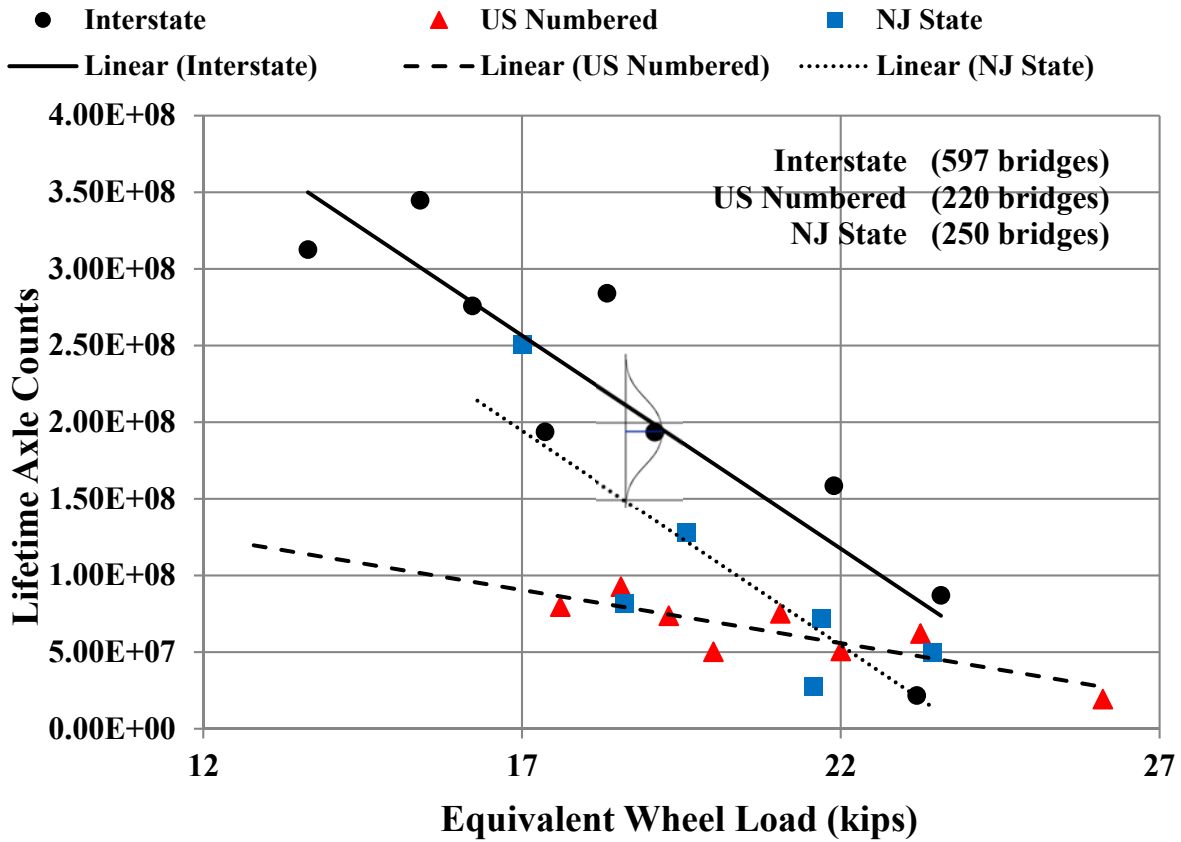
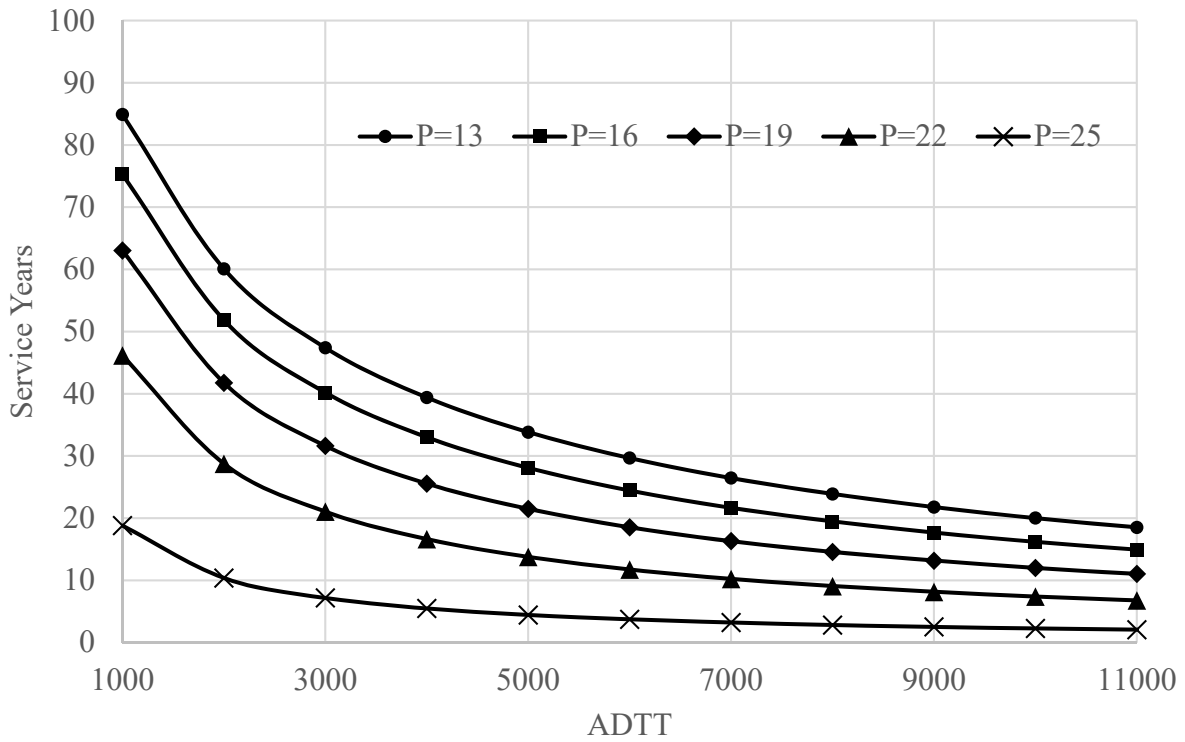
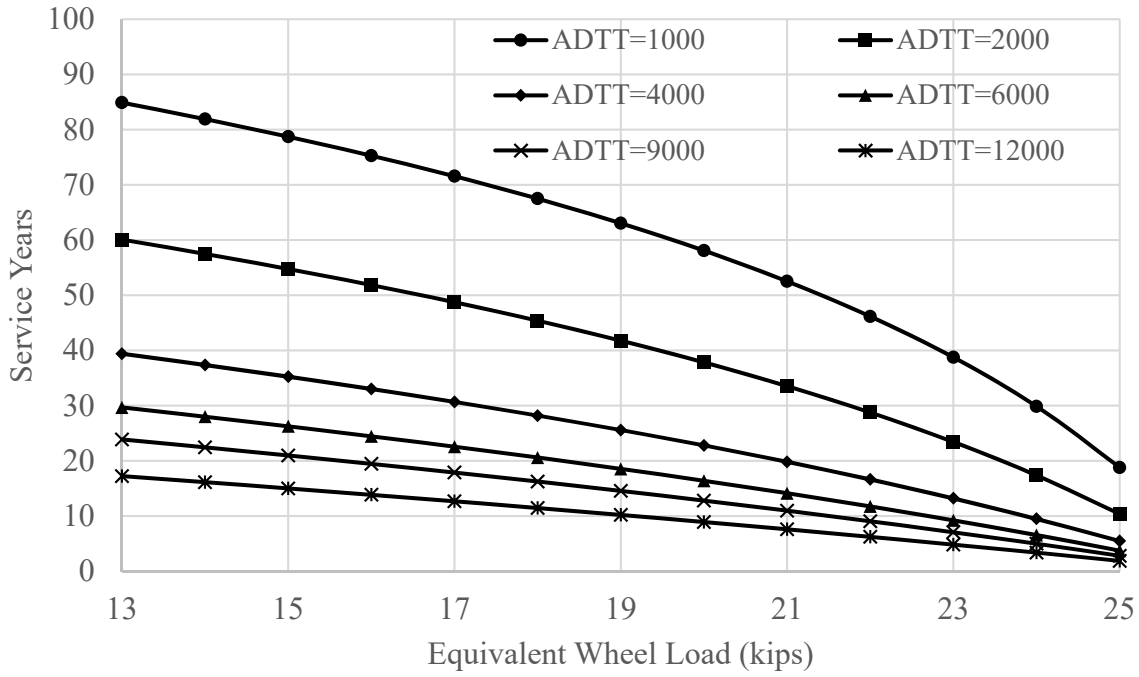
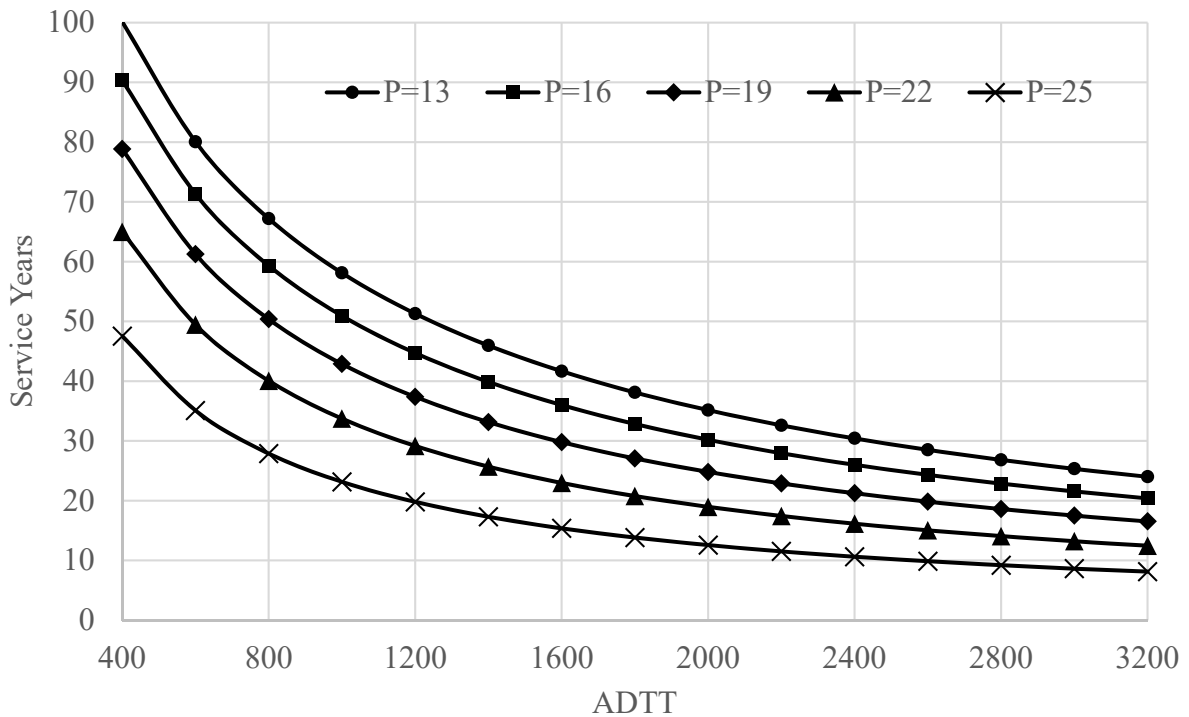
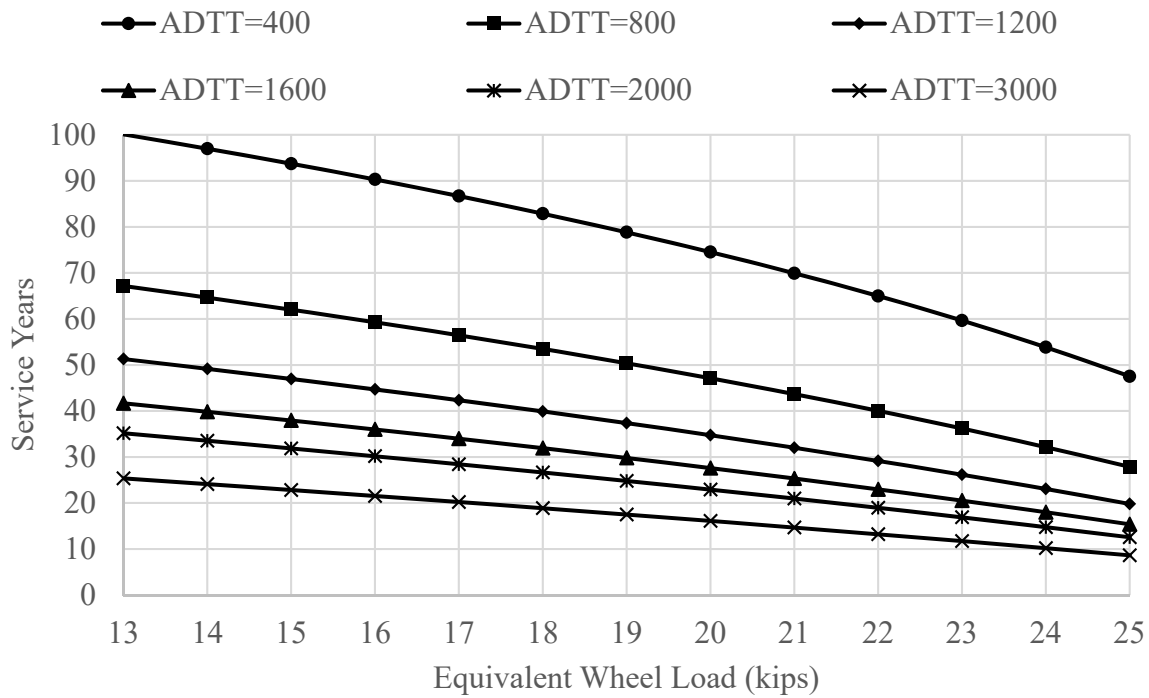


Figure 27. Correlation between lifetime axle counts vs equivalent wheel load



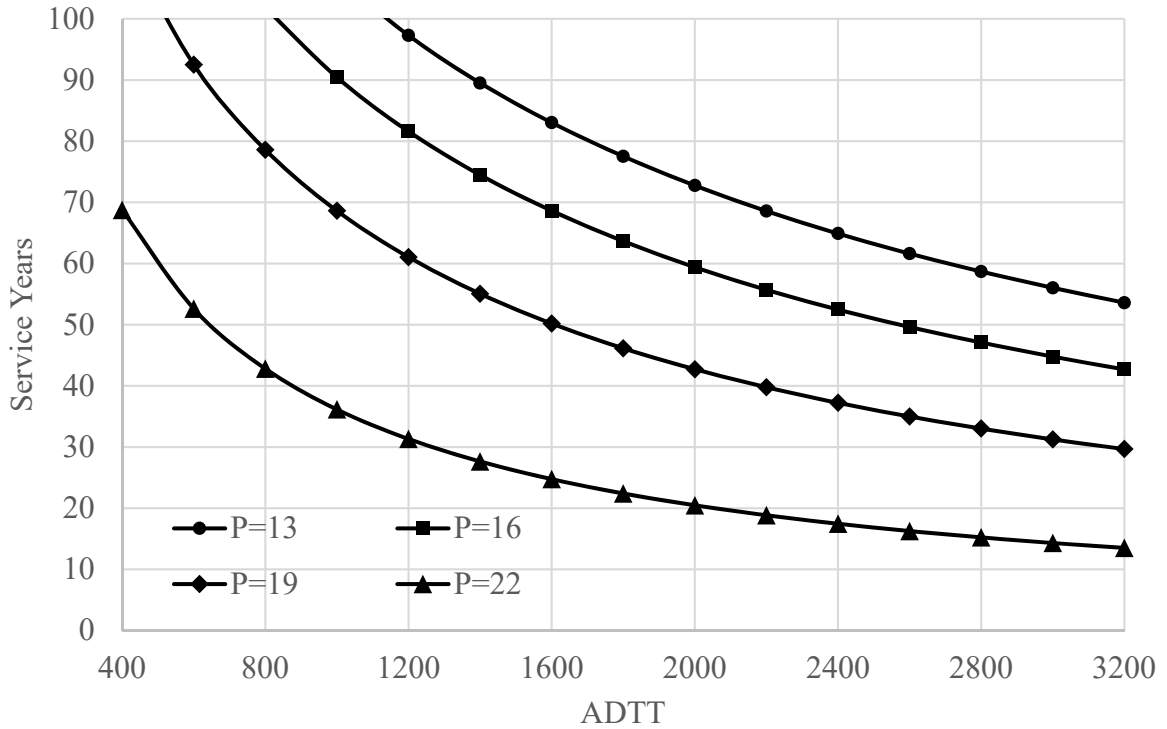
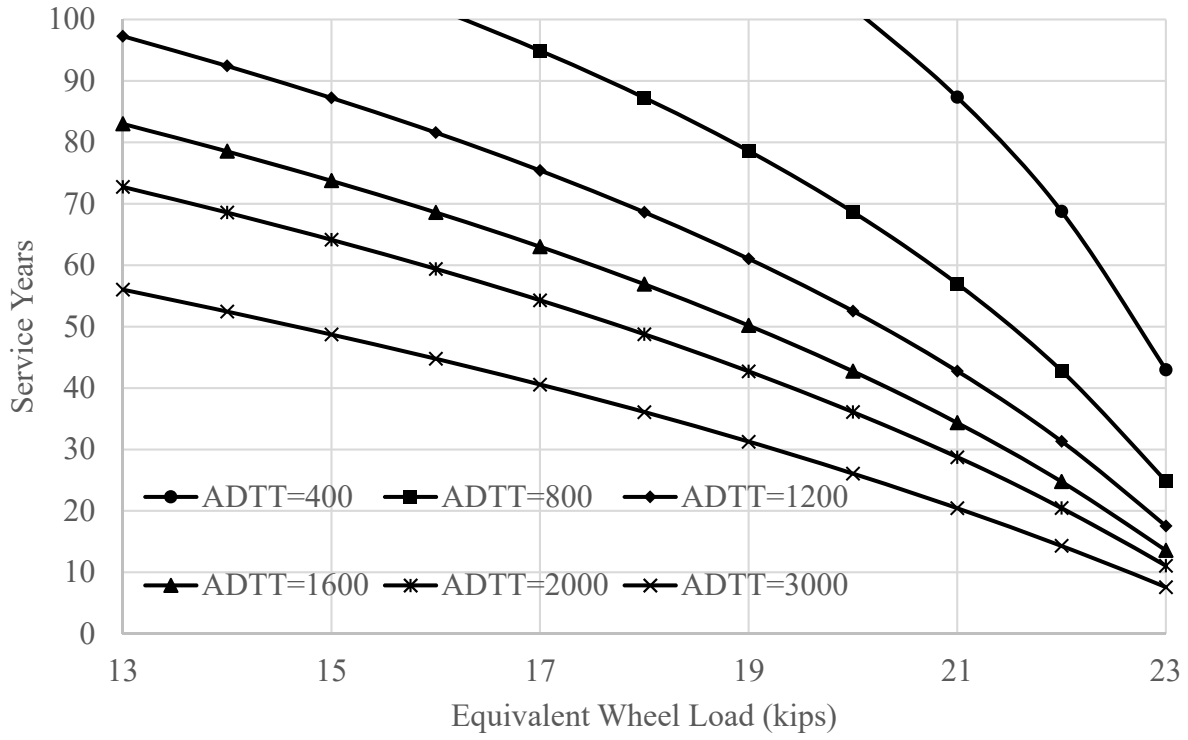
(a)

Figure 28. Predicted service life of deck; (a) interstate highway, (b) US numbered highway, and (c) NJ state highway



(b)

Figure 28. Predicted service life of deck; (a) interstate highway, (b) US numbered highway, and (c) NJ state highway (continued)



(c)

Figure 28. Predicted service life of deck; (a) interstate highway, (b) US numbered highway, and (c) NJ state highway (continued)

Economic impact of overweight trucks on bridge decks

After the prediction function was developed for the service lives of bridge decks, two scenarios are considered in this study to quantify the economic impact of overweight trucks; Case 1: “all trucks,” considers current truck traffic with all trucks—including overweight trucks, and, Case 2: “legal truck traffic,” considers all trucks—excluding overweight trucks. BLCCA is performed for both scenarios. The annual maintenance costs are assumed to be the same for both scenarios. An analysis period of 75 years was used. The deck replacement cost is \$150 per ft². Percentage increases in annual truck traffic are assumed as 2.25, 1.5, and 1.5 for interstate highways, US numbered highways, and NJ state highways, respectively. The discount rate is assumed as 3 percent. The analysis results of BLCCA were summarized in Table 21. Parameters needed from WIM data for two scenarios are also listed. EUAC is annual deck cost per deck area in ft² due to overweight trucks. The unit cost is the cost of unit weight of overweight trucks. It is in dollar per deck ft² per kip. Note that weight of overweight trucks here is the marginal weight of overweight trucks above the legal weight. Boxplots of service life reduction in percent and unit costs for three types of highways are shown in Figure 29. The percentage reductions of service life in average are 29.6, 26.2, and 49.2 for interstate highways, US numbered highways, and NJ state highways, respectively. The overweight trucks induced more costs on decks of NJ state highways than the other two factored highways. This result can be attributed to the following issues unique to NJ highways: 1) NJ state highways have the highest proportion of overweight trucks compared to the other two, 2) overweight trucks introduced much heavier wheel loads than the legal trucks did, and 3) the average number of axles per truck on NJ state highways is relatively less.

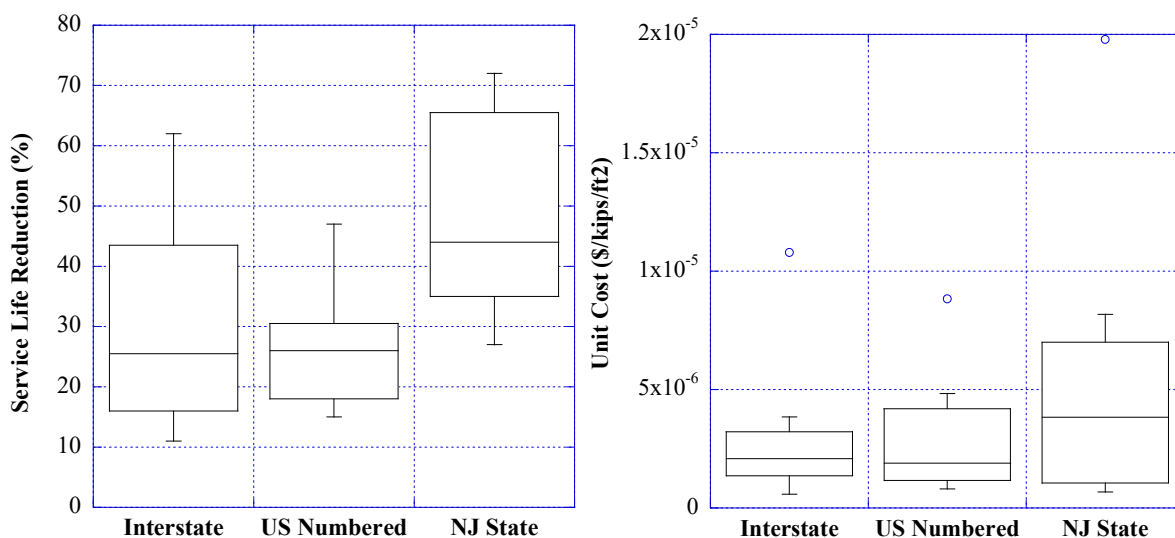


Figure 29. Effect of overweight trucks

Table 21 - Summary of bridge deck life cycle cost analysis

Route (WIM sites)	Service Life (Case 1)	Service Life (Case 2)	EUAC (Case 1)	EUAC (Case 2)	Cost Difference	Unit Cost (Overweight Part)	Unit Cost (Whole Truck)	Life Reduction
	(years)	(years)	(\$/year/ft ²)	(\$/year/ft ²)	(\$/year/ft ²)	(\$/kips/ft ² /year)	(\$/kips/ft ² /year)	(%)
I-195	30	59	7.71	5.53	2.18	1.07E-06	2.80E-07	49%
I-280	63	102	5.39	4.90	0.48	3.85E-06	6.97E-07	38%
I-287 (A87)	19	30	10.48	7.71	2.77	7.29E-06	6.97E-07	37%
I-287 (287)	19	23	10.48	9.16	1.32	2.60E-06	2.55E-07	17%
I-78 (78A)	7	9	23.35	19.23	4.12	2.15E-06	1.27E-07	22%
I-78 (78D)	22	26	9.45	8.41	1.04	2.07E-06	1.90E-07	15%
I-78 (78W)	16	19	11.97	10.48	1.49	7.06E-07	9.48E-08	16%
I-80	18	47	10.93	6.09	4.84	1.08E-05	1.78E-06	62%
I-95	32	43	7.41	6.33	1.09	5.84E-07	8.53E-08	26%
I-676	66	74	5.29	5.07	0.22	2.10E-06	1.57E-07	11%
I-295	21	28	9.77	8.05	1.73	1.66E-06	2.01E-07	25%
US-1	25	36	8.61	6.89	1.72	2.27E-06	3.15E-07	31%
US-30	111	117	4.87	4.85	0.02	4.36E-07	5.19E-08	5%
US-9	29	40	7.87	6.53	1.35	4.83E-06	7.71E-07	28%
US-22	68	85	5.23	4.99	0.25	1.04E-06	1.54E-07	20%
US-40	49	70	5.98	5.18	0.80	1.52E-06	2.34E-07	30%
US-46	80	105	5.02	4.89	0.12	1.31E-06	1.96E-07	24%
US-130	84	96	4.99	4.93	0.06	2.06E-06	3.33E-07	13%
US-202	42	50	6.39	5.93	0.46	3.56E-06	5.15E-07	16%
US-206	70	82	5.18	5.00	0.17	8.10E-07	1.40E-07	15%
US-322	48	90	6.03	4.96	1.07	8.83E-06	1.69E-06	47%
NJ-15	52	78	5.83	5.03	0.80	8.09E-07	1.17E-07	33%

Route (WIM sites)	Service Life (Case 1)	Service Life (Case 2)	EUAC (Case 1)	EUAC (Case 2)	Cost Difference	Unit Cost (Overweight Part)	Unit Cost (Whole Truck)	Life Reduction
	(years)	(years)	(\$/year/ft ²)	(\$/year/ft ²)	(\$/year/ft ²)	(\$/kips/ft ² /year)	(\$/kips/ft ² /year)	(%)
NJ-18 (18D)	54	86	5.74	4.98	0.76	1.98E-05	2.70E-06	37%
NJ-18 (018)	99	139	4.92	4.80	0.12	3.98E-07	5.76E-08	29%
NJ-31	29	103	7.87	4.90	2.97	3.84E-06	8.50E-07	72%
NJ-33	45	119	6.20	4.85	1.36	5.83E-06	9.30E-07	62%
NJ-34	139	171	4.80	4.74	0.06	7.65E-07	1.32E-07	19%
NJ-55	30	41	7.71	6.46	1.25	6.79E-07	8.65E-08	27%
NJ-68	141	183	4.79	4.73	0.07	4.06E-06	6.69E-07	23%
NJ-72	127	168	4.82	4.75	0.08	3.79E-07	6.14E-08	24%
NJ-73	77	137	5.04	4.80	0.23	1.30E-06	2.58E-07	44%
NJ-94	130	167	4.82	4.75	0.07	3.82E-07	6.13E-08	22%
NJ-124	191	261	4.72	4.66	0.06	7.77E-06	1.34E-06	27%
NJ-138	46	148	6.14	4.78	1.36	8.18E-06	2.18E-06	69%
NJ-168	177	207	4.73	4.70	0.03	3.72E-06	4.88E-07	14%

Deterioration and Prediction Models for Pavement

Impact of Overweight Truck on Pavement Life

The objective of this chapter is to evaluate the impact of overweight traffic on pavement life using a mechanistic-empirical analysis approach. The state-of-practice mechanistic-empirical pavement design and analysis software (Pavement-ME) was used to predict pavement life under different traffic loading scenarios. The axle load spectra obtained from WIM data are analyzed, respectively, for the non-overweight and overweight traffic. The pavement structures considered in the analysis include flexible pavement and composite pavement with different combinations of layer thickness. The life reduction ratio at different sites due to overweight traffic was calculated. At the same time, field performance data at the sites where the WIM data were collected are analyzed to estimate the pavement service life at field condition.

WIM Data and Axle Load Spectra

Traffic data is an important data input for MEPDG and the most accurate method to obtain traffic data is the weight-in-motion (WIM) system. WIM systems can continuously measure and store axle load and axle spacing with supplementary data such as date, time, speed, lane of travel, vehicle type, etc. In this study, WIM data at ten sites located at different routes were obtained from the New Jersey Department of Transportation (NJDOT) and used for level-1 traffic input in the M-E analysis. Axles per truck, monthly adjustment factors, and hourly distribution factors were obtained through the post-processing of WIM data.

Currently, the NJDOT regulations dictate the legal GVW as 80,000 lbs., the legal axle weight on a single axle is 22,400 lbs., and the legal tandem axle weight is 34,000 lbs. For a single permit, five dollars per ton is charged once the GVW or axle weight exceeds their legal limits. Besides the excess weight fee, a ten-dollar base fee, a 12-dollar transaction fee, and a 5 percent service fee are included in the permit fee structure. In this study, the WIM data is filtered into two traffic categories. The first category includes the vehicles within the legal weight limit and the second category includes the overloaded vehicles with the GVW or axle load exceeding the legal weight limit.

Table 22 shows the average annual daily truck traffic (AADTT) and the percentage of overweight trucks after analysis of WIM data in 10 selected sites. As expected, the AADTT on the interstate highway is much greater the AADTT on the minor road. However, the percentage of overweight trucks varies in a wide range from 3 percent to 25 percent.

Figure 30(a) and (b) show typical truck class distributions on the interstate highway and the minor road, respectively, for the non-overweight and overweight traffic. It

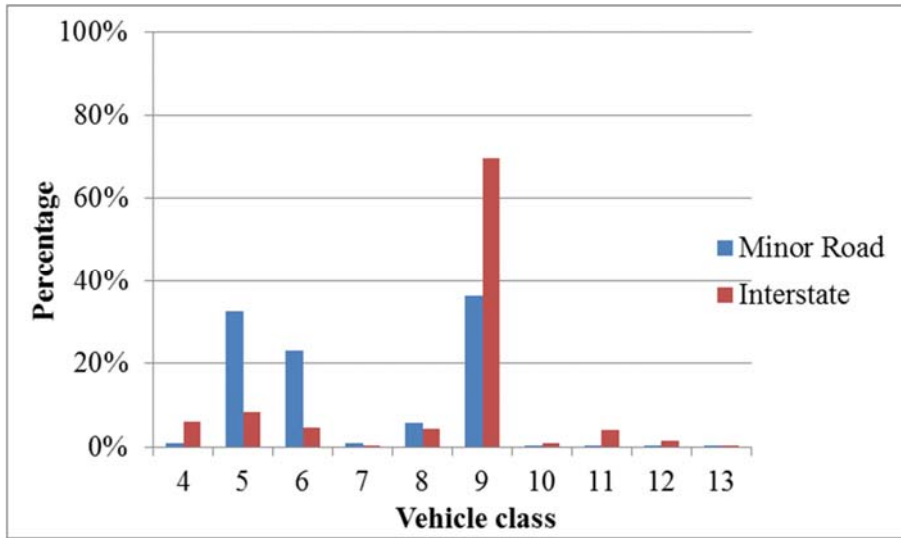
was found that on minor roads the truck traffic composition for the non-overweight traffic mainly includes class 9 (five-axle, single trailer), class 5 (two-axle, single unit), class 6 (three-axle, single unit); while the truck traffic composition for the overweight traffic mainly includes class 9 (five-axle, single trailer) and class 7 (four or more Axles, Single Unit). On the other hand, on the interstate highway, class 9 (five-axle, single trailer) is the dominant truck class for both the non-overweight and overweight traffic.

Table 22 - WIM data at the selected sites

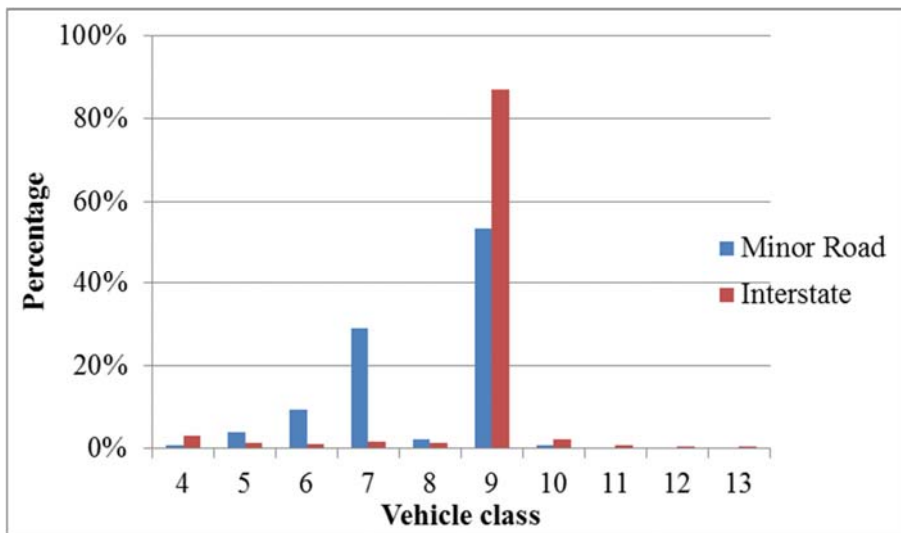
Road type	Site	Route type	Average annual daily truck traffic (AADTT)		Percentage of overweight truck
			Total	Overweight	
Major road	1	Interstate	11739	1970	17%
	2	Interstate	14131	1567	11%
	3	Interstate	3572	686	19%
	4	US Highway	8337	558	7%
	5	Interstate	10747	275	3%
	6	Interstate	13607	899	7%
Minor road	7	State Highway	928	230	25%
	8	State Highway	2710	239	9%
	9	State Highway	1348	143	11%
	10	State Highway	485	26	5%

Figure 31 shows the axle load spectra of Class 9 vehicles in the non-overweight traffic, respectively, on the Interstate highway and minor road. The results show that on minor road, the single axle and tandem axle have most axle loads around 10 kips. Most of tridem axles have loads between 10 and 20 kips. On the interstate highway, the single axle has the similar axle load spectra as the one on the minor road. However, the tandem axle has a wide distribution of load ranging from 6 kips to 36 kips and the tridem axle has a wide distribution of load ranging from 12 kips to 51 kips. The data clearly show that the trucks travelled on the interstate highway have the greater axle loads than the trucks on the minor road.

Figure 32 shows the axle load spectra of Class 9 vehicles in the overweight traffic, respectively, on the interstate highway and the minor road. The results show that the single axle and tandem axle have the similar loading distribution patterns on the interstate highway and the minor road, although the percentage of axle loads within the specific load ranges are different. Two peaks were observed in the distribution of single axle loads and one peak was observed in the distribution of tandem axle loads. On the interstate highway, the tridem axle has a peak distribution at 50 kips, which contributes significantly to the total vehicle weight.

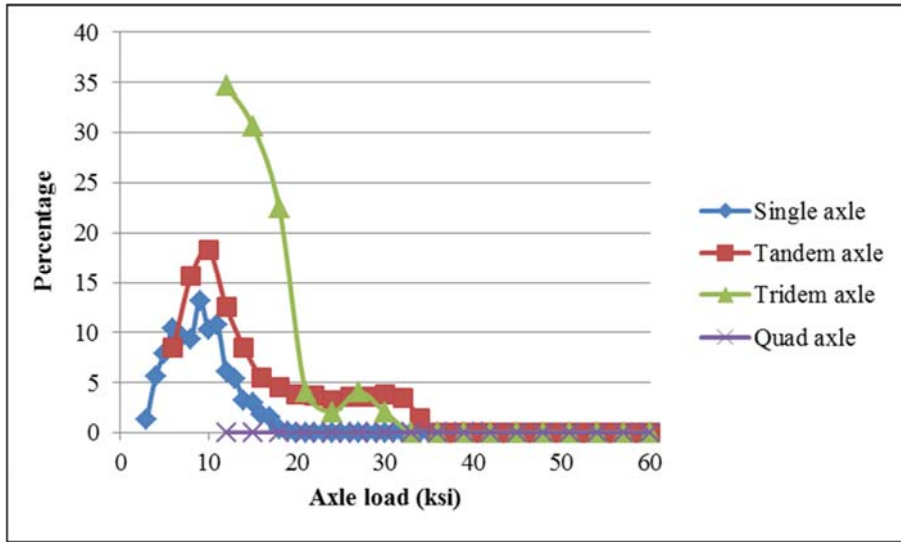


(a)

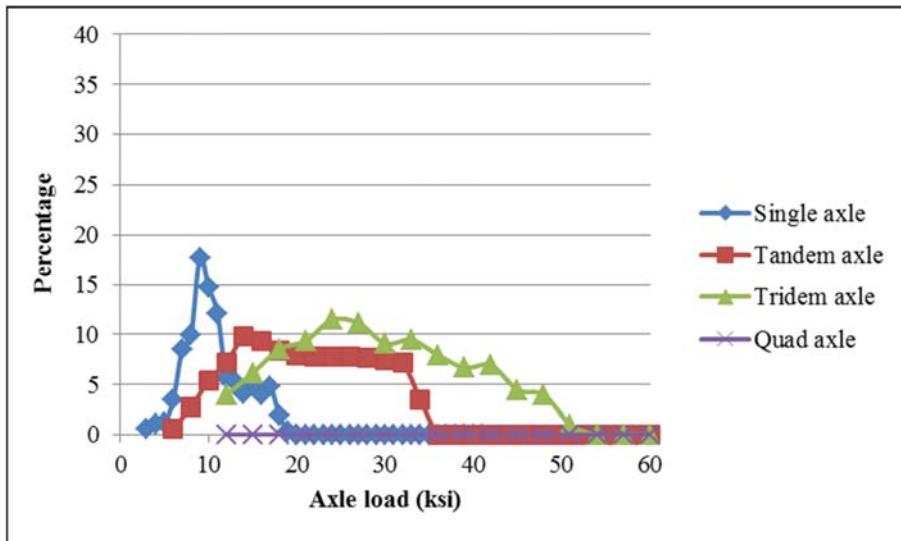


(b)

Figure 30. Vehicle class distributions for (a) non-overweight and (b) overweight traffic

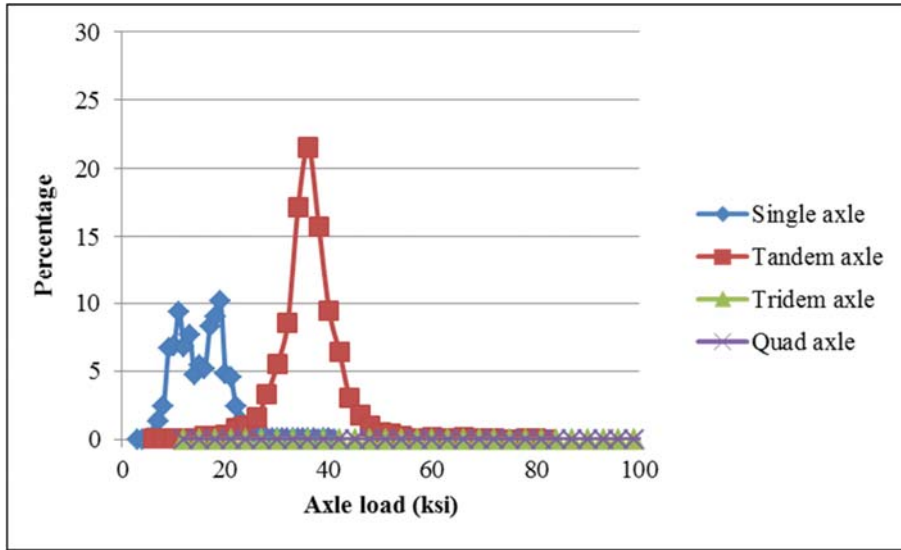


(a)

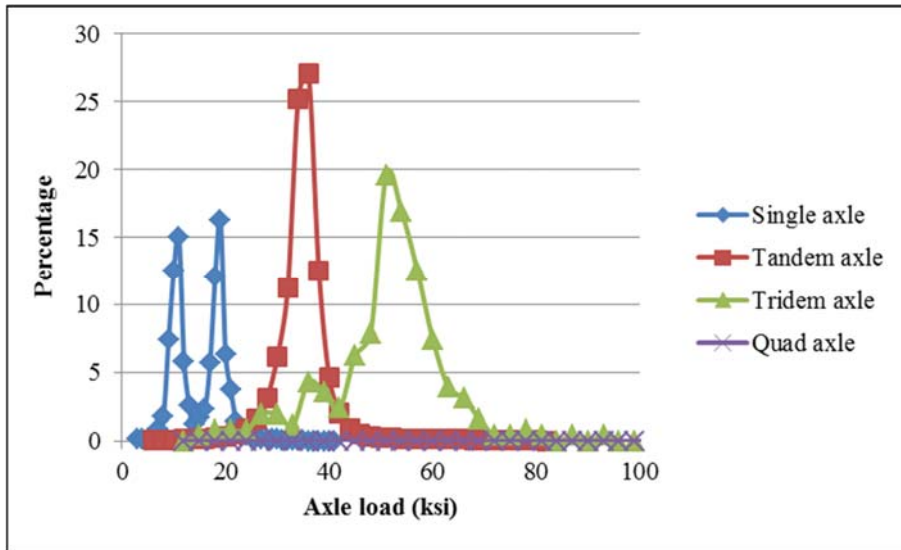


(b)

Figure 31. Axle load spectra of non-overweight traffic on (a) minor road and (b) major road (Class 9 vehicle)



(a)



(b)

Figure 32. Axle load spectra of overweight traffic on (a) minor road and (b) major road

M-E Analysis Using Different Loading Scenarios

The pavement life under traffic loading was analyzed using the Pavement-ME software. The pavement structures at the 10 selected sites include both flexible pavement and composite pavement, as shown in Table 23. The level 3 inputs were used for the material properties at each pavement layer, including the dynamic modulus of asphalt concrete, elastic modulus and tensile strength of Portland cement concrete, and resilient modulus of base/subbase layer and subgrade.

Table 23 - Summary of pavement structures

Site	Pavement type	Layer Thickness (inch)		
		Asphalt	PCC	Base/Subbase
1	Thick Flexible Pavement	11.5	/	20
2		16	/	20
3		12	/	10
4		10.5	/	10
5	Composite Pavement	4.5	10	12
6		3	9	12
7		3.5	7.5	12
8		3.5	7	12
9	Thin Flexible Pavement	4.5	/	20
10		2	/	18

The design reliability is 90 percent and the default design criteria for various performance indicators were used, as shown in Table 24. The load-related pavement distresses were mainly considered in the analysis including permanent deformation (AC and base rutting) and AC fatigue cracking (top-down and bottom-up). In the Pavement-ME, environmental conditions are simulated by the Enhanced Integrated Climatic Model (EICM) and this study selected Newark, NJ as the climate station.

Table 24 - M-E pavement design criteria

Performance criteria	Limit
Initial IRI (in/mi)	63
Terminal IRI (in/mi)	172
AC top-down fatigue cracking (ft./mi)	2000
AC bottom-up fatigue cracking (%)	25
AC thermal fracture (ft./mi)	1000
Permanent deformation - total pavement (in)	0.75
Permanent defamation - AC only (in)	0.25

In order to evaluate the effect of overweight traffic on pavement damage, the reduction ratio of pavement life is calculated using (35).

$$\text{Reduction ratio of pavement life} = \frac{L_0 - L_x}{L_0} \quad (35)$$

where

L_0 : Pavement life caused by total traffic; and

L_x : Pavement life caused by the non-overweight traffic.

Figure 33 shows the reduction ratio of pavement life as the percentage of overweight truck varies for the 10 selected sites. Linear regression fitting with a relatively high R-square value indicates that a linear relationship may exist regardless of the variation in traffic loading and pavement structure. In general, it shows that 1 percent increase of overweight truck may cause 1.8 percent reduction of pavement life. The use of reduction ratio of pavement life is to normalize the effect of overweight truck at different conditions and thus it is more applicable to quantify the impact of overloaded vehicle on pavement damage in the network level. It is expected that the absolute difference of pavement life caused by overweight trucks will vary depending on the traffic characteristics, pavement structure, and the in-situ condition at a specific pavement segment.

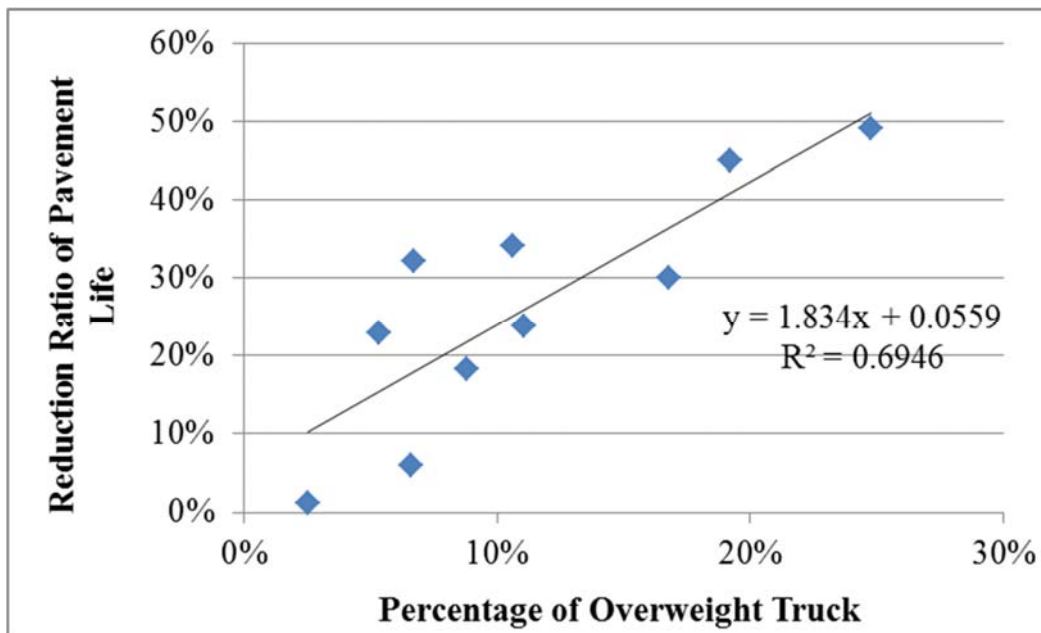


Figure 33. Reduction ratio of pavement life at different percentages of overweight truck

Allocation of Pavement Damage Cost Using Mechanistic-Empirical Pavement Analysis (Pavement-ME)

This part aims to develop a methodology to allocate asphalt pavement damage cost induced by truck loading using mechanistic-empirical (M-E) pavement analysis procedure. Load equivalency factors (LEFs) are developed from M-E analysis and used to convert truck traffic to the number of equivalent single axle load (ESAL) that would yield the same impact on pavement. Pavement life is predicted using Weigh-in-Motion (WIM) data and typical pavement designs in New Jersey. Life-cycle cost analysis is performed to derive the unit pavement damage cost considering the variations in economic analysis parameters and maintenance strategy. Finally, the pavement damage cost caused by individual trucks are determined based on the axle configurations of the truck.

Development of Load Equivalency Factor for Individual Pavement Distress

Pavement deterioration is caused by distribution of the GVW on axles, so it is important to quantify the effect of individual axle configurations on pavement damage. Historically, load equivalency factors (LEFs) have been derived from the AASHO Road Test in the 1950s to convert different axle configurations to ESALs. However, these LEFs were developed for a limited number of pavement types, load magnitudes, pavement ages, and environments and thus cannot reflect the recent developments in pavement material and structure design. In addition, these LEFs cannot reflect the effect of tire pressure on pavement damage.

In order to accurately compare pavement damage caused by different axle types (single, tandem, tridem, and quad) and load magnitudes, LEFs were calculated using mechanistic-empirical (M-E) pavement analysis in this study. The LEF was defined as the ratio between the damage caused by one single pass of the axle in consideration and the damage caused by one single pass of the standard 18-kip single axle load with dual tires (one ESAL), as shown in Equation (36). The calculated LEFs can be used to determine the equivalent number of ESALs for each specific axle that will provide the basis for allocation of pavement damage cost.

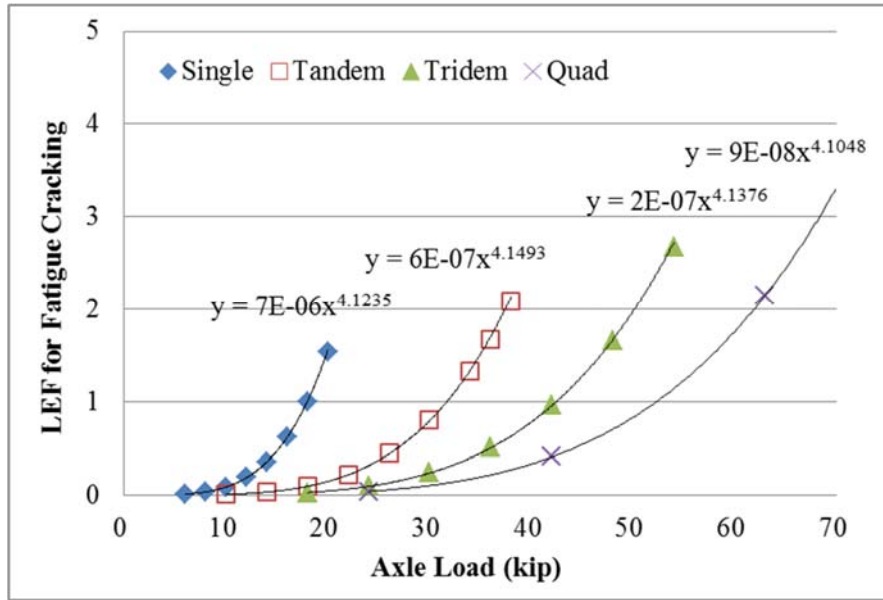
$$LEF = \frac{1/N}{1/N_{ESAL}} = \frac{N_{ESAL}}{N} \quad (36)$$

where

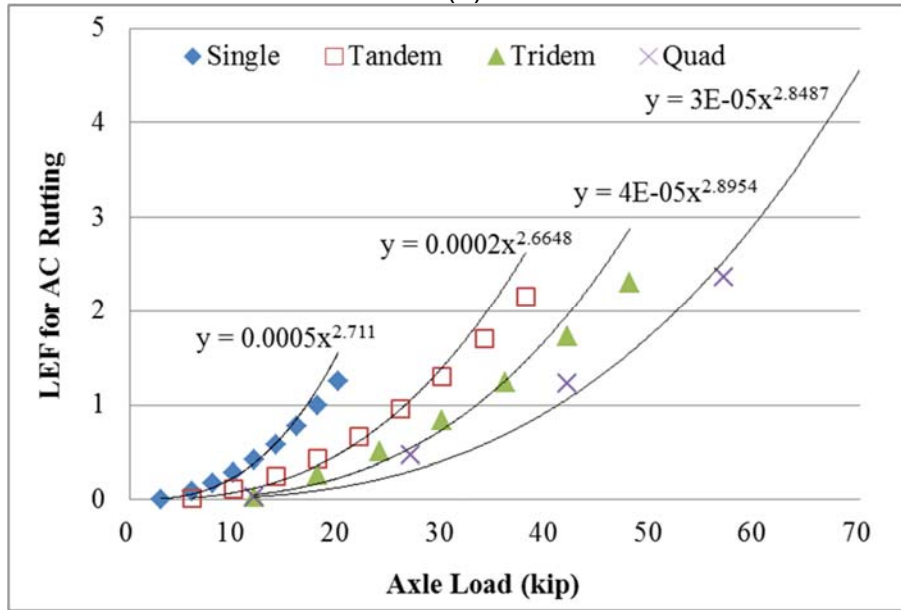
LEF = Load Equivalency Factor;

N_{ESAL} = allowable number of load repetitions to failure under the loading of the standard 18-kip single axle load with dual tires; and

N = allowable number of load repetitions to failure under the loading of the axle with different load magnitudes and configurations.



(a)



(b)

Figure 34. Load equivalency factors for (a) fatigue cracking and (b) AC rutting developed using Pavement-ME

In the M-E pavement analysis, structural responses (stresses, strains and deflections) are mechanistically calculated based on material properties, environmental conditions, and loading characteristics. These responses are used as inputs in empirical models to predict pavement performance. Particularly, the M-E approach characterizes traffic load as distribution of single, tandem, tridem, quad axles instead of converting to ESAL, which is critical for evaluating the pavement damage caused by trucks with different axle load and configurations (ARA 2004).

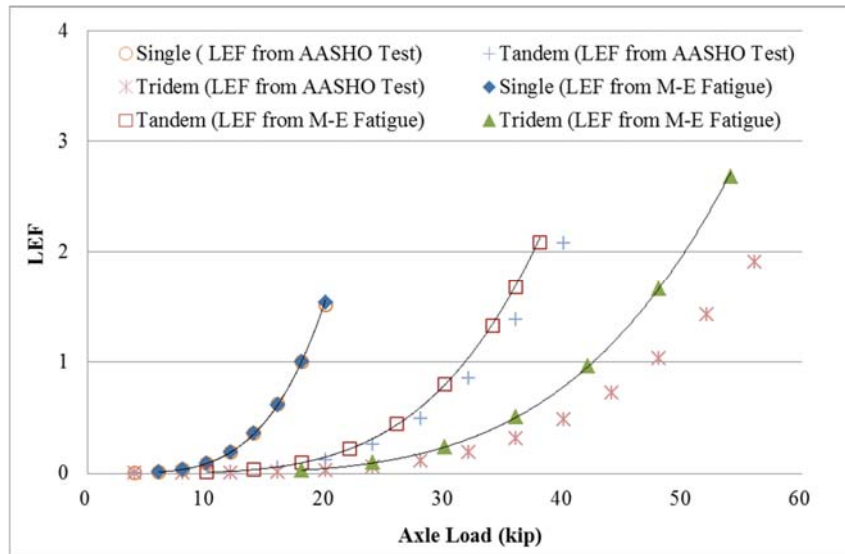
It is expected that the failure mechanism of pavement varies depending on structure, material, traffic loading, and environment. The failure criteria considered in this study mainly include load-related rutting and bottom-up fatigue cracking in the asphalt layer. The top-down cracking is not included considering that it is a combined effect of loading and thermal stress and the influence of tire-pavement interaction was not captured in the current version of Pavement-ME (Wang and Al-Qadi 2009). The design reliability of 90 percent and the default design criteria for various performance indicators were used. In the Pavement-ME, environmental conditions are simulated by the Enhanced Integrated Climatic Model (EICM) and this study selected Newark at New Jersey as the climate station.

Figure 34(a) and (b) plot the calculated LEFs of different axle loads and configurations, respectively, for fatigue cracking and rutting. Power functions were used to fit the relationship between the LEFs and the axle loads and high R-squares found for the fitting models. The results indicate that the potential of fatigue cracking in thin asphalt pavements are more sensitive to the load change compared to the potential of AC rutting in thick asphalt pavements.

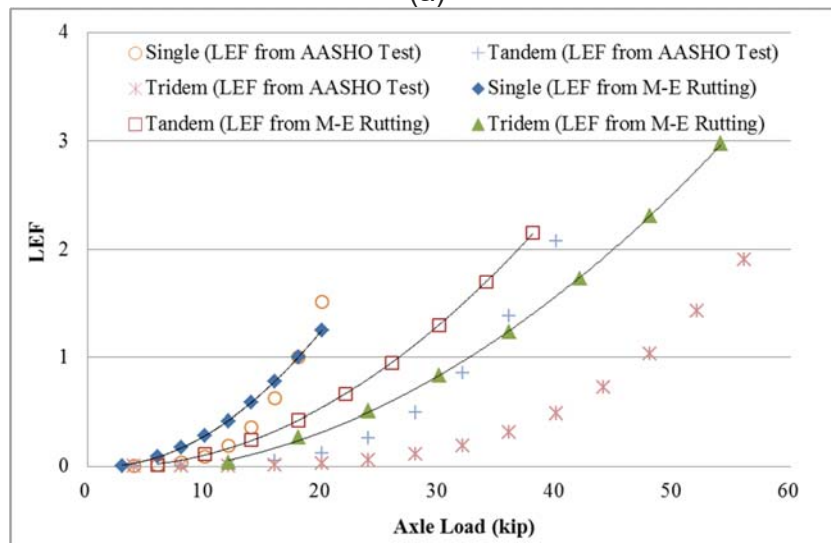
The exponents in the power models are around four for fatigue cracking and three for AC rutting. This is consistent with the exponential parameters used in the performance functions that relate pavement responses under vehicular loading to the allowable number of load repetitions before failure (ARA 2004). It is note that the parameters in the performance transfer functions are nationally calibrated using the long-term pavement performance (LTPP) database and need to be calibrated by state highway agencies using local material properties and climate conditions.

It is known that the LEFs from AASHO road test can be approximated as a “fourth power law” although the exact value of LEFs may vary depending on the structure number (SN) and the terminal Present Serviceability Index (PSIt) (AASHTO 1993). The LEFs from AASHTO road test is developed based on road surface serviceability that is affected by multiple distresses, including change in ride, rutting, cracking, and patching. These LEFs indicate that the damage to the pavement structure varies approximately according to the fourth power of the axle load, as known as “fourth power law”.

Figure 35 compares the LEFs from AASHO road test (SN=5, PSI_t = 2.5) and the M-E based LEFs for fatigue cracking and rutting, respectively. The results show that for single axle the LEFs for fatigue cracking calculated from the M-E approach are close to the classic LEFs from AASHO road test. On the other hand, for single axles the LEFs for rutting calculated from the M-E analysis are greater than the classical LEFs when the axle load is smaller than 18 kips, but become smaller than the classical LEFs when the axle load is greater than 18 kips. However, the classic LEFs underestimate the impact of multi-axle load on pavement damage compared to the LEFs calculated from the M-E analysis and the difference is more significant for the case of rutting.



(a)



(b)

Figure 35. Comparisons between load equivalency factors for (a) fatigue cracking and (b) rutting from Pavement-ME analysis and AASHO road test

Development of Tire Pressure Equivalency Factor

Truck tire inflation pressures have steadily increased in the recent decades since truck users tend to carry more load and reduce tire wear (Wang and Machemehl 2003). A most apparent effect of the increased tire pressure would be reduction in the tire-pavement contact area, which may result in an increase in the tire-pavement contact stress and then more pavement damage. Although the current load regulations do not include tire pressure, it is important to consider it in the allocation of pavement damage cost.

Charging vehicles only by the number of axles without considering axle load and tire inflation pressure, may encourage vehicles hauling heavy loads on fewer axles with overinflated tires. On the other hand, Central Tire Inflation (CTI) can be installed on a vehicle that enables the vehicle operator to adjust the tire inflation pressure as needed, for example, the US Forest Service uses CTI on trucks travelling on their logging roads (Greenfield 1993). The analysis results indicate that the deployment of CTI should consider not only tire wear and ride comfort but also pavement damage.

Figure 36 shows the distribution of tire pressure that is collected in a truck survey by the TXDOT. In their study, a statewide tire pressure survey identified the variations of truck tire pressures and the effect of tire pressure on pavement damage.

Similar to LEFs, an M-E pavement analysis was conducted to calculate the tire pressure equivalency factor (TPEF), Equation (37). Figure 37 shows the TPEFs, respectively, for fatigue cracking and rutting. The results indicate that the tire pressure has a more significant effect on rutting compared to fatigue cracking. The TPEFs show a linear relationship with tire pressure and are independent on the axle type and the load applied.

$$\text{TPEF} = \frac{1/N}{1/N_{120\text{psi}}} = \frac{N_{120\text{psi}}}{N} \quad (37)$$

where

TPEF = Tire Pressure Equivalency Factor;

$N_{120\text{psi}}$ = allowable number of load repetitions to failure under the tire pressure of 120 lbf/in²; and

N = allowable number of load repetitions to failure under the different tire pressure levels.

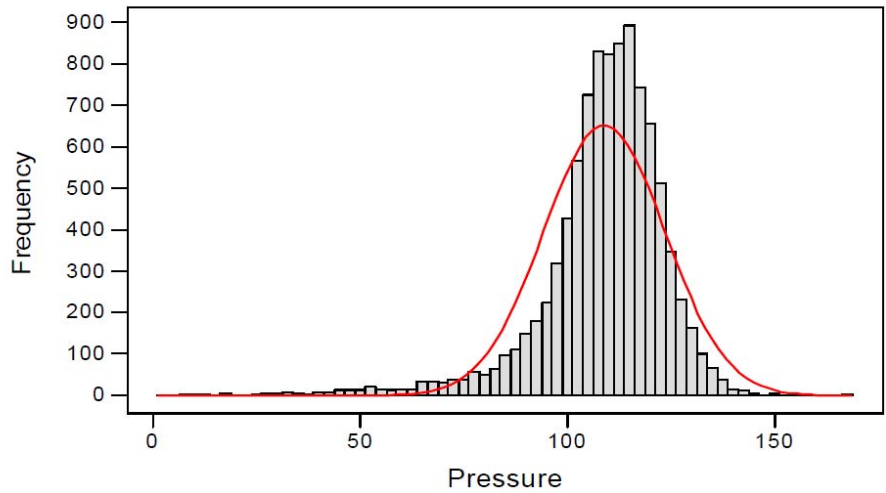


Figure 36. Tire pressure distributions from a TXDOT survey (After Wang and Machemehl 2003)

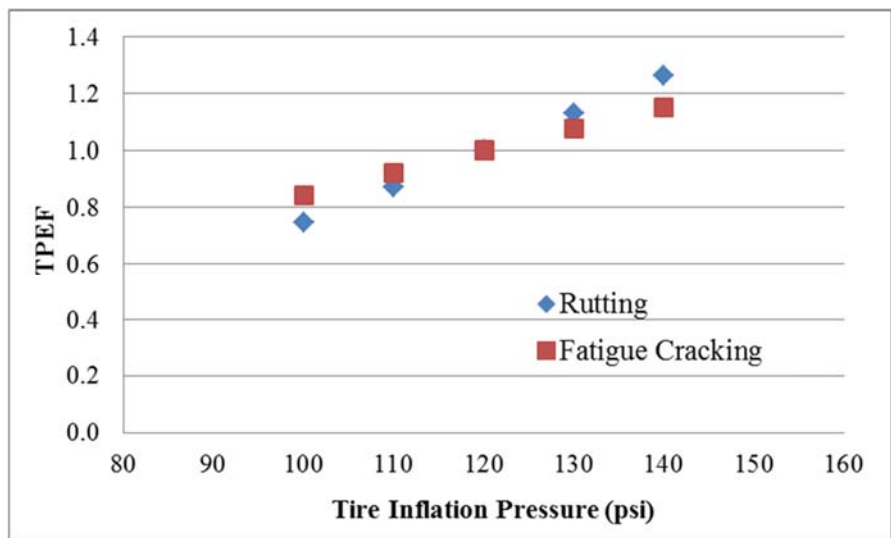


Figure 37. Tire pressure equivalency factors for fatigue cracking and rutting

Pavement Life at Different Traffic Scenarios

Based on practical pavement structures applied in New Jersey, flexible pavement and composite pavement were selected for analysis. Due to traffic volume difference, thicker pavement structures using better asphalt were designated for major roads. The layer type, material type, and thickness of flexible and composite pavements for each road type are summarized in Table 25 and Table 26.

Table 27 includes the truck traffic volume combinations for software input. Non-overweight AADTT and overweight truck percentage as of non-overweight AADTT are two factors which have influence on pavement service life. Based on traffic volume assumptions, the axle load spectra of non-overweight and overweight truck

traffic in Figure 31 and Figure 32 and the new axle load spectra for traffic inputs was recalculated. 30 cases were conducted for each pavement structure.

Table 25 - Representative pavement structures used for major road

Pavement Type	Layer Type	Material	Thickness (in.)
Thick Flexible Pavement	Flexible	Asphalt concrete (PG 76-22)	6
	Flexible	Asphalt concrete (PG 64-22)	6
	Non-stabilized	Crushed gravel	20
	Subgrade	A-1 soil	Semi-infinite
Composite Pavement	Flexible	Asphalt concrete (PG 76-22)	6
	Rigid	Cement concrete	9
	Non-stabilized	Crushed gravel	12
	Subgrade	A-1 soil	Semi-infinite

Table 26 - Representative pavement structures used for minor road

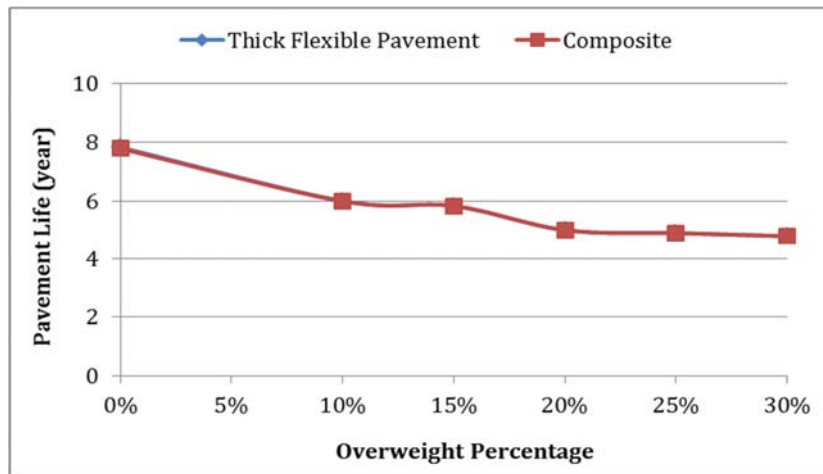
Pavement Type	Layer Type	Material	Thickness (in.)
Thin Flexible Pavement	Flexible	Asphalt concrete (PG 64-22)	2
	Flexible	Asphalt concrete (PG 64-22)	2
	Non-stabilized	Crushed gravel	20
	Subgrade	A-1 soil	Semi-infinite
Composite Pavement	Flexible	Asphalt concrete (PG 64-22)	4
	Rigid	Cement concrete	7
	Non-stabilized	Crushed gravel	12
	Subgrade	A-1 soil	Semi-infinite

Table 27 - Traffic Volume Assumption Matrixes

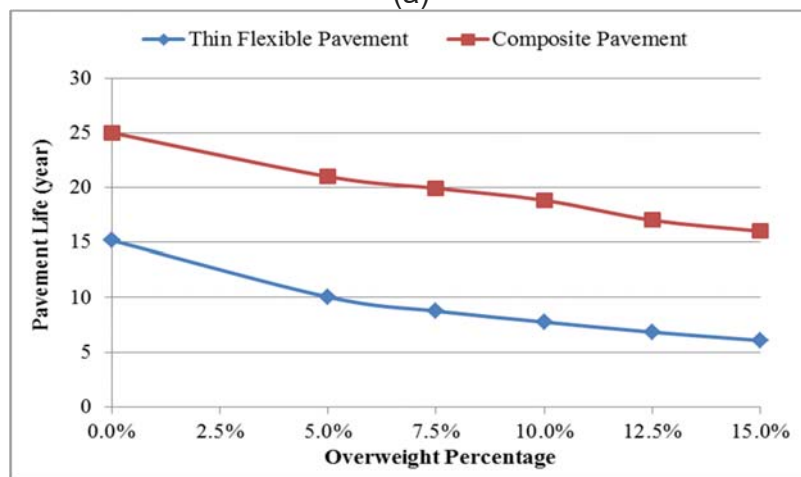
Axle Load Spectrum Used	AADTT without Overload	Overweight Truck Percent as of AADTT without Overload
Major Road	4000, 6000, 8000, 10000, 12000	0%, 10%, 20%, 30%, 25%, 25%
Minor Road	500, 1000, 1500, 2000, 3000	0%, 5%, 7.5%, 10%, 12.5%, 15%

The criteria for maximum bottom-up cracking is 10 percent (thin flexible pavement only) and for maximum subtotal AC rutting is 0.25in (thick flexible pavement and composite pavement). According to pavement life predictions, thick flexible pavement and composite pavement fail due to AC rutting, while thin flexible pavement fails due to fatigue cracking. The typical flexible pavement and composite pavement life at 90 percent reliability are predicted. Pavement life with 2000 AADTT for minor road and 8000 AADTT for major road is presented in Figure 38.

It is expected that pavement life decreases as overweight percentage increases. For major roads, the pavement life difference between thick flexible pavement and composite pavement is tiny, as presented in Figure 38(a). However, it is shown that the plots of pavement life for minor roads in Figure 38(b) are parallel. Comparing pavement life difference due to the changes of overweight percentages from 0 percent to 15 percent, overweight percentage has more influence on minor roads than major roads.



(a)



(b)

Figure 38. Pavement life comparisons between flexible pavement and composite pavement of (a) major road (b) minor road

Life Cycle Cost Analysis

In this study, it is assumed that road users were not charged user costs and only agency costs were considered in the pavement life-cycle cost analysis. Analysis periods and discount rates are the two most significant parameters affecting pavement life cycle cost. The analysis period should be chosen to be long enough to include major future rehabilitation treatments but not so long that it becomes unreasonable (Walls and Smith 1998). Pavement life-cycle cost analysis with different analysis periods, discount rates, and repair strategies are considered in the sensitivity analysis part.

According to the National Cooperative Highway Research Program (NCHRP) Guide for Pavement-Type Selection, an analysis period of at least 40 years was suggested for new construction or reconstruction of pavements, while an analysis period of at least 30 years was suggested for rehabilitation of pavements. A respectively longer analysis period should be selected for long-life pavements. A discount rate is used to convert future costs to present year costs. Historically, discount rates are in the range of 3 percent to 5 percent. The long-term real discount rate values supplied in the most recently updated edition of the Office of Management and Budget (OMB) Circular A-94, Appendix C, were suggested for use in life-cycle cost analysis. The current long-term real discount rate is approximately 2 percent. Thus, analysis periods of 30 and 60 years and 3 percent discount rate are used in the life-cycle cost analysis.

There are several economic indicators available to the analyst such as Benefit/Cost (B/C) Ratios, Internal Rate of Return (IRR), Net Present Value (NPV), and Equivalent Uniform Annual Costs (EUAC). IRR is a return rate that makes net present value of all cash flows from a certain project investment equal to zero. NPV converts all costs to a single base year costs, while EUAC converts all projects to a recurring yearly cost. After converting to NPV or EUAC, the costs of various investment options can be compared.

The NPV is defined as the sum of the present values of the individual cash flows of the same entity and has wide application in pavement life cycle cost analysis. The NPV of agency cost during the analysis period is computed using the discounted monetary value of future costs and salvages by transforming costs occurring in different time periods and salvages at the end of analysis period to a common unit of measurement. NPV is a common economic calculation and, for highways, which is expressed by Equations (38) and (39).

$$NPV = C + M_i \left(\frac{1}{1+r} \right)^{n_i} + \dots + M_j \left(\frac{1}{1+r} \right)^{n_j} - S \left(\frac{1}{1+r} \right)^N \quad (38)$$

where

NPV=Net present value or present worth;

C= Present cost of initial rehabilitation activity;

M_i = Cost of the i^{th} maintenance & rehabilitation (M&R) alternative in terms of constant dollars;

r=Discount rate;

n_i = Number of years from the present to the i^{th} M & R activity;

N= Length of the analysis period in years; and

S= Salvage value at the end of the analysis period.

$$S = \left(1 - \frac{L_A}{L_E}\right)C \quad (39)$$

where

S=Salvage value (or residual value) of rehabilitation alternative;

L_A =Analysis life of rehabilitation alternative in years;

L_E =Expected life of the rehabilitation alternative; and

C= Cost of the rehabilitation alternative.

In addition to analysis period and discount rate, pavement repair strategy is an essential factor affecting life-cycle costs. The NJDOT applied the typical rehabilitation strategy of milling to a depth of 2 in. and overlaying with 2 in. of new asphalt material. No preventive maintenance or annual maintenance was considered. Maintenance costs for different treatments were calculated using the formulas in a previous study conducted by Zaghoul et al. (2006) for the NJDOT. The unit cost (\$ per square yard) equations used for flexible pavements and composite pavements are shown in Equations (40) and (41).

$$\text{Flexible pavements: Mill + overlay: } 3.98M + 7.0T_{ac} \quad (40)$$

$$\text{Composite pavements: Mill + overlay: } 3.98M + 7.01T_{ac} \quad (41)$$

where

M= thickness of milling in inches;

T_{ac} = thickness of AC overlay in inches; and

D= thickness of concrete slab in inches.

Marginal Pavement Damage Cost

For the same pavement structure, the initial construction cost is unchanged, so pavement damage cost differences occur owing to pavement life and repair frequency. The average pavement damage cost is the total maintenance cost divided by the total road usage. The marginal pavement damage cost (MPDC) is defined as a unit cost of providing pavement structure for one extra passage of a unit road usage expressed as ESAL. Compared to average damage cost, it is more realistic and practical method to calculate pavement damage cost.

According to the prior work by Ahmed (2012), linear relationship between the pavement damage costs and the logarithm of average annual ESALs to base e was developed. Pavement type (flexible pavement and rigid pavement) and pavement age range from 0 to 50 years old were the optional parameters in the final functions. Hajek et al. (1998) explored power functions to establish relationship between EUAC and the logarithm of the annual ESALs to base 10, respectively, for new pavements and in-service pavements. The regional codes for southern Ontario and north Ontario were indicator variables in the fitting functions.

In reference to the EUAC and the average annual ESALs, several alternative regression functions were investigated to build models for marginal pavement damage cost estimation. The exponent regression in Equation (42) was selected based on statistical parameters:

$$NPV = \beta_0 e^{\beta_1 \log_{10}(ESALs)} \quad (42)$$

where

β_0, β_1 = Constant term and parameter estimates for model explanatory variables;
 NPV = Net present value per lane-mi over analysis period; and
 ESALs = Average annual number of equivalent single axle load per lane-mi.

Average annual ESALs were estimated through dividing the total ESALs by analysis period n. The total ESALs during analysis period is computed by Equation (43).

$$ESALs = AADTT \times G \times f_d \times f_l \times 365 \times ESAL \text{ factor} \quad (43)$$

where

AADTT = Average annual daily truck traffic;
 f_d = Directional distribution factor (0.5);
 f_l = Lane distribution factor (0.95);
 ESAL factor = Equivalent single axle load factor;
 $G = \text{Growth factor} \frac{(1+r)^n - 1}{r}$
 r = Growth rate (3%); and
 n = Analysis period.

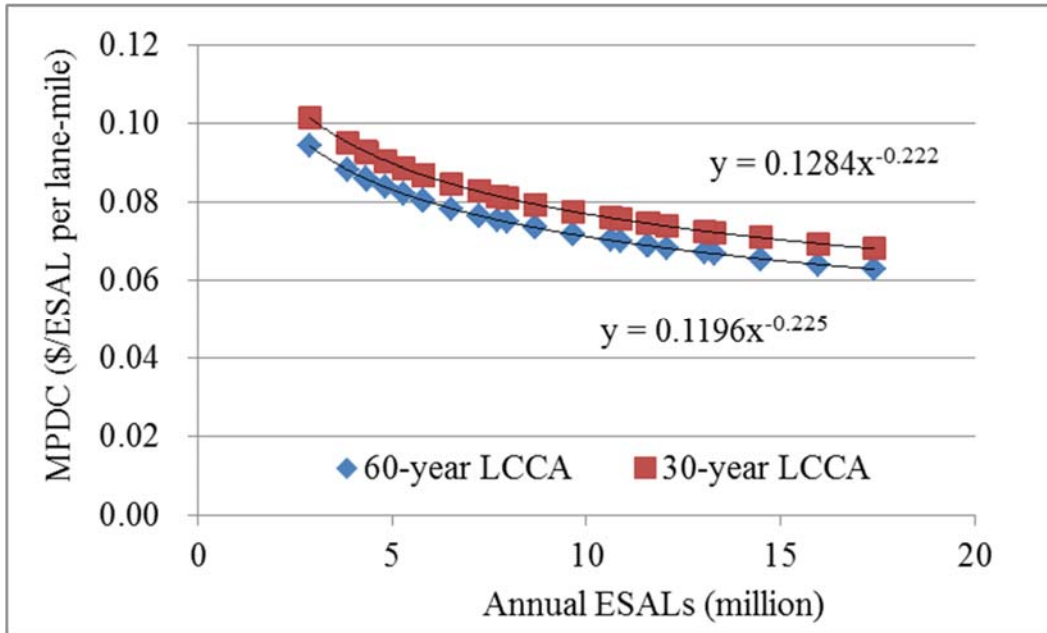
The estimated functions were differentiated with respect to average annual EASLs to obtain the marginal pavement damage costs as shown in Equation (44).

$$MPDC = \frac{\beta_0 \beta_1}{\ln(10)} (ESALs)^{\left(\frac{\beta_1}{\ln(10)} - 1\right)} \quad (44)$$

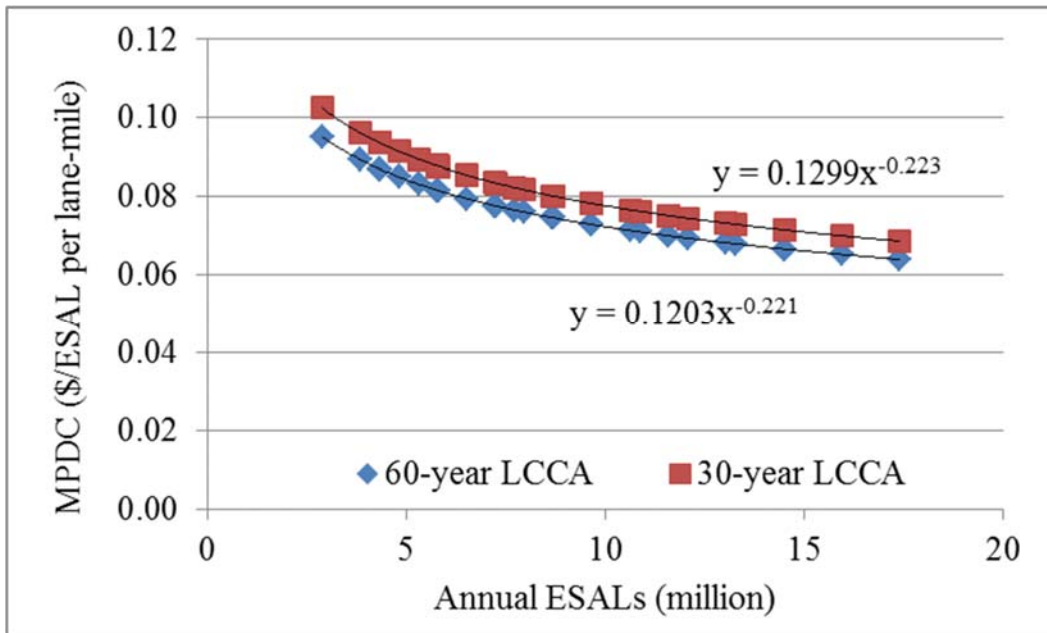
where

MPDC = Marginal pavement damage cost (\$/ESAL per lane-mi); and
 ESALs = Average annual number of equivalent single axle load per lane-mi.

The MPDC plots in Figure 39 and Figure 40 were plotted, respectively, for the different pavement structures on major and minor roads. The analysis periods were 30 and 60 years in the life-cycle cost analysis. When the traffic volume is low, fewer trucks share the pavement damage cost and the marginal pavement damage cost is higher. It should be noted that the MPDC of major road is significantly smaller than that of minor road.

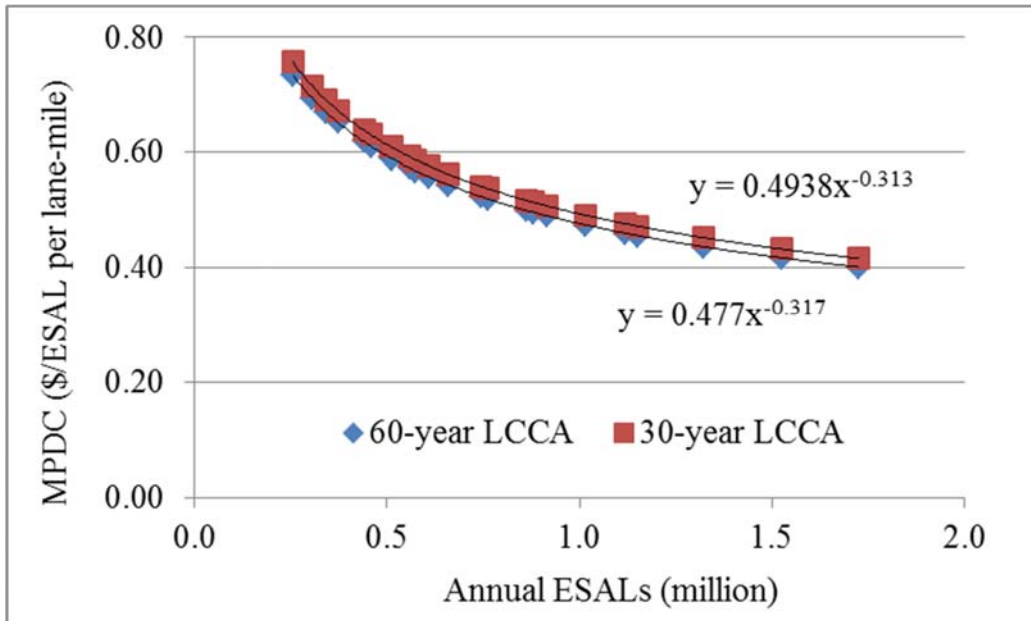


(a)

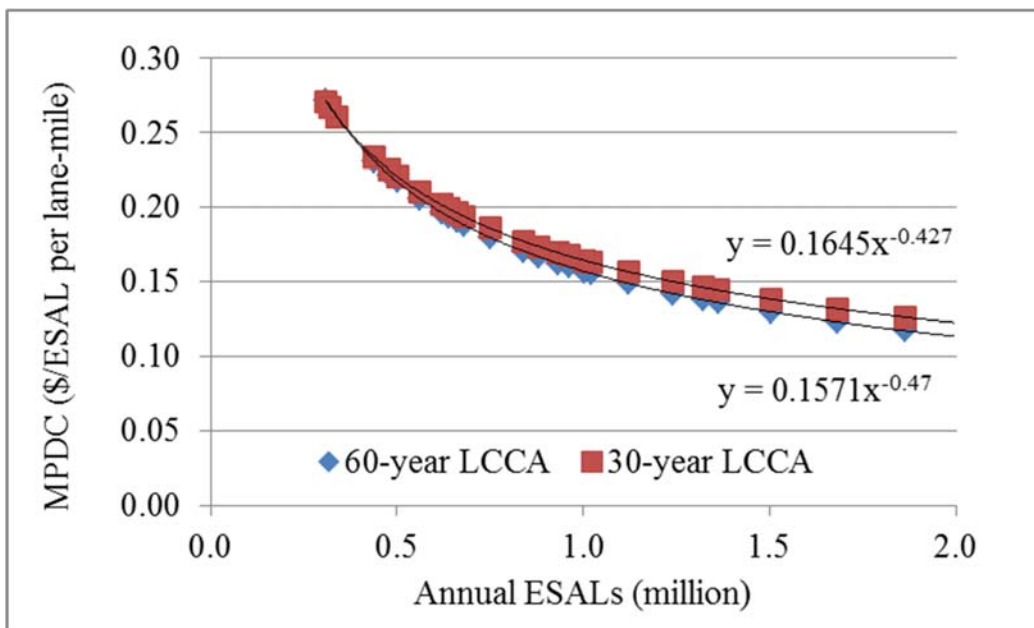


(b)

Figure 39. MPDC of (a) thick flexible pavement (b) composite pavement on major road for 30 and 60-year analysis period



(a)



(b)

Figure 40. MPDC of (a) thin flexible pavement (b) composite pavement on minor road for 30 and 60-year analysis period

Allocation of Pavement Damage Cost Using Pavement Performance Data

This part aims to develop a methodology to allocate asphalt pavement damage cost induced by truck loading using pavement performance data. Figure 41 illustrates flowchart of the methodology of quantifying pavement damage cost caused by truck loading. Pavement performance data were obtained from pavement management system (PMS) to predict pavement service life. Treatment costs spent on pavement rehabilitation were extracted from the construction database. Load equivalency factors (LEFs) that were developed from AASHO road test results were used to convert truck traffic to the number of equivalent single axle load (ESAL) that would yield the same impact on pavement. Life-cycle cost analysis (LCCA) was performed to derive the unit pavement damage cost considering the variations in economic analysis parameters. Finally, pavement damage cost caused by individual truck is determined based on the axle configurations of the truck. Figure 41 shows the flowchart of analysis methodology for pavement damage cost.

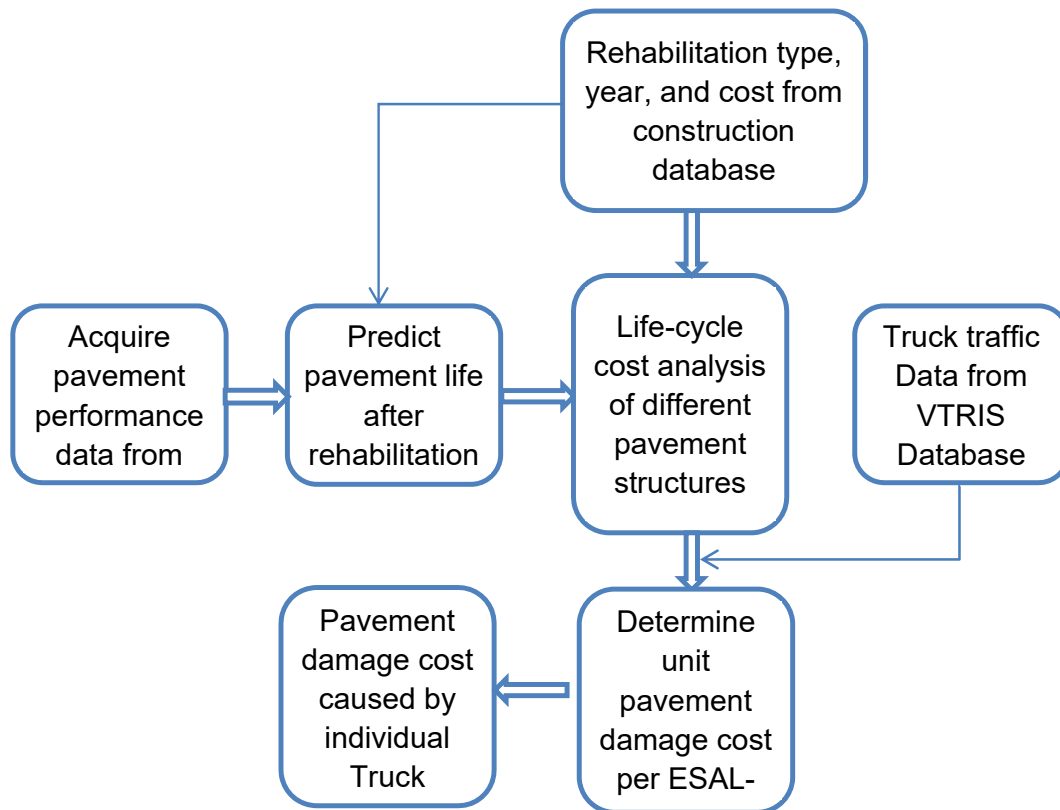


Figure 41. Flowchart of analyzing impact of truck loading on pavement damage cost

Pavement Structure and Maintenance Activities

In order to obtain realistic pavement damage cost caused by truck loading, representative road segments were selected for analysis. These segments were selected as the road section close to the weight-in-motion site so the accurate traffic data can be obtained. Each road section includes a two-mi segment in proximity to a WIM station. Totally, 12 WIM sites were selected and the corresponding road sections have different types of pavement structure and road classifications, as shown in Table 28 and Table 29.

The available construction activities and cost data at the road sections were extracted from the NJDOT construction database, as shown in Table 30. The results show that most treatments are milling and overlay of different depths of asphalt surfacing layers. For instance, M2.5/O2.5 indicates cold milling to a depth of 2.5 inch and overlaying with 2.5 inch of new asphalt material. Both pavement cost and project cost were obtained for the construction project that includes the 2-mi segment in proximity to the WIM site. The cost per lane-mi can be calculated by dividing the total cost by the total lane-mi constructed in the project. Only the cost data after 2004 were available in the construction database.

Table 28 - WIM stations and mileposts at selected sites

No.	Site	Direction	WIM Station	WIM Milepost
1	I-78A	E	78A	14.5
2	I-80A	W	80A	8.3
3	I-295	N	295D	2.9
4	I-78W	E	78W	42.2
5	I-80C	W	80C	38.1
6	I-80B	E	80B	32.4
7	US-202	N	202	3.5
8	NJ-33	W	33	23.5
9	US-202B	N	202B	19.2
10	NJ-55	N	55C	27.4
11	NJ-31	N	31C	40.8
12	NJ-70	W	70B	10.3

Table 29 - Pavement structures at selected sites

Road Type	Pavement Type	Site	Layer Thickness (inch)		
			Asphalt	Concrete	Base/Subbase
Interstate highway	Composite	I-78A	6	9	12
		I-80A	4	9	12
		I-295	3	9	15
	Flexible	I-78W	19.25	0	12
		I-80C	12	0	15
		I-80B	16	0	20
State road	Composite	US-202	3.5	7.5	12
		NJ-33	2.5	5.5	N/A
		US-202B	5	7	N/A
	Flexible	NJ-55	4.5	0	20
		NJ-31	4	0	N/A
		NJ-70	4	0	N/A

Table 30 - Treatment and cost data at selected sites

Site	Lane mi	Project (million\$)	Pavement (million\$)	Year	Treatment Type
I-78A	48	16.60	N/A	2008	M3/O3
I-80A	46.2	11.70	10.73	2006	M3/O3
I-295	14.2	5.00	N/A	2010	M3/O3
I-78W	50.4	24.95	18.30	2008	M2/O6
I-80C	42.42	19.60	12.38	2006	M2/O4
I-80B	51.44	11.44	8.00	2006	M2.5/O2.5
US-202	10.28	5.73	N/A	2009	M3.5/O3.5
NJ-33	6.0	3.17	2.69	2006	M2/O2
US-202B	20.9	3.10	2.50	2006	M2/O4
NJ-55	20.4	3.47	3.25	2004	M3/O4.5
NJ-31	5.4	3.71	3.09	2005	M3/O3
NJ-70	13.8	3.10	2.50	2006	M2/O4

Pavement Life Estimated from Field Data

Pavement performance data were extracted from the NJDOT PMS database to estimate pavement service life after different types of rehabilitation treatments. The extracted data include Surface Distress Index (SDI) and International Roughness Index (IRI) from 2000 to 2014. It was found that the IRI usually does not reach the failure criteria or the rehabilitation threshold after 10 years. Thus, the SDI is believed to be a better index reflecting pavement deterioration. Essentially, the SDI has a scale of 0-5 and incorporates both the non-load related distresses outside the wheel paths (NDI) and the load related distress index (LDI). The NJDOT defines the pavement condition as poor when SDI < 2.4 or IRI > 170 in/mi and as good when SDI > 3.5 and IRI < 95 in/mi. Therefore, the service life in the study is determined as the time period before the SDI reaches 2.4.

According to specific year in which the rehabilitation treatment was conducted, the SDI data after the treatment was selected for pavement service life prediction. Table 31 shows the average SDI in the two-mi segment used for pavement life estimation.

Various model forms (such as linear, exponential, logarithmic, power, and polynomial models) can be used to estimate the best fit to pavement condition data based on maximizing the goodness of fit, R-square, A majority of model forms do not constrain the curve to fit within the boundaries and may not simulate the development trend for SDI in a correct way. For instance, it can be observed from Table 31 that during the first couple of years, the SDI declines slowly. Afterward, it may start to drop rapidly and finally decrease gradually as a step function. Under this scenario, the linear model and exponential model can hardly predict the trend.

Table 31 - Average SDI at selected sites after maintenance treatments

Site	2004	2005	2006	2007	2008	2009	2010	2011	2012	2013	2014
I-78A	-	-	-	-	-	-	5	5	5	3.6	2.7
I-80A	-	-	-	-	5	5	3.9	3.5	3.4	2.6	1.9
I-295	-	-	-	-	-	-	-	5	-	3.9	2.7
I-78W	-	-	-	-	-	5	4.0	4.1	3.9	3.6	3.0
I-80C	-	-	-	5.0	5	5.0	2.8	2.8	2.8	1.3	1.3
I-80B	-	-	5	5	4.6	5	3.9	3.9	3.3	3.6	2.2
US-202	-	-	-	-	5	3.9	3.0	2.8	2.8	-	-
NJ-33	-	-	-	5.0	5.0	5.0	3.9	3.6	3.9	3.3	1.9
US-202B	-	-	-	-	5	3.9	3.1	2.8	2.8	-	-
NJ-55	5	3.9	3.9	3.9	2.7	1.1	1.1	-	-	-	-
NJ-31	-	-	5	5	3.3	2.7	-	0.7	0.7	-	-
NJ-70	-	-	-	5	5	5.0	4.3	3.8	2.8	2.8	2.1

Sigmoidal (S-shape) model has been shown to provide high accuracy as well as constraining the curve to fit within pavement condition boundaries (Hajek et al. 1985; Jackson et al. 1996) ^(106,107). Typical form of sigmoidal model is shown as below. It ensures that the performance curve is constrained within the condition model boundaries between SDI=0 and 5. After the model parameters are determined, the pavement life before the SDI reaching 2.4 was calculated for different sites. Figure 42 shows an example of deterioration trend of pavement performance with the measured and fitted SDI data. Table 32 presents the model fitting parameters and the predicted pavement life using S-shape model.

$$SDI = SDI_0 - \exp(a - b * c^{(\ln(\frac{1}{Age}))}) \tag{45}$$

where

SDI = Surface distress index;

SDI₀ = Surface distress index at year zero (usually 5);

Age = the year since the initial construction of the last rehabilitation treatment; and

a, b, c = Model coefficients with a = ln(SDI₀) and SDI_{terminal}=0.

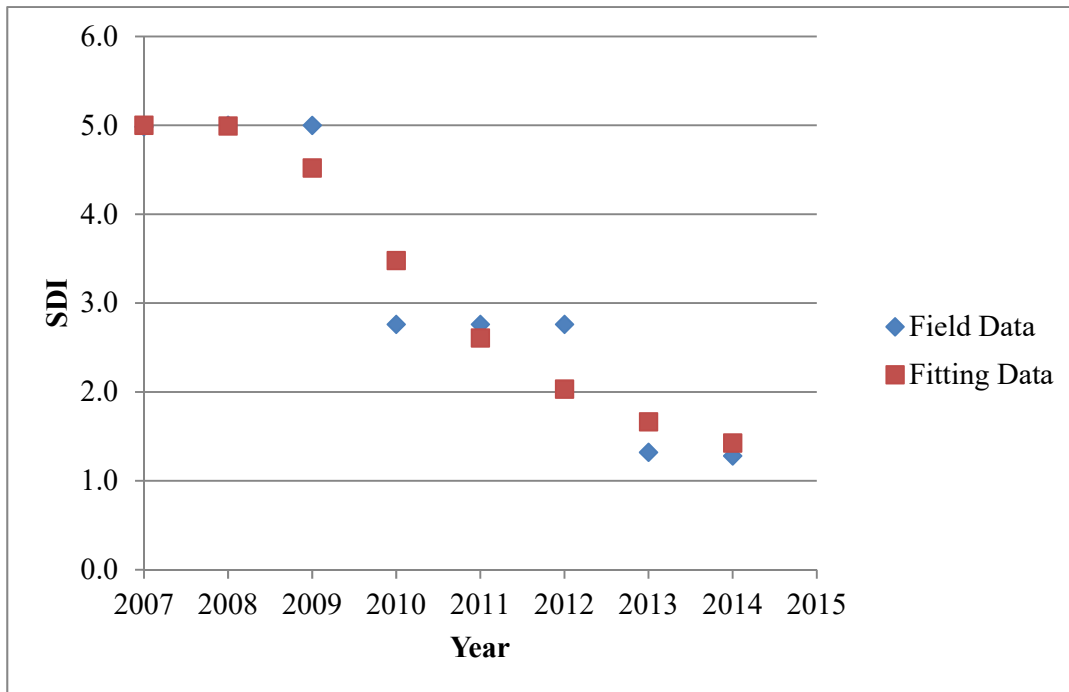


Figure 42. Example of deterioration trend of pavement performance (I-80B)

Table 32 - Predicted pavement service life using SDI data

Site	Sigmoidal model of SDI					Pavement Life
	a	b	c	R ²	SSE	
I-78A	1.60	70.37	17.02	97.8	0.10	5.2
I-80A	2.99	6.38	1.87	95.7	0.35	6.3
I-295	1.50	18.70	10.82	100.0	0.00	4.4
I-78W	4.34	5.72	1.27	86.7	0.29	9.1
I-80C	1.44	39.11	13.90	91.8	1.44	5.3
I-80B	12.69	17.06	1.18	88.6	0.81	9.2
US-202	1.53	2.68	2.46	93.2	0.25	5.6
NJ-33	19.06	22.90	1.12	89.1	0.85	7.8
US-202B	1.53	2.68	2.46	94.8	0.19	5.6
NJ-55	6.26	8.50	1.33	91.0	1.23	5.1
NJ-31	1.72	13.92	8.26	98.3	0.32	4.0
NJ-70	48.88	52.16	1.04	94.8	0.51	7.4

Load Equivalency Factor and Equivalent ESALs

Pavement deterioration is caused by distribution of the GVW on axles, so it is important to quantify the effect of individual axle configurations on pavement damage. Historically, load equivalency factors (LEFs) have been derived from the AASHO Road Test in the 1950s to convert different axle configurations to ESALs. The LEF was defined as the ratio between the damage caused by one single pass of the axle in consideration and the damage caused by one single pass of the standard 18-kip single axle load with dual tires (one ESAL), as below. The calculated LEFs can be used to determine the equivalent number of ESALs for each specific axle that will provide the basis for allocation of pavement damage cost.

$$LEF = \frac{1/N}{1/N_{ESAL}} = \frac{N_{ESAL}}{N} \quad (46)$$

where

LEF = Load Equivalency Factor;

N_{ESAL} = Allowable number of load repetitions to failure under the loading of the standard 18-kip single axle load with dual tires; and

N = Allowable number of load repetitions to failure under the loading of the axle with different load magnitudes and configurations.

It is noted that the LEFs from AASHO road test vary depending on the structure number (SN) and the terminal Present Serviceability Index (PSI_t) (AASHTO 1993) ⁽²⁾. The LEFs from AASHTO road test is developed based on road surface serviceability that is affected by multiple distresses, including changes in rideability, rutting, and cracking and patching. These LEFs indicate that the load-induced damage to the pavement structure varies approximately according to the fourth power of the axle load for single axles, as known as “fourth power law”. Figure 42 shows an example of the LEFs from AASHO road test and regression equations for flexible pavement (SN = 5, $PSI_t = 2.5$), respectively, for single, tandem, tridem, and quad axles. Figure 43 shows an example of the LEFs from AASHO road test and regression equations for rigid pavement (D = 9 in, $PSI_t = 2.5$), respectively, for single, tandem, tridem, and quad axles.

Weigh-in-motion (WIM) devices can continuously capture and record axle load, gross vehicle load and axle spacing with supplementary data such as date, time, speed, lane of travel, vehicle type, over a measurement site. The Office of Highway Policy Information (HPPI) has developed the Vehicle Travel Information System (VTRIS) web site. The online database at VTRIS can generate W-Tables in unified format including vehicle travel, weight, and classification characteristics which are collected from WIM stations.

In order to accurately compare pavement damage on different pavement structures, truck traffic volume and weights were collected from VTRIS database (2010-2013 data) in this study. The separate WIM data for 2007-2008 was used to compute ESALs in the analysis period for NJ-55 because VTRIS data are not available at the WIM station. It is noted that the ESAL calculation varies depending on pavement structures. Flexible LEFs were used for flexible pavements, while rigid LEFs were used for composite pavements.

It was found that daily ESALs from 2010 to 2013 either increases or decreases, so it is not realistic to predict total ESALs in analysis period using a constant growth rate. The power function model was utilized to estimate the accumulated total ESALs in 30-year and 60-year analysis periods. Table 8 presents the daily ESALs and ESALs calculated in 30-year and 60-year analysis period with lane factor of 0.95. Growth rate of 3 percent was assumed for NJ-55.

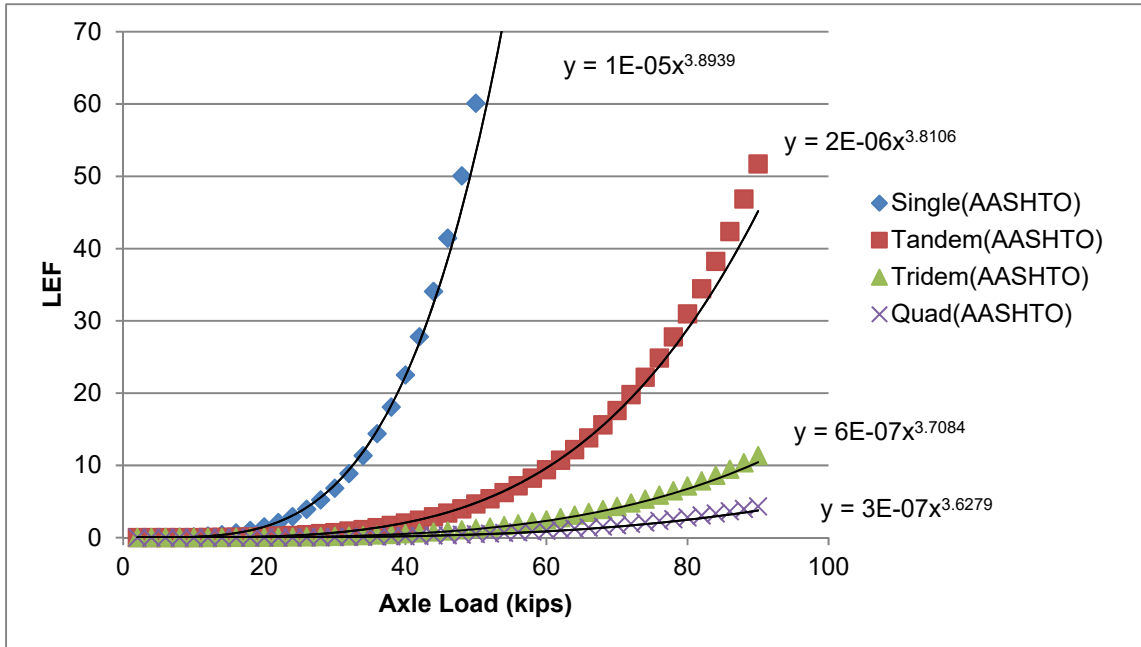


Figure 43. Example of LEFs from AASHO road test-flexible pavement (Structure Number = 5, Terminal $PSI_t = 2.5$)

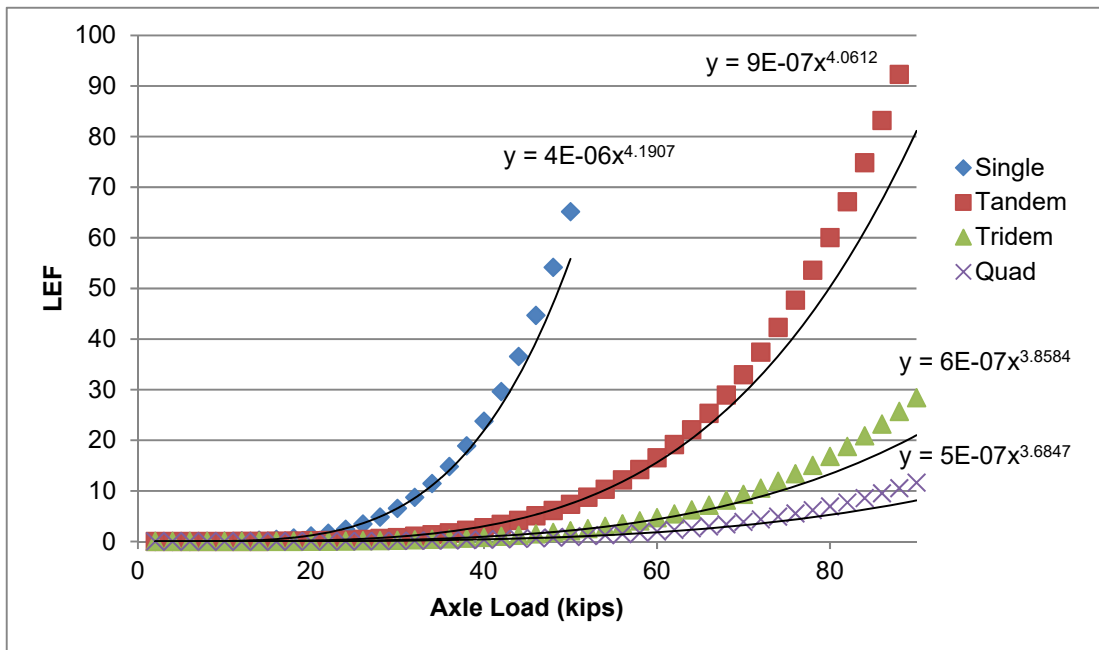


Figure 44. Example of LEFs from AASHO road test-rigid pavement (Slab thickness = 9 in, Terminal $PSI_t = 2.5$)

Table 33 - ESAL calculation in 30-year and 60-year analysis period

Route	2010	2011	2012	2013	30-year	60-year	Source
I-78A	17256	15675	15493	14198	1.43E+08	2.73E+08	VTRIS
I-80A	4540	3981	6759	956	4.38E+07	8.63E+07	VTRIS
I-295	N/A	1074	1846	1619	3.46E+07	8.68E+07	VTRIS
I-78W	2816	3176	2775	2524	3.05E+07	6.13E+07	VTRIS
I-80C	6017	4707	4332	3021	3.24E+07	5.66E+07	VTRIS
I-80B	3363	3022	1509	N/A	1.77E+07	3.07E+07	VTRIS
US-202	972	589	365	460	2.97E+06	4.62E+06	VTRIS
NJ-33	358	471	293	376	4.20E+06	8.53E+06	VTRIS
US-202B	383	363	356	1125	7.15E+06	1.64E+07	VTRIS
NJ-55	514	514	514	514	8.48E+06	2.91E+07	WIM
NJ-31	420	401	361	604	4.54E+06	9.20E+06	VTRIS
NJ-70	241	198	183	194	1.64E+06	3.00E+06	VTRIS

Pavement Damage Cost per Truck

The unit pavement damage cost was obtained by dividing the NPV of total cost by the number of total ESALs in the analysis period. Table 9 shows the calculated average values of unit pavement damage cost (\$ per ESAL lane-mi), respectively, for thick/thin flexible pavements and thick/thin composite pavements. As expected, the unit pavement damage cost decreases as the analysis period increases. Generally, the pavement damage cost of the thick pavement is less than the pavement damage cost of the thin pavement. This is consistent with the findings reported by previous literature. Table 34 lists the unit pavement damage cost from different sites summarized in two road categories.

After the load equivalency factors and the unit pavement damage cost are known, the pavement damage cost caused by an individual truck can be estimated using the equation below. In this case, the pavement damage caused by an individual truck with a combination of different axles is equivalent to the linear combination of the damage caused by each axle. The proposed methodology provides a universal approach to allocate the cost responsibility among different vehicle classes with different axle types, loads, and tire pressure levels.

$$\text{Cost per truck} = \sum_{i=1}^k LEF_i \times \text{unit pavement damage cost} \quad (47)$$

where

LEF_i = Load equivalency factor for each axle group.

Examples of pavement damage cost caused by individual truck on Interstate highways and state highways are shown in Table 35 and Table 36. The truck weights and axle loads represented the most common axle configurations as observed in the WIM data. The total equivalent ESALs of each individual truck with

different axle loads and configurations were shown in the tables. The results clearly indicate that a truck having the same GVW but different axle configurations could cause significantly different pavement damage and thus be responsible for different cost shares.

The data presented here provide a basis for the axle-weight-distance based pricing strategy for single-trip permit fee if the axle load distribution of overweight trucks and the travel distance of each truck trip are known. On the other hand, if the total annual mileage is reported by the truck operator, the annual permit fee could be charged based on the registered GVW and the axle configuration. In this case, enforcement becomes important to capture the violations on the real weight that is carried by the truck during the trip or the deviation of truck trips or mileage from the planned routes.

Table 34 - Unit pavement damage costs (FY2015 \$ per ESAL lane-mi)

Analysis Period	Road Category	Pavement cost		Project cost	
		Average	Range	Average	Range
30 years	Interstate highway	0.038	0.027-0.052	0.048	0.013-0.083
	State road	0.250	0.092-0.483	0.314	0.115-0.599
60 years	Interstate highway	0.027	0.018-0.038	0.032	0.009-0.061
	State road	0.161	0.046-0.345	0.215	0.049-0.428

Table 35 - Example of pavement damage cost per truck on Interstate highways

Truck class	Class 4		Class 5		Class 6		Class 7		Class 8		Class 9		Class 10		Class 11		Class 12		Class 13	
GVW (kip)	29.9	44.9	30.6	42	31.5	48.6	44.2	69.7	38.9	57.9	48.6	70.8	41.6	63.4	43.3	66.4	59.2	79.9	77.2	108
Single axle (kip)	11.9	18.7	10.8	18	13.4	14.5	12.8	10.3	8.36	9.24	10.8	10.1	10.6	10.1	9.46	9.9	7.7	10.3	5.28	9.24
	18		19.8	24					14.3	17.4					13	13.4	14.3	16.3		
															7.48	16.3	11	13.6		
															6.82	11	9.02	16.9		
Tandem axle (kips)		26.2			18	33.9			16.3	31	20.5	29.7	16.1	20.7			17.2	22.7		
										17.4	31									
Tridem axle (kips)							31.5	59.4					15	32.3					34.5	54.8
																				44.4
Quad axle (kips)																			47	
Total Equivalent ESALs	0.93	1.4	1.22	3.14	0.37	1.69	0.42	2.36	0.44	1.7	0.41	1.87	0.19	0.53	0.34	1.43	0.52	1.51	0.66	2.51
Damage cost (\$ per mi)	0.04	0.05	0.05	0.12	0.01	0.06	0.02	0.09	0.02	0.06	0.02	0.07	0.01	0.02	0.01	0.05	0.02	0.06	0.03	0.1

Table 36 - Example of pavement damage cost per truck on state roads

Truck class	Class 4		Class 5		Class 6		Class 7		Class 8		Class 9		Class 10		Class 11		Class 12		Class 13	
GVW (kip)	29.9	44.9	30.6	42	31.5	48.6	44.2	69.7	38.9	57.9	48.6	70.8	41.6	63.4	43.3	66.4	59.2	79.9	77.2	108
Single axle (kip)	11.9	18.7	10.8	18	13.4	14.5	12.8	10.3	8.36	9.24	10.8	10.1	10.6	10.1	9.46	9.9	7.7	10.3	5.28	9.24
	18		19.8	24					14.3	17.4					13	13.4	14.3	16.3		
															7.48	16.3	11	13.6		
															6.82	11	9.02	16.9		
															6.38	15.8				
Tandem axle (kips)		26.2			18	33.9			16.3	31	20.5	29.7	16.1	20.7			17.2	22.7		
											17.4	31								
Tridem axle (kips)							31.5	59.4					15	32.3					34.5	54.8
																				44.4
Quad axle (kips)																			47	
Total Equivalent ESALs	0.93	1.4	1.22	3.14	0.37	1.69	0.42	2.36	0.44	1.7	0.41	1.87	0.19	0.53	0.34	1.43	0.52	1.51	0.66	2.51
Damage cost (\$ per mi)	0.23	0.35	0.31	0.78	0.09	0.42	0.1	0.59	0.11	0.42	0.1	0.47	0.05	0.13	0.08	0.36	0.13	0.38	0.16	0.63

Greenhouse Gas Emissions and Fuel Consumption Attributable to Overweight Freight Vehicles

A model was developed to estimate the costs to road users of excess fuel consumption and greenhouse gas (GHG) emissions from pavement deterioration due to overweight freight vehicles. Fuel consumption, consumer costs and GHG emissions were estimated for the areas around bridges on nine restricted access highways in New Jersey. Results are expressed on a per mile of highway basis.

This model was applied to nine bridges and two mile segments of highway in New Jersey, as were other analysis done for this report. These include:

- I-195 between mileposts 9.0 and 11.0
- I-78 between mileposts 4.0 and 6.0
- I-80 between mileposts 31.0 and 33.0
- US 1 between mileposts 47.0 and 49.0
- I-287 between mileposts 61.0 and 63.0
- I-295 between mileposts 39.0 and 41.0
- NJ 34 between mileposts 0.0 and 2.0
- US 202 between mileposts 2.0 and 4.0
- NJ 55 between mileposts 26.0 and 28.0

For each segment IRI values were obtained based on WIMS data and AADT for trucks and all vehicles, as noted in the section on pavements.

Methods and Assumptions

Fuel consumption of the vehicles using each road segment is estimated using the World Bank's Highway Development and Management System (HDM4) (Bennett and Greenwood, 2013a 2003b) as calibrated for US roads based on NCHRP Report 720 (Chatti and Zaabar, 2012). The mix of vehicles using the roads is estimated based on default assumptions for restricted roads in New Jersey between 2012 and 2050 using EPA's MOVES model. Average speed is estimated as free flow speed adjusted for congestion based on the Highway Capacity Model (Transportation Research Board, 2010). The NJDOT Straight Line Diagrams (2010) were used to determine road characteristics. AADT for trucks and for all vehicles and indicators of road deterioration in particular IRI were obtained. Other data inputs needed for the HDM4 model are discussed below. Fuel consumption by weight is the basis for estimations of direct emissions of CO₂ and upstream emissions of CO₂, CH₄, and N₂O. Consumer fuel costs are assumed to be constant between 2012 and 2031 at the rates of \$3.742 per gallon for gasoline and \$4.176 per gallon for diesel (EIA, 2014) in 2014 dollars.

Fuel Consumption

NCHRP 720 provides estimates of modeling factors for 15 types of vehicle (Chatti and Zaabar, 2012). Fuel consumption estimates are based on vehicle speed, vehicle mix, engine efficiency, power, congestion, and AADT. Engine efficiency is taken from NCHRP defaults for gasoline engines of various sizes and for diesel engines. Power includes tractive power, power to the vehicle's accessories and the power necessary to overcome friction in the engine. Adjustments to speed are accounted for using HCM 2010.

Any effect of road deterioration on fuel consumption will be as a result of an increase in the tractive power needed to move vehicles. Tractive power requirements are the result of aerodynamic forces, gradient forces, curvature forces, rolling resistance and inertial forces. Aerodynamic forces are determined by air drag, vehicle frontal area, air density and speed. Speed is the only factor for which NCHRP 720 does not offer a default. Gradient force is determined by vehicle weight, grade, and gravity. Of these there are default vehicle weights by vehicle type and gravity is a constant (Chatti and Zaabar, 2012).

It is assumed that the nine segments modeled here are level (grade = 0%). Curvature forces include the sharpness of the average directional adjustment (curvature radius), vehicle weight, number of wheels, and speed, and tire stiffness. The default value of 3000 meters was used for the curve radius. Of these only speed does not have a default value. Rolling resistance includes tire factors, and three measures of pavement texture or distress: mean profile depth (MPD), international roughness index (IRI), and the Benkelman Beam rebound deflection (DEF). Of these only the tire factors have defaults in NCHRP 720. Inertial forces are a result of acceleration and deceleration. Please refer to the report (Chatti and Zaabar, 2012) for additional information necessary to implement this model. The variables that cannot be taken from defaults in NCHRP 720 include:

- Vehicle Speed (m/sec)
- Vehicle Acceleration (m/sec²)
- Mean Profile Depth (MPD) (mm)
- International Roughness Index (IRI) (m/km)
- Benkelman Beam Rebound Deflection (DEF) (mm)
- Gradient (radians)
- Surface Type (asphalt or concrete)
- Congestion (dFuel) (percentage)

Velocity is estimated as the free flow speed calculated by the 2010 Highway Capacity Model. Idling is calibrated in NCHRP 720 (Chatti and Zaabar, 2012) by vehicle type. Acceleration is expected to be a minimal non-zero number to account for accelerations and decelerations. Acceleration is assumed to be 1 m/sec² for all facilities and vehicle types. Ranges were given as generalized estimates for MPD (1.5 – 2.5 mm) and DEF (0.2-0.5). The midpoints of these ranges were used for all facilities, i.e. 2.0 for MPD and

0.35 for DEF. IRI was estimated for all facilities using the Mechanistic-Empirical Design Guide (MEPDG). The grade was assumed to be level, i.e. equal to zero, for all segments. With one exception for each type of wearing surface, all bridge surfaces are concrete and all road surfaces are asphalt. A congestion penalty of one percent was included for all vehicles and facilities to account for further loss of fuel efficiency to account for extremes of slower speeds and accelerations/decelerations beyond the very conservative estimates made here.

Vehicle Mix

The vehicle mix assumptions of this model are that the distribution of vehicle types on restricted access New Jersey highways is uniform for all restricted access facilities in New Jersey. A MOVES script was run that specified the State of New Jersey and restricted roads to both urban and rural for years 2012 through 2031. Other years from 2032 to 2050 were extracted as well in hopes that more years of WIMS data would be available. The output variables of that run were vehicle type, year and VMT. For each year, each vehicle type was standardized by total VMT for the year, which produced each vehicle type's proportional share of total VMT. It is assumed that traffic volume is unchanged from year to year.

Table 37 - MOVES Vehicle Types

Vehicle Class	Weight		Fuel Type
	Pounds	Kilograms	
Passenger Cars	Not Classified by Weight		Gasoline
Passenger Cars	Not Classified by Weight		Diesel
Light Duty Gasoline Trucks	≤6,000	≤2,722	Gasoline
Light Duty Gasoline Trucks	6,000-8,500	2,722-3,856	Gasoline
Light Duty Diesel Trucks	≤8,500	≤3,856	Diesel
Heavy Duty Gasoline Vehicles and Buses	>8,500	>3,856	Gasoline
Heavy Duty Diesel Vehicles	8,501-10,000	3,857-4,536	Diesel
Heavy Duty Diesel Vehicles	10,001-19,500	4,537-8,845	Diesel
Heavy Duty Diesel Vehicles	19,501-33,000	8,846-14,969	Diesel
Heavy Duty Diesel Vehicles	>33,000	>14,969	Diesel
Diesel Transit and School Buses	Not Classified by Weight		Diesel

Adjustments to Vehicle Mix

There are important differences in the way HDM4 and MOVES classify vehicles. The MOVES run produced VMT data for eleven vehicle types shown in Table 37. These include gasoline and diesel passenger cars, light duty gasoline and diesel trucks, heavy duty gasoline trucks, and buses over 8,500 pounds, heavy duty diesel trucks in four weight classes from over 8,500 pounds, and diesel buses. The assignment to NCHRP 720 vehicle types is shown in Table 38, with changes of fuel type to accommodate MOVES's more complete classification of vehicle types. Changes to the fuel type-determined base efficiency are also noted. Changes to tire type are also noted.

HDM4 includes three types of passenger cars, including small, medium, and large. All have gasoline engines. The calibrated values in NCHRP 720 for engine, tire, and vehicle characteristics are identical for all three, including weight. MOVES refers to passenger cars as a whole but models gasoline and diesel engines. It is assumed that all passenger cars have a weight of 1.9 MT (4,189 lbs.). The base efficiency factor is reduced from 0.096 to 0.059 ml/kW/sec to account for a diesel engine in a diesel passenger car.

Smaller light duty gasoline trucks (< 6,000 lbs. or 2,722 kg) in MOVES are modeled as light delivery cars in HDM4 (2,540 kg. or 5600 lbs.). The vehicle types in both models are gasoline engines. The base efficiency is not adjusted.

In HDM4 light trucks weigh 4,500 kg (9,921 lbs.) and have gasoline engines. This category provides the best available match for heavy duty gasoline vehicles (over 8500 lbs. or 3,856 kg.) and lighter heavy duty diesel vehicles (up to 4,536 kg. or 10,000 lbs.) It is also used for light duty diesel trucks and the heavier light duty gasoline trucks (up to 3,856 kg. or 8,500 lbs.). For gasoline vehicles, the base efficiency is unchanged. For diesel vehicles, the base efficiency was lowered from 0.062 to 0.059 ml/kW/sec to account for diesel engines.

Other MOVES vehicle type categories are assigned to HDM4 as follows: below 19,500 lbs. (8,845 kg) medium truck (6,500 kg), up to 33,000 lbs. (14,969 kg) heavy truck (13,000 kg.), above 33,000 lbs. (14,969 kg) articulated truck (13,600 kg). Diesel buses were assigned to medium buses (4,500 kg)

HDM4 gives unrealistically low estimates of tire stiffness for radial tires above 2,500. The model predicts fuel efficiency below one mile per gallon for light delivery cars and light trucks when radial tires are specified at any speed (HDM4 default for these vehicle types). By changing the specification to bias tires, fuel efficiency rose to roughly 20 mpg for light delivery cars and to roughly 10 mpg for light trucks. Because of this, bias tires are assumed for all vehicles except passenger cars.

Table 38 - Conversions of MOVES Vehicle Types to HDM4 Vehicle Types

Vehicle Class		Fuel Type		Efficiency (ξb)	
MOVES	HDM4	HDM4	Adjusted	HDM4	Adjusted
Passenger Cars	Medium car	Gasoline	Gasoline	0.096	0.096
Passenger Cars	Medium car	Gasoline	Diesel	0.096	0.059
Light Duty Gasoline Trucks up to 6000 lbs.	Light delivery car	Gasoline	Gasoline	0.072	0.072
Light Duty Gasoline Trucks up to 6001 - 8500 lbs.	Light truck	Gasoline	Gasoline	0.062	0.062
Light Duty Diesel Trucks Up to 8500 lbs.	Light truck	Gasoline	Diesel	0.062	0.059
Heavy Duty Gasoline Vehicles and Buses >8500 lbs.	Light truck	Gasoline	Gasoline	0.062	0.062
Heavy Duty Diesel Vehicles 8501-10000 lbs.	Light truck	Gasoline	Diesel	0.062	0.059
Heavy Duty Diesel Vehicles 10001-19500 lbs.	Medium truck	Gasoline	Diesel	0.059	0.059
Heavy Duty Diesel Vehicles 19501-33000 lbs.	Heavy truck	Diesel	Diesel	0.059	0.059
Heavy Duty Diesel Vehicles >33000 lbs.	Articulated truck	Diesel	Diesel	0.059	0.059
Diesel Transit and School Buses	Medium bus	Diesel	Diesel	0.059	0.059

Vehicle Class		Tire Type		Weight (MT)	
MOVES	HDM4	HDM4	Adjusted	HDM4	Adjusted
Passenger Cars	Medium car	Radial	Radial	1.9	1.9
Passenger Cars	Medium car	Radial	Radial	1.9	1.9
Light Duty Gasoline Trucks up to 6000 lbs.	Light delivery car	Radial	Bias	2.54	2.54
Light Duty Gasoline Trucks up to 6001 - 8500 lbs.	Light truck	Radial	Bias	4.5	4.5
Light Duty Diesel Trucks Up to 8500 lbs.	Light truck	Radial	Bias	4.5	4.5
Heavy Duty Gasoline Vehicles and Buses >8500 lbs.	Light truck	Radial	Bias	4.5	4.5
Heavy Duty Diesel Vehicles 8501-10000 lbs.	Light truck	Radial	Bias	4.5	4.5
Heavy Duty Diesel Vehicles 10001-19500 lbs.	Medium truck	Bias	Bias	6.5	6.5
Heavy Duty Diesel Vehicles 19501-33000 lbs.	Heavy truck	Bias	Bias	13	13
Heavy Duty Diesel Vehicles >33000 lbs.	Articulated truck	Bias	Bias	13.6	13.6
Diesel Transit and School Buses	Medium bus	Bias	Bias	4.5	4.5

Average Speed

The HCM 2010 model was used to estimate adjusted free flow speed for the nine segments modeled. AADT in both directions was ranges from 13,400 – 123,375 based on the WIMS data. The proportion of trucks and buses were taken for each year from the MOVES run, as previously discussed. Other variables are based on the 2010 NJDOT Straight Line Diagrams. The inputs are shown in Table 39.

Table 39 - HCM 2010 Inputs

	Funct. Class	Speed Limit	Median Present	Access Points	AADT	Shoul der Width	Lane Width	Number of Lanes	Urban or Rural	Grade	Prop. Trucks / Buses	Avg. Speed
		mph		per mile		Feet	Feet					mph
I-195	Freeway	65	TRUE	0.667	48,796	12	12	2	Rural	Level	MOVES	73
I-78	Freeway	65	TRUE	0.667	87,602	12	12	2	Urban	Level	MOVES	73
I-80	Freeway	65	TRUE	1.000	84,740	12	12	3	Urban	Level	MOVES	73
US 1	Arterial	50	TRUE	10.000	123,375	10	12	4	Urban	Level	MOVES	52
I-287	Freeway	65	TRUE	0.167	105,620	12	12	2	Urban	Level	MOVES	70
I-295	Freeway	65	TRUE	0.500	101,040	12	12	3	Urban	Level	MOVES	75
NJ 34	Arterial	55	TRUE	8.000	24,481	10	12	2	Urban	Level	MOVES	58
US 202	Arterial	55	TRUE	0.500	13,400	12	12	2	Rural	Level	MOVES	60
NJ 55	Freeway	65	TRUE	2.000	21,500	12	12	2	Urban	Level	MOVES	70

Greenhouse Gases

Both direct and upstream GHG emissions are estimated from fuel consumption based on estimates from the GREET model (Argonne National Laboratory, 2011) that are used in the GASCAP model (Noland and Hanson, 2014). Carbon equivalence was estimated using the IPCC AR4 standard (Le Treut et al. 2007) in which the carbon dioxide equivalence of GHGs is as follows:

- CO₂ 1
- CH₄ 25
- N₂O 298

Results

Data were run for 2012 through 2031 for the nine road segments. Because the data were restricted to the bridge surfaces themselves rather than segments of known length, costs and GHG emissions are presented as factors per mile of highway. The pavement of the bridge surface differed from that of the road surface in seven of nine cases. All the bridge pavement surfaces are concrete, with the exception of I-195, which is asphalt. All the road surfaces (within one mile of the bridge) are asphalt, with the exception of I-287, which is concrete. While our data reflects the bridge pavement

conditions, we assume that this applies to the nearby road surfaces; however, this is calculated for both asphalt and concrete pavements.

IRI values increase with road surface deterioration and this leads to increases in GHG emissions. The analysis focuses on the marginal increase due to overweight trucks on the road segments. Figure 45 shows a comparison of the change in IRI over time with overweight truck traffic compared to no overweight trucks using US 1 as an example (and assuming asphalt pavement). Overweight trucking accounts for a small but linear and increasing difference in the total IRI over 20 years. Figure 45 shows that over 20 years IRI increased on US 1 from roughly 1.5 m/km to 2.25 m/km with no overweight trucks and 2.5 m/km with overweight trucks. The range of 2012 IRI values is 1.351 to 1.545 m/km. The range for 2031 is 1.775 to 2.546 m/km.

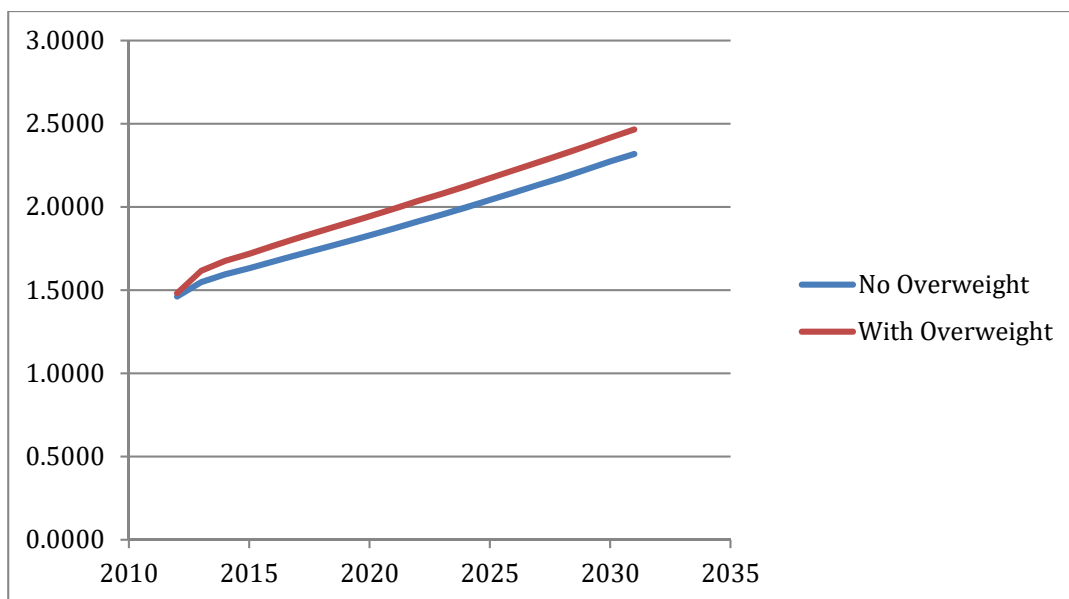


Figure 45. IRI progression on US 1 (m/km)

Table 40 and Table 41 display results for each of the highway segments analyzed assuming asphalt pavements, over a 20-year lifetime. For gasoline, total consumption increases vary from a minimum of 500 gallons on NJ 34 to a maximum of roughly 28,000 gallons on US 1. For diesel, total consumption varies from a minimum of 131 gallons to a maximum of 7,430 gallons on the same facilities. The cost of fuel consumption to all users increases between \$2,423 (\$121 per year) and \$135,964 (\$6,730 per year) per mile on these highways in 2014 dollars. Proportionally the largest percent increases in fuel consumption are I-195 (0.14% gasoline – 0.09% diesel) and NJ 55 (0.13% gasoline – 0.09% diesel). GHG emissions increases (over 20 years) are relatively minor. Table 42 and Table 43 present results assuming concrete pavements. The differences are negligible, thus despite not having IRI data that matches the road segment pavement type, these results suggest that differences in the deterioration rates, and their effect on fuel consumption, are likely minor.

Table 40 - Predicted Fuel Consumption and Costs Attributable to Highway Use by Overweight Trucks over 20 years - Asphalt

	Predicted Gasoline Consumption per Mile					Predicted Diesel Consumption per Mile					Total Extra Cost to Consumer
	With Overweight Gallons	No Overweight Gallons	20-year Difference Gallons	Difference per cent	Added Consumer Cost	With Overweight Gallons	No Overweight Gallons	20-year Difference Gallons	Difference per cent	Added Consumer Cost	
I-195	17,067,122	17,043,617	23,505	0.138%	\$88,191	6,953,242	6,947,000	6,242	0.090%	\$26,067	\$114,257
I-78	30,722,838	30,697,796	25,042	0.082%	\$93,958	12,182,933	12,176,345	6,588	0.054%	\$27,511	\$121,469
I-80	29,154,743	29,131,330	23,413	0.080%	\$87,846	10,863,763	10,857,987	5,776	0.053%	\$24,121	\$111,966
US 1	28,299,400	28,271,432	27,968	0.099%	\$104,936	10,104,916	10,097,486	7,430	0.074%	\$31,028	\$135,964
I-287	39,166,007	39,163,425	2,582	0.007%	\$9,688	13,557,904	13,557,344	560	0.004%	\$2,339	\$12,026
I-295	36,471,360	36,464,423	6,937	0.019%	\$26,028	13,079,162	13,077,542	1,620	0.012%	\$6,765	\$32,793
NJ 34	6,225,272	6,224,772	500	0.008%	\$1,876	2,246,633	2,246,502	131	0.006%	\$547	\$2,423
US 202	3,495,110	3,494,017	1,093	0.031%	\$4,101	1,497,758	1,497,468	290	0.020%	\$1,211	\$5,312
NJ 55	7,615,226	7,605,166	10,060	0.132%	\$37,745	2,825,802	2,823,284	2,518	0.090%	\$10,515	\$48,260

Table 41 - Predicted GHG Emissions Attributable to Highway Use by Overweight Trucks over 20 years - Asphalt

	Predicted Greenhouse Gas Emissions with Overweight Trucks per Mile						Predicted Greenhouse Gas Emissions with No Overweight Trucks per Mile						Total increase in GHG CO ₂ e MT	Difference %
	Upstream			Direct			Upstream			Direct				
	CO ₂ MT	CH ₄ MT	N ₂ O MT	CO ₂ e MT	CO ₂ MT	CO ₂ e MT	CO ₂ MT	CH ₄ MT	N ₂ O MT	CO ₂ e MT	CO ₂ MT	CO ₂ e MT		
I-195	46,575	372.345	2.377	56,592	225,189	281,780	46,604	372.595	2.380	56,628	224,913	281,541	239	0.085%
I-78	83,193	665.354	4.275	101,100	401,953	503,053	83,132	664.867	4.271	101,026	401,660	502,686	367	0.073%
I-80	77,431	619.800	4.036	94,128	374,305	468,434	77,375	619.351	4.033	94,061	374,035	468,096	338	0.072%
US 1	74,202	594.299	3.905	90,224	358,823	449,046	74,135	593.754	3.901	90,141	358,494	448,635	411	0.092%
I-287	101,767	815.399	5.393	123,759	492,238	615,996	101,761	815.351	5.392	123,751	492,209	615,960	36	0.006%
I-295	95,752	766.848	5.035	116,423	463,015	579,438	95,736	766.717	5.034	116,403	463,015	579,418	20	0.003%
NJ 34	16,375	131.128	0.860	19,909	79,177	99,086	16,373	131.119	0.860	19,908	79,171	99,078	8	0.007%
US 202	9,707	77.551	0.489	11,792	46,871	58,662	9,705	77.530	0.489	11,789	46,858	58,646	16	0.027%
NJ 55	20,199	161.695	1.054	24,556	97,648	122,204	20,175	161.502	1.053	24,526	97,531	122,058	146	0.119%

Table 42 - Predicted Fuel Consumption and Costs Attributable to Highway Use by Overweight Trucks over 20 years - Concrete

	Predicted Gasoline Consumption per Mile					Predicted Diesel Consumption per Mile					Total Extra Cost to Consumer
	With Overweight	No Overweight	20-year Difference		Added Consumer Cost	With Overweight	No Overweight	20-year Difference		Added Consumer Cost	
	Gallons	Gallons	Gallons	per cent		Gallons	Gallons	Gallons	per cent		
I-195	16,754,776	16,731,288	23,488	0.140%	\$88,127	6,530,296	6,524,010	6,286	0.096%	\$26,250	\$114,377
I-78	30,160,818	30,135,827	24,991	0.083%	\$93,766	11,442,558	11,436,127	6,431	0.056%	\$26,856	\$120,622
I-80	28,617,303	28,593,890	23,413	0.082%	\$87,846	10,196,152	10,190,492	5,660	0.056%	\$23,636	\$111,482
US 1	27,714,965	27,687,047	27,918	0.101%	\$104,748	9,355,329	9,348,027	7,302	0.078%	\$30,493	\$135,241
I-287	38,458,104	38,455,538	2,566	0.007%	\$9,628	12,757,963	12,757,398	565	0.004%	\$2,359	\$11,987
I-295	35,807,107	35,800,179	6,928	0.019%	\$25,994	12,296,103	12,294,473	1,630	0.013%	\$6,807	\$32,801
NJ 34	6,099,513	6,099,027	486	0.008%	\$1,823	2,085,934	2,085,800	134	0.006%	\$560	\$2,383
US 202	3,425,364	3,424,261	1,103	0.032%	\$4,138	1,391,689	1,391,377	312	0.022%	\$1,303	\$5,441
NJ 55	7,476,569	7,466,493	10,076	0.135%	\$37,805	2,654,955	2,652,402	2,553	0.096%	\$10,661	\$48,466

Table 43 - Predicted GHG Emissions Attributable to Highway Use by Overweight Trucks over 20 years - Concrete

	Predicted Greenhouse Gas Emissions with Overweight Trucks per Mile						Predicted Greenhouse Gas Emissions with No Overweight Trucks per Mile						Total increase in GHG CO ₂ e MT	Difference %
	Upstream			Direct			Upstream			Direct				
	CO ₂ MT	CH ₄ MT	N ₂ O MT	CO ₂ e MT	CO ₂ MT	CO ₂ e MT	CO ₂ e MT	%	N ₂ O MT	CO ₂ e MT	CO ₂ MT	CO ₂ e MT		
I-195	45,079	360.608	2.325	54,787	218,043	272,830	45,108	360.858	2.328	54,824	217,767	272,591	239	0.088%
I-78	80,546	644.578	4.181	97,906	389,307	487,214	80,486	644.095	4.178	97,833	389,016	486,849	365	0.075%
I-80	74,987	600.604	3.949	91,179	362,626	453,805	74,932	600.157	3.945	91,112	362,357	453,468	337	0.074%
US 1	71,494	573.032	3.809	86,955	345,881	432,836	71,427	572.490	3.805	86,873	345,554	432,427	409	0.095%
I-287	98,721	791.436	5.279	120,080	477,666	597,746	98,715	791.388	5.279	120,073	477,637	597,710	36	0.006%
I-295	92,824	743.823	4.927	112,888	449,010	561,897	92,807	743.692	4.926	112,868	448,931	561,798	99	0.018%
NJ 34	15,793	126.562	0.839	19,207	76,398	95,605	15,792	126.553	0.839	19,206	76,392	95,598	7	0.008%
US 202	9,348	74.737	0.478	11,359	45,156	56,515	9,345	74.715	0.477	11,355	45,143	56,498	17	0.029%
NJ 55	19,572	156.766	1.031	23,798	94,649	118,447	19,548	156.572	1.030	23,769	94,532	118,301	146	0.124%

These calculations provide a per mile estimate of the fuel consumption and GHG emissions associated with the road deterioration from overweight trucks. Factoring these up to the entire state networks requires the assumption that the same fraction of overweight trucks uses the network throughout the state. This can also be broken down by Interstates/Turnpikes and Principal Arterials. According to FHWA Highway Statistics Table HM-20, (FHWA, 2012), the road mileage in New Jersey of Interstates and Other Freeways and Expressways is 920 miles, while Principal Arterial road length totals 1961 miles.

Using the results in Table 40 and Table 41, and both low and high ranges for Interstates versus Principal Arterials, total increases fuel consumption, fuel costs, and GHG emissions, attributable to overweight trucks, are shown in Table 44. While the range is quite broad, total costs could be as high as over \$300 million. The excess GHG emissions range up to over 700,000 MT. Total state GHG emissions are currently about 112 million MT, so the high range is less than 0.1% of current total statewide GHG emissions. While this appears trivial, given the difficulty of achieving reductions, even small amounts should not be ignored.

Table 44 - Estimated total excess fuel consumption, costs, and GHG emissions attributable to overweight trucks over 20 years

	Interstates/Turnpikes	Other Principal Arterials	Total
Low gasoline consumption (gal)	2,375,440	980,500	3,355,940
High gasoline consumption (gal)	23,038,640	54,845,248	77,883,888
Low diesel consumption (gal)	515,200	256,891	772,091
High diesel consumption (gal)	6,060,960	14,570,230	20,631,190
Low cost (\$)	\$11,063,920	\$4,751,503	\$15,815,423
High cost (\$)	\$111,751,480	\$266,625,404	\$378,376,884
GHG emission – low (MT CO ₂ e)	18,400	7,360	25,760
GHG emission – high (MT CO ₂ e)	337,640	378,120	715,760

Conclusions

A spreadsheet tool was developed to estimate increased highway user costs and GHG emissions based on increased IRI due to road deterioration. The increased cost and GHG emissions increase for overweight trucks are relatively small but still add to total costs for consumers. Fuel consumption does not increase much beyond one eighth of one percent for any of the highways. However, the results shown here are for one mile of highway in both directions. Factoring the deterioration factors over the entire network would add significantly to total costs, fuel consumption, and GHG emissions, although our estimate of this relies on fairly liberal assumptions concerning the condition of the road network and the extent of overweight truck traffic.

As with pavement LCAs generally (Noshadravan et al 2013), there are important concerns with this model regarding uncertainty. The model is static in terms of real fuel prices. The MOVES model is based on adjusted national data, even though New Jersey was specified. The HCM as applied is based on many national defaults. The HDM model presents the same problem, although it has been calibrated to be valid in the United States. Default inputs were used for most of the inputs. Where necessary to accommodate all diesel vehicle types modeled by MOVES, a diesel engine efficiency factor was added to four types of gasoline vehicles—most notably passenger cars. This is potentially a large source of error since it is the same efficiency factor used for all diesel vehicles including the largest trucks. Where necessary to get realistic fuel efficiency results, the default tire type was changed from radial to bias. Bias tires are stiffer than radial tires and handle heavy loads more efficiently. As modeled in NCHRP 720 radial tires on vehicles weighing more than 2.5 MT have fuel efficiencies of less than one mph. The aggregated error from the combination of these models is not known. A further difficulty was in establishing initial IRI values. The literature recognizes that an important problem with estimating rolling resistance is establishing initial IRI (Santero and Horvath 2009).

Development of a Decision-support Tool and Data-driven Life Cycle Cost Analysis

Decision Support Tool

The final step in this analysis is to assess and predict the maintenance and rehabilitation needs of highways based on a comprehensive Life Cycle Cost Analysis methodology. This step makes use of a user-friendly computerized decision support tool that will be driven by the available data and deterioration models to assess pavement and bridge conditions. Supplemented with traffic and weight data from the WIM and other sensors in NJ, the data is regularly integrated into the decision-support tool to update loads and the deterioration model results to keep up with potential changing traffic patterns.

The decision support (DS) tool is a GIS-based software that seamlessly integrates available pavement, bridge, and traffic data to predict the effect of increased loads and traffic on NJ's infrastructure through the use of NJ specific deterioration models described in the previous tasks. This DS tool produce predictions of the life cycle costs of these facilities using a comprehensive life cycle cost analysis methodology. The structure of the tool can be seen in Figure 46.

This software is achieved by deploying a client-server architecture where all the data is stored in a remote server where it is easy to update. The clients can access the server using a web browser if they have credentials for access.

It is important to emphasize that in the absence of a comprehensive LCCA, it is not possible to accurately predict the impact of increased loads and thus make sound policy decisions such as the pricing of heavy vehicles, types of permits for heavy trucks, sequence and type of maintenance and replacement of certain infrastructure components. The Rutgers ICS team has already developed a GIS-based economic evaluation tool that is being used or tested by NJDOT, NYMTC, NJTPA, and other area agencies, known as NJCost. The NJCost has been used by NJDOT for the preparation of economic analysis section of NJDOT's TIGER applications in 2009 and 2010. Thus, we used ASSIST-ME & NJCost as the basis of the DS tool and build it around our previous research results.

One of the major innovations of this task is to integrate a range of infrastructure data and NJ specific deterioration models to predict the cost implications of various traffic and related loading scenarios.

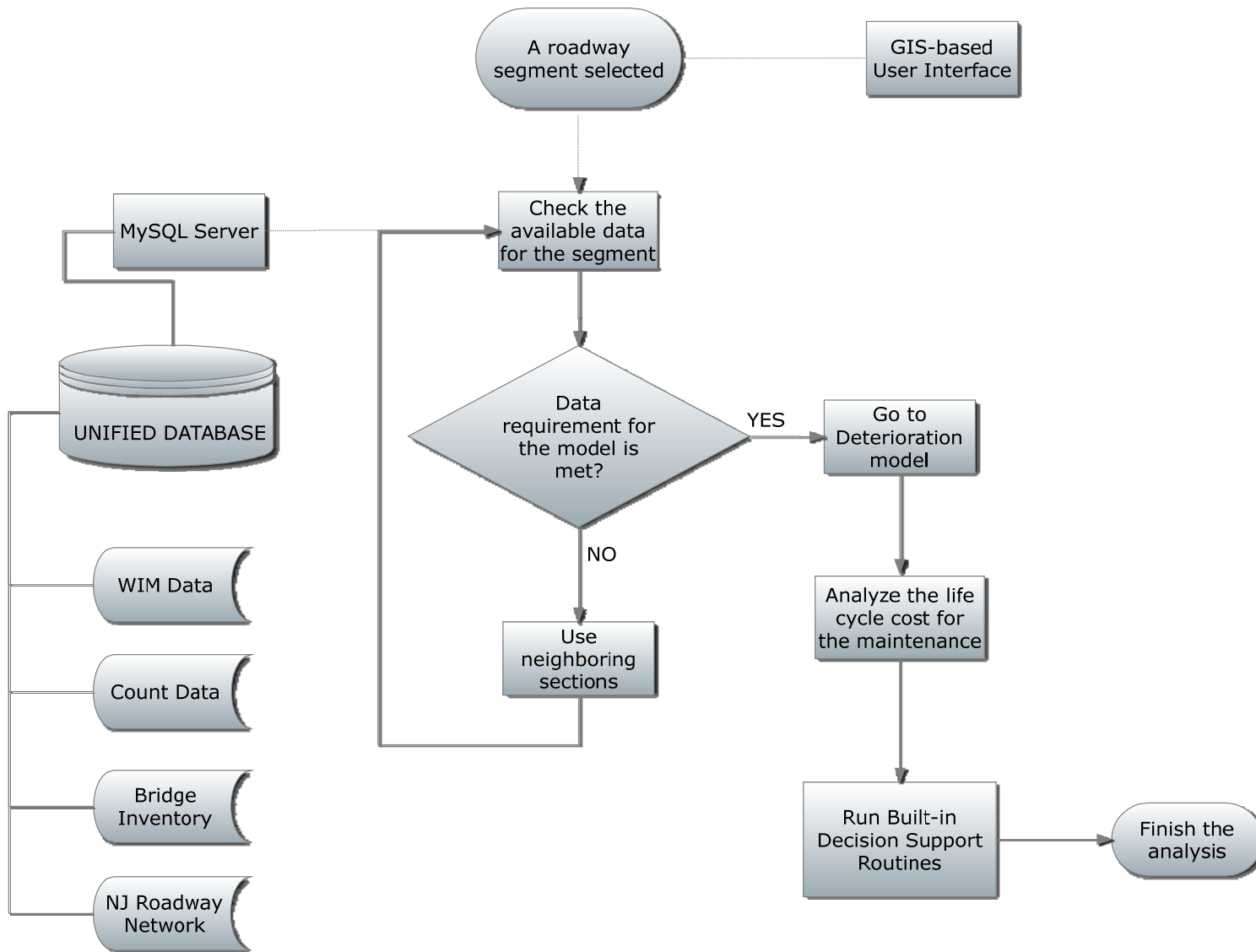


Figure 46. Decision support (DS) tool structure

Software Architecture

For the DS tool, an existing stable web-based interface, developed by Rutgers team, is employed. The interface provides a platform for decision support tool and life cycle cost analysis and make use of the features of ASSISTE-WIM, which is a software developed for NJDOT's Truck Monitoring program.

The tool utilizes spatial features of Google Maps to visualize roadways and WIM stations using the tables in the unified database. As mentioned earlier, MySQL Database Server is used as the backend for storing, managing and processing the data in unified database.

The results for NJ-specific deterioration models are used to assess pavement conditions and bridge conditions based on the available data in the database. Pavement and bridge damage cost functions are incorporated to the tool for calculating the costs of freight on the roadway infrastructure.

Functional Requirements

Functional requirements of the tool are summarized as follows:

- **User Interface:** The software interface is developed using PHP and JavaScript languages. The web-based interface is platform-independent and it can be easily accessed by the users anywhere in the world provided that they have an internet connection and the required credentials. The interface utilizes spatial features of Google Maps to visualize facilities and WIM stations. The bridge locations and WIM stations are geocoded in the software. With the help of GoogleMaps interface, the bridges, WIM stations and roadways are displayed on a web-based map.
- **Background Processing Engine:** This is the key part of the software. All the queries to the database and all the analyses are processed in the background only at the server. As the complex processes run at the server, the user does not need high processing power on his/her computer. Finally, the results are converted to JSON feed and automatically transferred to the user's computer for visualization on the interface.
- **Data Visualization:** To visualize the results in the user interface, first, the analysis results are interpreted by a JavaScript code. Then, the results are displayed on the map in the interface. The visualization features in the software include: (i) annual damage cost for a roadway, (ii) single trip cost for a truck. These features will be explained in detail in Section 5.3.

Data driven Life Cycle Cost Analysis

As mentioned above it is important to clearly explain the data driven LCCA methodology that is at the heart of this task. Even though most transportation policies are local, their

influence often spreads out beyond the area of implementation, as discussed in the previous sections. For example, policy shifts such as weight restrictions can cause truck traffic to change route and utilize highways. As a result, traffic will shift from the impacted part of the network to other areas, and the intensity of the shift will depend on several factors, such as road characteristics, demand structure, and network configuration (Safirova et al., 2007) ⁽¹⁰⁸⁾. Thus, quantification of changes in the transportation costs after the capacity expansion is crucial for policy planners to determine the possible benefits from capacity expansion projects, and select the projects that are most likely to generate highest benefits.

Methodology and Approach

Budget tightening, escalating costs for the maintenance of the public services functioning at an acceptable level, and increased public scrutiny of government-related expenditures had made all segments of our socioeconomic system tuned into the importance of effective management of resources and assets. Transportation agencies are especially concerned in this pursuit because of many reasons; to mention a few, they rank among the top sectors in public spending, the impacts of their investment decisions touch upon every member of the society, which makes public scrutiny rather strenuous. Furthermore, an asset base of \$3 trillion dollars (i.e, the value of the transportation system in the US as estimated by the FHWA) is under the influence of numerous natural and man-made dynamics, many of which are uncontrollable and/or uncertain. Decision-making and management in the transportation sector must be based on informed and conversant support. One of the most recognized techniques that provide such informed support, when applied properly, is the LCCA. This part of the research aims at establishing the guidelines for LCCA.

General Methodology of LCCA

LCCA refers to the systematic process for evaluating long-term public projects of considerable impacts on various domains. The process is performed by summing up the monetary equivalency of all benefits and costs at their respective time of occurrence throughout the analysis period. Then they are converted into a common time dimension so that different alternatives can be compared correctly.

After the costs and benefits are discounted, the appraiser may use a number of indicators that have been developed and applied in the economic evaluation of projects. The most common are the Net Present Value (NPV), the Cost-Benefit Ratio (B/C), the Equivalent Uniform Annual Costs (EUAC), and the Internal Rate of Return (IRR). The choice of the appropriate indicator depends largely on the level and context of the analysis. It may also depend on the degree of uncertainty in some parameters. For example, when projects are evaluated in developing countries where the discount rate is highly uncertain, the IRR format is the preferred format. When the analysis period of the project is unknown or the project is expected to last indefinitely, then EUAC is considered to be the better final format, because the EUAC equation is derived with the

assumption that the project will last indefinitely (ACPA, 2002)⁽⁸⁰⁾. The formulas of each format are presented in Table 45.

In principle, the choice of the economic indicator should consider the following questions:

- Are benefits included in the analysis?
- What is the level of decision-making and/or analysis involved?
- What methods suit the requirements of the particular agency involved?
- How important is the initial capital investment in comparison to future expenditure?
- What method of analysis is the most understandable to the decision-maker?

When the LCCA is used to evaluate project alternatives that result in equal primary benefits but entail uneven costs (i.e., evaluating different types of pavement for a highway, or different types of bridges), the NPV is considered the appropriate indicator (also the most popular) for comparing the differential economic worth of projects

Table 45 - Equations of economic indicators

Equation	Indicator	Abbreviation	Equation
(48)	Net Present Value	NPV	$NPV = \sum_{t=0}^T \frac{B_t - C_t}{(1+d)^t}$
(49)	Benefit-Cost Ratio	B/C	$\frac{PVB}{PVC} = \frac{\sum_{t=0}^T \frac{B_t}{(1+d)^t}}{\sum_{t=0}^T \frac{C_t}{(1+d)^t}}$
(50)	Equivalent Uniform Annual Costs	EUAC	$EUAC = NPV \left[\frac{1(1+d)^t}{(1+d)^t - 1} \right]$
(51)	Internal Rate of Return	IRR	$\sum_{t=0}^T \frac{B_t - C_t}{(1+IRR)^t} = 0$
NPV = Net present value of future costs and benefits; IRR = Internal Rate of Return; B/C = Benefit/Cost; PVB = Present value of future benefits; PVC = Present value of future costs; d = Discount Rate; t = time of incurrence (year); and T = Lifetime of the project or Analysis period (years).			

The NPV indicator, with its additive function, allows the analyst to account only for the differential costs (or benefits), while at the same time maintaining the consistency in the evaluation process. This characteristic reduces the computations needed in the analysis tremendously. All costs or benefits that are known (or assumed) to be equal need not be evaluated. This advantage becomes clear in the later discussion of the costs component in LCCA. With equal benefits among alternatives, Equation (48) (from Table 45) is reduced to:

$$NPVC = \sum_{t=0}^T \frac{C_t}{(1+d)^t} \quad (52)$$

where

C_t is the cost occurring at year t which should include all types of costs, monetary and non-monetary, encountered throughout the analysis periods.

Many LCCA documents restrict these costs to the initial construction cost, rehabilitation cost, annual maintenance cost, and salvage value (considered negative) by assuming that all user and societal costs are equal between alternatives. A detailed discussion of the type of costs that might be encountered as a result of the traditional projects (i.e., bridges and pavements) is presented in Chapter Six. Based on the above categorization of costs, the Net Present Value equation can be rewritten as:

$$NPV = \text{Initial Cost} + \text{pwf}^*(\text{rehabilitation Costs}) + \text{pwf}^*(\text{Maintenance Costs}) - \text{pwf}^*(\text{Salvage}) \quad (53)$$

where

$$\text{pwf}_t = \frac{1}{(1+d)^t} = \text{present worth factor of costs incurring at year } t.$$

LCCA Procedure

Life Cycle Cost Analysis structured approach can be outlined in the following steps:

- (1) Define project's alternatives;
- (2) Deciding on the approach: probabilistic or deterministic;
- (3) Choose general economic parameters: Discount Rate, Analysis Period;
- (4) Establish expenditure stream for each alternative;
- (5) Design rehabilitation strategies and their timings;
- (6) Estimate agency costs;
- (7) Estimate user costs;
- (8) Estimate societal costs;
- (9) Compute Net Present Value for each alternative;
- (10) Compare and interpret results;
- (11) Re-evaluate design strategies if needed.

(1) Defining project's alternatives

This is the first step in LCCA procedure. Experts and experienced professionals suggest strategies that might be potential options for the project. Each pavement design strategy specifies initial design and its performance, time-dependent rehabilitation/treatment activities, their timings and respective performances. At this stage, common costs between different strategies can be identified. For example, in evaluating new pavement projects, right-of-way costs are common to all alternatives. Marginal costs—especially occurring in the future—can be insignificant with respect to the total value of the project, thus it is helpful to identify such costs beforehand.

(2) Decide on the approach that would be followed

Probabilistic vs. Deterministic

Deciding the approach to be followed at this time should be done based on information and data available for the LCCA model parameters. In all cases, most of the LCCA parameters are uncertain and experts generally recommend that the probabilistic approach be adopted. Chapter three presents the methodology for the probabilistic approach.

(3) Choose general economic parameters

General economic parameters are the discount rate and the analysis periods. Both parameters should be equal for all options. We explain the choice of the parameters in detail in their respective sections.

(4) Establish expenditure stream

Expenditure stream diagram can be constructed as shown in the Figure 47.

- Set the design strategies, these design strategies include scope, timing of each activity.
- Compute agency costs (in real dollars) for each year of the analysis period.
- Compute user costs (real dollars) for each year of the analysis.
- Compute societal costs (real dollars) for each year of the analysis.

A typical expenditure stream diagram is shown in Figure 47.

(5) Compute the Net Present Value

After constructing the expenditure stream, computing the Net Present Value of each alternative becomes a straightforward calculation using Eq. #1 or #2 and #3 (from Table 45). It is advisable to compute agency, user, and society costs in separate manner before computing the total value of project to better understand the exact contribution of each cost category to the total final worth.

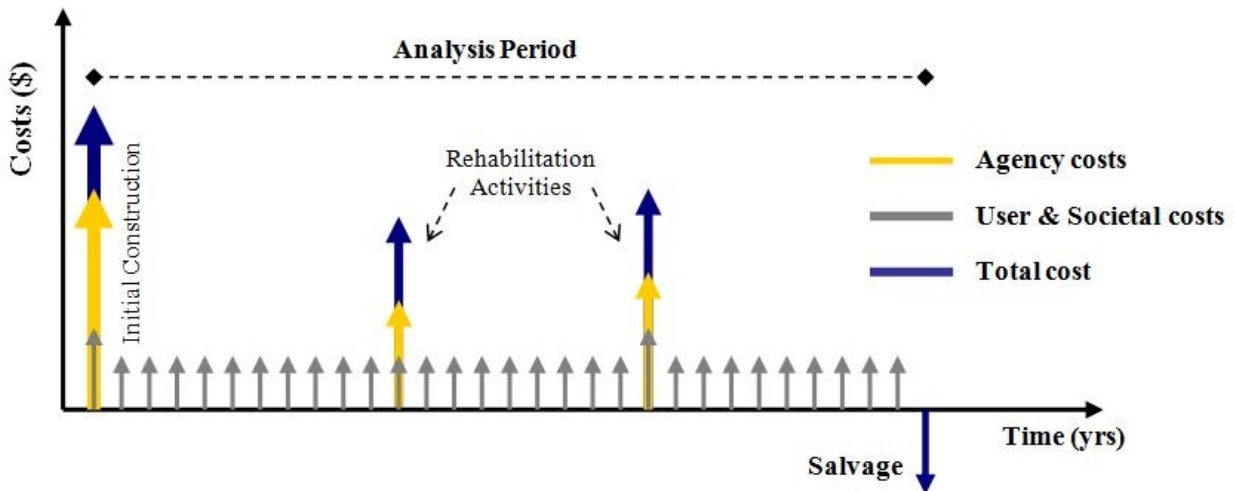


Figure 47. Conceptual cash flow diagram of a project ⁽¹⁰⁹⁾

(6) Compare and interpret results/ Sensitivity Analysis

Once NPV for each alternative is computed, with agency, user, and societal costs presented distinctively, one can interpret the results. Generally, an alternative is preferred if its NPV is less a minimum of 10 percent than the NPV of other competing alternatives. If the difference between NPV of alternatives is less than 10 percent, than such alternatives are considered similar or equivalent. A detailed discussion of results interpretation and the treatment of uncertainty is given in the next chapter, which presents the preferred probabilistic approach. On the other hand, if the deterministic approach is adopted in the analysis, sensitivity analysis should be conducted as a minimum. The sensitivity analysis should examine the variability of the main parameters in the analysis on the overall results. This is done by performing the analysis over a range of possible values of the parameter under testing while holding all other parameters constant. This analysis can give the decision-maker a better representation of the comparison and to some extent it can rule out bias toward certain alternatives.

The most significant parameters in the analysis that should be tested for sensitivity are:

- The discount rate;
- Timing of future rehabilitation activities;
- Traffic growth rate; and
- Unit costs of the major construction components.

(7) Re-evaluate Design Strategies

Presenting results and analyzing them help the process of re-assessing the design strategies, whether in scope, timing, or other factors. Sometimes minor alterations of the design strategies can lead to a better choice for the project.

Uncertainties and Reliabilities

Uncertainty characterizes many of the input parameters in any appraisal process. This characterization is more manifested in transportation projects when the lifetime of the project stretches over long periods of time. No one can be completely sure what interest rate should be applied twenty years from now, or how much traffic volume will be on a particular road in ten years. Engineers and economists have been working hard to estimate the uncertain parameters by deriving empirical models based on scientific research that observe and measure these uncertain variables and the influencing factors. An example of such undertaking was the research of the effects of pavement roughness on user costs, which started in the sixties by the World Bank (Wilde, 1999)⁽¹¹⁰⁾. Nevertheless, no matter how good these models are, the reliability of their outcome can never reach 100 percent level that is anticipated in Life Cycle Cost models.

Regardless of the uncertainties, many analysts appraising public projects in the past, have used (and some still use) deterministic values for the uncertain parameters by either making assumptions about their values using expert opinions or by using the deterministic results obtained from the prediction models, a process identified as the deterministic approach. According to our recent survey, 80 percent of the DOT respondents indicated that they are employing LCCA deterministically.

In best-case scenarios of evaluation processes, highly uncertain and sensitive variables such as the discount rates were treated with a simple risk analysis approach. This approach consisted of performing the analysis a number of times using a range of possible values for that specific variable, then comparing and reporting the results.

The nature of the costs incurred as a result of highway investments can be certain or uncertain (or deterministic or probabilistic). In reality, only a couple of these costs are actually deterministic. As such, the analysis results may be justifiably mistrusted when LCCA models are applied deterministically. The deterministic approach, or using discrete values for the parameters, would provide point-estimates of the outcome, which can result in a misleading decision support system and consequently an unsupported judgment.

For example, in a life cycle cost model that is analyzing two alternatives for a maintenance project, the deterministic approach may yield a point estimate for NPV of \$900,000 for alternative A and \$1,000,000 for alternative B. This makes alternative A the preferred choice, without giving any indication about the inherent variability in the model parameters. Whereas, using other possible values for the parameters (i.e. using a discount rate of 3 percent instead of 5 percent or varying the timing of the future rehabilitation by three years) might reverse the outcome, making alternative B the preferred choice.

Realizing this inherent flaw of using the deterministic approach, the Federal Highway Administration has been promoting the use of reliability concepts in appraising

transportation investments for the past five years (Herbold, 2000) ⁽¹¹¹⁾. Reliability concepts are best applied by adopting the probabilistic approach.

After the life cycle cost model is constructed, the probabilistic approach is employed by:

- (1) Identifying parameters that carry inherent variability in their values.
- (2) Constructing a probability distribution for the chosen parameters that indicates all possible values of the parameter and their relative likelihood of occurrence. Probability distributions can be defined in various function depending on the information and data available. The most common distributions are the uniform, triangular, normal, lognormal, and general.
- (3) After the probability distribution is defined/constructed for all uncertain variables, the final result of the model/problem can then be calculated in two ways, namely, the analytical approach, and simulation:
 - a. The analytical approach requires that the distribution of the uncertain variables in the model be described mathematically. Then the equations for these distributions are combined analytically according to the model to derive the resulting function, which describes the distribution of the possible outcomes. This approach is not practical and was developed when today's computing power was not available. It is not a simple task to describe constructed distributions as equations and it is more difficult to combine distributions analytically given even moderate complexity in the models. Furthermore, the mathematical skills necessary to implement the analytical techniques are significant.
 - b. Monte Carlo simulation is performed. The Monte Carlo simulation uses randomly or sample selected values for each variable in the model, based on the probability of that value occurring for the specific parameter, then obtains the system or model response and records this value. The sequence is performed many times. Each repetition will result in a value for the system response, and these responses will be used to construct the probability distribution of the final outcome. The number of iterations depends on the required level of accuracy and the available computing power. The larger the number of iterations, the better the result, until the simulation starts to converge and any additional iteration will not affect the final distribution (see Figure 48).
- (4) The final step of the probabilistic approach is interpreting the results. The final outcome of the simulation will be a probability distribution of the NPV or EUAC that gives the risk associated with each value (see Figure 49). This outcome format provides an effective support tool for the decision-making process. A wider distribution means a riskier alternative in comparison to the narrower distribution. Sometimes decision makers prefer less risky projects even if the mean of the net present value is higher than the riskier alternatives. Comparing two alternatives can be done by constructing the distribution of the difference between alternatives.

Another method includes plotting the cumulative probability distribution of both alternatives on the same graph where the comparison can be interpreted directly.

The probabilistic approach can also be extended to perform the sensitivity analysis. This type of analysis can help to identify the significant parameters for reevaluating the design strategies when needed. This process is done by plotting a Tornado graph that indicates the parameters and their correlation coefficient for each alternative. Parameters that have the larger correlation coefficient, generally more than 0.5, are considered the most significant.

The key element in the probabilistic approach is defining the probability density function/distribution for every component. These distributions must be defined as accurately as possible based on the information available. Probability distributions of the input variables may be developed using either objective or subjective methods. The objective method uses real data (such as compiled records of the recent bid items prices, or published discount rates) to define the distribution; the subjective method uses expert opinion. Subjective method is used in the absence of hard data. This method requires that the expert(s) choose pre-defined probability distribution that can best fit the variability of the parameter according to his expertise and experience.

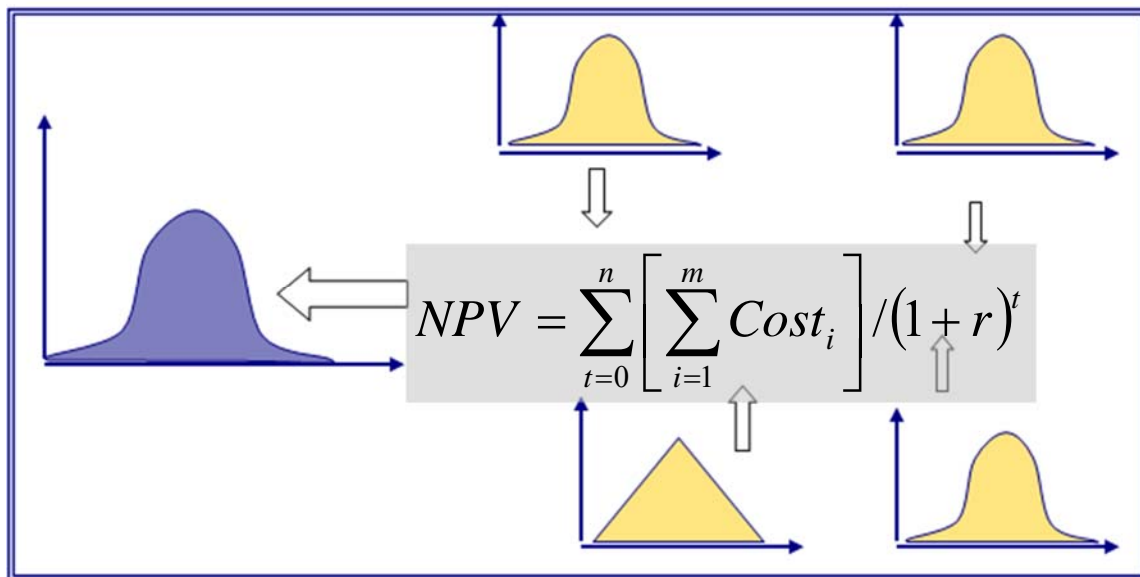


Figure 48. Calculating NPV using Monte Carlo simulation

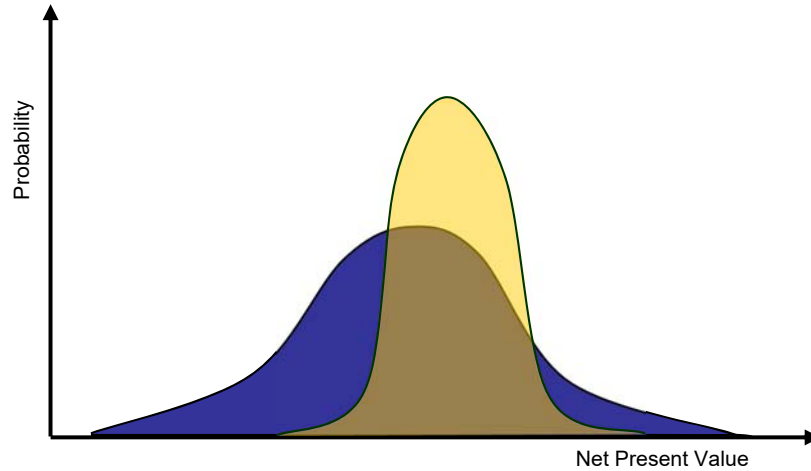


Figure 49. Conceptual probability distribution of LCCA output (NPV)

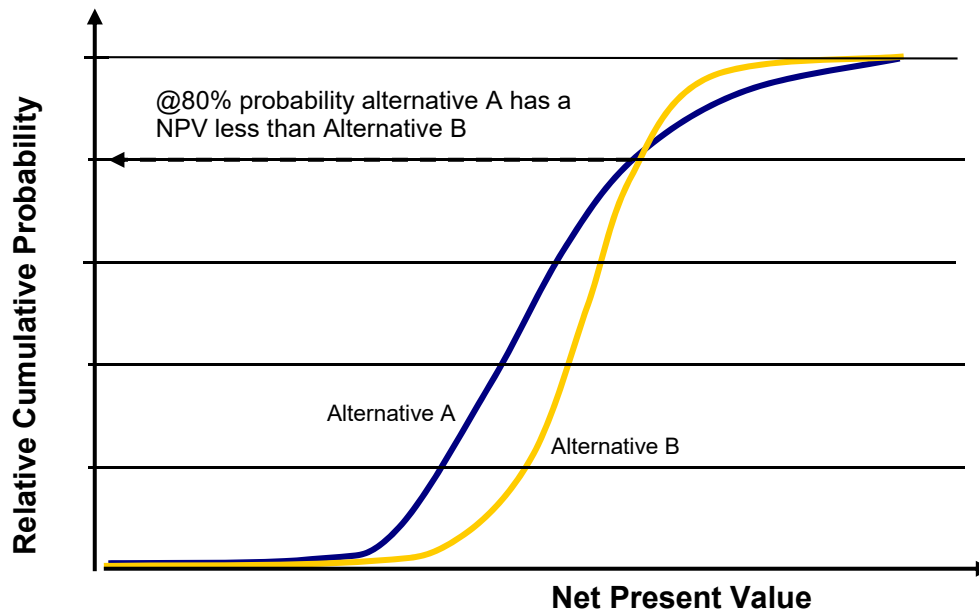


Figure 50. Cumulative probability distribution for two alternatives in LCCA

Wide distributions indicate high uncertainty in the parameters' values (i.e. the range of possible values for the parameter is quite large relative to its value), while narrower distribution indicates less uncertainty (Figure 50). In general, parameters that deal with activities occurring in present or near future are more certain than parameters for activities occurring in the distant future. For example, the values used for initial costs are relatively more certain than the costs of future rehabilitation, and therefore the distribution shape for initial costs is expected to be narrower than the distribution shape of the costs of future rehabilitation. This is exhibited in the probabilistic approach when the uncertainty in initial costs is accounted for by the variability in bid items prices (minimum, average, and maximum), while the future costs takes that variability and combine it with the uncertainty in interest rate, inflation rate, and the timing of future rehabilitation.

So far, the steps in LCCA are discussed in detail. However, it should be noted that the decision tool developed in this study has a limited implementation of LCCA where only the agency cost due to overweight trucks are calculated.

In the future, all other cost items such as user costs and environmental costs can be calculated using the same tool. However, in this study, we focused on the overweight trucks due to the requirement of the project. Ozbay et al. (2007) summarizes the data needed for calculating other cost items in LCCA as seen in Table 46 ⁽¹¹²⁾.

Table 46 - Types of data needed for calculating the other cost items ⁽¹¹²⁾

Cost Category	Data Sources and Type of Data
Vehicle Operating	Cost of fuel, cost of oil, cost of tires, cost of insurance, cost of parking and tolls, depreciation cost, mileage over “n” years, vehicle age
Congestion	Link volume, capacity, and free flow speed
Accident	Length of the road section, number of fatal accidents per year for each highway type, number of injury accidents per year for each highway type, number of property damage accidents per year for each highway, volume, capacity and number of lanes for the corresponding road section
Air Pollution	Fuel consumption at cruising speed, average speed, volume, capacity and free flow speed
Noise	Depreciation value and current housing prices FHWA Traffic Noise Level Model Current noise function TP + Output: % of autos and trucks on the road, % of constant speed autos, % of constant speed trucks, speed of autos, speed of trucks

Self-vehicle operating costs are affected by many factors, such as road design, type of the vehicle, environmental factors, and flow speed of traffic. Vehicle operating costs can be estimated considering depreciation cost, cost of fuel, oil, tires, insurance, and parking/tolls. Congestion costs can be defined as the drivers’ time loss and discomfort in the traffic. Its magnitude depends on volume, capacity of roadway and free flow speed. Accident costs can be classified into two major groups: (1) foregone production/ consumption by individuals, and (2) life-injury damages. In order to estimate the accident costs, the accident occurrence rate and unit cost of accident should be known.

Highway transportation agency accounts for air pollution due to the release of pollutants during motor vehicle operations. Its contribution is either through the direct emission of the pollutants from the vehicles or the resulting chemical reactions of the emitted pollutants with each other and with the existent materials in the atmosphere. Estimating costs attributed to highway air pollution is not a straightforward task, since there are no reliable methods to narrow down the origins of the existing air pollution levels. However, Ozbay et al. (2007) suggests adopting an emission function to estimate the

pollutant quantity generated by motor vehicles ⁽¹¹²⁾. Next, unit cost values of each pollutant can be calculated based on the methods presented in the literature.

There are several methods used to define noise in a numerical range such that any noise source can be examined by the human ear. In general, it is accepted that a sound above 50dB is a nuisance that imposes a cost on society. The social cost of noise is usually estimated by calculating the depreciation in the value of residential units alongside highways (i.e., the closer a house is to a highway, the lower the value of the house, and the higher the cost of the noise).

ASSISTME-WIM Weigh-In-Motion Data Analysis Tool

As a result of the several practical problems in using Weigh-In-Motion data, the research team previously designed an integrated visualization tool, ASSISTME-WIM, to integrate all of this data and provide a visual and analytical framework to utilize the data. The tool uses the benefits of Geographic Information Systems (GIS) and Structured Query Language (SQL) platforms within a single software tool.

ASSISTME-WIM uses a number of databases for WIM station locations and data. The stations' database is a geographic database that includes the specific details of all WIM stations in New Jersey, such as the location, route, milepost, and lane configuration. The SQL database includes three tables for each station, as the software can analyze raw data, classification data, and weight data from WIM stations. Upon launching the application, the data can be loaded to the SQL database if it was not done previously. Data availability on all stations can be checked for a selected time frame, if needed. Then, with the help of a GIS map, there are four different ways to select station(s) to analyze: single, double, route-based, and multiple. Upon selection of the stations, different analysis options for that choice appear, and the user will be able to select date ranges and the desired type of analysis (grouped under seven tabs).

Before executing an analysis, the data filters can be applied to raw ASCII data so that just valid truck traffic is observed. Depending on type of analysis, graphs and/or tables are generated based on the results of queries on the data. Moreover, Microsoft Excel® reports including same graphs and/or tables are generated to give more flexibility to the user for reporting and analyzing the data. There are 7 basic functionalities of the ASSISTME-WIM tool, which are accessible from the user interface:

- **Station Info:** The user selects WIM stations to analyze. There are four options: single selection, double selection (for comparison), route-based selection and multiple selections. These options give the user the ability to select all stations under investigation and automatically run the analysis for all of them.
- **GIS Map:** These WIM station locations are displayed on a map of New Jersey, clearly depicting counties, major roadways, and locations of WIM stations as nodes,

shown in Figure 29. Multiple map views can be chosen in the program to perform comparison studies between different time periods or different stations. Moreover, if a station selected on the map, brief information about the station can be seen in a pop window when hovering over the station with the mouse.

- **Type of Analysis:** There are various ways to analyze data and extract tables and graphs instantly. These are classified under seven main categories: Counts, Class, Comparison, Duration, Multi-year, Canned Report, and WGT Summary.
- **Data Filters:** There is an option to apply filters to the data. If this option is selected, misclassified vehicles and light vehicles (cars and motorcycles) are removed from the data and just valid truck traffic can be monitored at the station.
- **Database Loading:** The data from several stations are extracted from comma-separated text files (for raw ASCII data) or fixed-length text files (for CLA or WGT data) and inserted into the SQL database. This functionality minimizes the labor of dealing with single files for the analyses. Another advantage of a single database is that the machine where the database loaded, if configured accordingly, can be accessed from other clients having the software without need for loading the data again.
- **Data Availability Check:** This functionality enables users to query the whole CLA database and automatically map the available data visually for a selected time frame. A table also can be generated showing how much data is on the database for that period. History/Warnings: After analyzing the data, users can track their actions from the History tab. Every analysis executed by the user is recorded on this tab and users can see the details of the action and open the Excel report of the analysis results from this part. The warning tab is another informational part that makes it easy to follow the batch processes of the program, such as loading data or analyzing data for multiple stations.
- **Reporting:** As soon as executing the analyze command, temporary Excel reports are created which include the same graphs and tables displayed in the software as a result of an analysis. Later, users can view or delete these reports from the History tab.

Although it was developed as a desktop software tool, recently, a web version of ASSISTME-WIM is developed as seen in Figure 51. The geographic map support of the tool is provided by means of Google Maps API. Security vulnerabilities are also considered while developing the application to protect the sensitive data from unauthorized users. In the development of the module both Java Script and PHP languages are used for full interaction of the authorized clients with the web server and Google Maps® server.

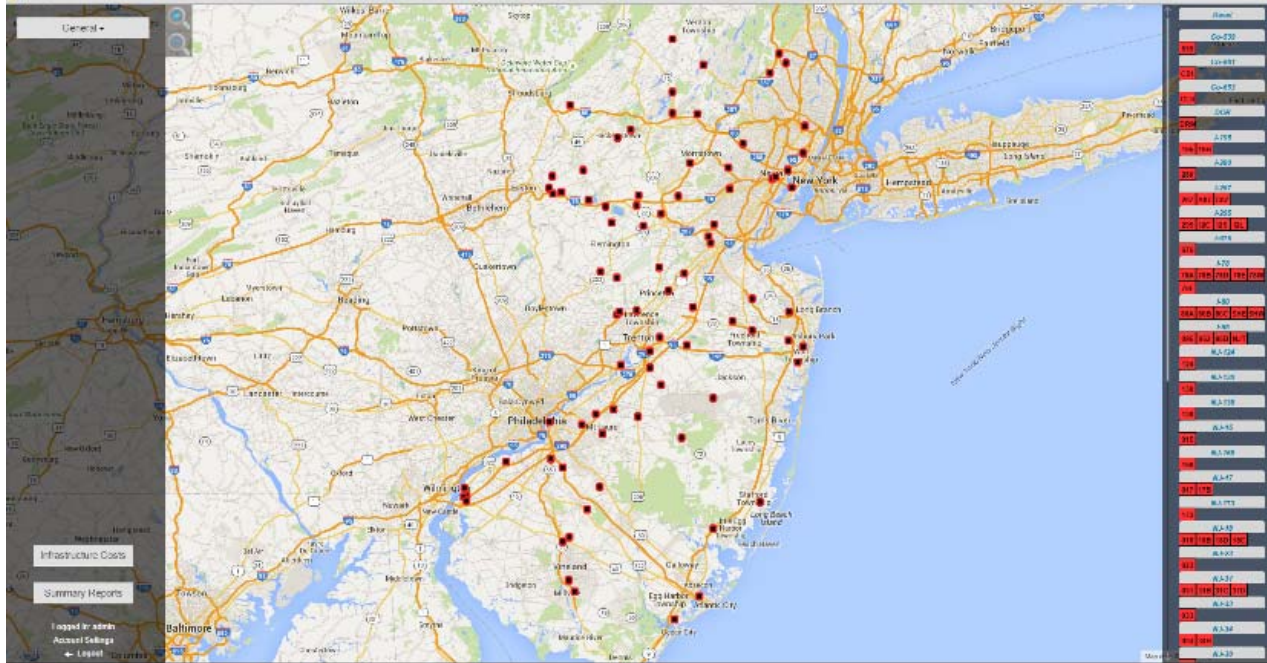


Figure 51. ASSISTME-WIM web user interface

ASSISTME-WIM web runs on a dedicated web server at Rutgers University. The server also runs MySQL to maintain WIM database. The decision tool developed in this study utilize ASSISTME-WIM web interface due to similarities in the data sources and the unified database is also maintained in the same machine as a separate MySQL database.

Features of the Web-based Tool:

Roadway Damage Cost Calculation

Figure 52 shows the flowchart of roadway life cycle cost calculation. First, a roadway is selected using the software interface. Based on the selection, WIM database is queried on the server side to locate the closest WIM station to the roadway. If the closest WIM station is on the selected roadway, the total ESALs and ADTT (truck traffic) for the latest available year calculated from the WIM data (using weight data). If there are no WIM stations on the selected roadway, another query is executed to find the WIM station closest to the roadway. In this case, we need to consider the different traffic patterns on the different roadways. Hence, AADT on the roadway where the closest WIM station located and AADT on the selected roadway are calculated using WIM data (count data in this case). It is assumed that the truck traffic is proportional to AADT of the roadways. As a result, the ADTT and total ESALs for the selected roadway are estimated using the proportionality of AADT of the two roadways. Then, the pavement cost is calculated based on the estimated ESALs and the unit pavement damage costs. To calculate the bridge costs, first, the bridges table in the database is queried for the bridges and their properties. Then, AADT on the roadway is calculated or estimated as explained for the pavement cost part. Using the bridge damage cost equation developed in this study and

the bridge properties, individual damage cost is calculated for the all bridges on the roadway and then summed up.

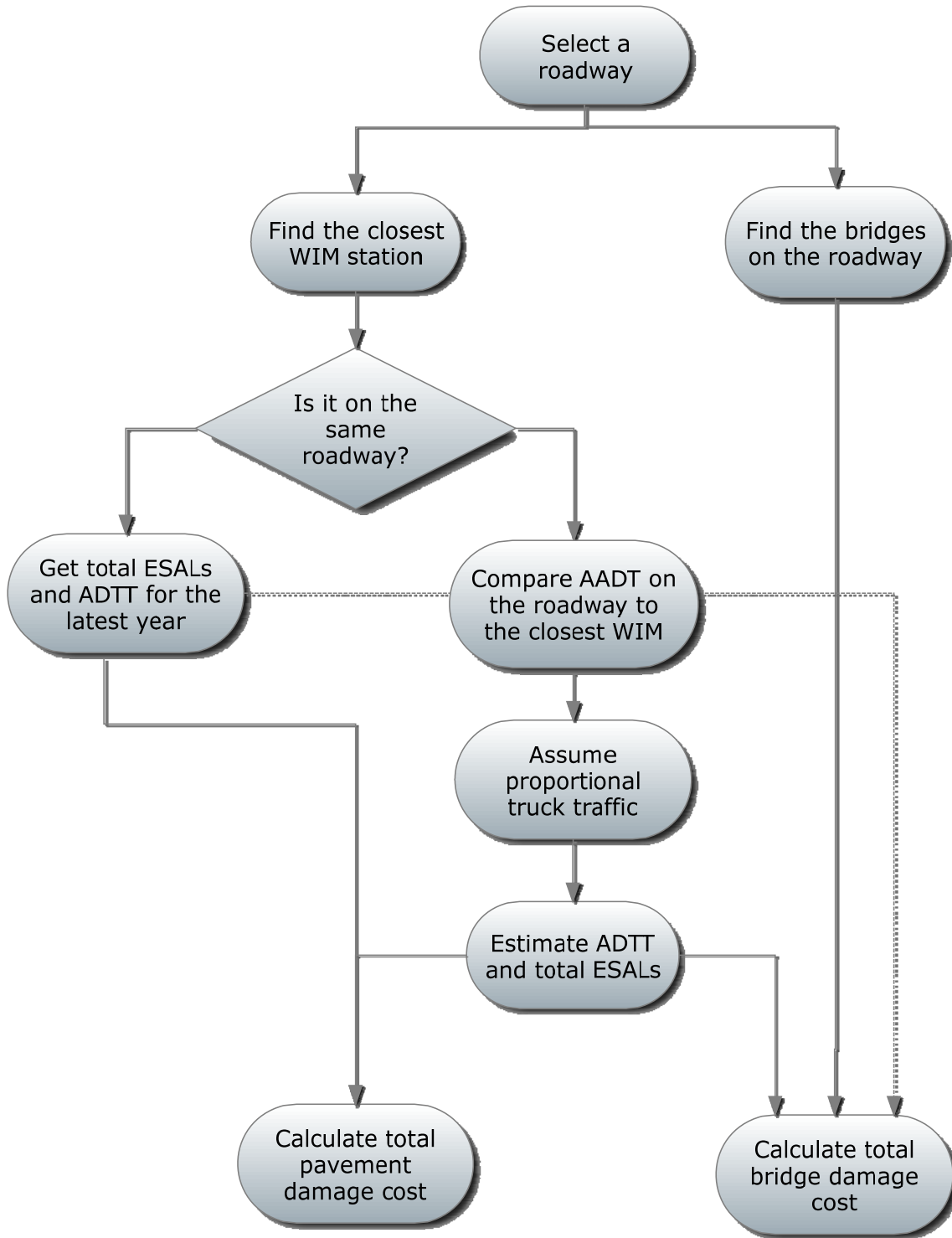


Figure 52. Flowchart for calculation of roadway LCC

Single Trip Cost Calculation

Figure 53 shows the flowchart of permit cost calculation for a truck. To calculate the permit cost, the program requires user input for the class and the gross weight of the truck (GVW). Then, the user also needs to define the links that truck will take on its route using SRI, and start and end mileposts. Since only average ESALs for the selected class is used for calculating the permit cost and based on the assumption that the closest WIM has the similar traffic trend, for each selected link, the WIM station closest to selected link is identified. Then, the pavement cost is calculated for each selected link. For the bridge cost, the bridges on the selected link are identified based on SRI, and start and end milepost. Then, using the bridge damage cost equation, the damage cost for each bridge is calculated and summed up for a single truck.

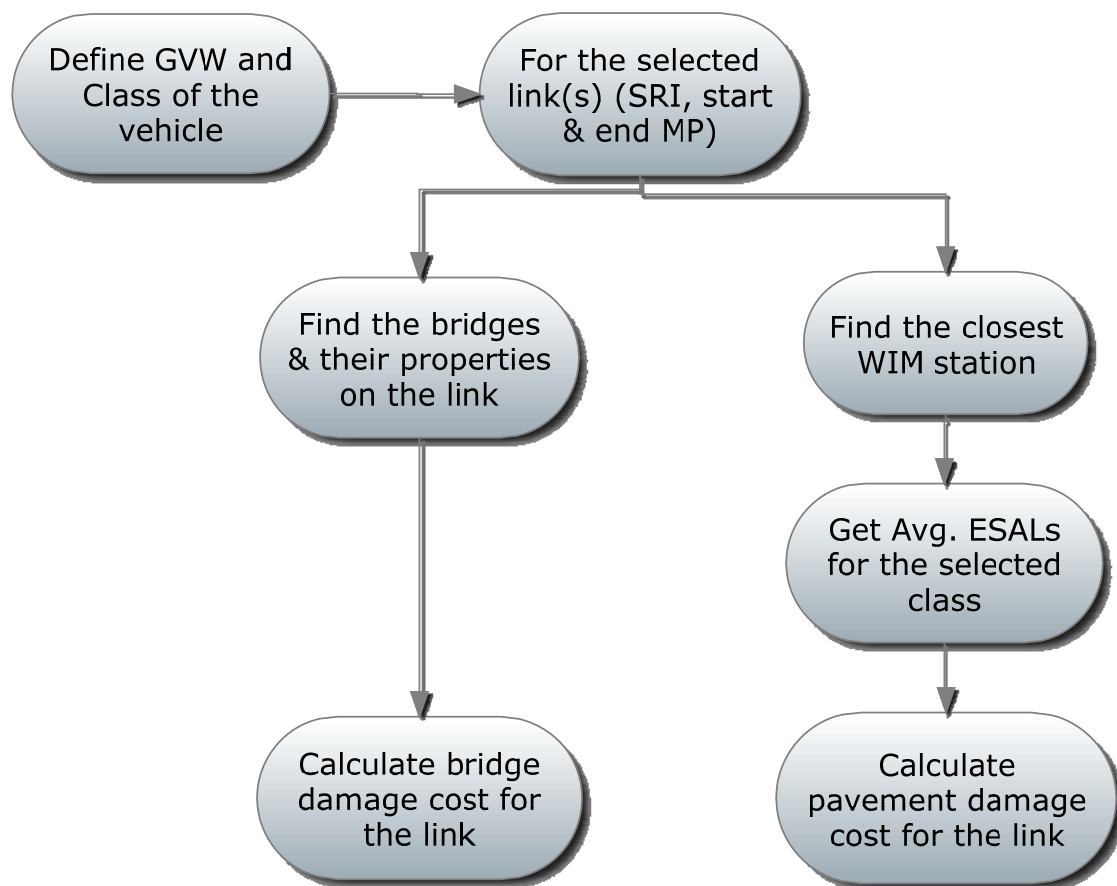


Figure 53. Flowchart for calculating permit cost for a truck

Cost Calculations in the Decision Tool

Unit Damage Costs

Pavement Unit Costs

After the life-cycle cost was calculated, the unit pavement damage cost was obtained by dividing the NPV of total cost by the number of total ESALs in the analysis period. The number of total ESALs was converted from truck traffic using the LEFs depending on the specific failure mechanism (rutting or fatigue cracking).

Table 47 shows the calculated unit pavement damage cost (per ESAL-mi) for Interstate highway and minor road, respectively. Two difference discount rates and analysis periods were used to obtain the variation of cost due to economic analysis parameters.

Table 47 - Unit pavement damage costs of interstate highway (\$ per ESAL lane-mi)

Analysis Period	Road Category	Pavement cost		Project cost	
		Average	Range	Average	Range
30 years	Interstate highway	0.038	0.027-0.052	0.048	0.013-0.083
	State road	0.250	0.092-0.483	0.314	0.115-0.599
60 years	Interstate highway	0.027	0.018-0.038	0.032	0.009-0.061
	State road	0.161	0.046-0.345	0.215	0.049-0.428

After the load equivalency factors and the unit pavement damage cost are known, the pavement damage cost caused by an individual truck can be estimated as below. In this case, the pavement damage caused by an individual truck with a combination of different axles is equivalent to the linear combination of the damage caused by each axle.

$$\text{Cost per truck} = \sum_{i=1}^k LEF_i \times \text{unit pavement damage cost} \quad (54)$$

Pavement unit costs presented in Table 47 are similar to the costs reported by other researchers. For example, Hajek et al. (1998) used the marginal cost method to analyze pavement cost allocation⁽⁶⁵⁾. They found that the annual life-cycle pavement costs were highly dependent on the highway type. The marginal pavement cost per ESAL per year for new pavement was found from \$0.0025 to \$0.5968; while for in-service pavement from \$0.0013 to \$0.307 (Canadian dollars).

Bridge Unit Costs

Using bridge fatigue models, the expected service life of different type of bridges are calculated. Then, unit cost of bridge construction from FHWA website is used for analyses. Table 18, Table 19, and Table 20 show the unit girder costs calculated for overweight vehicles and for all trucks while Table 21 shows the unit deck costs for overweight vehicles and for all trucks. Then, cost ratio for each class is calculated based on their damage on the bridges with different span lengths (see Table 48).

Table 48 - Cost ratio for each Class (Class unit cost/basic unit cost)

Class	Cost Ratio
Class 4	0.77
Class 5	0.51
Class 6	0.84
Class 7	1.6
Class 8	0.77
Class 9	1.06
Class 10	1.27
Class 11	0.95
Class 12	1.44
Class 13	1.76

Details of the Cost Calculation Steps

Details of Roadway Damage Cost Calculation

Inputs: SRI

Figure 54 shows the flowchart of damage cost calculation. First, a roadway is selected using the software interface. Based on the selection, WIM database is queried on the server side to locate the closest WIM station to the roadway. If the closest WIM station is on the selected roadway, the total ESALs and ADTT (truck traffic) for the latest available year calculated from the WIM data (using weight data). If there are no WIM stations on the selected roadway, another query is executed to find the WIM station closest to the roadway. In this case, we need to consider the different traffic patterns on the different roadways. Hence, AADT on the roadway where the closest WIM station located and AADT on the selected roadway are calculated using WIM data (count data in this case). It is assumed that the truck traffic is proportional to AADT of the roadways. As a result, the ADTT and total (annual) ESALs for the selected roadway are estimated using the proportionality of AADT of the two roadways. To calculate annual ESALs for the selected roadway, first ESALs for each vehicle is calculated using the equations in Figure 47 and Figure 48, and WIM data. In Figure 43 and Figure 44, the dots show ESAL calculation from AASHTO formula and it can be seen that the equations used in this study produce similar results. Finally, the annual damage cost is calculated for the selected roadway assuming that the trucks passing over the closest WIM station travel through from beginning to the end of the selected roadway.

The annual damage cost includes two cost items: pavement cost and bridge cost. To calculate the cost items for the selected route, the following equations are used:

$$\text{Pavement Cost} = \frac{\text{Total ESALs} * \text{Unit Damage Cost} * \text{Length of the selected segment}}{\text{Number of Lanes}} \quad (55)$$

where

unit pavement damage cost is in per ESAL per mi.

Interstate and US Routes are assumed to have thick pavement while other roadways are assumed to have thin pavement. Bridge cost is calculated from:

$$\text{Bridge Cost} = \frac{\text{Total sq-footage of bridges} * \text{Unit Damage Cost}}{\text{Total Weight}} \quad (56)$$

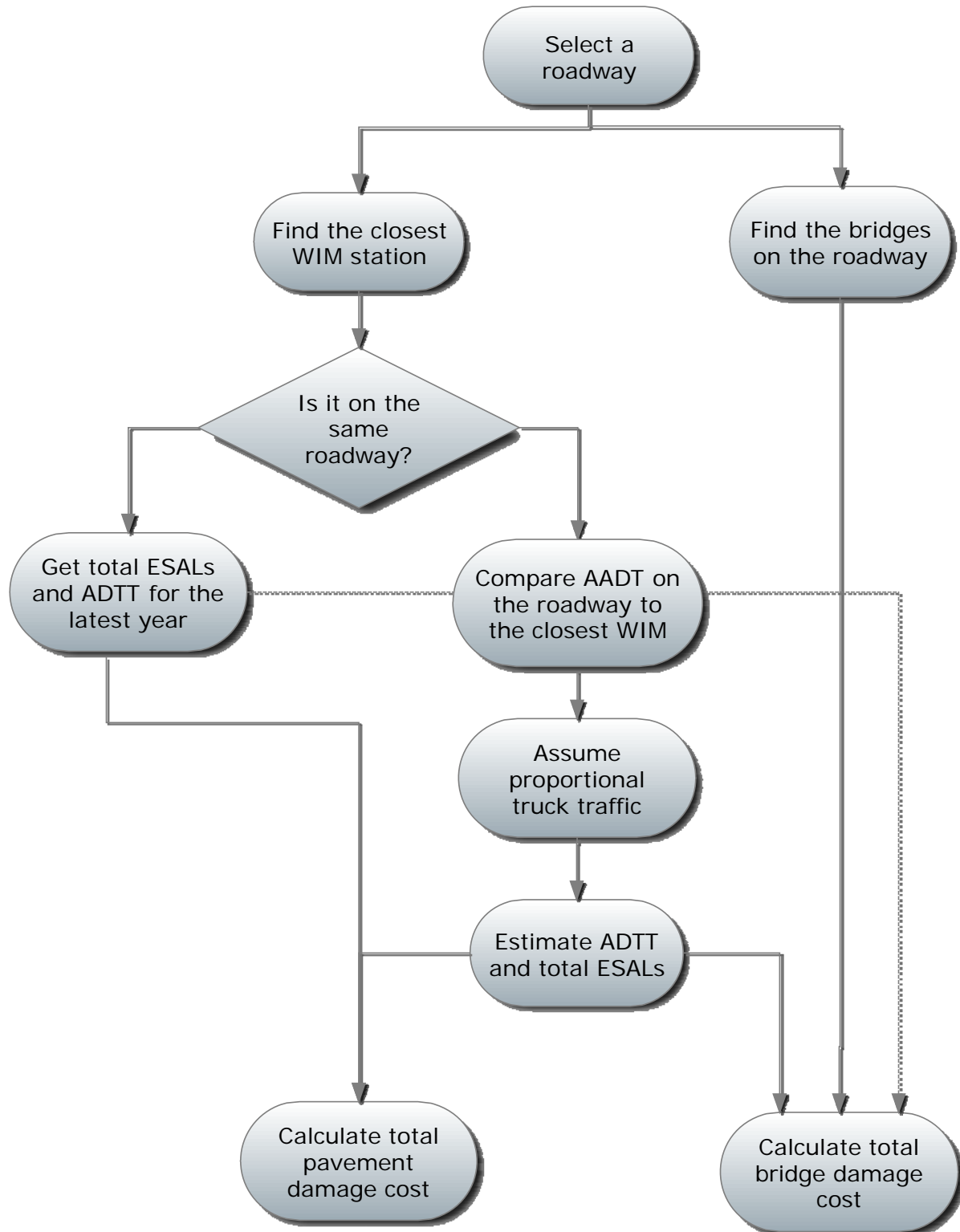


Figure 54. Flowchart of damage cost calculation

Details of Single Trip Cost Calculation

For this part inputs are:

Pavement Inputs: Axle load, axle configuration

Bridge Inputs: Truck class, Weight (tons)

Figure 55 shows the flowchart of permit cost calculation for a truck. To calculate the permit cost, the program requires user input for the class and the gross weight of the truck (GVW). Then, the user also needs to define the links that truck will take on its route using SRI, start and end milepost. Since only average ESALs for the selected class is used for calculating the permit cost and based on the assumption that the closest WIM has the similar traffic trend, for each selected link, the WIM station closest to selected link is identified. Then, the pavement cost is calculated for each selected link.

$$\text{Single Trip Cost} = \sum [(\text{Pavement Cost due to an overweight truck} + \text{Bridge Cost due to an overweight truck}) \text{ for each segment}] \quad (57)$$

For each segment:

$$\begin{aligned} \text{Pavement Cost} &= (\text{Average ESALs of overweight truck passing the} \\ &\quad \text{selected segment}) * \text{Unit Damage Cost} * \text{Number of} \\ &\quad \text{Lanes} * \text{Length of the selected segment} \\ \text{Bridge Cost} &= (\text{Total sq-footage of bridges}) * \text{Unit Girder Damage} \\ &\quad \text{Cost} * \text{Gross Veh. Weight of Overweight trucks} \\ &\quad (\text{GVW}) + (\text{Total sq-footage of bridges}) * \text{Unit Deck} \\ &\quad \text{Damage Cost} \end{aligned} \quad (58)$$

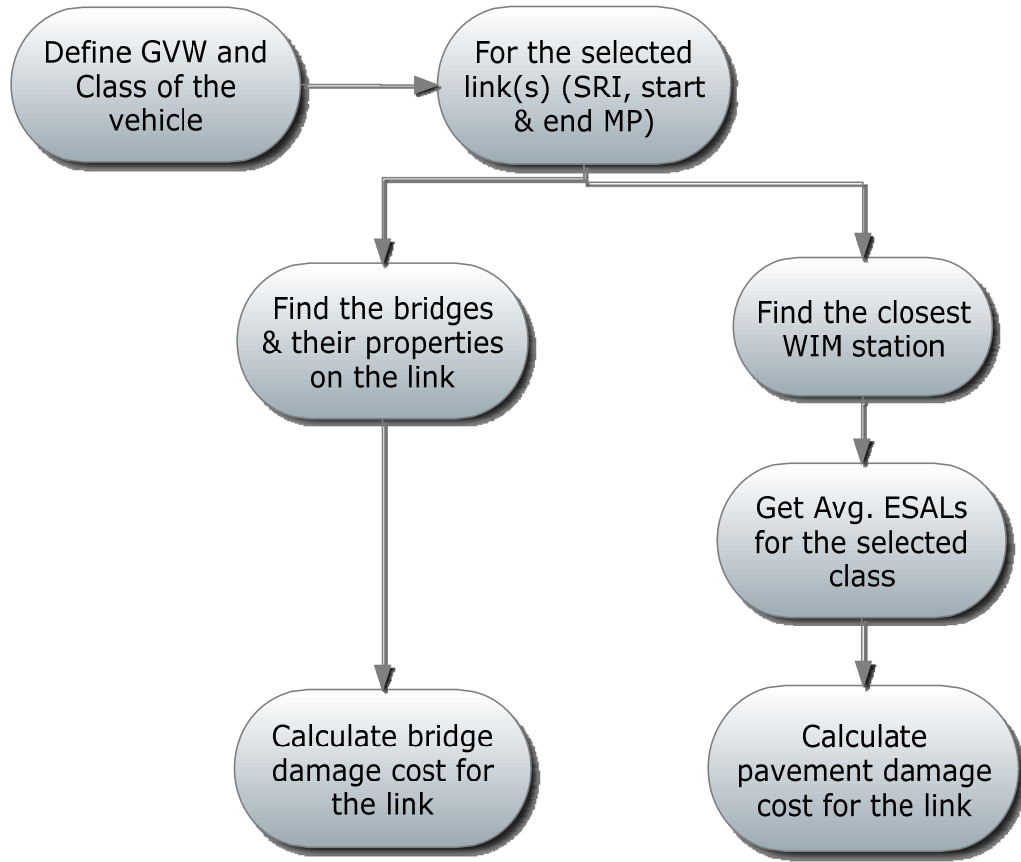


Figure 55. Flowchart for calculating permit cost for a truck

Analyzing NJ Permit Data using the Decision Tool

The permit database covers the permits issued by NJDOT between 8/16/2010 and 12/1/2010. The permit database has many tables but three of them are needed to analyze vehicles and their routes. These tables are the TripRequest, Vehicle, and LinksPerRequest tables. There are three types permits that are issued by NJDOT—the annual Ocean-borne container, single trip, and special oversize trailer permit. Unfortunately, only single trip permits issued for overweight trucks (16,832 records) contain the actual trip details.

Table 49 and Table 50 shows the statistics of permit vehicles by weight and trip length categories. It can be seen that average trip length for close to 60 miles. At the same time, as the weight increases, the trip length also increases based on the data (Figure 56). Average weight among the permit vehicles is close to 110 kips. Moreover, the vehicle weight increases as the trip length increases (Figure 57).

Table 49 - Mileage statistics of permit vehicles by weight categories

Weight Range (kips)	miles Statistics	Min.	1st Quantile	Median	Mean	3rd Quantile	Max.
80-90		0.16	31.12	57.69	60	78.86	201.32
90-100		0.34	30.78	56.19	58.62	79.23	193.52
100-110		0.33	33.74	60.09	62.71	80.06	200.39
110-120		0.42	35.08	60.09	59.68	77.15	202.82
120-130		0.08	28.45	54.61	57.41	76.87	196.34
130-140		0.86	31.98	48.07	55.01	74.52	194.53
140-150		1.76	35.72	62.67	61.79	86.31	179.21
150-160		0.95	39.28	65.42	62.68	79.2	206.5
160-170		0.39	36.82	65.28	59.68	76.58	162.86
170-180		0.64	61.33	76.04	67.93	77.11	182.41
180-190		2.18	26.04	53.34	58.47	67.97	152.98
>190		19.9	48.53	77.11	96.54	159.17	159.17

Table 50 - weight statistics of permit vehicles by mileage categories

Miles Range (miles)	Weight Statistics	Min.	1st Quantile	Median	Mean	3rd Quantile	Max.
0-30		80.1	94.2	104.0	109.5	122.0	207.0
30-60		80.1	92.6	106.0	110.0	124.0	200.1
60-90		80.3	95.0	109.0	112.3	123.5	211.0
90-120		80.4	92.2	102.0	108.7	120.0	192.0
120-150		81.0	96.0	107.4	111.1	120.0	198.0
150-180		80.1	95.0	105.0	110.6	120.0	211.0
180-210		88.0	99.0	117.1	117.5	136.0	172.0

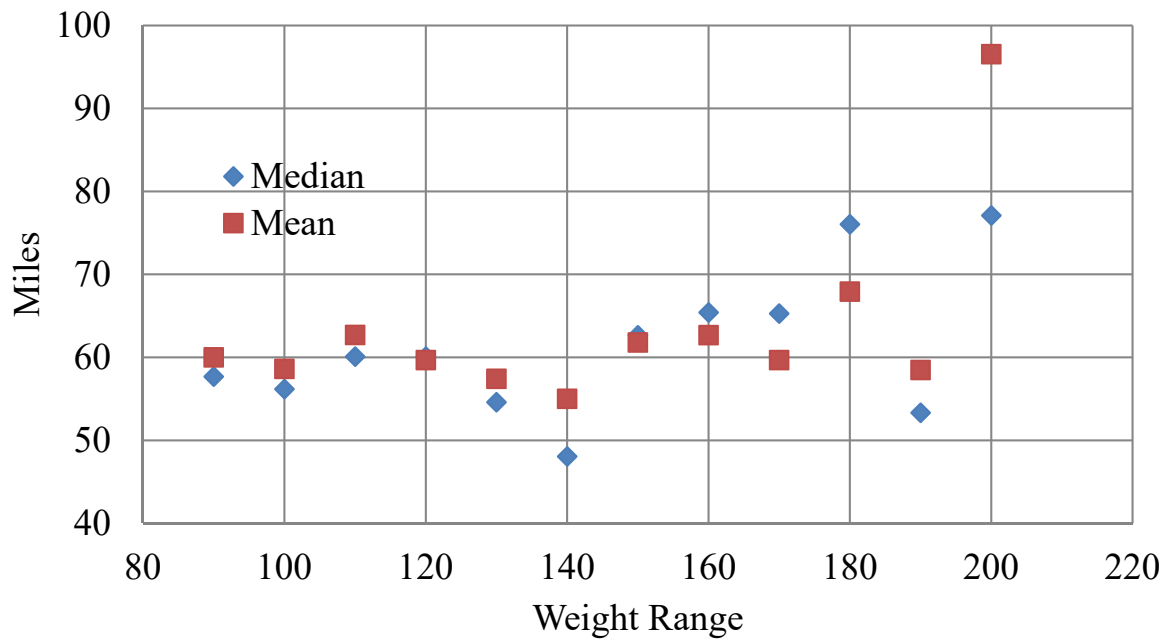


Figure 56. Average and Median Miles for Each Weight Categories

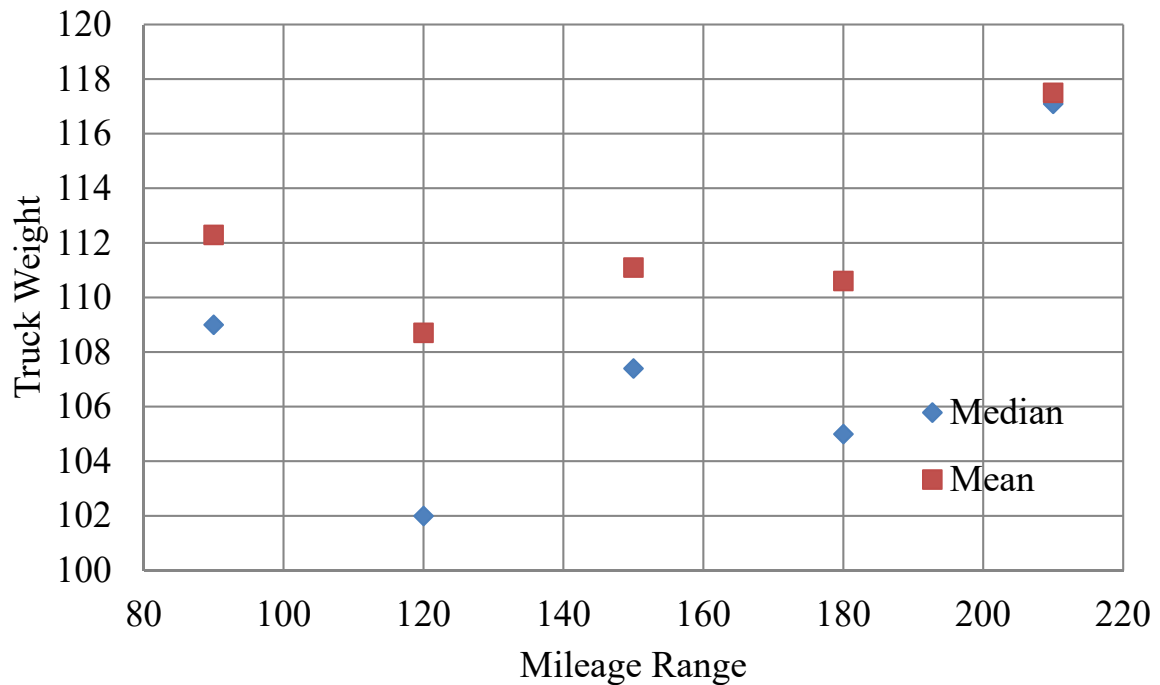


Figure 57. Average and Median Weight for Each Mileage Categories

When we investigate the distribution of the trip length inside each weight category, it is clear that the lighter weight categories (up to 110 kips) are distributed more uniformly (**Figure 58**). Whereas, the probability of a longer trip length increases as the gross vehicle weight increases.

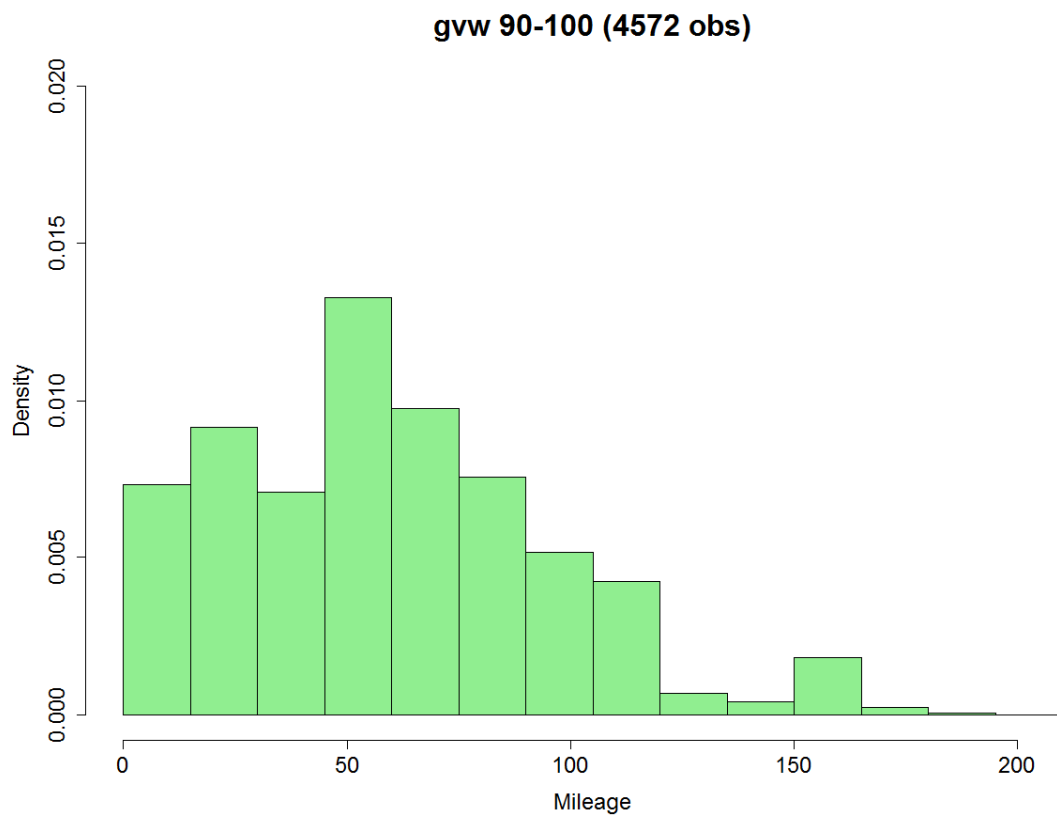
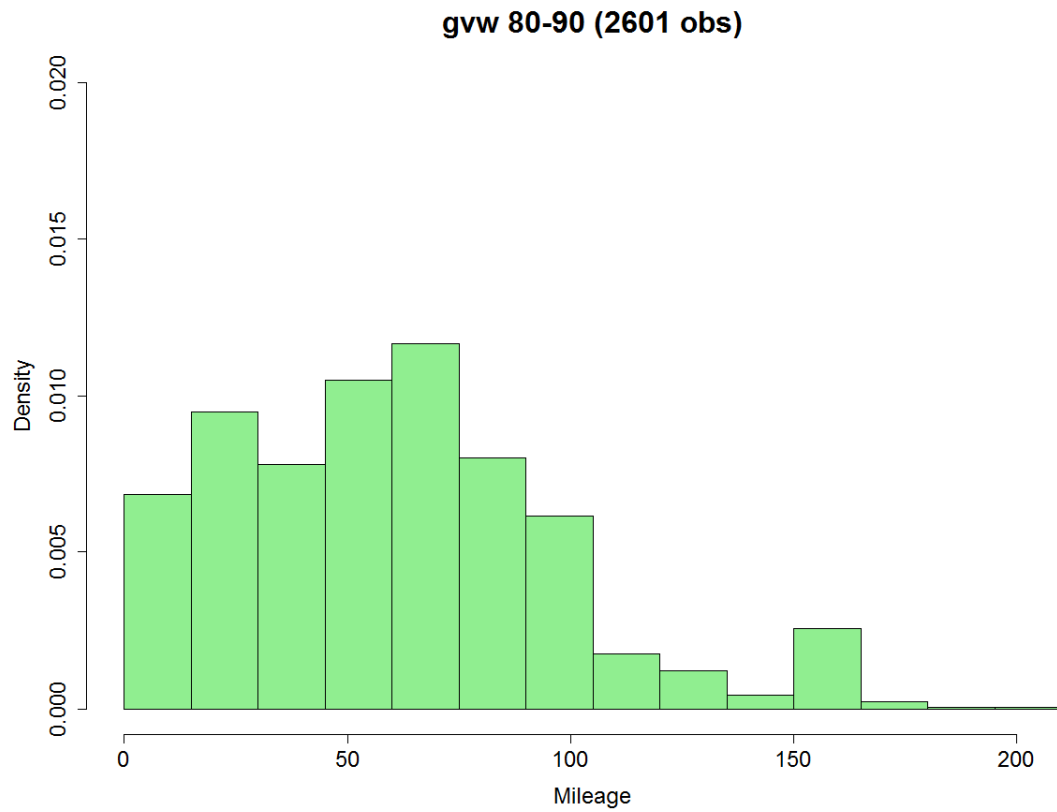


Figure 58. Distribution of trip length in each weight category

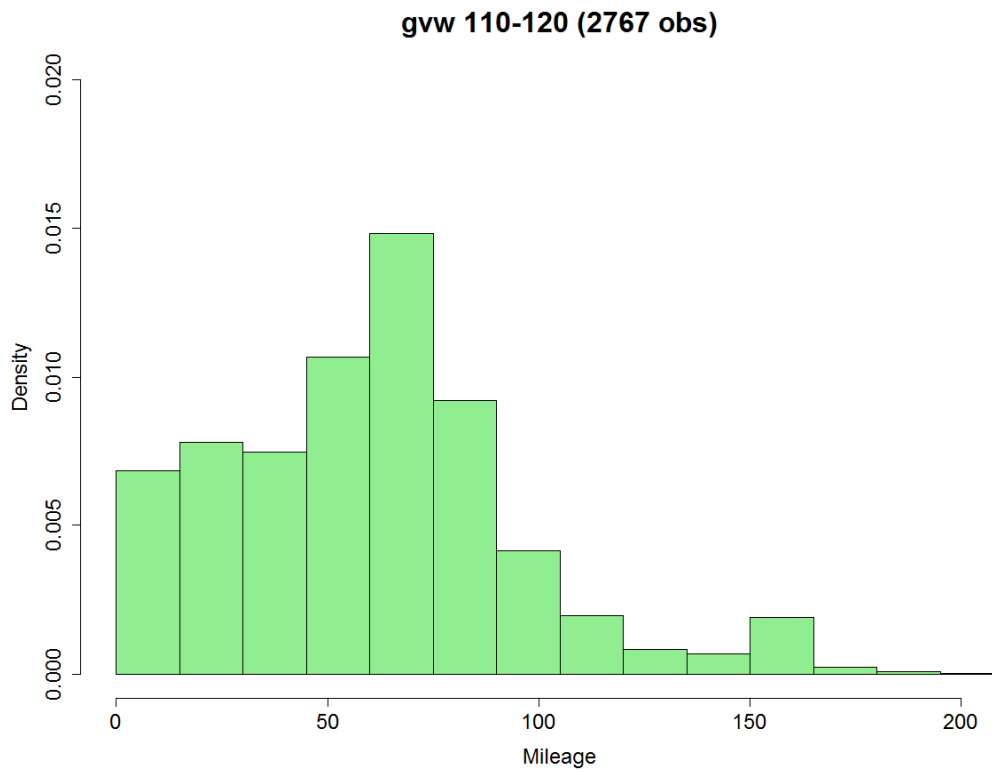
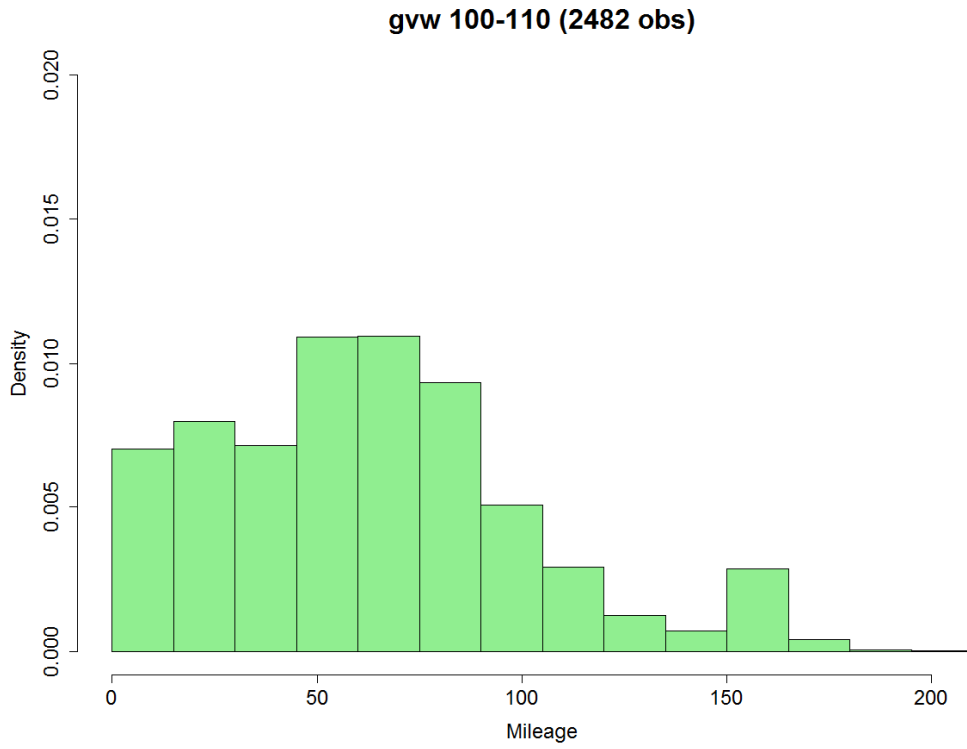


Figure 58. Distribution of trip length in each weight category (continued)

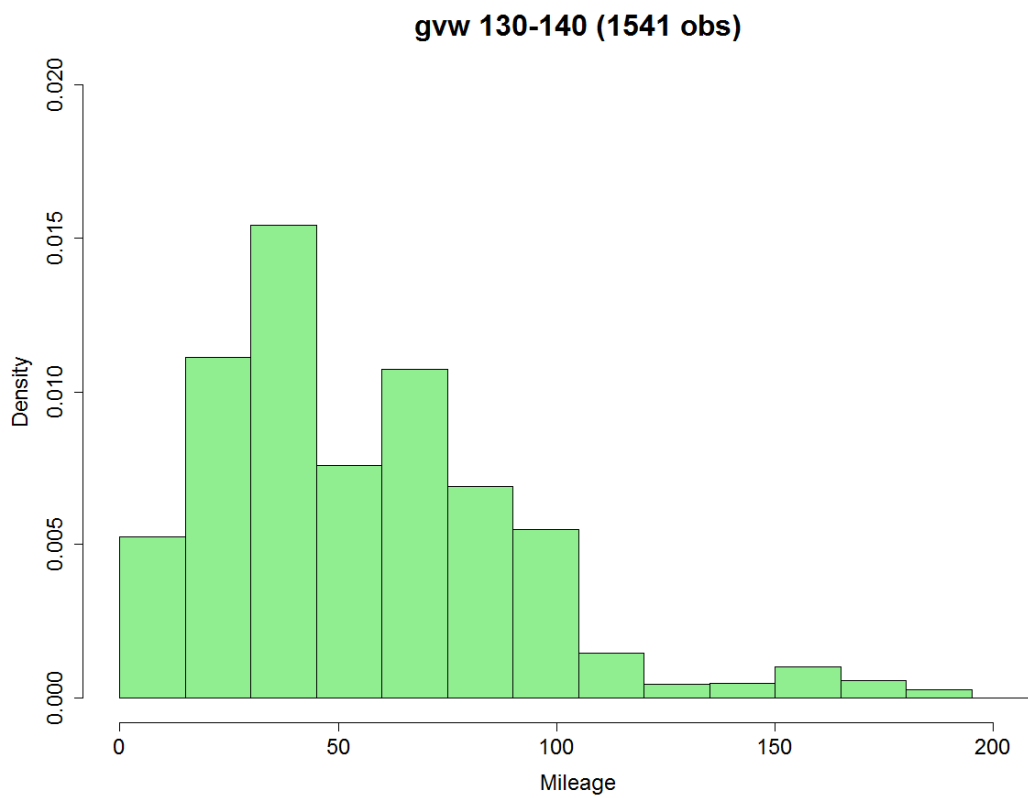
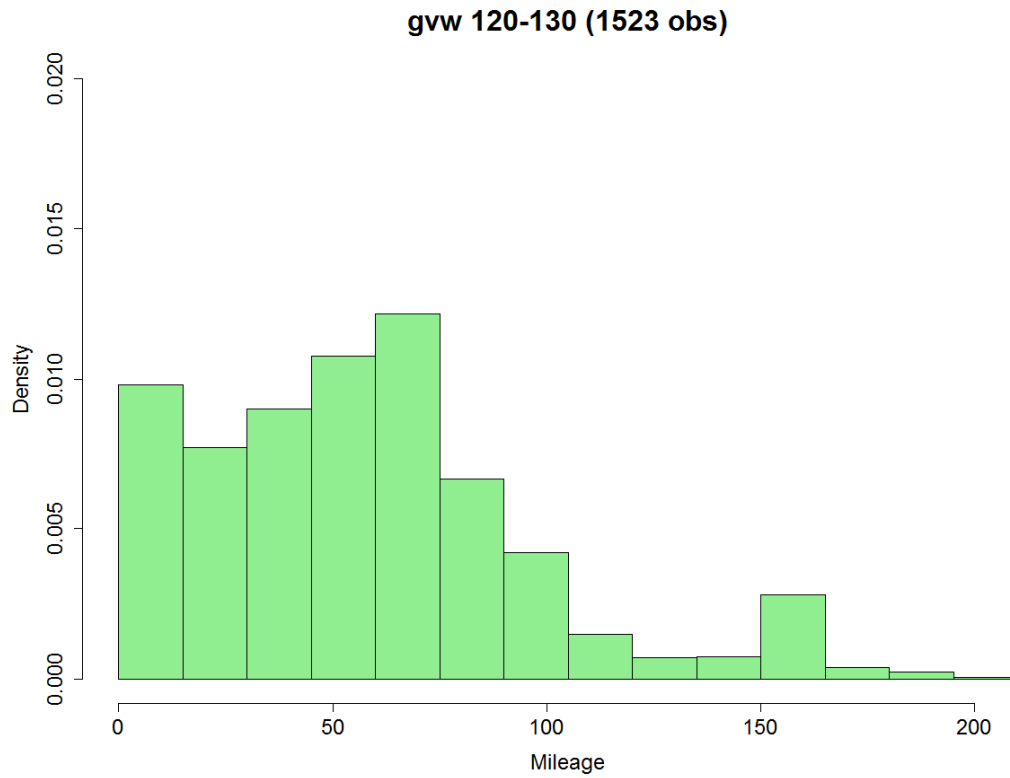


Figure 58. Distribution of trip length in each weight category (continued)

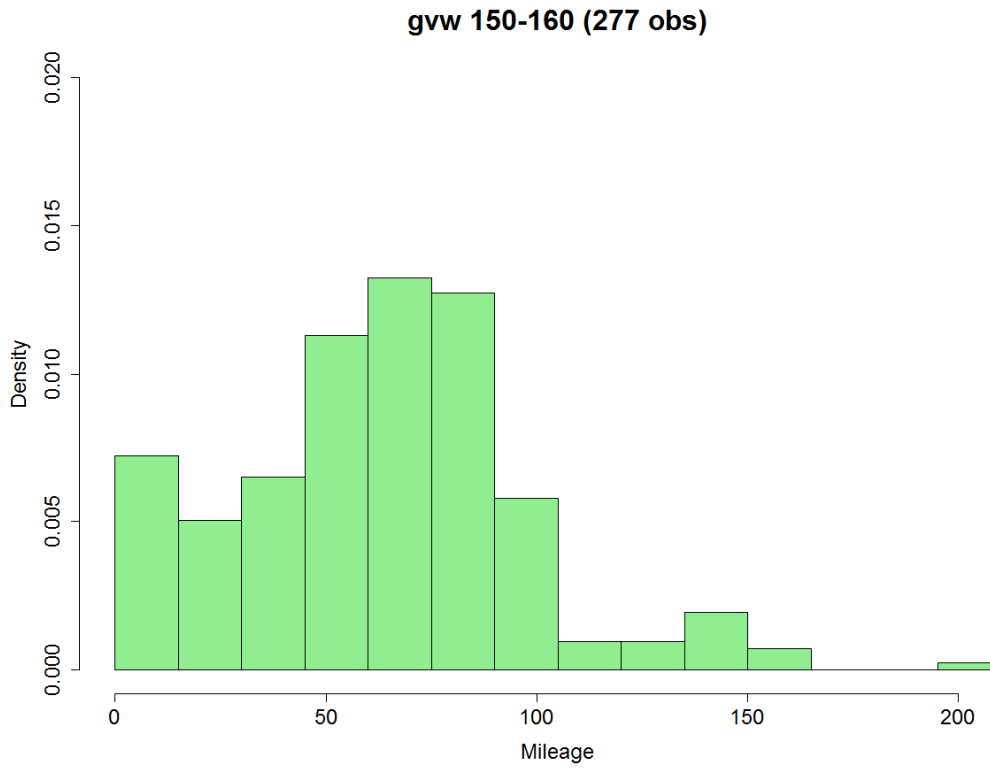
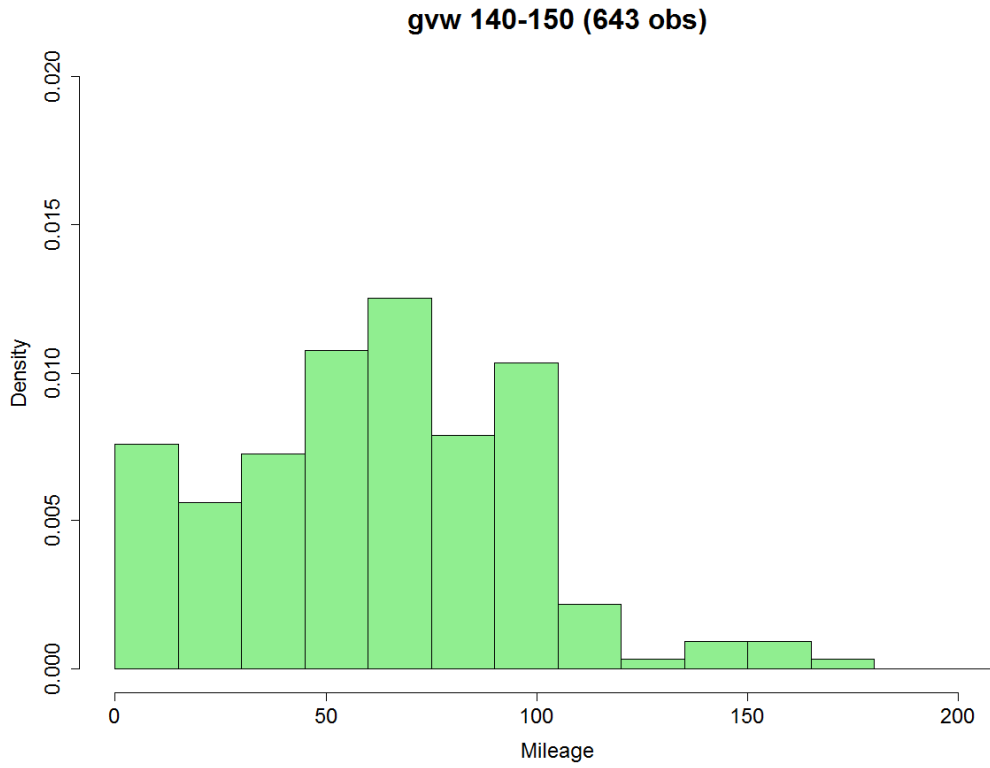


Figure 58. Distribution of trip length in each weight category (continued)

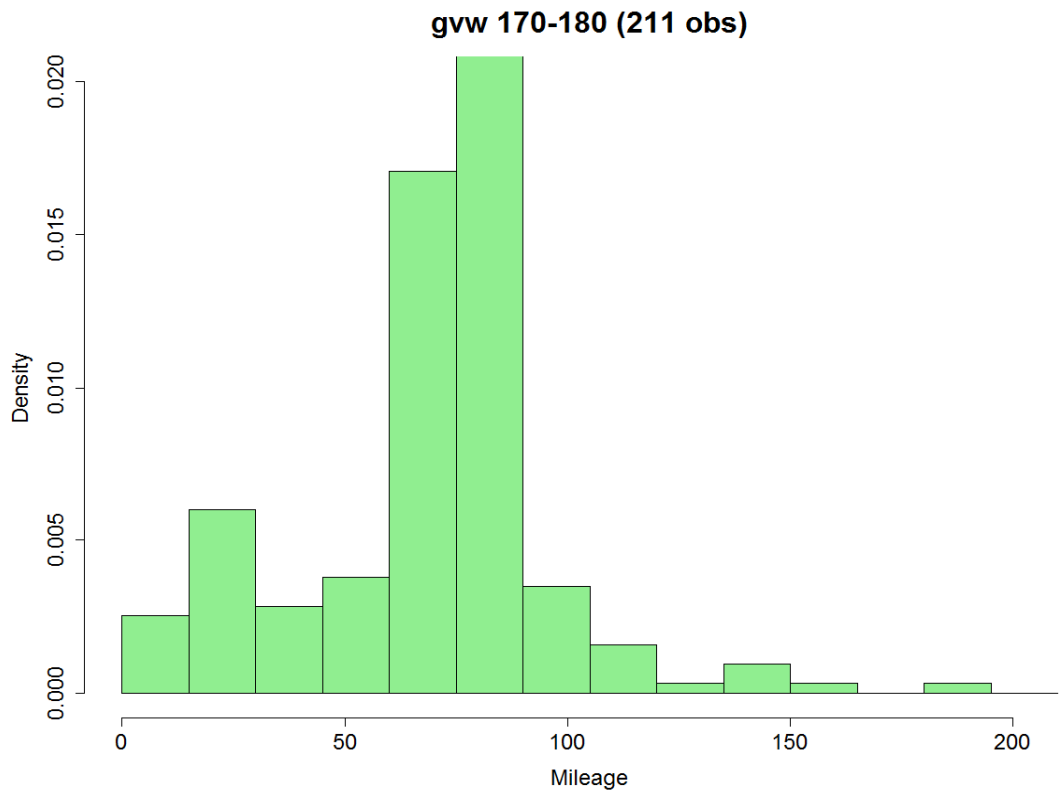
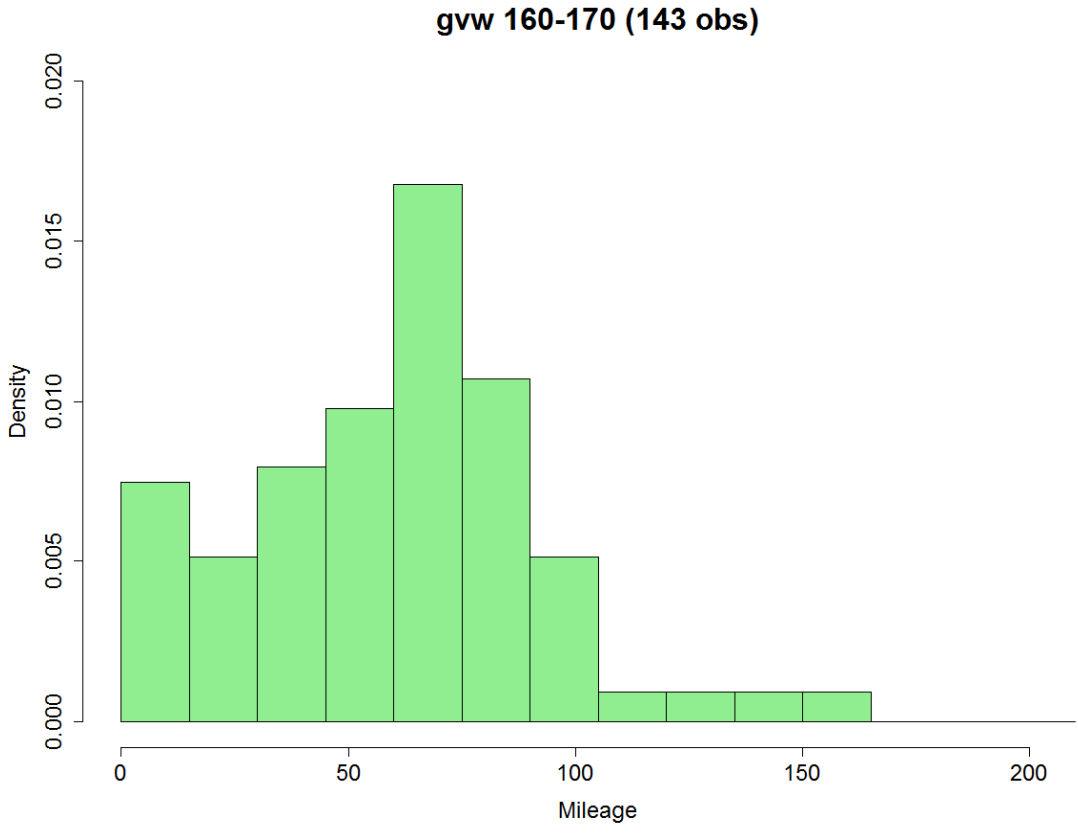


Figure 58. Distribution of trip length in each weight category (continued)

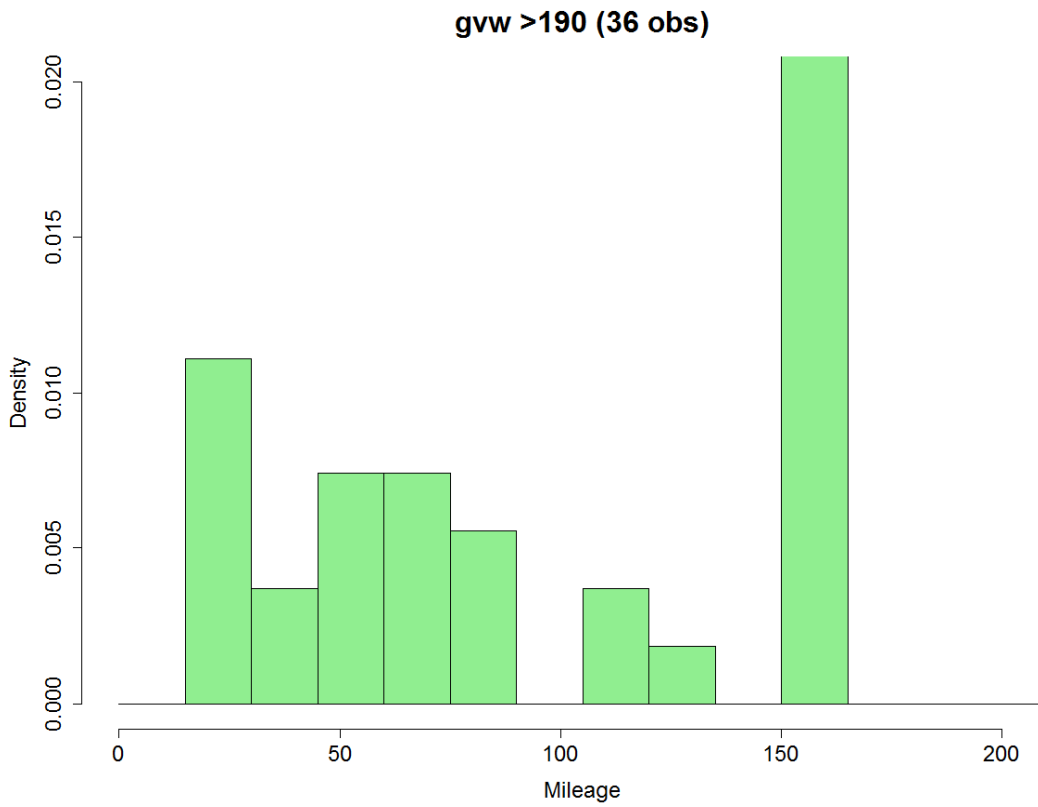
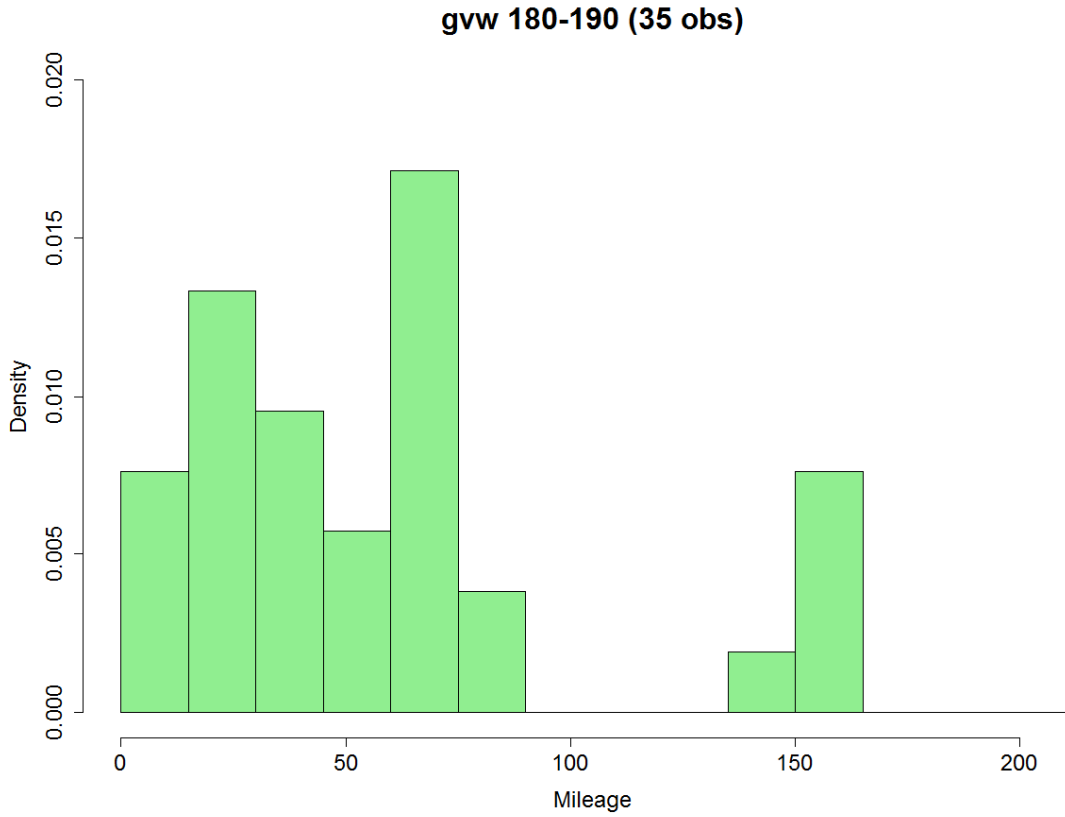


Figure 58. Distribution of trip length in each weight category (continued)

Distribution of weight in mileage categories are similar (skewed to left), except the longest trip length category (180-210 miles). In the last category, the probability of heavier weight increases dramatically compared to other categories. (see **Figure 59**).

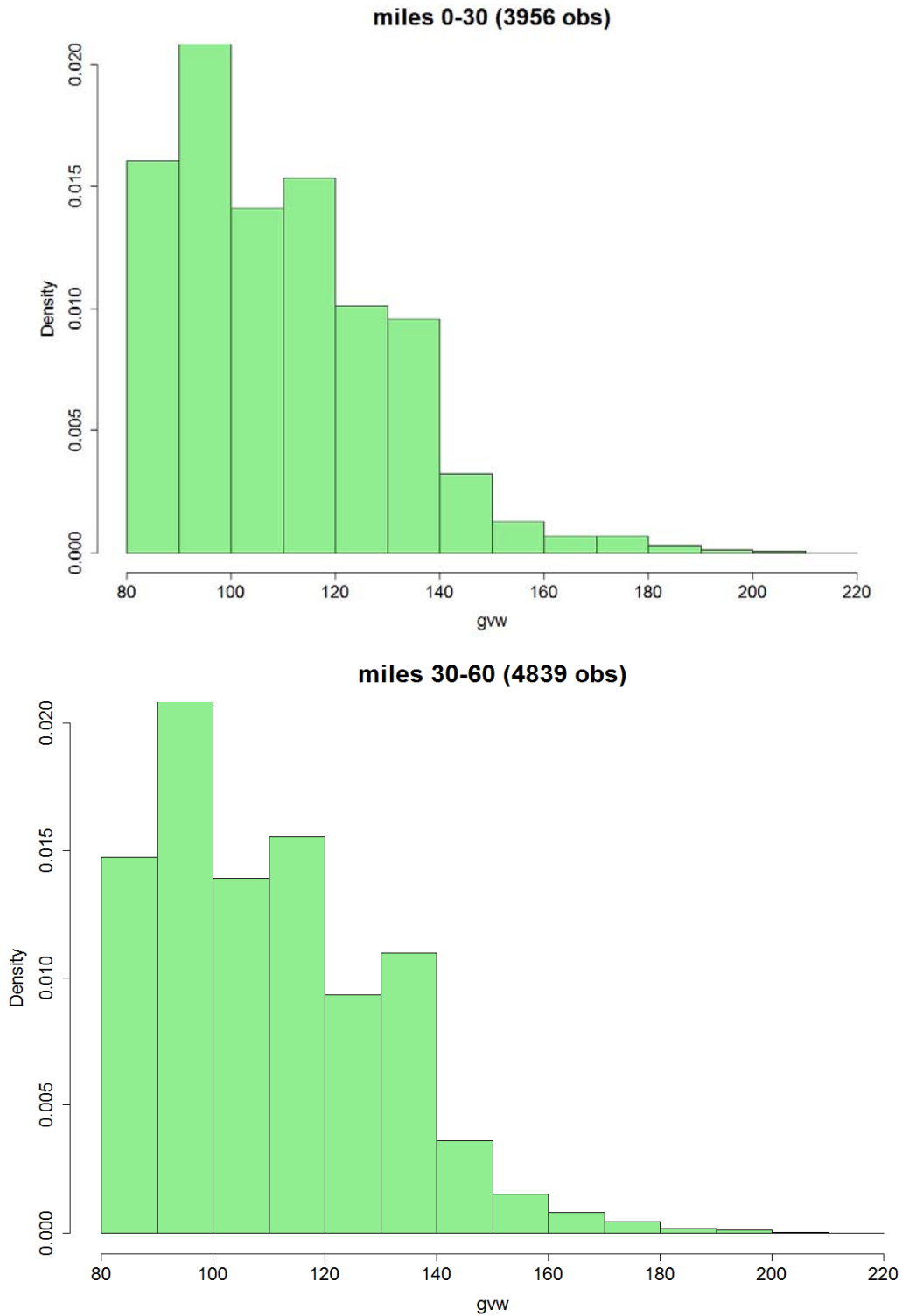


Figure 59. Distribution of weight in each of trip length category

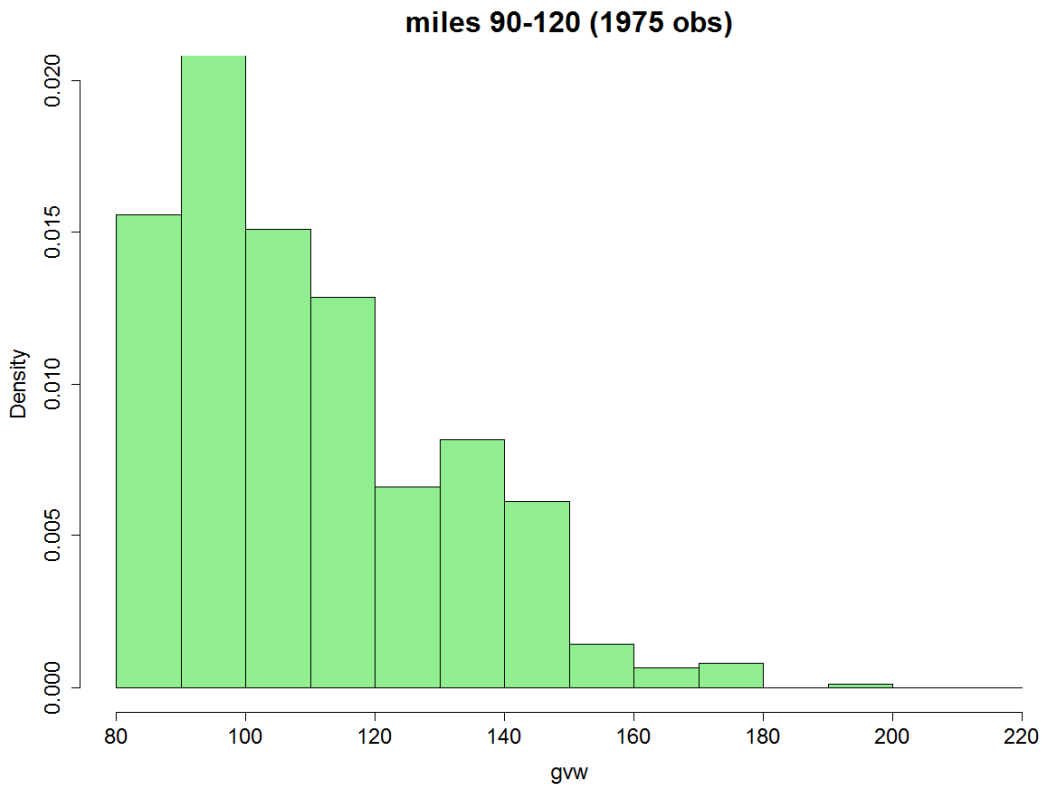
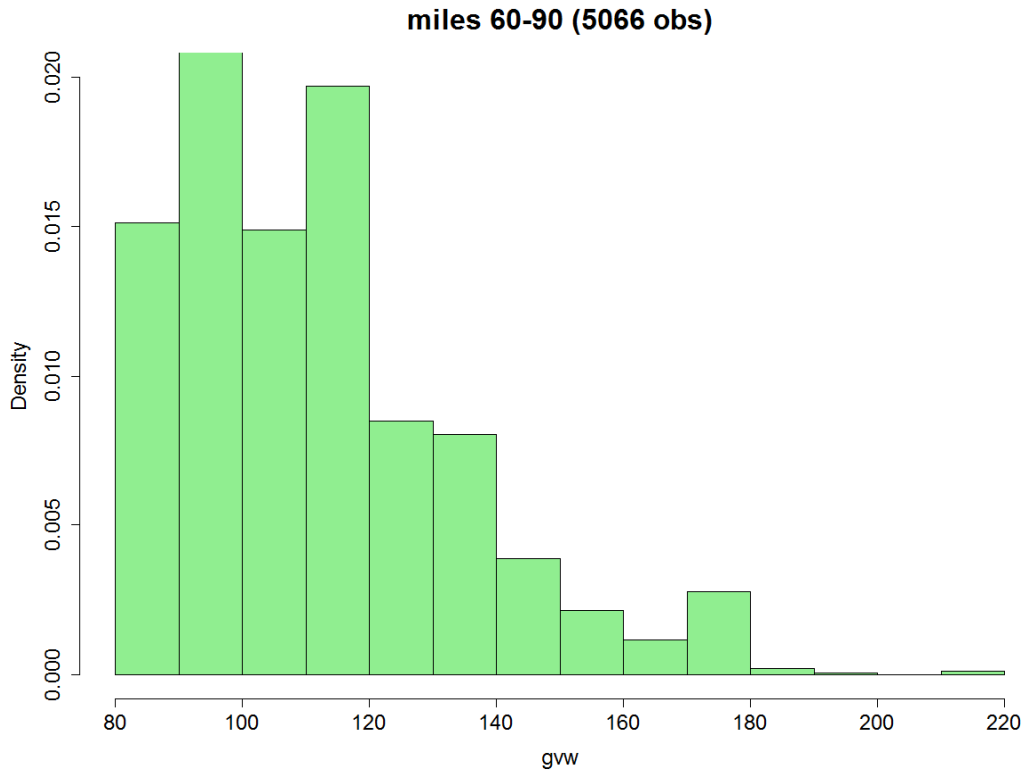


Figure 59. Distribution of weight in each of trip length category (continued)

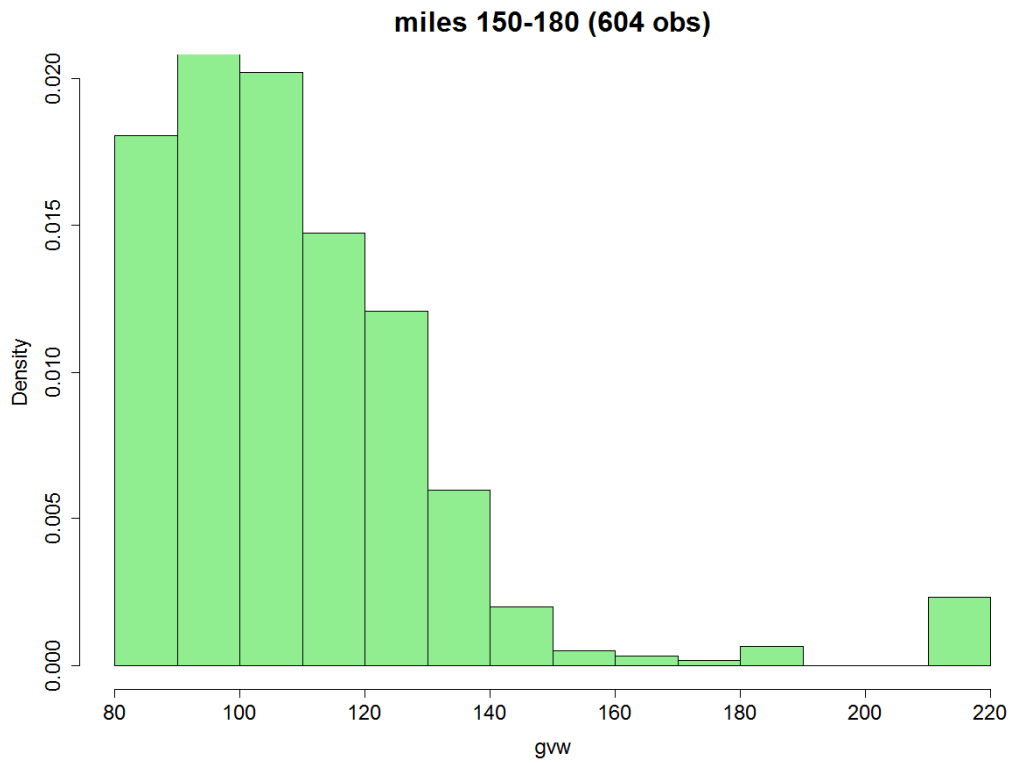
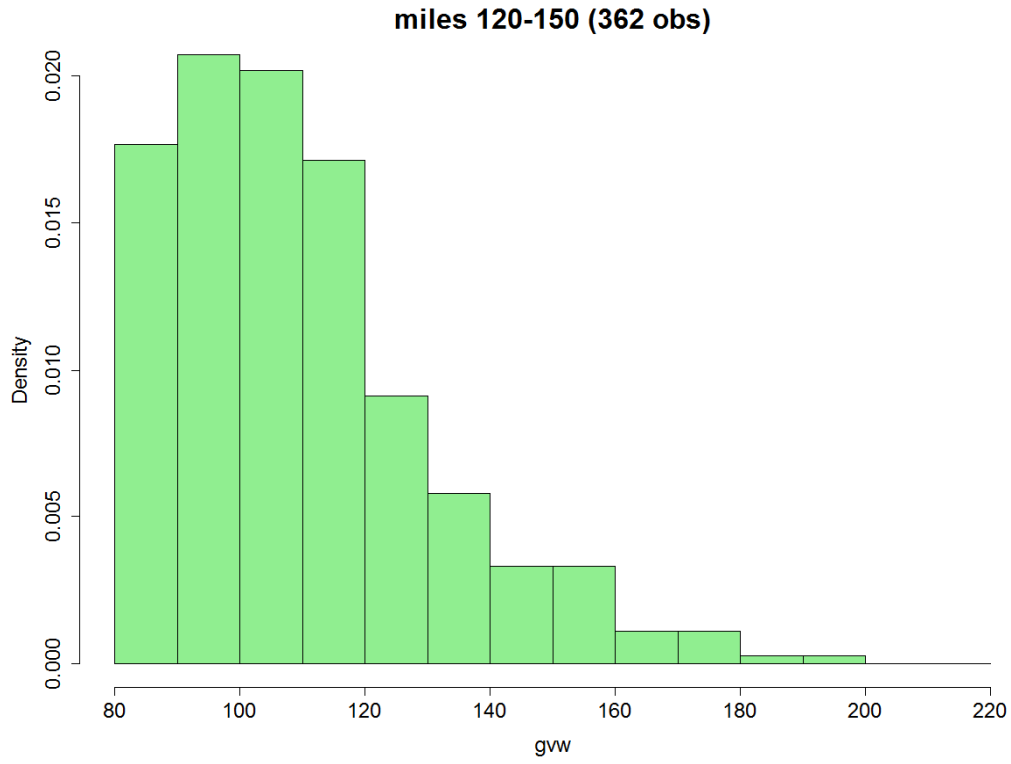


Figure 59. Distribution of weight in each of trip length category (continued)

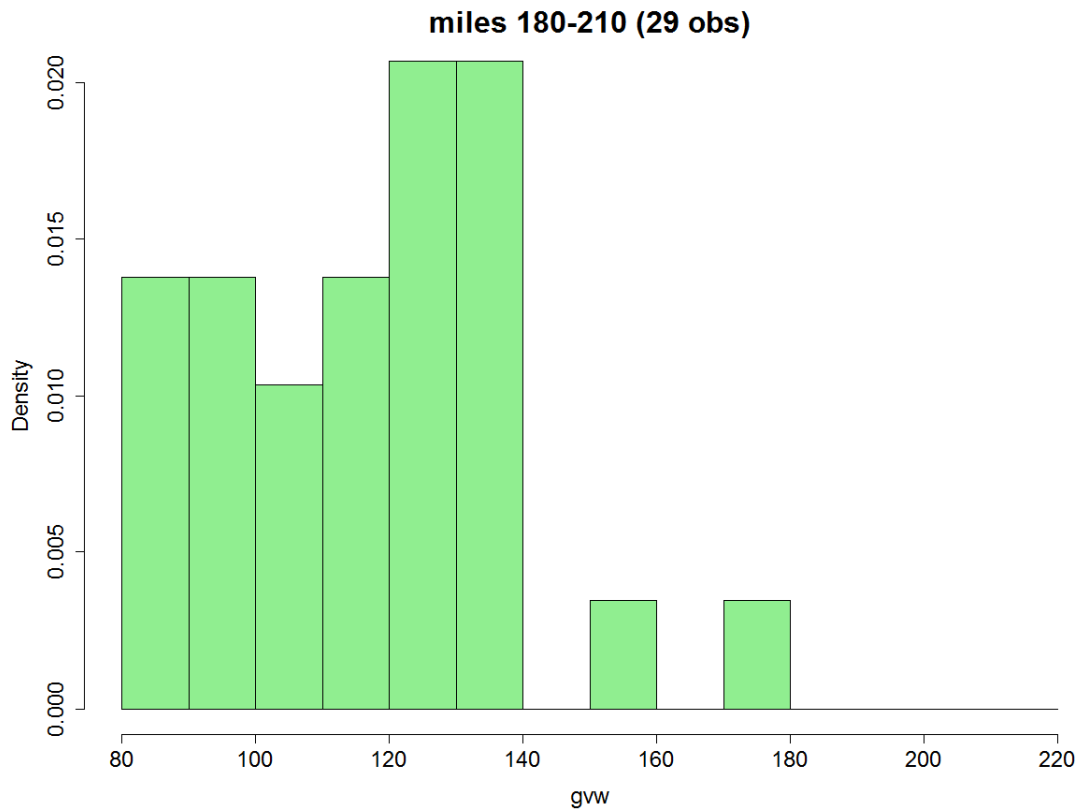


Figure 59. Distribution of weight in each of trip length category (continued)

To analyze the damage costs of each permitted vehicle, new routines are developed in the decision tool. The same cost equations for bridge costs and pavements costs from the previous sections are used in the developing the decision tool below. Two approaches are used for calculating the pavement cost: average cost and marginal cost.

While calculating damage costs using the first approach, minimum, average, and maximum costs are used for unit pavement damage cost ranges. This produces three cost categories: low, average, and high as shown in Figure 60 and Figure 61.

Instead of calculating the costs in per ton or per mile, the research team considered the effect of both weight of the vehicles and the trip length. As the trip length increases, there is a higher chance of passing more bridges on the roadway network. Hence, in both figures the cost are presented in per ton per mile. We also converted the permit fee (basic fee + ton fee) in these figures.

Although it is not evident in Figure 60, in which the weight categories are used, Figure 61, in which trip length categories are used, reveals the rationale behind the approach used in this study. Figure 61 demonstrates that as the trip length increases, the damage costs increase, and the damage costs are higher than the permit fee.

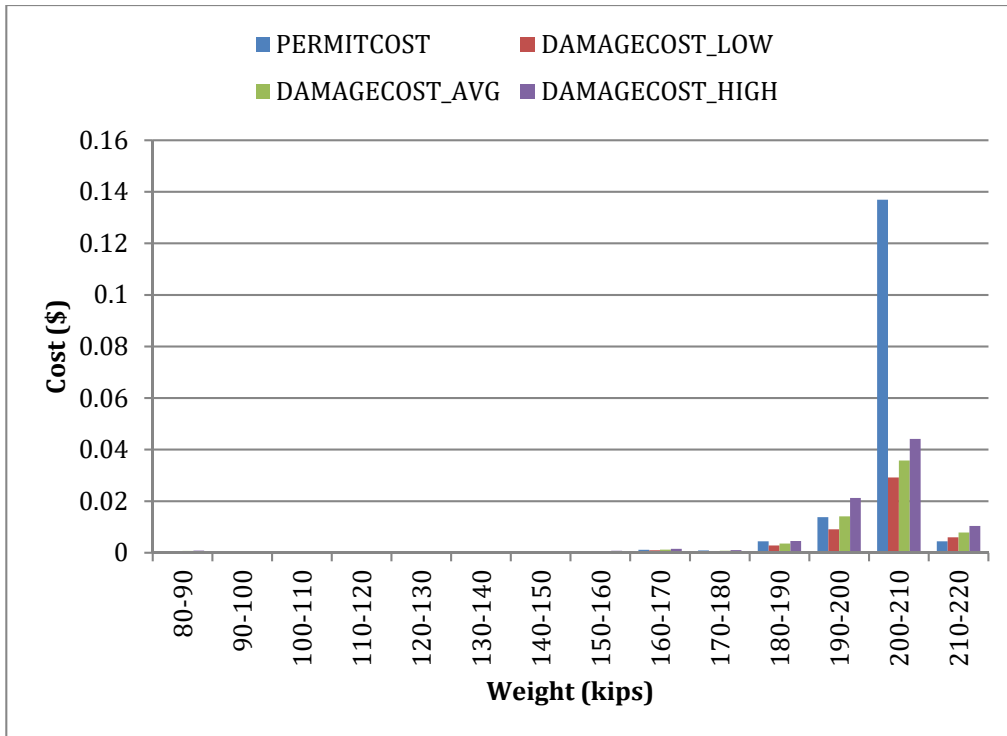


Figure 60. Damage and permit costs for weight categories (per ton per mile)

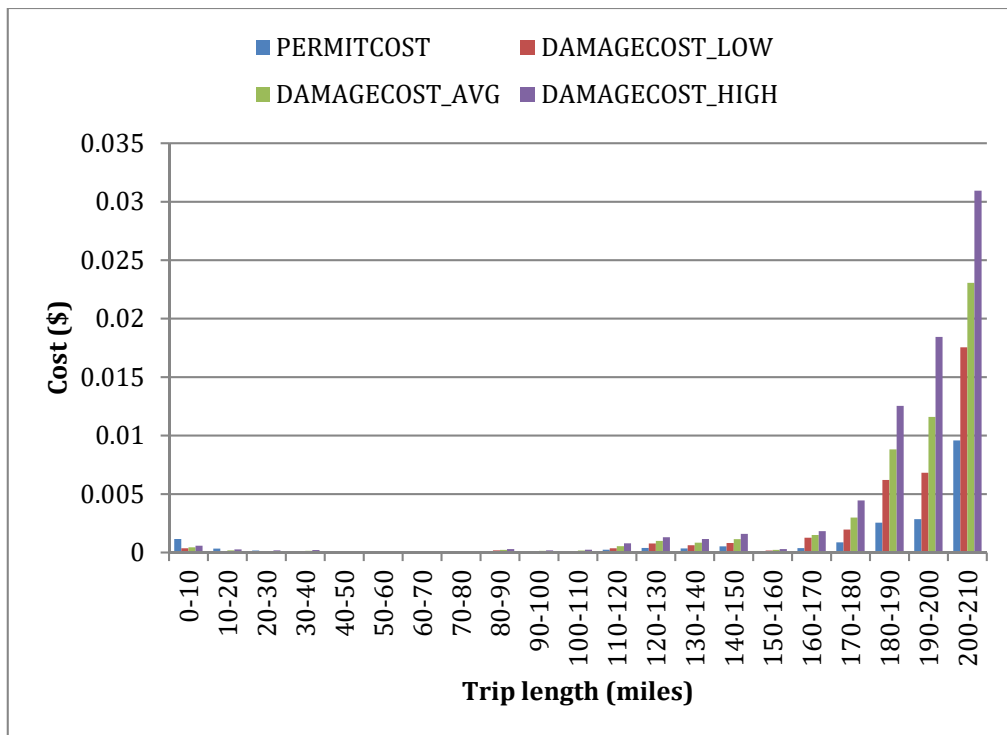


Figure 61. Damage and permit costs for trip length categories (per ton per mile)

Surface plots of permit costs and each damage cost scenario in Figure 62 and Figure 63 show more clearly that our damage cost approach penalizes both mileage and weight. On the other hand, the current permit fee only increases by weight as shown in Figure 62.

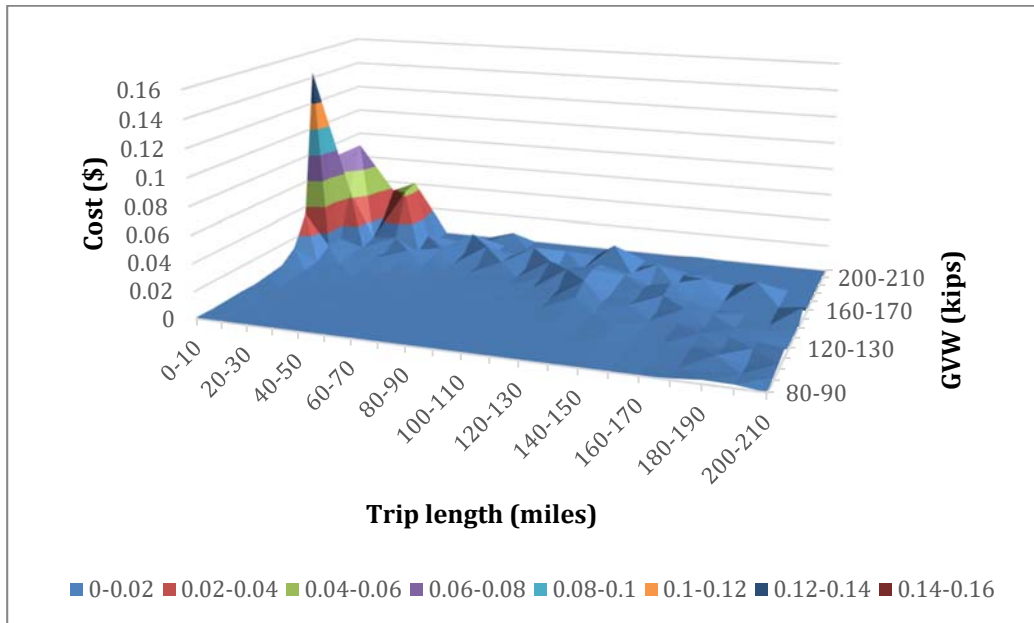
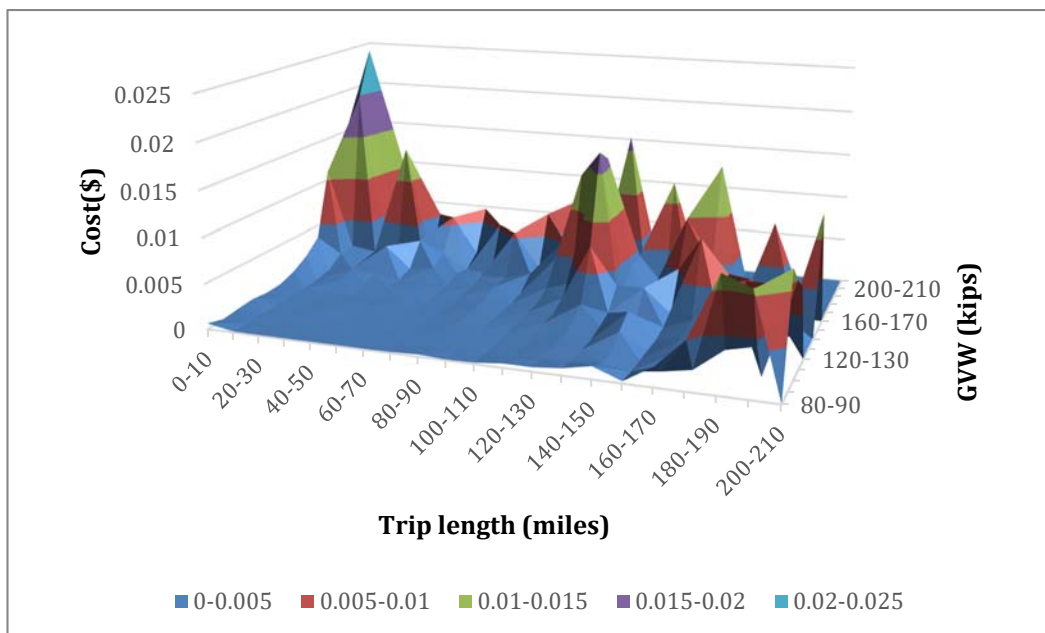
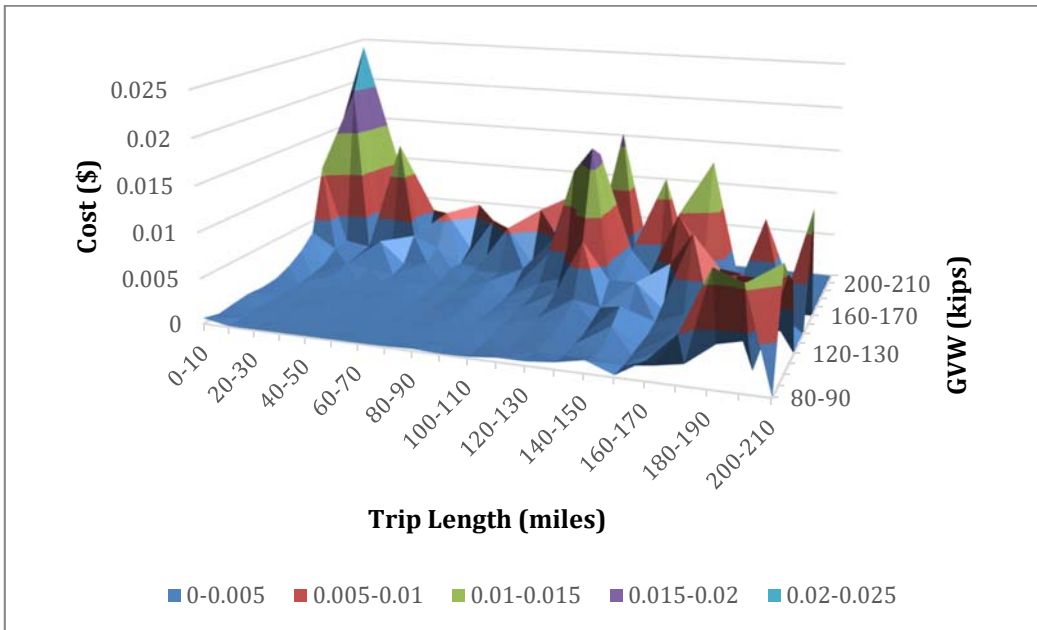


Figure 62. Surface plot of permit costs (per ton per mile) by weight and by trip length

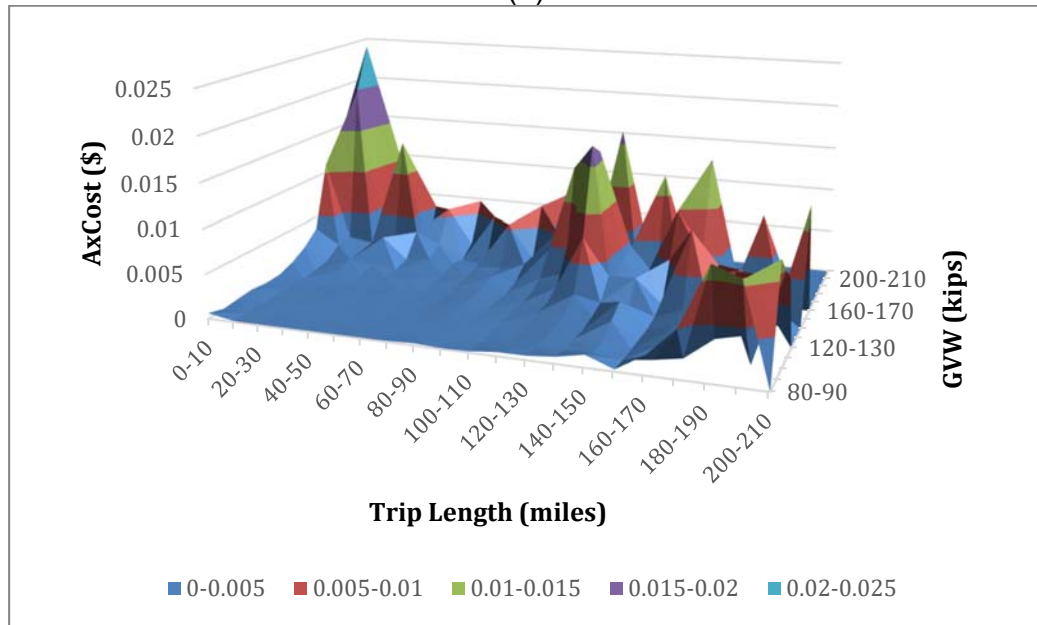


(a)

Figure 63. Surface plots of (a) low, (b) average, (c) high damage costs (per ton per mile) by weight and by trip length



(b)



(c)

Figure 63. Surface plots of (a) low, (b) average, (c) high damage costs (per ton per mile) by weight and by trip length (continued)

For the marginal pavement costs approach, the damage costs are calculated in two ways. First, pavement structure of interstate and US highways are considered similar (thick pavement) while state roads are assumed to have thin pavement structure, which produces a lower damage cost. Then, US highways and state highways both are assumed to have thin pavement structure, which yields higher damage cost estimates as shown in Figure 64 and Figure 65. While the costs in Figure 64 do not have a definite trend, Figure 65 shows that the per ton per mile damage costs increase by using the approach in this study, and they are again higher than the permit costs.

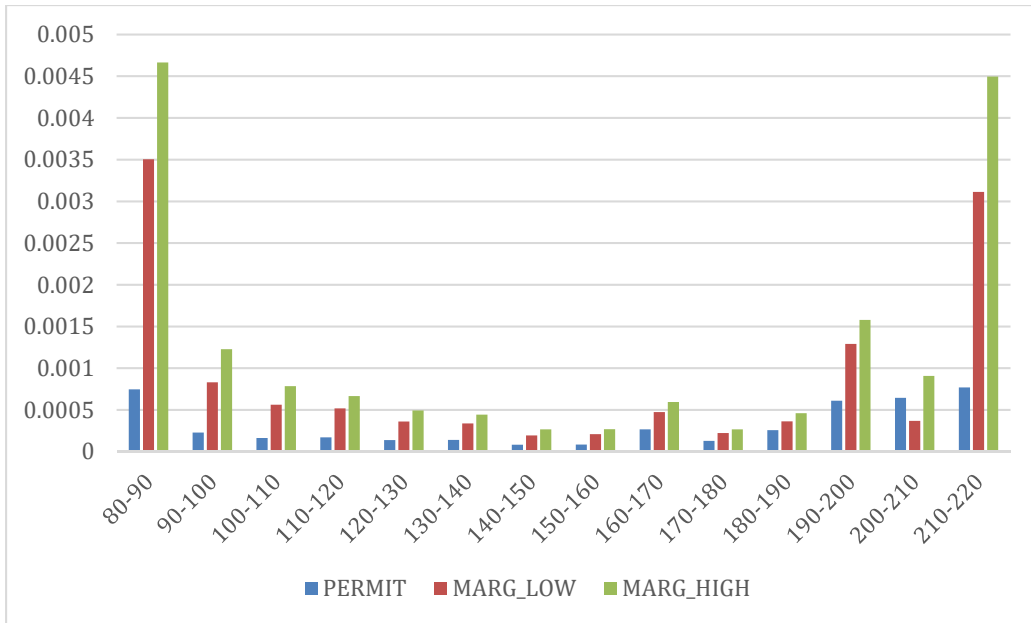


Figure 64. Damage and permit costs for weight categories (per ton per mile) using marginal unit pavement costs

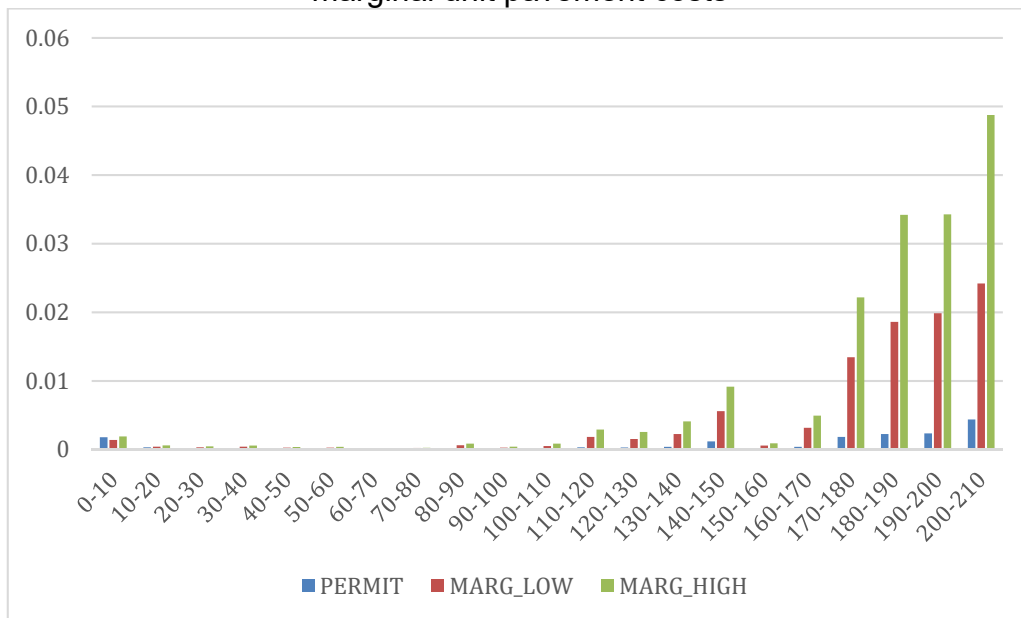


Figure 65. Damage and permit costs for trip length categories (per ton per mile) using marginal unit pavement costs

It is also possible to calculate average per trip costs to observe the real differences between the current approach and permit fee structure as in Figure 66. In fact, it is clear that the damage costs are increasing while trip length increases.

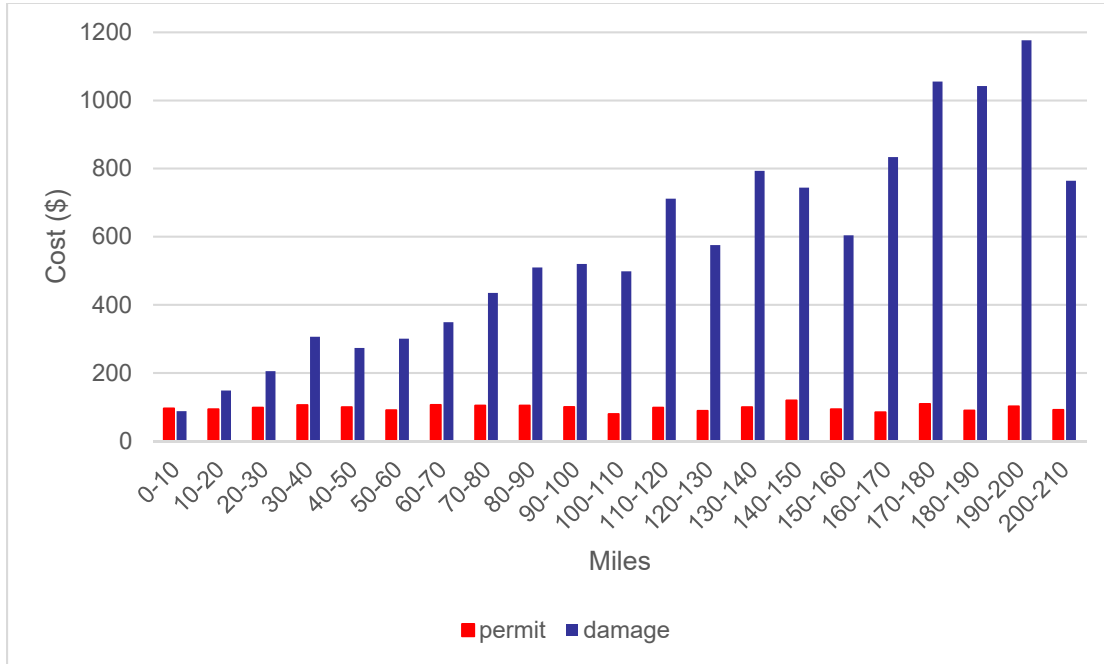


Figure 66. Comparison of average trip costs based on trip length using marginal unit pavement costs

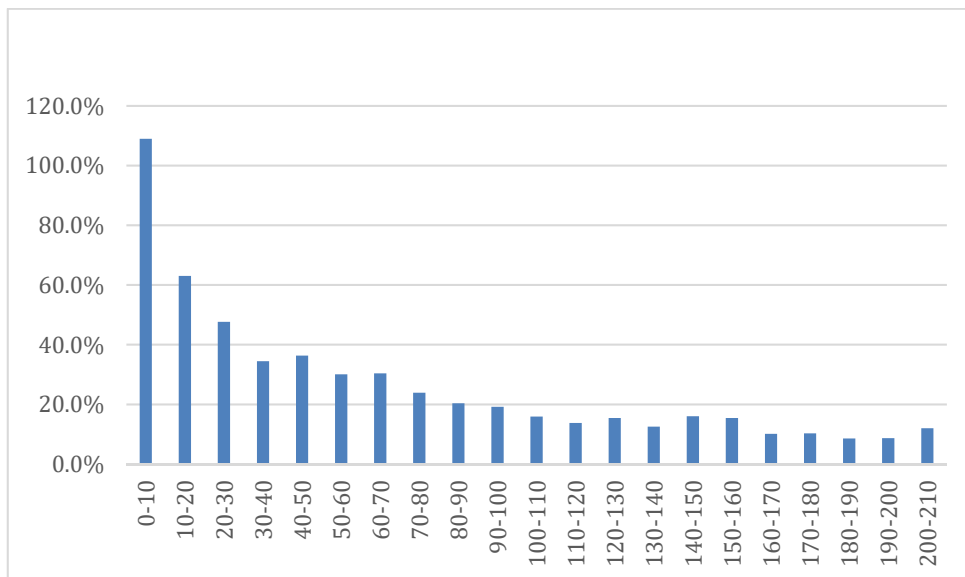


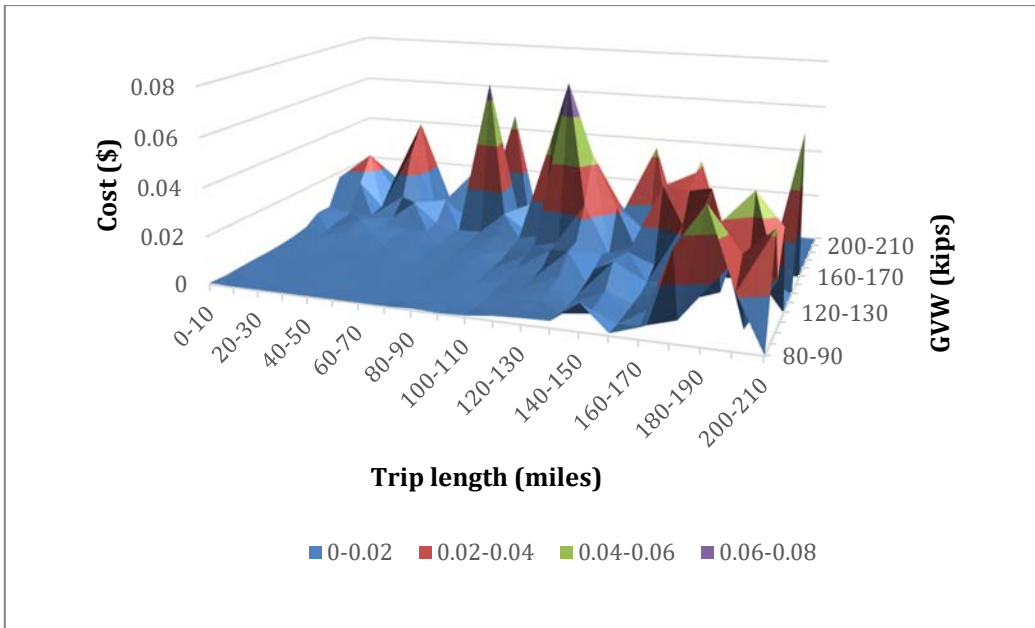
Figure 67. Percentage of damage cost paid through the current permit fee structure

Using the permit records, average damage costs were also calculated for different overweight and trip length categories as shown in Table 51. From Figure 67, it can be observed that for trip lengths between 0-10 miles, the damage costs are close to the paid permit costs. However, as the trip length increases, the damage costs are generally higher than the permit costs. The readers should note that, these values are calculated from the permit records. The use of major/minor roads and the number of bridges passed during the trip have major impacts on our approach. However, since some categories do not have enough samples, and the trips in those categories mainly consist of major roads, those categories do not follow the increasing trend.

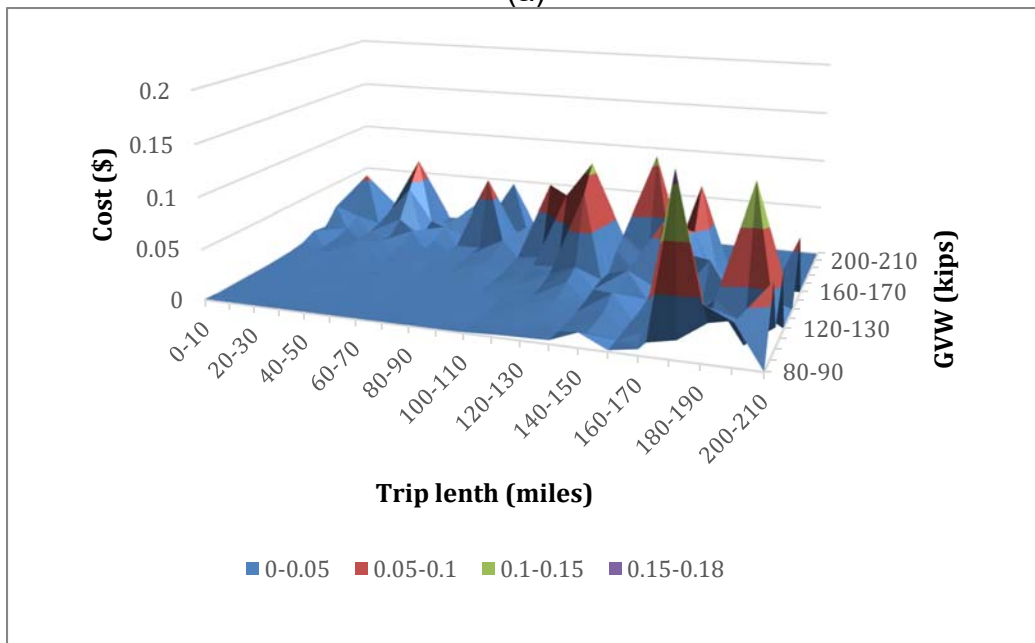
Table 51 - Average damage costs for different overweight and trip length categories

Tons\Miles	0-10	10-20	20-30	30-40	40-50	50-60	60-70	70-80	80-90	90-100	100-110
0-10	51.69987	97.42765	145.055	189.0242	176.8668	258.2277	232.4844	310.7401	386.7251	344.9117	393.8479
10-20	95.52967	149.9606	196.0201	273.4119	266.7087	275.343	333.837	475.4784	474.727	515.4291	579.8548
20-30	114.8806	206.2788	259.0935	400.2553	364.5109	360.5336	423.6076	522.9908	727.4625	694.6634	689.1233
30-40	140.0607	251.2497	450.779	447.8997	453.1922	470.7513	570.4155	571.9395	683.4559	785.9347	946.0719
40-50	329.8896	264.4077	343.655	648.3515	323.1547	556.3786	583.9745	528.2479	643.131	748.7657	1048.463
50-60	275.063	255.025	416.2239	969.839	574.195	715.6225	482.9825	433.33	654.47	611.375	1225.8
60-70			443.485	103.38				620.342			
Tons\Miles	110-120	120-130	130-140	140-150	150-160	160-170	170-180	180-190	190-200	200-210	
0-10	443.8585	448.4003	444.6846	338.0869	402.9795	609.2514	553.722	600.6325	591.9025	1225.2	
10-20	535.0821	597.8634	1019.738	620.1118	558.3408	880.1512	1033.7	813.2188	1237.01	533.885	
20-30	1377.575	661.009	879.9454	1132.329	760.7653	1220.193	1313.851	1937.365	1730.7		
30-40	1102.82		1330.725	1232.254	671.5471	1330.298	1408.878				
40-50	1662.211	1155.685	1039.915	706.87							
50-60		1875.17		1160.125							
60-70					2305.55						

Similar to the first approach, surface plots of the damage costs by trip length and by weight in Figure 68 show the big picture clearly: Shorter trips of lighter vehicles impart less damage to the infrastructure, and incur lower costs. Conversely, longer trips incur higher costs. Longer trips are more likely to damage roadway structures when longer strips of pavement are exposed to damage and there is a higher chance of passing over bridges on the roadway, which all increases damage to the infrastructure in its entirety.



(a)



(b)

Figure 68. Surface plots of (a) low, (b) high damage costs (per ton per mile) by weight and by trip length using marginal unit pavement costs

CONCLUSIONS

Conclusions for Bridge Part

This study aims to quantify the economic impact of overweight trucks on bridge structures. Two main structural components were considered in the analysis, bridge deck and bridge girders. Two loading scenarios were assumed to quantify the effect of overweight trucks. In Case 1, “all trucks” represents current truck traffic with all overweight trucks, and in Case 2, “legal truck traffic” excludes overweight trucks. We selected three bridge prototypes after analyzing the bridge inventory in New Jersey: simple span steel multi-beam bridges, simple span steel girder-floorbeam bridges, and simple span prestressed concrete multi-beam bridges. Fatigue deterioration was used to estimate the service life of bridge girders under different loading scenarios, and the current AASHTO fatigue approach was used to establish girder fatigue. Condition ratings from the NBI database were used to derive the deterioration models of bridge decks over time, and the actual service lives of decks on available highways were obtained. Additionally, WIM data from stations spread over New Jersey highway networks were used to extract the “all truck” and the “legal truck traffic” datasets. Correlation between truck load statistics and service life on available major routes were quantified. Lastly, the life-cycle cost analysis for two scenarios were presented along with the economic impact of overweight trucks on bridge decks.

The results of this on-going study lead to the following conclusions:

- Most of damage cost from overweight trucks was attributed to the deterioration of bridge decks. Deck unit costs are about 6-7 times of girder unit costs.
- Overweight trucks caused more damage to bridge girders of interstate highways, however, overweight trucks caused more damage to bridge decks of NJ state highways due to the presence of a larger proportion of overweight trucks, larger wheel loads from overweight trucks, and fewer axles per truck.
- Based on NBI data, the average service life of bridge decks on interstate highways, US numbered highways, and NJ state highways are 36.8 years, 48.4 years, and 52 years, respectively. The bridge decks on interstate highways deteriorated the most while those on NJ state highways deteriorated the least.
- Compared to US numbered highways and NJ state highways, interstate highways have highest ADTT and axles per day. This is the reason that decks on interstate highways have shorter service lives. Interstate highways have higher effective truck weight than the other two highway types. However, the equivalent wheel loads are comparable for all three highway types since the trucks on interstate highways usually have more axles. More axles help distribute the GVW. The highest equivalent wheel load is found to be on US-322 rather than on interstate highways.
- NJ state highways have the highest proportion of overweight trucks. Most overweight trucks on interstate highways are Class 9 with five axles. The majority of overweight trucks travelling on the other two highway types are Class 7 with four axles
- Service life prediction functions for decks were proposed based on equivalent wheel loads, helping to quantify service life reduction due to increased wheel load.

Future Work for Bridge Deterioration Models

In this study, fatigue of prestressed tendons was considered as the critical deterioration model for prestressed concrete girders. However, based on recent research of our team, the failures of prestressed concrete girders are caused by the shear failure at beam-end of manufactured PC girders. We have observed that the PC I-girders are under high shear stress exceeding the shear strength of concrete around the bottom flange and on the web near the beam end. Based on the new findings, the damage cost of prestressed concrete girders will be investigated in the future.

Conclusions for Pavement Part

This study aims to quantify the effect of vehicular loading on pavement deterioration and thus more reliably assess the relative cost shares of damage caused by heavy weight vehicles.

This report analyzed the impact of overweight vehicles on pavement using WIM data and mechanistic-empirical pavement analysis. Different distribution patterns were observed between the overweight and non-weight traffic in terms of truck classes and axle load spectra. The reduction ratio of pavement life was used to normalize the effect of overweight truck at different conditions. A linear relationship was found between the overweight percentage and the reduction ratio of pavement life regardless of the variation in traffic loading and pavement structure. In general, a 1 percent increase of overweight trucks may cause 1.8 percent reduction of pavement life.

We developed a methodology for allocating asphalt pavement damage cost to individual trucks based on the gross vehicle weight (GVW), axle load, and configuration. The pavement damage cost was estimated using two different approaches: mechanistic-empirical (M-E) pavement analysis, and pavement performance data from PMS. Although the marginal pavement damage cost is developed using the M-E analysis, local calibration of performance function is recommended to increase the accuracy of pavement life prediction and refine the cost values.

The developed methodology was used to derive pavement damage cost considering a wide range of pavement structures and traffic conditions in interstate highway and state roads. The study results indicate that the unit pavement damage costs vary depending on road category and analysis period of LCCA. The analysis of pavement damage cost caused by an individual truck clearly indicates that a truck having the same GVW but different axle configurations could cause significantly different pavement damage costs.

Therefore, a different permit fee structure is recommended. The developed methodology allows allocating costs to different trucks in a manner that is commensurate with their respective contributions to pavement damage and developing an “axle-weight-distance” based permit fee structure for overweight trucks. This will help allocate costs to different vehicle classes in a manner that is commensurate with their

respective contributions to pavement damage. It is expected that by doing so, state agencies can be placed in a better position to optimize the existing road use charging system, update permit fee structures for overweight trucks, and ultimately preserve investments in highway infrastructure without sacrificing the competitive position of the state.

Conclusions for Decision Tool

In this study, an integrated methodology was developed for estimating the infrastructure costs related to pavement and bridges. Advanced models were developed for both parts, however, the advanced nature of the models made it harder to implement this detailed approach to real-life situations. Hence, the research team developed a user-friendly web based tool that utilizes the user interface of ASSISTME-WIM (another tool developed by the same research team to process and to analyze WIM data). This tool is capable of using the modeling results along with the unified database to automatically calculate the infrastructure costs for a roadway or a single truck trip (given that truck properties). Moreover, the software can display selected roadways and segments on a GIS interface that uses GoogleMaps API.

Based on the results, this report concludes the following:

1. ASSISTME-WIM can effectively and quickly estimate the roadway damage to pavement and bridges from freight (overweight trucks as well as other heavy vehicles).
2. ASSISTME-WIM provides a relative indication of how overweight trucks damage infrastructure by calculating overweight units on multiple roadways.
3. Damage to minor roads caused by freight is currently underestimated. Trip length is a major factor affecting the degree of damage to infrastructure caused by overweight trucks. As trip length increases, trucks are more likely to travel across more bridges and minor roadways, causing more aggregate damage. Future estimates of damage to minor roads and bridges should consider trip length.
4. Based on the analysis of permit records from 2011, the estimated state-wide average cost of moving one ton of overweight load for one miles is about \$0.33, in which about 60% of the damage cost attributed to pavement and 40% to bridges. Based on NJDOT's current permit fee structure, the damage cost is not fully recovered using weight-based fee structure only. ASSISTME-WIM can be used to adjust NJDOT permit fees for overweight trucks. The single trip cost function can calculate damage caused by single vehicles for a single trip. Future research work is needed to account for the damage cost by using a fee structures based per overweight ton per mile traveled.

REFERENCES

1. *AASHTO Guide for Design of Pavement Structures*. American Association of State Highway and Transportation Officials, Washington, D.C, 1986.
2. *AASHTO Guide for Design of Pavement Structures*. American Association of State Highway and Transportation Officials, Washington, D.C, 1993.
3. ARA, Inc., ERES Division. **“Guide for Mechanistic-Empirical Design of New and Rehabilitated Pavement Structures”** in NCHRP 1-37A, TRB, Transportation Research Board of the National Academies, Washington, D.C., 2004.
4. N.A. Parker and S. Hussain. “Pavement damage and road pricing”. In *Proceedings of 85th Transportation Research Board Annual Meeting*, Washington, D.C., 2006.
5. F. Hong, J. A. Prozzi and J. Prozzi. “A new approach for allocating highway cost”. *Journal of Transportation Research Forum*, Vol. 46, No. 2, 2007, pp. 5-20.
6. E. J. Yoder, B., Colucci-Rios, J. Fraczek and J. A. Skees. *Effects of Raising Load Limits on Pavements and Bridges in Indiana*. Joint Highway Research Project, IN/JHRP-79-23, FHWA, U.S. Department of Transportation, 1979.
7. BTML Division of Wilbur Smith Associates. *Effects of Truck Weights on Deterioration, Operations, and Design of Bridges and Pavements*. Final report to NYSDOT, ERDB, 1987.
8. **“Truck Weight Limits: Issues and Options.”** In *Transportation Research Board Special Reports 225*, TRB, National Research Council, Washington, D.C., 1990.
9. **“New Trucks for Greater Productivity and Less Road Wear: An Evaluation of the Turner Proposal.”** In *Transportation Research Board Special Reports 227*, TRB, National Research Council, Washington, D.C., 1990.
10. F. Moses. (1989) **“Effects on Bridges of Alternative Truck Configurations and Weights.”** Draft Final Report to NCHRP TRB, Transportation Research Board of the National Academies, Washington, D.C., 1989.
11. J. Mohammadi, S.A. Guralnick and R. Polepeddi. *The Effects of Increased Truck Weights Upon Illinois Highway Bridges*. Final Report to IDOT, FHWA/IL/RC-013, Illinois Institute of Technology, FHWA, U.S. Department of Transportation, 1998.
12. A.H.S. Ang and W.H. Tang, *Probability Concepts in Engineering Planning and Design, Vol. 1, Basic Principles*. John Wiley, Inc., New York, 1975.
13. R.J. Heywood and R.A. Person **“Adequacy of Australian Bridges”**, Department of Transport and Regional Development, 1997.
14. A. Saber, F. Roberts, Z. Zhou and W. Alaywan. *Monitoring System to Determine the Impact of Sugarcane Truckloads on Non-Interstate Bridges*. Report No. FHWA/LA.06/418, FHWA, U.S. Department of Transportation, 2008.

15. J. Chang and M.J. Garvin. "Sensitivity Analysis to Assess the Impact of Truck Weight Reform on Bridge Network Costs". #07-0222, In *Proceedings of 86th Transportation Research Board Annual Meeting*, Washington, D.C., 2007.
16. A. K. Altay, D. S. Arabbo, E. B. Corwin, R. J. Dexter and C. E. French. *Effects of Increasing Truck Weight on Steel and Prestressed Bridges*. MDOT Report MN/RC-2013-16, Minnesota Department of Transportation, 2003.
17. M. Dicleli, and M. Bruneau. "Fatigue-Based Methodology for Managing Impact of Heavy-Permit Trucks on Steel Highway Bridges." *J. Struct. Eng.*, Vol. 121, No. 11, 1995, pp. 1651–1659.
18. M. P. Culmo, J. T. DeWolf and M. R. DelGrego. "**Behavior of Steel Bridges Under Superload Permit Vehicles.**" In *Transportation Research Record* No. 1892, TRB, National Research Council, Washington, D.C., 2004, pp. 107-114.
19. J. A. Reisert and M. D. Bowman. *Fatigue of Older Bridges in Northern Indiana due to Overweight and Oversized Loads, Volume 1: Bridge and Weigh-In-Motion Measurements*. Report FHWA/IN/JTRP-2005/16-1. FHWA, U.S. Department of Transportation, 2006.
20. F. L. Roberts, A. Saber, A. Ranadhir and X. Zhou. *Effects of Hauling Timber, Lignite Coal, and Coke Fuel on Louisiana Highways and Bridges*. Report No. 398, Louisiana Department of Transportation and Development, 2005.
21. Ohio Department of Transportation. *Impacts of Permitted Trucking on Ohio's Transportation System and Economy*. 2009.
22. H. Bae and M. Oliva. *Bridge Analysis and Evaluation of Effects under Overload Vehicles-Phase I*. CFIRE 02-03, 2009.
23. H. Bae and M. Oliva. *Bridge Analysis and Evaluation of Effects under Overload Vehicles-Phase II*. CFIRE 02-03, 2012.
24. Z. Lin, J. Zhao, and H. Tabatabai. *Impact of Overweight Vehicles (with Heavy Axle Loads) on Bridge Deck Deterioration*. CFIRE 04-06, 2012.
25. T. Adams, E. Perry, A. Schwartz, B. Gollnik, M. Kang, J. Bittner and S Wagner. *Aligning Oversize/Overweight Fees with Agency Costs: Critical Issues*. WisDOT ID No. 0092-10-21, CFIRE ID No. 03-17, 2013.
26. M. Chowdhury, B. Putman, W. Pang, A. Dunning, K. Dey and L. Chen. *Rate of Deterioration of Bridges and Pavements as Affected by Trucks*. Report No. FHWA-SC-13-05, FHWA, U.S. Department of Transportation, 2013.
27. A.K. Azad, M.H. Baluch, M.Y. Al-Mandil and Al-Suwaiyan. *Static and Fatigue Tests of Simulated Bridge Decks. Experimental Assessment of Performance of Bridges*. Proceedings of ASCE Convention, Boston, MA., 1986, pp. 30-41.
28. K. Okada, H. Okamura and K. Sonada. "**Fatigue Failure Mechanism of Reinforced Concrete Deck Slabs**". In *Transportation Research Record* 664, TRB, National Research Council, Washington, D.C., 1978, pp.136-144.

29. T. Kato and Y. Goto. "**Effect of Water Infiltration of Penetration Deterioration of Bridge Deck Slabs.**" In *Transportation Research Record 950*, National Research Council, Washington, D.C., 1978, pp. 202-209.
30. *AASHTO The Manual for Bridge Evaluation*. American Association of State Highway and Transportation Officials, Washington, D.C., 2011.
31. B. Batchelor, B.E. Hewitt and P. Csagoly. "**An Investigation of the Fatigue Strength of Deck Slabs of Composite Steel/Concrete Bridges.**" In *Transportation Research Record 664*, TRB, National Research Council, Washington, D.C., Vol.1, 1978, p.153-161.
32. I. K. Fang, C.K.T. Tsui, N. H. Burns, and R.E. Klinger. "Fatigue Behavior of Cast-in-Place and Precast Panel Bridge Decks with Isotropic Reinforcement." *PCI Journal*, Vol. 35, No.3, 1990, pp.28-39.
33. M. Petrou, P.C. Perdikaris and A. Wang. "**Fatigue Behavior of Non-composite Reinforced Concrete Bridge Deck Models.**" In *Transportation Research Record 1460*, TRB, National Research Council, Washington, D.C., 1994, pp.73-80.
34. P.C. Perdikaris, M.F. Petrou, and A. Wang. *Fatigue Strength and Stiffness of Reinforced Concrete Bridge Decks*, Final Report FHWA/OH-93/016, FHWA, U.S. Department of Transportation, 1993.
35. S. Youn and S. Chang. "Behavior of Composite Bridge Decks Subjected to Static and Fatigue Loading." *ACI Structural Journal*, Vol. 95, No.3, 1998, pp.249-259.
36. Z. Lin, J. Zhao and H. Tabatabai. *Impact of Overweight Vehicles (with Heavy Axle Loads) on Bridge Deck Deterioration*. No. CFIRE 04-06, 2012.
37. R. E. Weyers, M. G. Fitch, E. P. Larsen, I. L. Al-Qadi, W. P. Chamberlin and P. C. Hoffman. *Concrete Bridge Protection and Rehabilitation: Chemical and Physical Techniques. Service Life Estimates*. No. SHRP-S-668, 1994.
38. Y. Liu and R. E. Weyers. "Modeling the time-to-corrosion cracking in chloride contaminated reinforced concrete structures". *ACI Materials Journal*, Vol. 95, No. 6, 1998.
39. M.G. Stewart and D.V. Rosowsky. "Time-dependent reliability of deteriorating reinforced concrete bridge decks." *Structural Safety*, Vol. 20, No. 1, 1998, pp. 91-109.
40. K. A. T. Vu and M. G. Stewart. "Structural reliability of concrete bridges including improved chloride-induced corrosion models". *Structural Safety*, Vol. 22, No. 4, 2000, pp. 313-333.
41. G. Fu, J. Feng, W. Dekelbab, F. Moses, H. Cohen, D. Mertz and P. Thompson. "**Effect of Truck Weight on Bridge Network Costs**". In *NCHRP Report 495*, TRB, Transportation Research Board of the National Academies, Washington, D.C., 2003.

42. F. Moses, C.G. Schilling and K.S. Raju. "**Fatigue Evaluation Procedures for Steel Bridges.**" In *NCHRP Report 299*, TRB, Transportation Research Board of the National Academies, Washington, D.C., 1987.
43. A. Nowak, H. Nassif and L. DeFrain. "Effect of Truck Load on Bridges." *ASCE Journal of Transportation Engineering*, Vol. 119, No. 6, 1993, pp. 853-867.
44. *AASHTO Guide Specifications for Fatigue Evaluation of Existing Steel Bridges*. American Association of State Highway and Transportation Officials, Washington, D.C., 1990.
45. *AASHTO LRFD Bridge Design Specifications*. American Association of State Highway and Transportation Officials, Washington, D.C., 2012.
46. *ASTM E206-72: Definitions of Terms Relating to Fatigue Testing and the Statistical Analysis of Fatigue Data*. American Society for Testing and Materials, 1979.
47. W.H. Munse. *Fatigue, Brittle Fracture, and Lamellar Tearing*. Structural Engineering Handbook, 3rd Ed. E.H. Gaylord Jr. and C.N. Gaylord, eds., McGrawHill Inc., New York, 1990, 4.1-4.24.
48. W. Schutz. "A History of Fatigue." *Engineering Fracture Mechanics*, Vol. 54, No. 2, 1996, pp. 263-300.
49. C. G. Schilling, K. H. Klippstein, J. M. Barsom and G.T. Blake. "**Fatigue of Welded Steel Bridge Members under Variable-Amplitude Loadings**". In *NCHRP Report 188*, TRB, Transportation Research Board of the National Academies, Washington, D.C., 1978.
50. J.W. Fisher, G.L. Kulak, and I.F. Smith. *A Fatigue Primer for Structural Engineers*. National Steel Bridge Alliance, American Institute of Steel Construction, 1998.
51. M.A. Miner. "Cumulative Damage in Fatigue". *Journal of Applied Mechanics*, Vol. 12, No. 3, 1945, pp. 159-164.
52. D.F. Socie and M.A. Pompetzki. "Modeling Variability in Service Loading Spectra." *Journal of ASTM International*, Vol. 1, No. 2, Paper ID JAI11561, 2004.
53. J.W. Fisher, J. Jian, D.C. Wagner, and B.T. Yen. "**Distortion-induced fatigue cracking in steel bridges.**" In *NCHRP Report 336*, TRB, Transportation Research Board of the National Academies, Washington, D.C., 1990.
54. J. Laman and A. Nowak. "Fatigue-load model for girder bridges". *Journal of Structural Engineering*, ASCE, Vol. 122, No 7, 1996, pp. 726-733.
55. C. G. Schilling. "Stress cycles for fatigue design of steel bridges." *Journal of Structural Engineering*, Vol. 110, No. 6, 1984, pp. 1222-1234.
56. P. B. Keating and J. W. Fisher. *Review of Fatigue Tests and Design Criteria on Welded Details*. Fritz Engineering Laboratory Report 488-1(85), Lehigh University, Bethlehem, PA, 1985.

57. C. Hahin, J.M. South, J. Mohammadi and R.K. Polpeddi. "Accurate and Rapid Determination of Fatigue Damage in Steel Bridges." *Journal of Structural Engineering. ASCE*, Vol. 119, No. 1, 1993, pp. 150-168.
58. J. Mohammadi, S. A. Guralnick and R. Polepeddi. *The Effects of Increased Truck Weights Upon Illinois Highway Bridges*. Final Report to IDOT, FHWA/IL/RC-013, FHWA, U.S. Department of Transportation, 1998.
59. F. L. Roberts and L. Djakfar. *Preliminary Assessment of Pavement Damage due to Heavier Loads on Louisiana Highways*. Report No. FHWA/LA-98/321. FHWA, U.S. Department of Transportation, 1999.
60. T. E. Freeman and T. M. Clark. "Performance of pavements subject to higher truck weight limits in Virginia." *Transportation Research Record: Journal of the Transportation Research Board*, No. 1806, 2002, pp. 95-100.
61. J.M., Sadeghi and M. Fathali. "Deterioration Analysis of Flexible Pavements under Overweight Vehicles." *Journal of Transportation Engineering-ASCE*, Vol. 133, No. 11, 2007, pp. 625-633.
62. J. C. Pais and S. I. R. Amorim, and M. J. C. Minhoto. "Impact of Traffic Overload on Road Pavement Performance." *Journal of Transportation Engineering*, Vol. 139, No. 9, 2013, pp. 873-879.
63. R. Gibby, R. Kitamura and H. Zhao. "Evaluation of Truck Impacts on Pavement Maintenance Costs." *Transportation Research Record: Journal of the Transportation Research Board*, No.1262, 1990, pp. 48-56.
64. R. Ghaeli, B. G. Hutchinson, R. Haas and D. Gillen. "Pavement and Bridge Cost Allocation Analysis of the Ontario, Canada, Intercity Highway Network." *Transportation Research Record: Journal of the Transportation Research Board*, No. 1732, 2000, pp. 99-107.
65. J. J. Hajek, S.L. Tighe and B.G. Hutchinson. "Allocation of Pavement Deterioration due to Trucks Using a Marginal Cost Method." *Transportation Research Record: Journal of the Transportation Research Board*, No. 1613, 1998pp. 50-56.
66. Z. Li, K. C. Sinha and P. S. McCarthy. "Methodology to Determine Load-and Non-Load-Related Shares of Highway Pavement Rehabilitation Expenditures." *Transportation Research Record: Journal of the Transportation Research Board*, No. 1747, 2001, pp. 79-88.
67. T.C. Martin. "Estimating Heavy Vehicle Road Wear Costs for Bituminous-Surfaced Arterial Roads." *Journal of Transportation Engineering*, Vol. 128, No. 2, 2002, pp. 103-110.
68. J.K. Fortowsky and J. Humphreys. "Estimating Traffic Changes and Pavement Impacts from Freight Truck Diversion Following Changes in Interstate Truck Weight Limits." *Transportation Research Record: Journal of the Transportation Research Board*, 1966, pp. 71-79.

69. C. Tirado, C. Carrasco, J. M. Mares, N. Gharaibeh, S. Nazarian and J. Bendaña. "Process to Estimate Permit Costs for Movement of Heavy Trucks on Flexible pavements." *Transportation Research Record: Journal of the Transportation Research Board*, No. 2154, 2010, pp. 187-196.
70. A. Ahmed. *Pavement Damage Cost Estimation using Highway Agency Maintenance, Rehabilitation, and Reconstruction Strategies*. Dissertation, Purdue University, 2012.
71. M. Chowdhury, B. Putman, W. Pang, A. Dunning, K. Dey and L. Chen. *Rate of Deterioration of Bridges and Pavements as Affected by Trucks*. Report No. FHWA-SC-13-05, FHWA, U.S. Department of Transportation, 2013.
72. D. Peterson. "**Life-Cycle Cost Analysis of Pavements.**" In *NCHRP Synthesis of Highway Practice 122*, TRB, Transportation Research Board of the National Academies, Washington, D.C., 1985.
73. R. Winfrey. *Economics Analysis for Highways*. International Textbook Company, Pennsylvania, 1969.
74. P.D. Cady. "Inflation and Highway Economics Analysis", *ASCE Journal of Transportation Engineering*, Vol.109, No. 5, Paper No. 18248, 1983, pp. 631-639.
75. D. Arditi and H. Messiha. "Life Cycle Cost Analysis (LCCA) in Municipal Organizations." *Journal of Infrastructure Systems*, Vol. 5, No. 1, 1999
76. J. Walls and M. Smith, *Life-Cycle Cost Analysis in Pavement Design-In search of Better Investment*, Report No. FHWA-SA-98-079, FHWA, U.S. Department of Transportation, 1998
77. G.P. Demos. *Life Cycle Cost Analysis and Discount Rate on Pavements for the Colorado Department of Transportation*, Report No. Cdot-2006-17, Colorado Department of Transportation, 2006.
78. D. Lee. "Fundamentals of Life-Cycle Cost Analysis", In *Proceedings of 81st Transportation Research Board Annual Meeting*, Washington, D.C., 2002.
79. K.T. Hall, C. Correa, S.H. Carpenter and R. Elliott. "Guidelines for Life-Cycle Cost Analysis of Pavement Rehabilitation Strategies", In *Proceedings of 82nd Transportation Research Board Annual Meeting*, Washington, D.C., 2003.
80. ACPA, *Life Cycle Cost Analysis: A Guide for Alternate Pavement Designs*, American Concrete Pavement Association, 2002.
81. J. Reigle and J. Zaniewski, "Risk-based Life Cycle Cost Analysis for Project-level Pavement Management." In *Proceedings of 81st Transportation Research Board Annual Meeting*, Washington, D.C., 2002.
82. T. Papagiannakis and M. Delwar. "Computer Model for Life-Cycle Cost Analysis of Roadway Pavements." *Journal of Computing in Civil Engineering*, Vol. 15, No. 2, 2001, pp.152-156.

83. K. Abaza, S. Ashur, S. Abu-Eisheh and A., Rabay's. "Macroscopic Optimal System for Management of Pavement Rehabilitation." *Journal of Transportation Engineering*, No. 6, 2001.
84. T. Zayed, L. Chang and J.D. Fricker. "Life-Cycle Cost Analysis using Deterministic and Stochastic Methods: Conflicting Results", *Journal of Constructed Facilities*, Vol. 16, No.2, 2002.
85. O. Salem, S. AbouRizk and S. Ariaratnam. "Risk-based Life-cycle Costing of Infrastructure Rehabilitation and Construction Alternatives." *Journal of Infrastructure Systems*, 2003.
86. H. Hwak, "**Life-Cycle Cost Analysis for Bridges.**" In *NCHRP Report 483*, TRB, Transportation Research Board of the National Academies, Washington, D.C., 2003.
87. Y. Huang, T. M. Adams and J.A. Pincheira. "Analysis of Life-Cycle Maintenance Strategies for Concrete Bridge Decks." *Journal of Bridge Engineering*, 2004, pp. 250-258.
88. S. Labi and K. C. Sinha. "Life-Cycle Evaluation of Flexible Pavement Preventive Maintenance." *Journal of Transportation Engineering*, 2005, pp. 744-751.
89. L. Daigle and Z. Lounis. *Life cycle cost analysis of high performance concrete bridges considering environmental impacts*. NRCC-49675, NRC Publications Record, 2006.
90. C. Chen and G.W. Flintsch. "Fuzzy Logic Pavement Maintenance and Rehabilitation Triggering Approach for Probabilistic Life-Cycle Cost Analysis." *Transportation Research Record: Journal of the Transportation Research Board*, No. 1990, 2007, pp. 80–91.
91. A. Kendall, G.A. Keoleian and G.E. Helfand. "Integrated Life-Cycle Assessment and Life-Cycle Cost Analysis Model for Concrete Bridge Deck Applications." *Journal of Infrastructure Systems*, 2008, pp. 214-222.
92. E. Lee, C. Kim and J.T. Harvey. "Selection of Pavement for Highway Rehabilitation Based on Life-Cycle Cost Analysis Validation of California Interstate 710 Project, Phase 1" *Transportation Research Record: Journal of the Transportation Research Board*, No. 2227, 2011, pp. 23–32.
93. H. Zhang, G.A. Keoleian and M.D. Lepech. "Network-Level Pavement Asset Management System Integrated with Life-Cycle Analysis and Life-Cycle Optimization." *Journal of Infrastructure Systems*, Vol. 19, 2013, pp. 99-107.
94. D. Su, H. Nassif and E. S. Hwang. "Probabilistic Approach for Forecasting Long Term Performance of Girder Bridges." In *Proceedings of 94th Transportation Research Board Annual Meeting*, No. 15-5515, Washington, D.C., 2015.
95. Office of Engineering Bridge Division. *The Recording and Coding Guide for the Structure Inventory and Appraisal of the Nation's Bridges provides instructions for coding of condition rating for bridge structure*. Report No. FHWA-PD-96-001, FHWA, U.S. Department of Transportation, 1995.

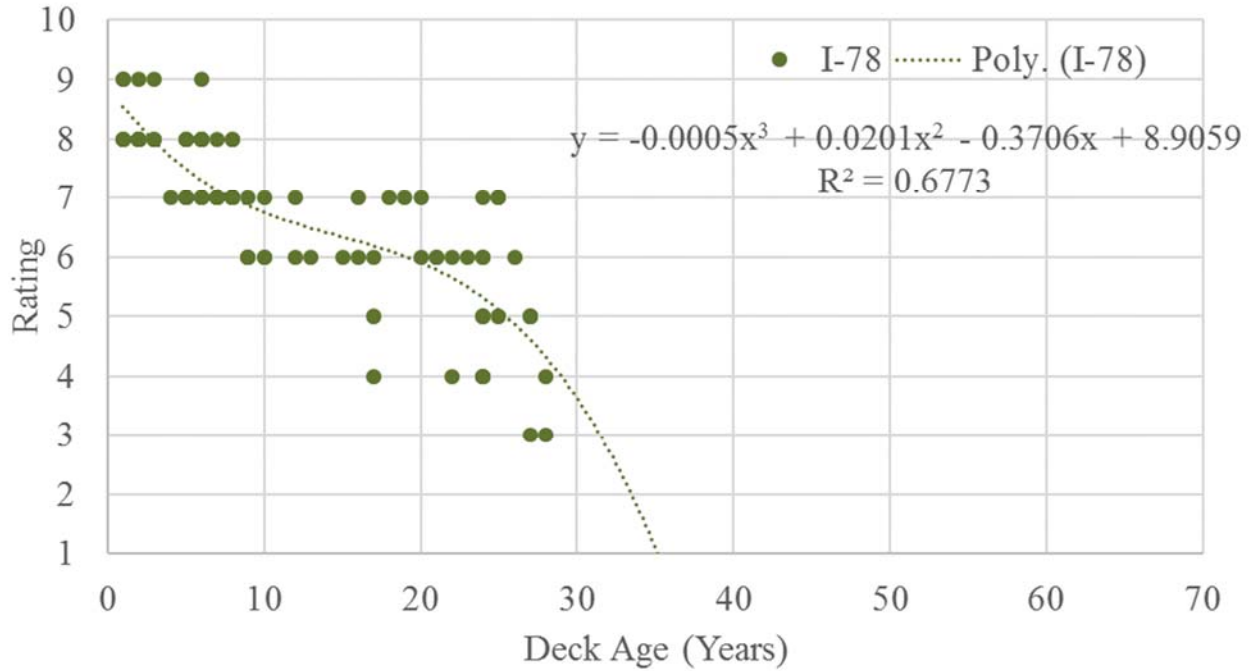
96. FHWA. *Bridge Formula Weights*. Report No. FHWA-HOP-06-105, FHWA, U.S. Department of Transportation, 2006 (revised 2015).
97. T. R. Overman, J. E. Breen and K. H. Frank. *Fatigue Behavior of Pretensioned Concrete Girders*, Report No. FHWA/TX-85/39+300-2F, FHWA, U.S. Department of Transportation, 1984.
98. ACI Committee 215, "Considerations for Design of Concrete Structures Subject to Fatigue Loading," *ACI Journal*, Vol. 71, No. 3, March 1974, pp. 97-121.
99. C. Paulson, K. H. Frank, J. E. Breen. *A Fatigue Study of Prestressing Strand*, Report No. FHWA/TX-82/54+300-1, FHWA, U.S. Department of Transportation, 1983.
100. T. Helgason, J. M. Hanson, N. F. Somes, W. G. Corley and E. Hognestad. "**Fatigue Strength of High-Yield Reinforcing Bars.**" In *NCHRP Report 164*, TRB, Transportation Research Board of the National Academies, Washington, D.C., 1976.
101. C. Bathias and P. C. Paris. *Gigacycle Fatigue in Mechanical Practice*. Marcel Dekker, New York, 2005.
102. M. Bolukbasi, J. Mohammadi and D. Ardit. "Estimating the future condition of highway bridge components using national bridge inventory data." *Practice Periodical on Structural Design and Construction*, Vol. 9, No. 1, 2004, pp. 16-25.
103. A. Hatami and G. Morcou. *Developing deterioration models for Nebraska bridges*. Report No. SPR-P1 (11) M302, Nebraska Department of Road, 2011.
104. NJDOT Structural Evaluation. *Bridge re-evaluation survey report Structure No. 0218-161*, Cycle No.16, New Jersey Department of Transportation, 2012.
105. A. Azizinamini, E. H. Power, G. F. Myers and H.C. Ozyildirim. "**Bridges for Service Life Beyond 100 Years: Innovative Systems, Subsystems, and Components**". In *SHRP 2 Report No. S2-R19A-RW-1*, Transportation Research Board of the National Academies, Washington, D.C., 2014.
106. J. J. Hajek, W. A. Phang, A. Prakash and G. A. Wrong. "Performance Prediction for Pavement Management." *Proceedings Vol. 1 of North American Pavement Management Conference*, Toronto, Canada, 1985.
107. N. C. Jackson, R. Deighton and D .L. Huft. "Development of Pavement Performance Curves for Individual Distress Indexes in South Dakota Based on Expert Opinion, Pavement Management Systems for Streets, Highways, and Airports." *Transportation Research Record: Journal of the Transportation Research Board*, No. 1524, 1996, pp. 130-136.
108. E. Safirova, K. Gillingham and S. Houde. "Measuring Marginal Congestion Costs of Urban Transportation: Do Networks Matter?" *Transportation Research A*, Vol. 41, 2007, pp. 734-749.
109. K. Ozbay, D. Jawad, N. Parker and S. Hussain L"ife Cycle Cost Analysis: State-of-the Art vs. State-of-Practice". *Transportation Research Record: Journal of the Transportation Research Board*, No. 1864, 2004, pp. 62-71.

110. W. Wilde, S. Waalkes and R. Harrison. *Life Cycle Cost Analysis of Portland Cement Concrete Pavements*. Report No. FHWA/TX-00/0-1739-1, FHWA, U.S. Department of Transportation, 1999.
111. K. Herbold. "Using Monte Carlo Simulation for Pavement Cost Analysis", *Public Roads*, Vol. 63, No. 4, 2000.
112. K. Ozbay, O. Yanmaz-Tuzel and B. Bartin. *Cost of Transporting People in New Jersey: Phase 2*. Report No. FHWA/NJ-2007-003, FHWA, U.S. Department of Transportation, 2007.
113. Straus, Sandy H., and John Semmens. *Estimating the cost of overweight vehicle travel on Arizona highways*. No. FHWA-AZ-06-528. Arizona Department of Transportation, 2006.
114. M. Ghosn, G. Fiorillo, V. Gayovyy, T. Getso, S. Ahmed, and N. Parker. *Effects of Overweight Vehicles on NYSDOT Infrastructure* (No. C-08-13), 2015.

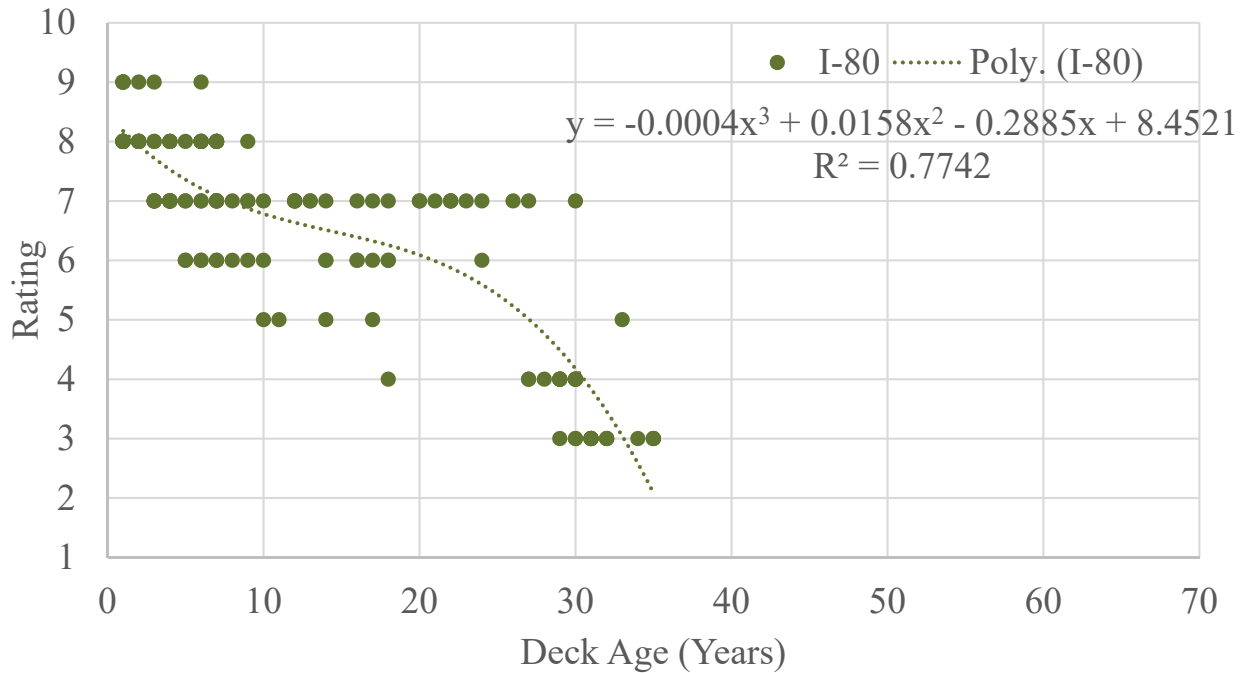
APPENDIX A OBTAINED DECK DETERIORATION CURVE FROM NBI DATABASE

The obtained deterioration curve for bridge decks on various highways

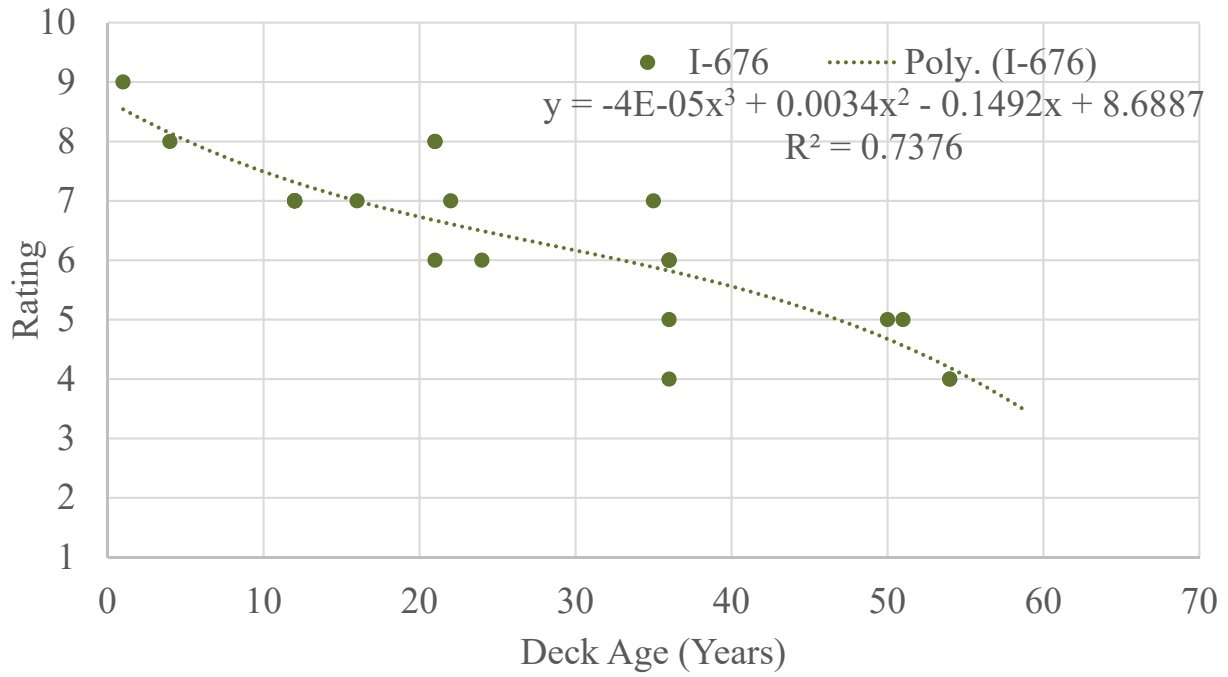
I-78



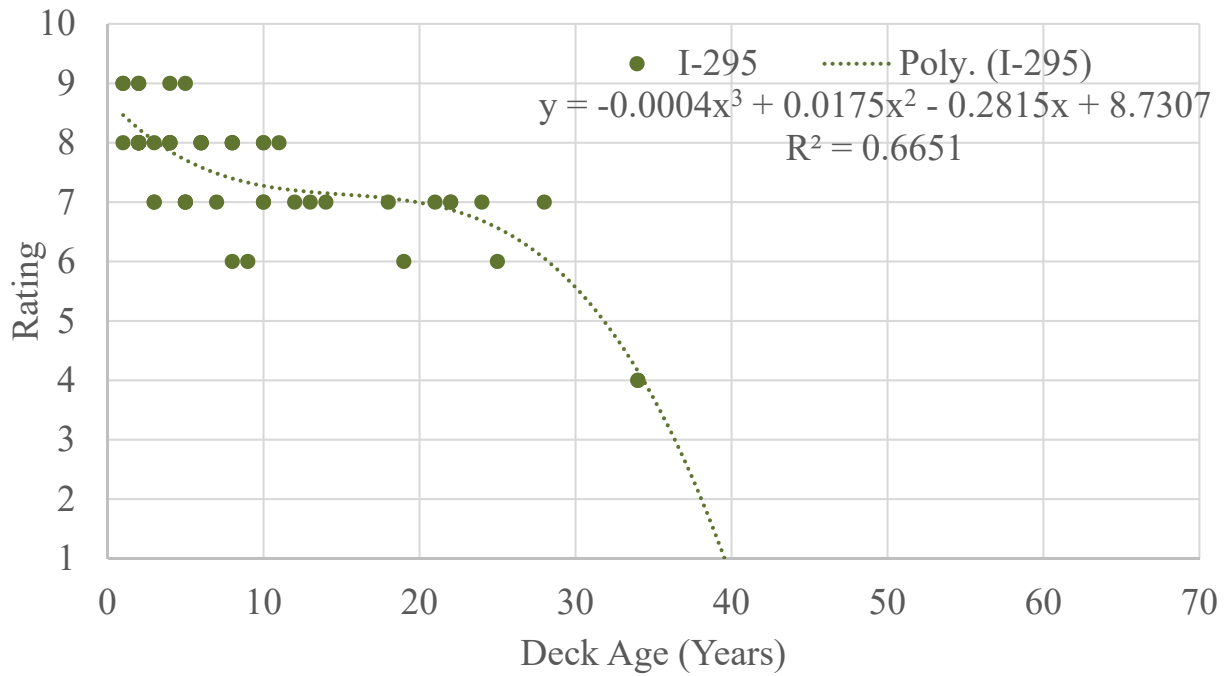
I-80



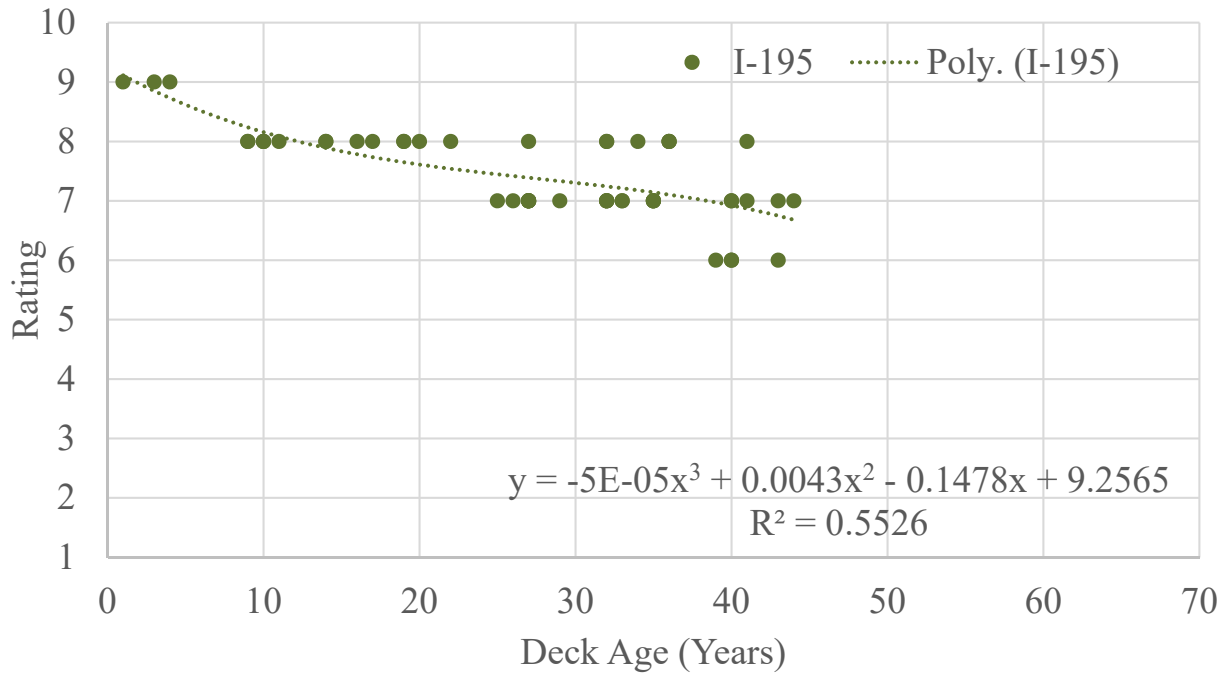
I-676



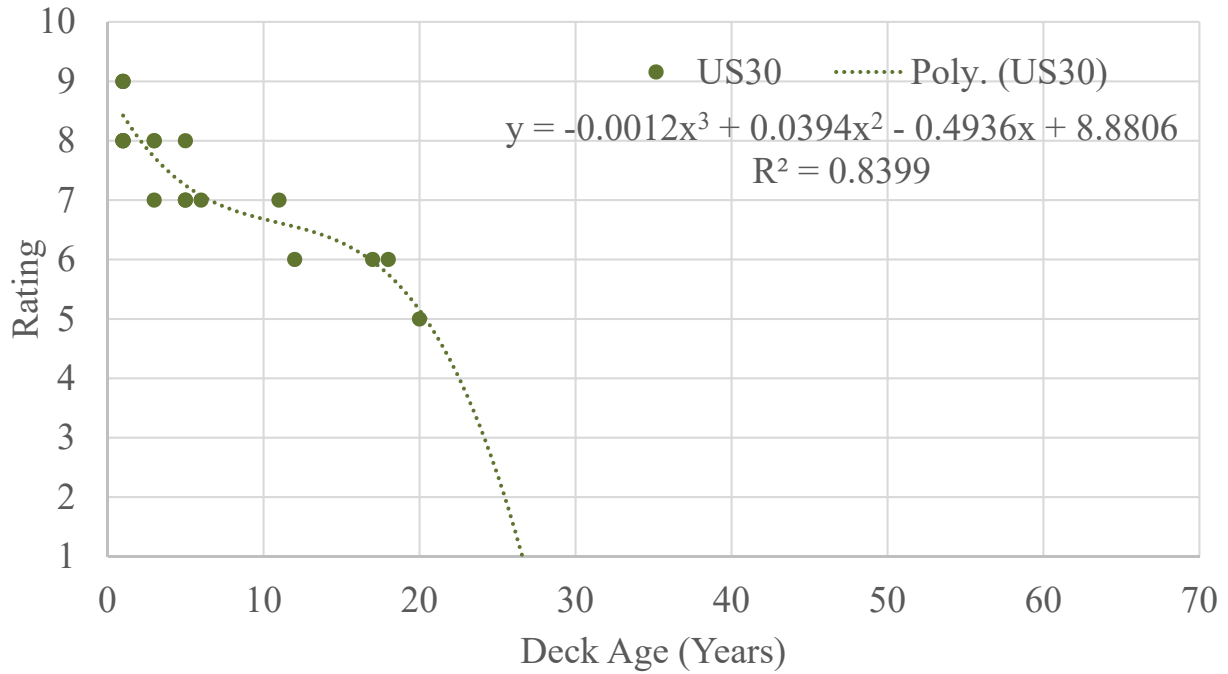
I-295

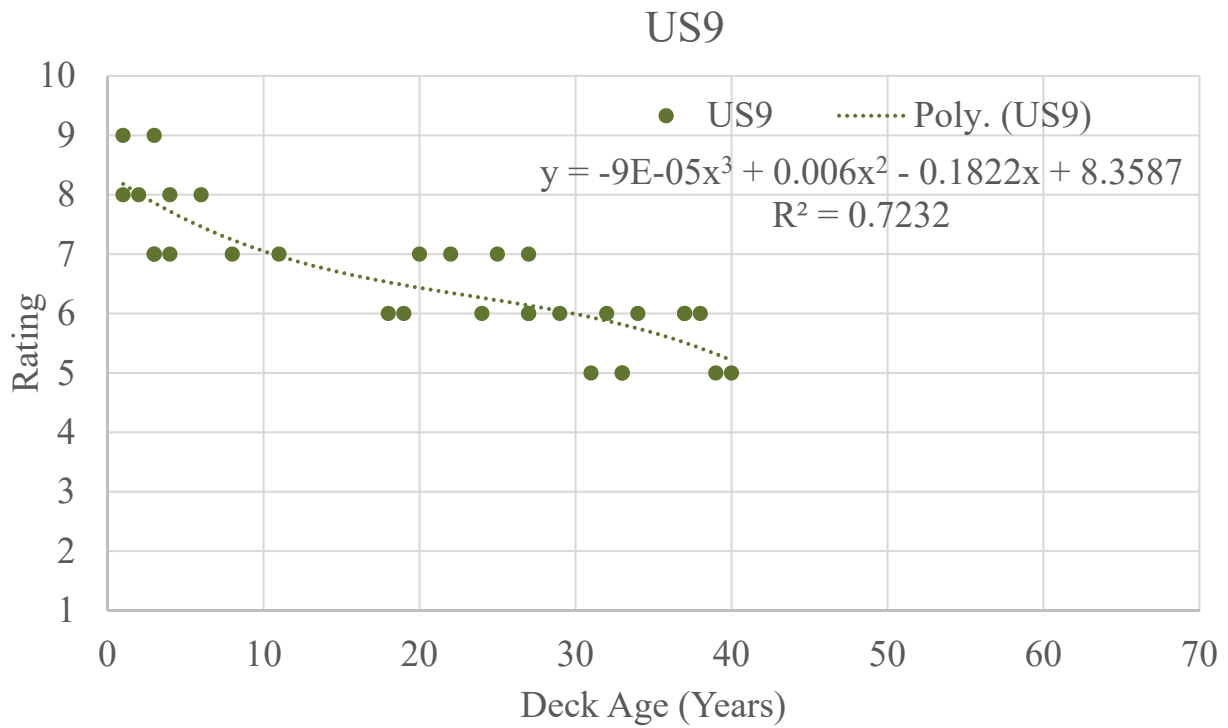
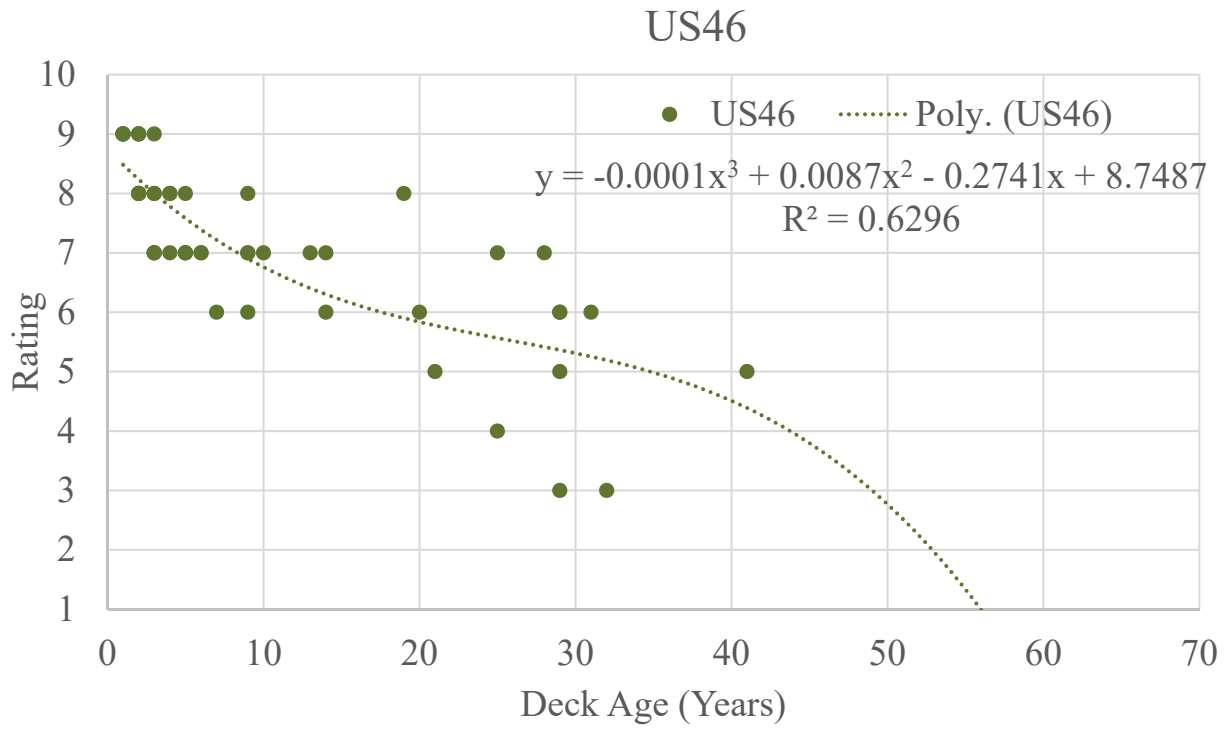


I-195

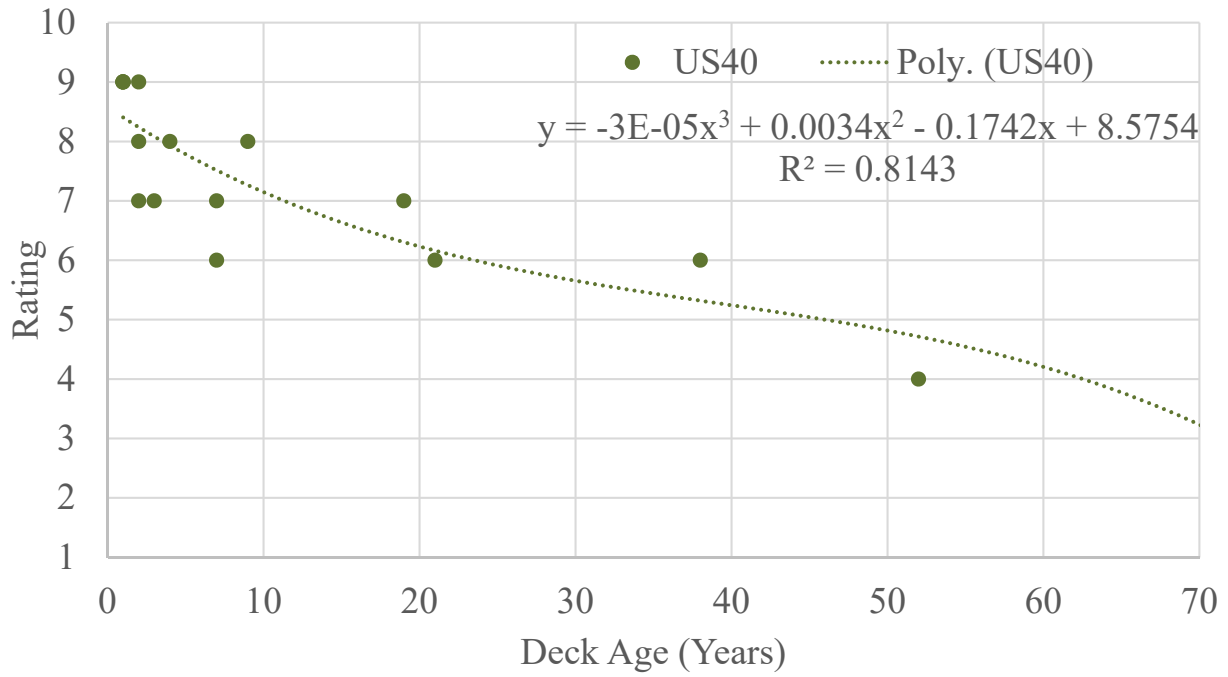


US30

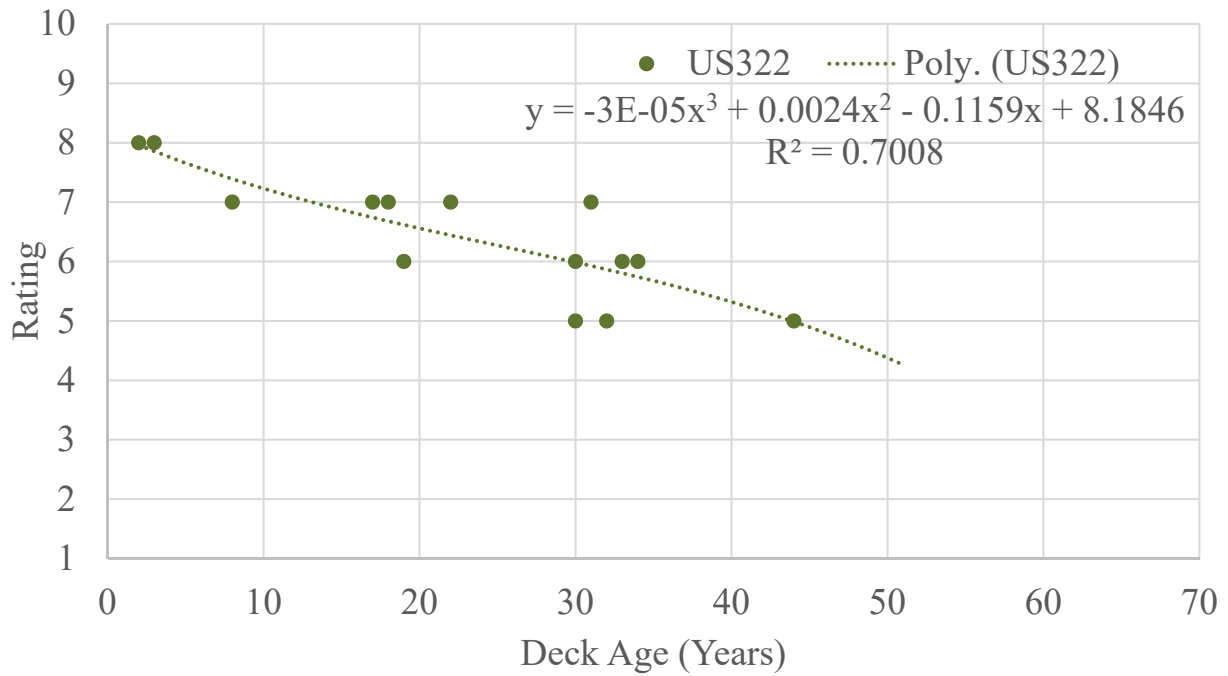




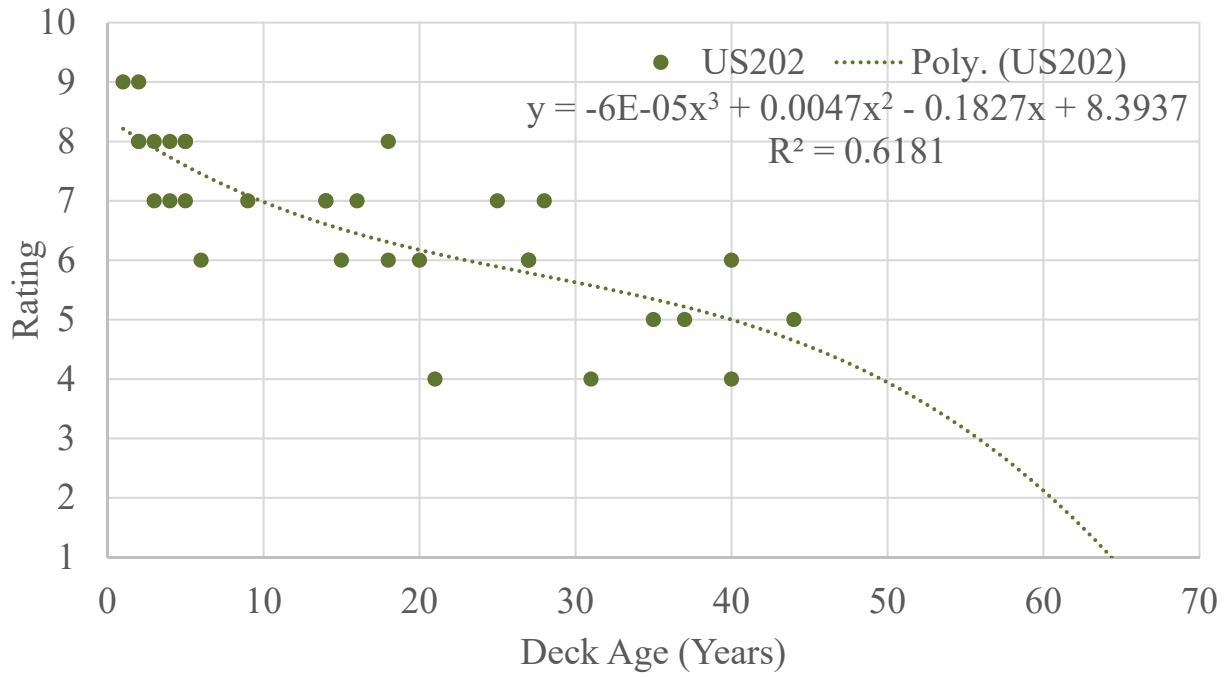
US40



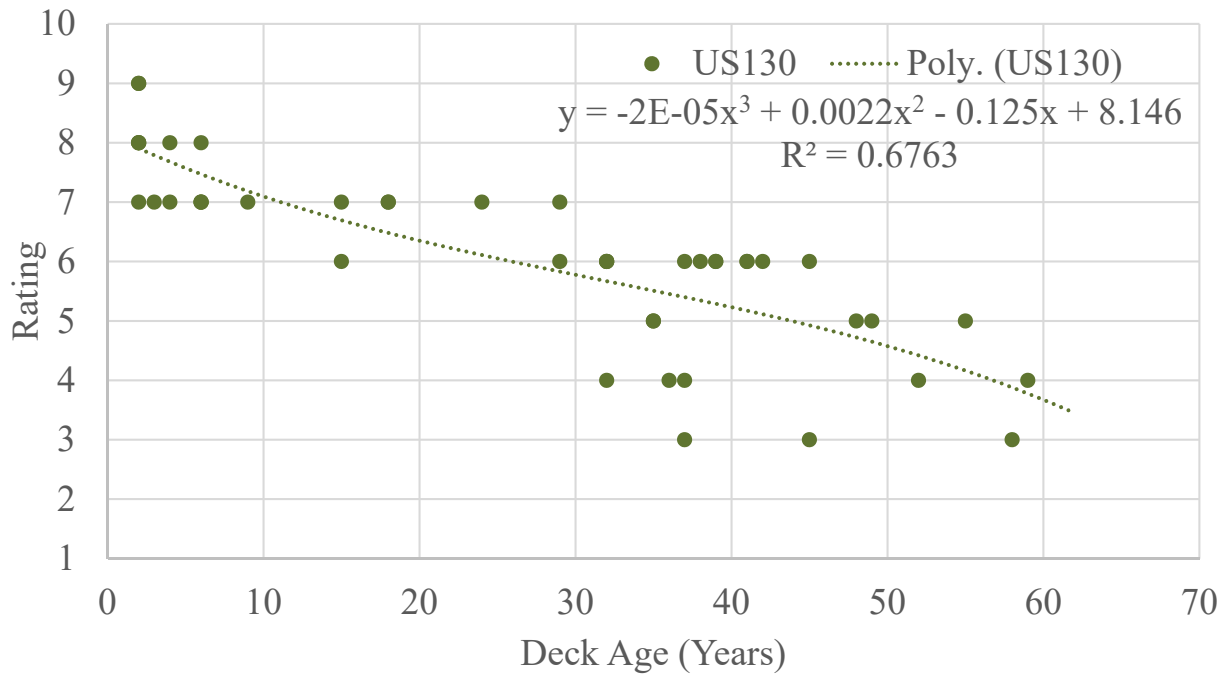
US322



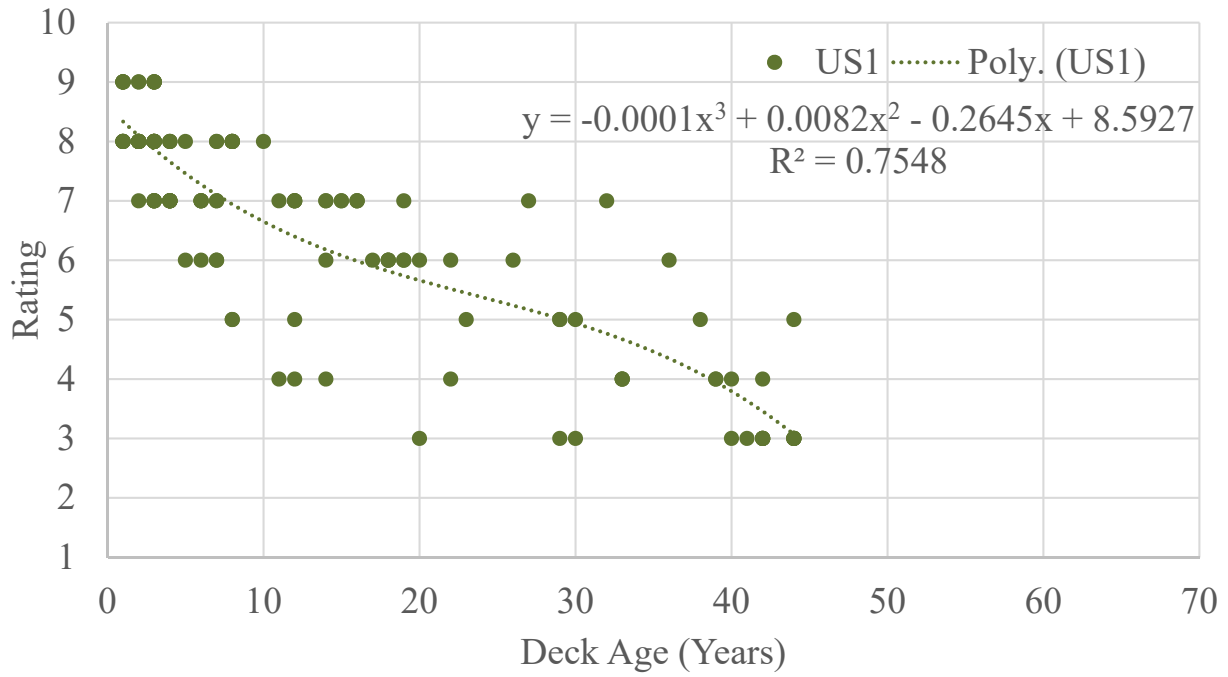
US202



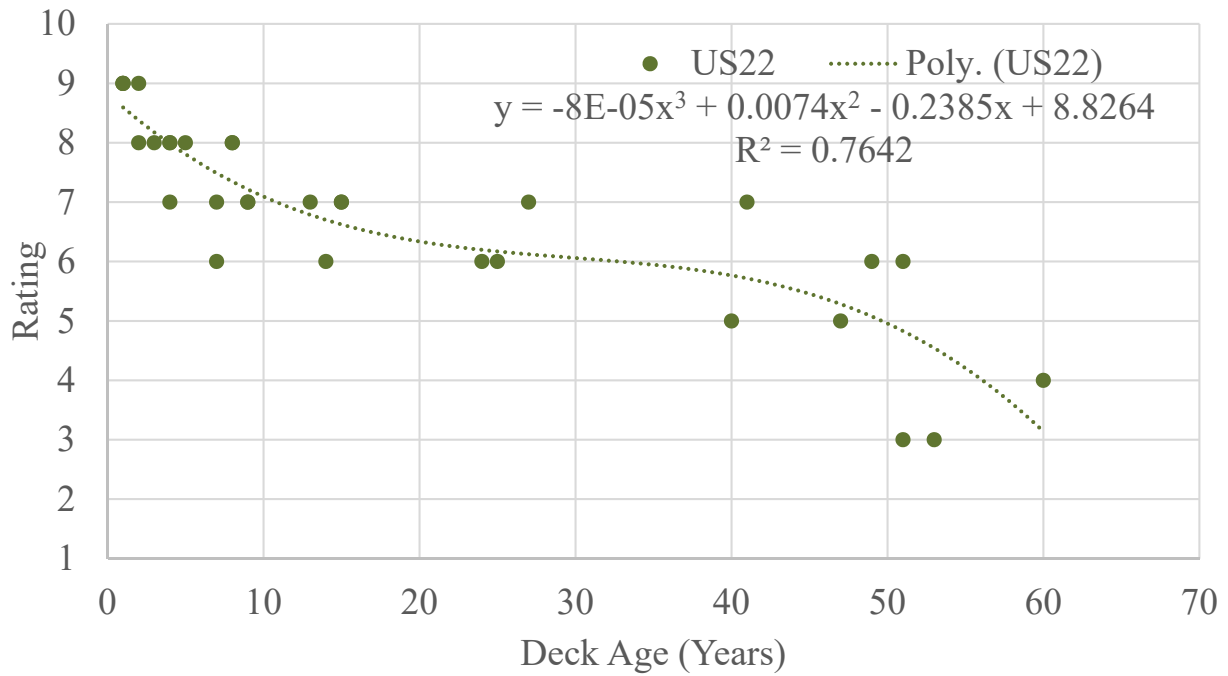
US130



US1



US22



APPENDIX B STRUCTURAL ANALYSIS OF SELECTED BRIDGES

From the classification of highway bridge inventory in New Jersey, in the “**Bridge Classification**” section, four types of bridges were selected for structural analysis in order to obtain their response under various truck loading, including 1) simple span steel multi-beam bridges, 2) simple span steel girder-floorbeam bridge, 3) simple span prestressed concrete multi-beam bridges, and 4) continuous span steel multi-beam bridges. The following section describes structural analysis using the Finite Element approach and the AASHTO approach to verify the results. AASHTO fatigue evaluation were then used to predict the fatigue life.

Prototype Bridge I: Simple Span Steel Multi-Beam Bridge

Due to the large inventory of simple span steel multi-beam bridges, three bridges were selected to represent the bridges with short, average and long span lengths. The bridges selected for analysis are summarized in Table 52 include the NJ Route 34 over I-195 and NJ Route 138 (Str. No. 1307-155), Route I-295 over Clements Bridge Road (Str. No. 0428-164), Route US 202 over County Route 605 (Queens Road) and Alexauken Creek. Respectively, these structures represent average span length, short span length and long span length bridges.

Table 52 - Summary of selected bridges

Structure No.	Span Length (ft.)	Total Width (ft.)	Skew Angle	Number of Girders	Girder Spacing (ft.)	Slab Thickness (in)	Girder Depth (in)
1307-155	86.5	112.75	21	16	7.25	10	54
0428-164	62.5	56.50	11	7	8.75	9.5	36
1023-153	106	57.25	11	8	7.42	8	57.5

Finite Element Bridge Analysis

Material Properties

The modulus of elasticity of the steel girders and diaphragms are taken as 29,000 ksi, and the Poisson’s Ratio taken as 0.3. For the concrete slab, the elastic modulus and Poisson’s Ration were taken as 3,600 ksi and 0.18, respectively. Neither the concrete nor steel components are expected to deform beyond the elastic range due to design loads, so only elastic material properties are considered.

Element Selection and Analysis Report

The FE models were developed using the general FEA program, ABAQUS. The modeled bridges are shown in Figure 69. A 4-node shell element (S4) was selected for the concrete slab. Element type S4 in ABAQUS is a fully integrated, finite membrane strain shell element. Simpson’s rule is used to calculate the cross-sectional behavior of

the shell elements. For the steel girders, floor beams, stringers, and diaphragms, a 2-node linear beam element (B31) was selected in the model. Element type B31 is a first-order, shear deformable beam elements, meaning that shear deformation as well as flexural deformation can be accounted in the analysis. The slab elements are connected to beam elements using the multi-point constraint, or MPC, which rigidly constrains rotations and translations of the slave node to those of the master node.

With the developed model, a set of point loads simulating one or multiple truck loading was applied on the concrete deck. A multiple load case analysis was adopted to apply the truck load at various locations of the concrete deck. This analysis method in ABAQUS allows for the change of applied loads and boundary conditions. The results can then be scaled and linearly combined during post-processing.

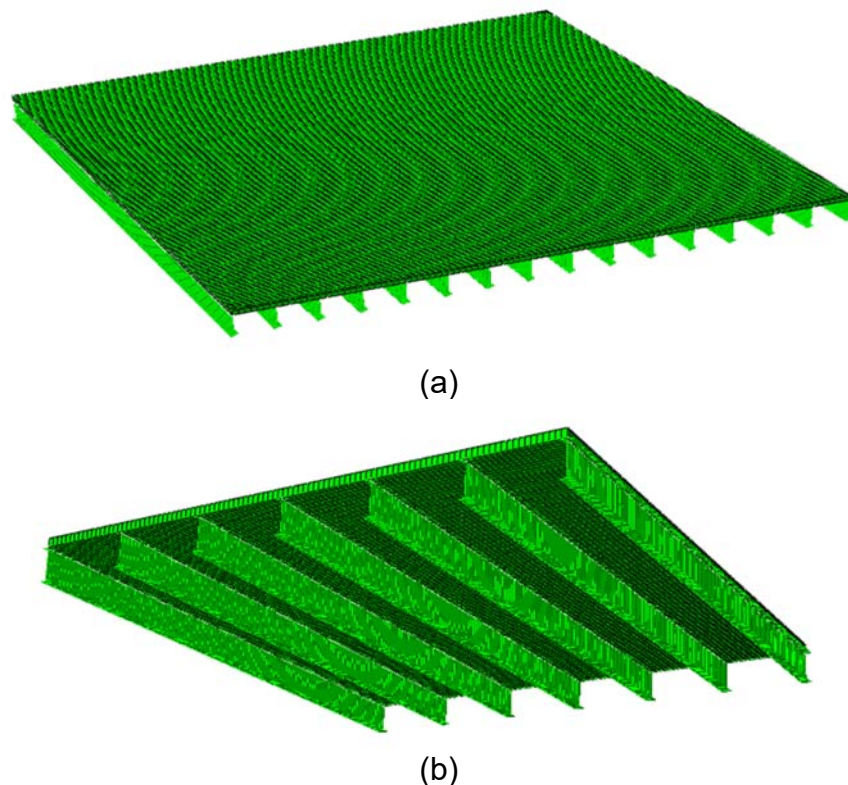


Figure 69. Finite element models for (a) Structure No. 1307-155, and (b) Structure No. 0428-164

Maximum Stress Range Induced By AASHTO Fatigue Trucks and Girder Distribution Factor

The load cases in the FEA are generated to represent an HS-20 truck for the fatigue limit state, which uses a fixed distance of 30 ft. between the middle and rear axles, as shown in Figure 70. A dynamic impact factor of 0.15 for fatigue is included. For interior girders, the truck is centered over the girder. For exterior girders, the truck is positioned 1 ft. from the sidewalk or the inside face of the parapet. For structures with different

girder sections at splice locations, bottom flange stress is evaluated at both mid-span and the cutoff location. Figure 71, for example, shows that the maximum cutoff stress determined from the FE analysis was 2811 lb/in^2 for exterior girders on Str. No. 1307-155. For comparison, the AASHTO method was used to compute the girder stresses and distribution factors manually, shown in detail in Appendix A. The results, given in Table 53 through Table 55, show that AASHTO stresses for “one lane loaded” are on average 64 percent higher than the stress results from the FE analysis. From the analysis, the bridge with Str. No. 1023-153 has the maximum stress ranges under the same fatigue truck loading.

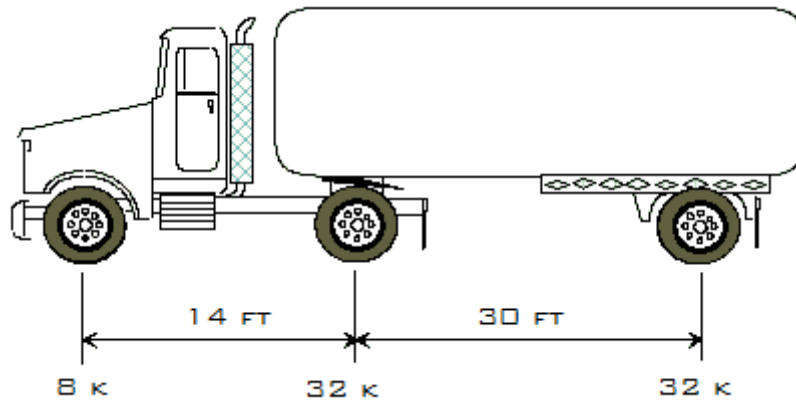


Figure 70. HS-20 design truck for fatigue

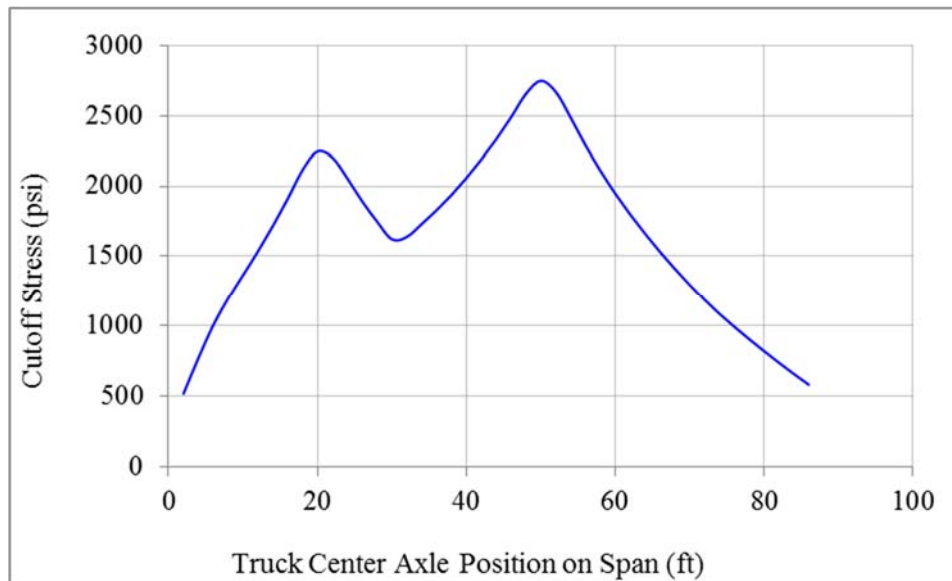


Figure 71. Exterior girder bottom flange stress at splice cutoff, located 24 ft. from midspan, due to HS-20 including impact (Str. No. 1307-155)

Table 53 - Str. No. 1307-155

Member	Span Position	GDF		Stress (lbf/in ²)	
		FEM	AASHTO	FEM	AASHTO
Exterior Girder	Midspan	0.29	0.51	2709	4333
	Cutoff	0.33	0.51	2811	4600
Interior Girder	Midspan	0.24	0.41	2130	3446
	Cutoff	0.27	0.40	2393	3586

Table 54 - Str. No. 0428-164

Member	Span Position	GDF		Stress (lbf/in ²)	
		FEM	AASHTO	FEM	AASHTO
Exterior Girder	Midspan	0.39	0.66	3957	6749
	Cutoff	--	--	--	--
Interior Girder	Midspan	0.33	0.54	3174	5565
	Cutoff	--	--	--	--

Table 55 - Str. No. 1023-153

Member	Span Position	GDF		Stress (lbf/in ²)	
		FEM	AASHTO	FEM	AASHTO
Exterior Girder	Midspan	0.46	0.594	3704	5240
	Cutoff	0.54	0.594	4383	5290
Interior Girder	Midspan	0.38	0.637	3125	5620
	Cutoff	0.48	0.625	3965	5560

Prototype Bridge II: Simple Span Steel Girder-Floorbeam Bridge

The Newark Bay Bridge is a bridge crossing over the Newark Bay that connects the cities of Newark and Bayonne, New Jersey. The bridge was constructed in 1956 as part of New Jersey Turnpike (I-95) network. The bridge provides the access from the New Jersey Turnpike main line at interchange 14 to Lower Manhattan in New York City via the Holland Tunnel. Newark Bay Bridge contains three different types of superstructures: Floor-Beam Spans (Type A), Beam Span (Type B), and Main Truss Span (Type C). The layout of each type of spans was shown in Figure 72.

A comprehensive field testing was conducted to understand the behavior of the Newark Bay Bridge and collect the data for the model calibration. The bridge was monitored using an array of sensors to understand truck loading on the bridge under normal traffic conditions and the structural behavior under the truck loading. The results of the field tests and monitoring were used to improve accuracy of analytical modeling. An array of sensors were adopted for bridge monitoring, including Laser Doppler Vibrometer (LDV), strain transducer, foil strain gages, and Weigh-In-Motion (WIM) sensors as shown in Figure 73 and Figure 74. The strain transducers and the LDV were placed on various bridge components to collect data under truck loading. With the WIM sensors, information about truck traffic on the bridge was gathered and the results were used as

an input for the analytical studies. The truck traffic information gathered using the WIM sensors can also be used for future design and maintenance of bridges, since the data includes detailed information of the truck traffic.

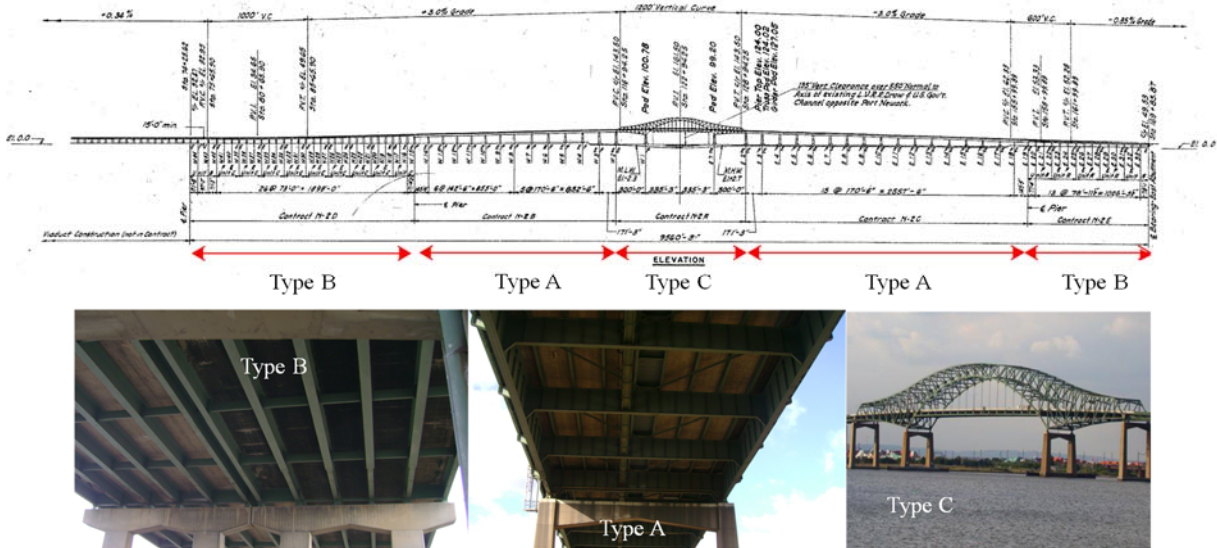


Figure 72. Newark Bay Bridge

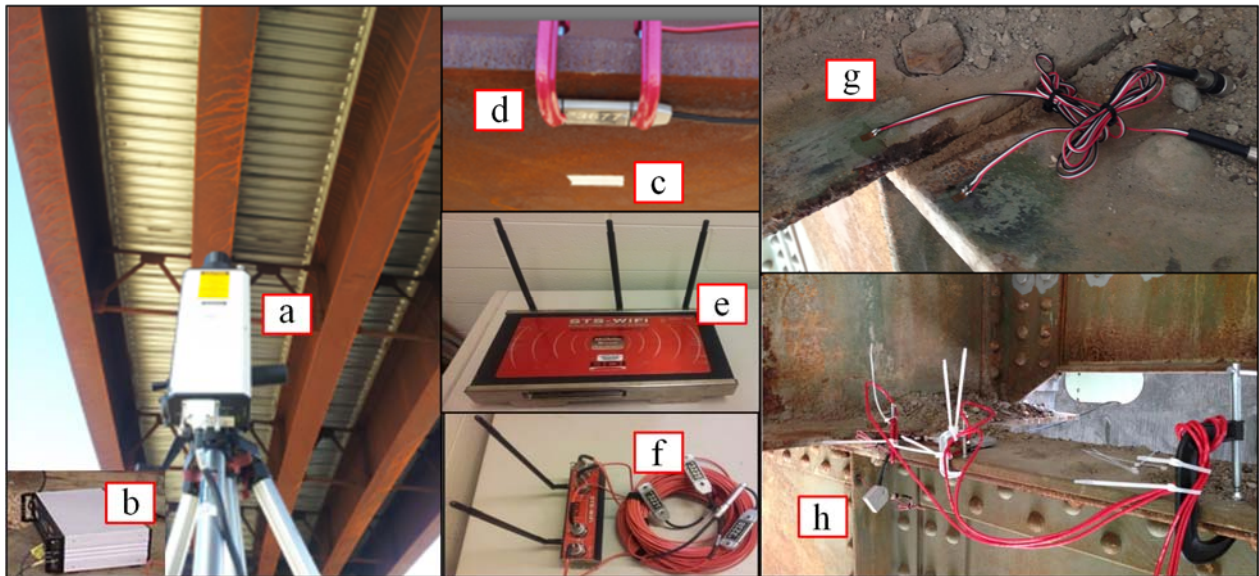


Figure 73. Field instrumentation equipment

The Laser Doppler Vibrometer (LDV), is a non-contact sensor that measures displacement and velocity of a remote point. The LDV uses laser interferometer to measure vibration. The system is composed of three parts: the helium neon Class II laser head (Figure 73 a), the decoder unit (Figure 73 b), and the reflective target

(reflector) attached to the structure (Figure 73 c). The laser head is mounted to a tripod that is positioned underneath the target. The reflective target, typically retro-reflective tape, provides a strong signal. The Structural Testing System (STS) is a modular data acquisition system. The system consists of a main processor (Figure 73 e), junction boxes (Figure 73 f), and strain transducers (Figure 73 c) or a foil strain gauge completion unit (Figure 73 h). The general-purpose standard 350 Ω foil gauges (Figure 73 g) used here were connected to the STS system with a quarter arm foil strain gauge completion unit. The permanent Weigh-In-Motion (WIM) system was installed on the east abutment of the bridge to collect traffic information regarding traffic volume, traffic pattern, and truck weight. The piezoelectric sensors were installed on all 4 traffic lanes on the abutment. The east bound sensors were installed approximately about 120-ft away from the east abutment and the west bound sensors were installed approximately about 60-ft away from the east abutment. Layout of the WIM sensors is shown in Figure 74.

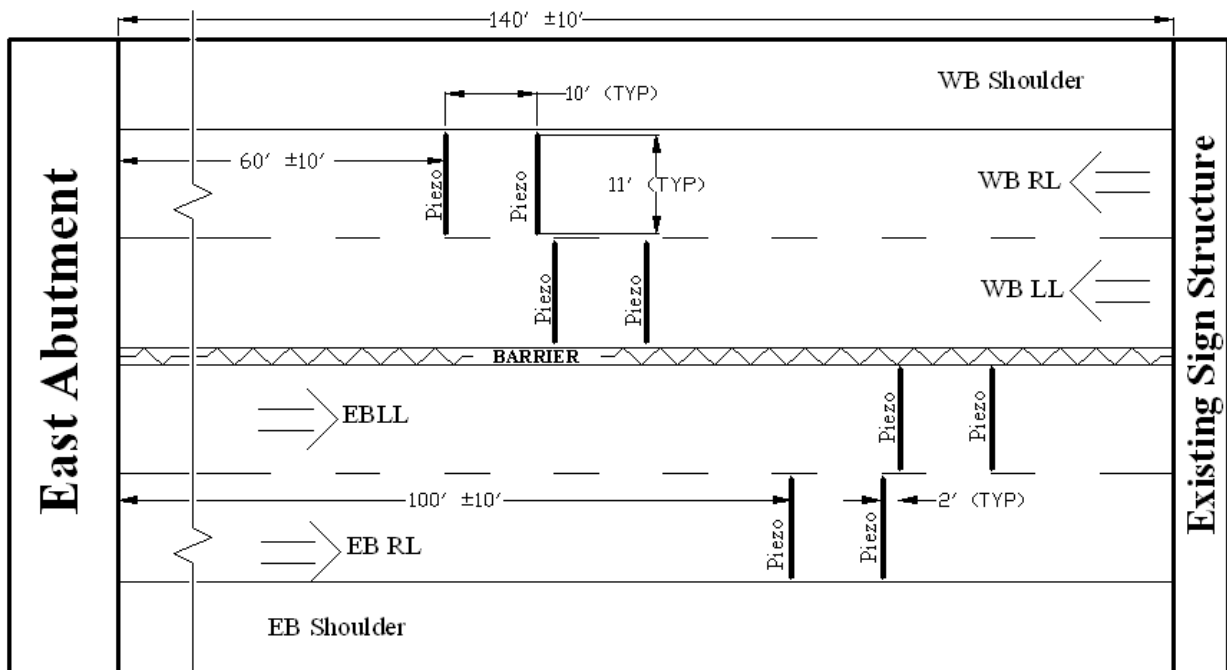


Figure 74. Weight-In-Motion sensor locations

Span W14 was selected for field instrumentation and testing. 7 strain transducers, 5 reflective tapes and 6 foil strain gauges were installed as shown in Figure 75. The foil strain gauges were installed on selected fatigue critical details, which is the connection of end floor beam and stringers in this case. Two locations were chosen as shown in Figure 76. The detail information of each sensor was listed in Table 56. The configuration of testing truck was shown in Figure 77. Both static test and dynamic test (5 mph and 30 mph) were performed on the selected span.

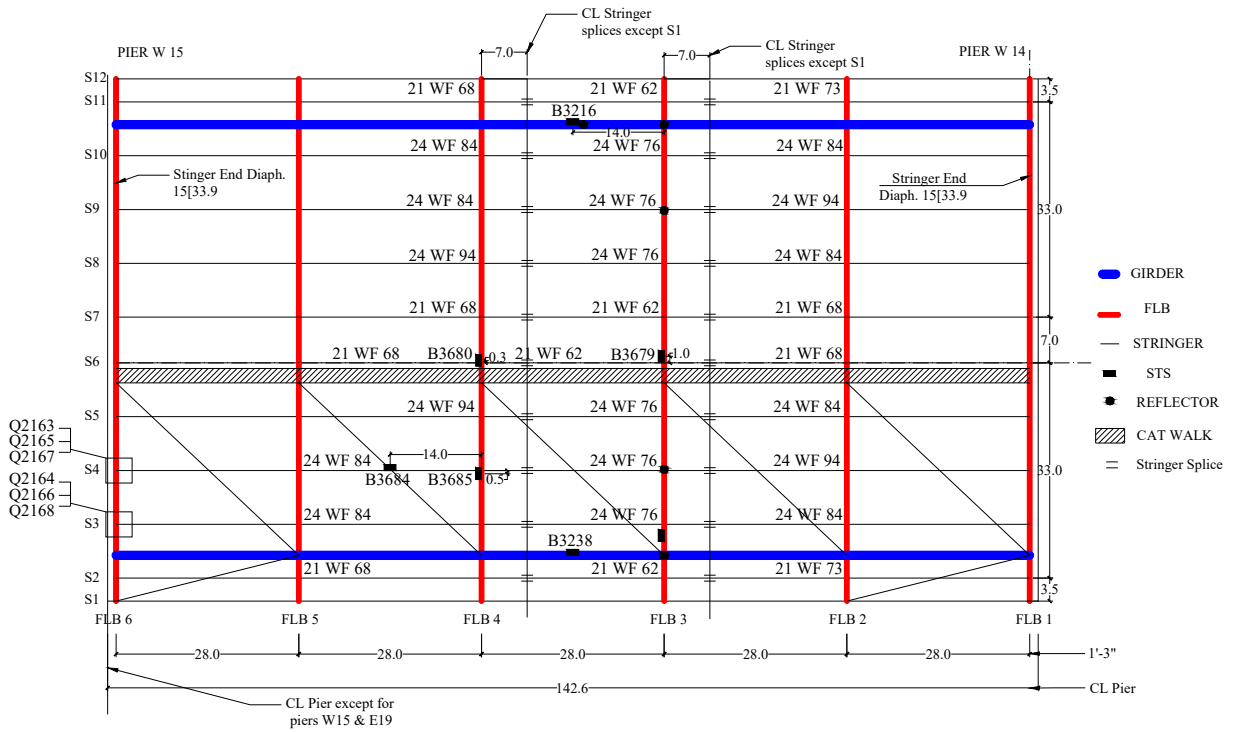


Figure 75. Instrumentation on Span W14 (Type A span) (ft.)

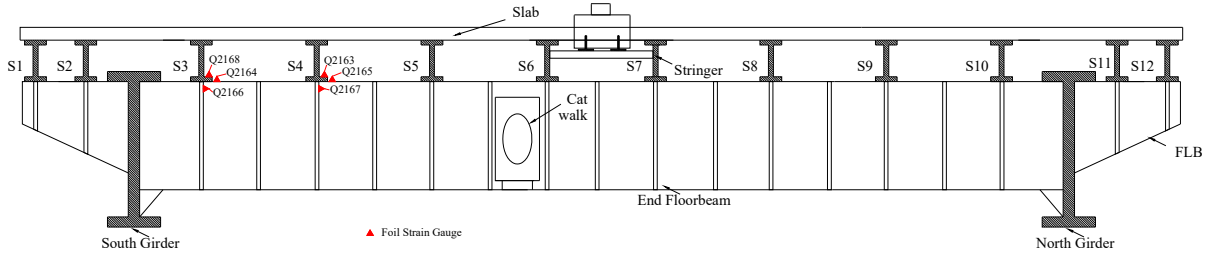


Figure 76. Cross section of instrumented Span W14 (Type A span) (ft.)

Table 56 - Location of each sensor

Sensor ID	Sensor type	Location
B3216	Strain Transducer	on North Girder, 14 ft. from FLB3
B3238	Strain Transducer	on South Girder, 14 ft. from FLB3
B3679	Strain Transducer	on FLB3, 1 ft from S6
B3680	Strain Transducer	on FLB4, 0.3 ft from S6
B3684	Strain Transducer	on S4, 14 ft from FLB 4
B3685	Strain Transducer	on FLB4, 0.3 ft from S6
Q2163	Foil strain gage	S4 and FLB6 connection, on the top of bottom flange of S4
Q2165	Foil strain gage	S4 and FLB6 connection, on the top of top flange of FLB6
Q2167	Foil strain gage	S4 and FLB6 connection, on the stiffener of FLB6 under S4
Q2164	Foil strain gage	S3 and FLB6 connection, on the top of top flange of FLB6
Q2166	Foil strain gage	S3 and FLB6 connection, on the stiffener of FLB6 under S3
Q2168	Foil strain gage	S3 and FLB6 connection, on the top of bottom flange of S3

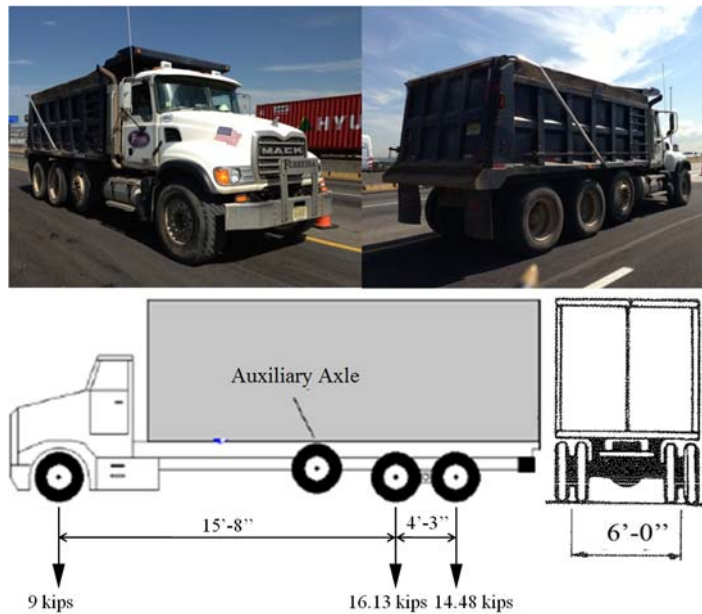


Figure 77. Configuration and axle weights of calibration truck

Three Dimensional Finite Element Modeling and Verification

The bridge span that was tested was also modeled and analyzed using the finite element (FE) program ABAQUS (Version 6.10). Various element types were used to validate and ascertain the accuracy of the FE model, the FE analysis results were compared with data collected from field tests and various items were adjusted to improve the model including 1) section properties, 2) material behavior, 3) boundary conditions, and 4) interaction between different members. The modulus of elasticity of the steel girder, floorbeam, and stringer, E , and Poisson's Ratio, ν_s , is used as 29,000 ksi and 0.3, respectively. It is noted that the steel girders, floorbeams, and stringer are expected to undergo deformation within the elastic region only and therefore the inelastic behavior of the steel material was not considered. The compression strength for concrete was considered as 8000 lbf/in². The established model is shown in Figure 78 and the comparisons shown in Figure 79 confirm the good agreement between the FE model and field testing data.

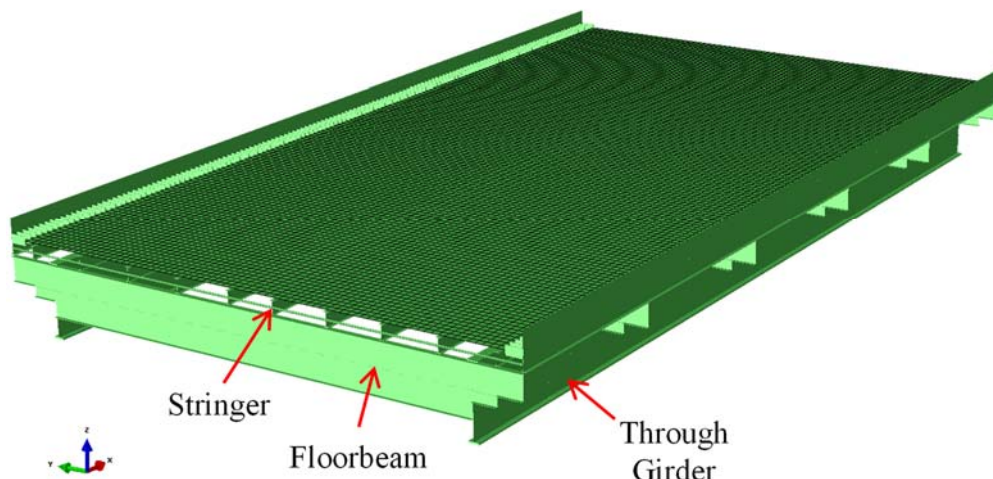


Figure 78. FE Model for Span W14

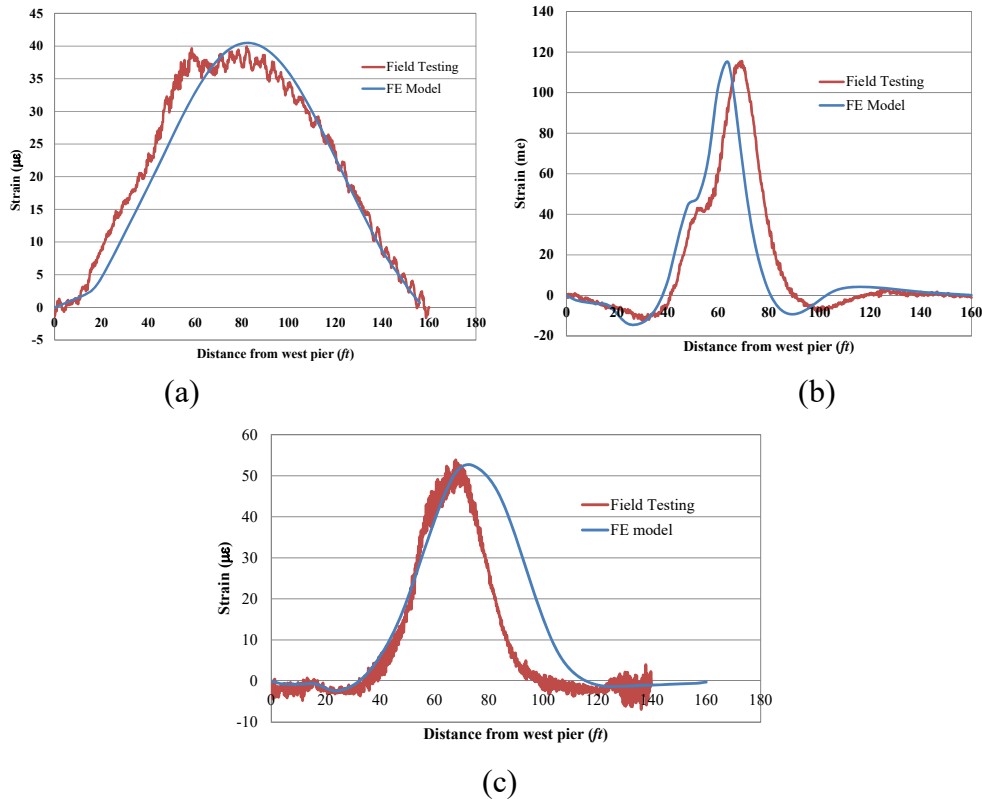


Figure 79. Comparison of strain profiles under truck loading on south lane (17 ft. from curb): (a) main girder Sensor B3238, (b) S4 Sensor B3684, and (c) floorbeam FLB 4 Sensor B3685

Fatigue Truck Model Analysis

A fatigue truck is typically used to represent truck traffic conditions at the bridge site. The fatigue truck models provided in the AASHTO LRFD, 2010 [9] is shown in Figure 80 (a) with a 6 ft. (1.82 m) axle width. However, the AASHTO Manual for Bridge Evaluation indicate that when the GVW distribution at the investigated site is available, an effective GVW can be determined by Eq. (1) and this effective GVW can be used to modify the GVW of AASHTO fatigue truck model.

$$W_{eq} = \left(\sum f_i W_i^3 \right)^{1/3} \quad \text{Eq. 1}$$

where f_i is the frequency of occurrence of trucks with a GVW weight of W_i . After deriving the effective gross vehicle weight by analyzing the WIM data, the gross weight of the modified AASHTO fatigue truck will be distributed proportionally into each axle as illustrated in Figure 80 (b).

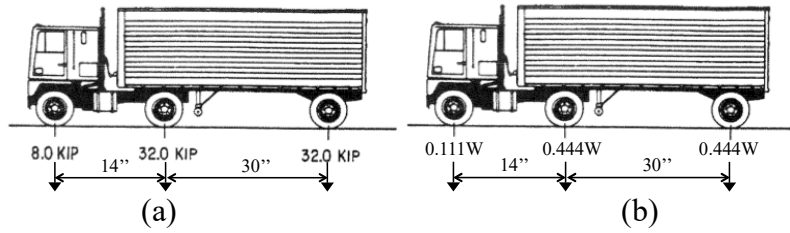
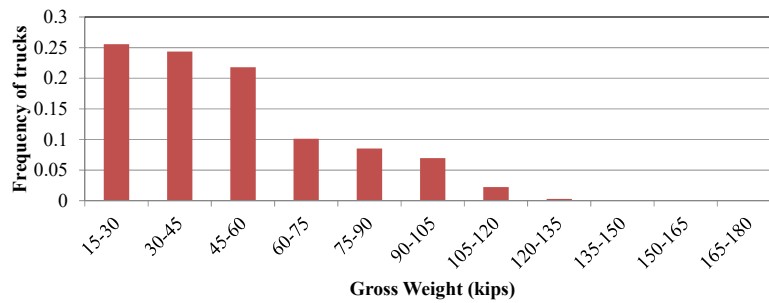
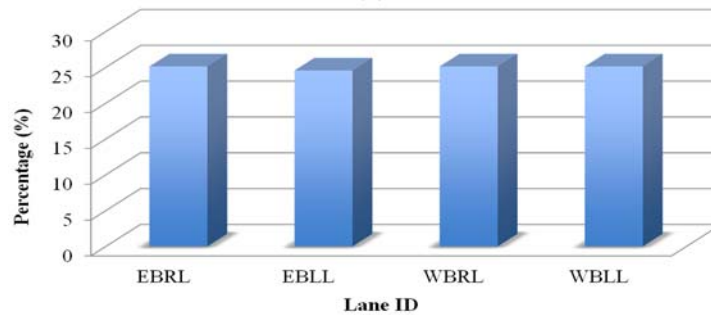


Figure 80. (a) AASHTO fatigue truck model (b) modified AASHTO fatigue truck model

WIM data collected at this bridge site were used in this study to develop the modified fatigue truck model in this study. The distribution of gross weight and truck distribution in each lane were shown in Figure 81. The effective gross weight for fatigue truck calculated in this case was 61.4 kips.



(a)



(b)

Figure 81. (a) Distribution of gross weight; (b) Distribution of trucks in each

The maximum stress range caused by the site-specific fatigue trucks and the estimated remaining fatigue life was shown in Table 57.

Table 57 - Stress range caused by site specific fatigue trucks and estimated remaining fatigue life

Structural member	Critical location	Δf (ksi)	Δf_{LL+IM} (ksi)	Δf_{eff} (ksi)	$(\Delta f_{eff})_{max}$ (ksi)	Remaining fatigue life prediction by AASHTO	
						Category C	Category D
Girder	Main girder and FLB4 intersection	1.87	2.15	1.46	2.91	Infinite	Infinite
Floorbeam	End floor beam and S6 intersection	3.93	4.52	3.06	6.12	Infinite	Infinite
Stringer	midspan of stringer	4.65	5.35	3.62	7.24	Infinite	57 (evaluation life), 32 (minimum life), 83 (mean life)

Prototype Bridge III: Simple Span Prestressed Concrete Multi-Beam Bridges

Before the finite element modeling, a prestressed concrete bridge with span length of 60 ft. was designed according the AASHTO LRFD Bridge Design Specification using an in-house design program. Using the information of this designed bridge, a 3-dimensional finite element model was developed for this bridge using ABAQUS. The following sections explains each model element used as well as the constraint/release conditions applied.

Geometric Modeling

The structure of the bridge can be modeled using nodes, elements and sections provided by ABAQUS.

Elements

The ABAQUS program library itself provides numerous options for selection of geometric elements. Out of which for this project, Beam and Shell elements have been identified as the most appropriate and dependable for bridge related problems.

Beam Element

Due to its one-dimensional characteristics, definition of stringers and girders can be modeled with the help of Beam Element. A two-node beam element is used to model girders. It should be noted here that the segment generally won't deform out of plane. This fact/ condition can be considered a constraint while defining the problem statement. This restriction ensures that the plane section will remain the plane section until the whole analysis is done. Figure 82 below depicts the beam element with various integration localities. The more minute the modeling, the more precision is achieved. This means the accuracy of the outcome depends upon the degree of discretization. But the problem a user encounters during working with highly discretized bridge is, slow processing of the program.

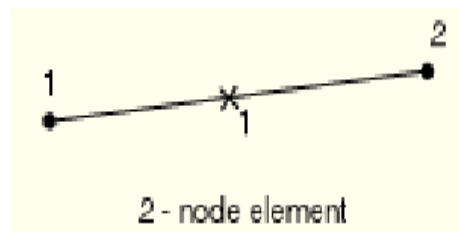


Figure 82. Integration points of two-node linear beam B31

Shell Element

For concrete bridge decks in FE models, a shell element has been used very commonly due to their thickness. The inbuilt library resource for the shell element is very rich. The majority are four-node type of shell elements. The element is of a completely integrated, general purpose type with finite-membrane-strain shell elements that allow in-plane bending able to permit planar bending (in plane bending). In addition to this, it also allows deflection/deformation in transverse direction. It should be noted that this element is considered to be of a thick shell theory. It is obvious that with the increase in the thickness value, the predicted pattern for thin shell explained by the Kirchhoff-Love hypothesis gets dulled. This is very certain as this hypothesis banks upon the condition of homogeneous isotropic materials. Thus, implementing it for thick-shelled, laminated anisotropic materials, such as the steel reinforced concrete bridge deck, will not yield a proper result. The four-node shell element has six degrees of freedom at each node and four integration points for each element. Figure 18 illustrates the integration point and nodes used by the four-node shell elements.

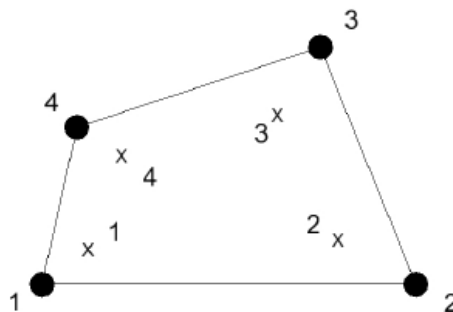


Figure 83. Integration points of a four-node shell element (ABAQUS)

Tendon Element

For the modeling of prestressing tendons, a truss element is introduced to the model. A 2-node linear displacement truss element T2D2 is used to model the tendon elements.

Sections

It is extremely important to incorporate the properties of an element into the model. The definitions of the properties and characteristics are incorporated into the model using sections. From the numerous available sections, the following types are associated with the current analysis. A section corresponds to a specific material. After identifying sections, certain sets of elements are imposed on related sections.

Beam Section

The beam section is used to define the cross-section for beam elements when numerical integration over the section is required. Girder of the bridge is modeled using an I beam section. The integration points for the I beam section in stress are shown in Figure 84.

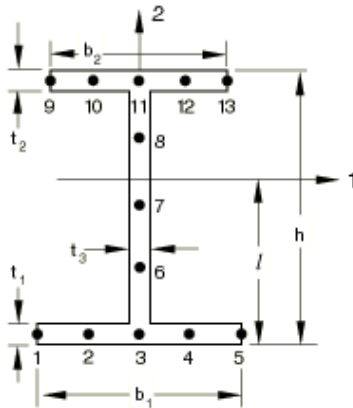


Figure 84. Integration points on I section

Shell Section

The use of the shell section is to specify or define a shell cross section in ABAQUS input file. The thickness of deck in bridge model is provided using this section.

Rebar Layer

For modeling, all the steel reinforcement of the inbuilt rebar element was implemented. In ABAQUS this element is capable of providing embedment within the beam or shell elements. Steel Reinforcing rebars are placed in both transverse layers and longitudinal layers within the shell.

Solid Section

The prestressing tendons in girder are defined using solid section.

Constraint Elements

The model built in ABAQUS model is an assembly of individual structural components., such as beams, shells, studs, etc. Unless these constituent elements are merged to build a bridge, analysis cannot be run. As for joining these elements, constraint elements must be employed. The most commonly used constraint element used a multipoint Constraint (MPC). Rigid joints simulating a beam is ensured by beam MPC. The simulation is between two nodes. And this simulation is mostly employed for slab and beam elements to generate composite action. The displacement and rotation of one node is directly associated with those of the connected node.

Material Properties

Material modeling consists of defining the properties of the different materials used in the structure. Each material definition is actually a combination of various independent characteristics.

- Density
- Elastic Modulus
- Poisson's ratio
- Thermal expansion
- Dependent variables
- User defined field

For accurate results the properties of these materials must be determined and input into the program.

Loading

The standard fatigue loading that defined by AASHTO Bridge Design Specification was used. In addition, the loading was placed at the location where the maximum stress is produced at the tendons. The initial prestressing force is applied using two commands from ABAQUS: initial condition and prestress hold.

Finite Element Analysis

Using the information described above, a 3-D FE model was developed as shown in Figure 85 and Figure 86. Applying the HS-20 fatigue loads, the stress that obtained from the prestressing tendon at the midspan is 140.4 ksi. The initial stress was 200.16 ksi. Therefore, the stress range of prestressed tendon for this bridge is 59.76 ksi under AASHTO fatigue truck model.

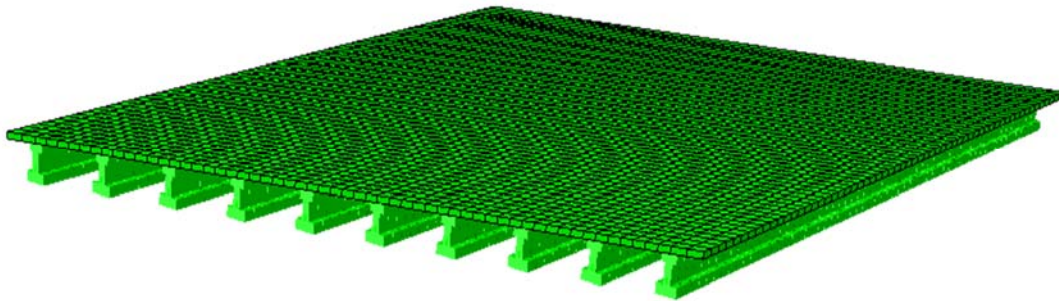


Figure 85. 3-D FE model for prestressed concrete bridge

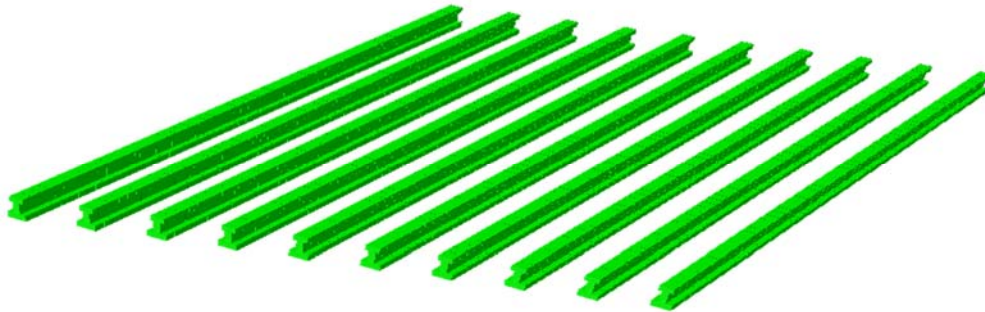


Figure 86. 3-D FE model for prestressed concrete girder